

DTIC FILE COPY

UNIVERSITY OF NOTTINGHAM

DEPARTMENT OF CHEMISTRY

①

ARMY/NAVY/AIR FORCE LIBRARY
EDISON HOUSE

AD-A218 047

ABSTRACTS

DTIC
ELECTE
FEB 20 1990
S D D

unlimited

8TH. INTERNATIONAL
SYMPOSIUM
ON GAS KINETICS

15 - 20 JULY 1984

DISTRIBUTION STATEMENT A

Approved for public release
Distribution Unlimited

00 02 16 028

Organised by the Gas Kinetics Group,
of the Faraday Division of the Royal Society of Chemistry

Organising Committee

I. M. T. Davidson (Leicester)
J. A. Kerr (Birmingham)
M. J. Pilling (Oxford)
I. Powis (Nottingham)

P. J. Sarre (Nottingham)
J. P. Simons (Nottingham)
I. W. M. Smith (Cambridge)
R. Walsh (Reading)

We gratefully acknowledge sponsorship of this Conference by:-

BP Company plc
British Council
British Gas
Exxon Research and
Engineering Company

ICI plc
Shell Research Limited
United States Air Force (EOARD)
United States Army
Coherent (UK) Ltd
Lambda Photometrics Ltd

Printed in England by Chas Goater & Son Ltd.

UNIVERSITY OF NOTTINGHAM

DEPARTMENT OF CHEMISTRY

ABSTRACTS

Approved for public release;
distribution unlimited.



8TH. INTERNATIONAL SYMPOSIUM ON GAS KINETICS

15 – 20 JULY 1984

*"The intensity of the conviction that a hypothesis is true
has no bearing on whether it is true or not."*

Sir Peter Medawar, Advice to a Young Scientist

CONFERENCE PROGRAMME

SCIENTIFIC SESSIONS

The formal scientific sessions will be held in the Large Lecture Theatre in the Department of Chemistry and posters will be displayed in Hugh Stewart Hall.

REGISTRATION

Registration will take place at the following times:

Sunday 15 July	15.00 - 20.30 at Hugh Stewart Hall
Monday 16 July	08.30 - 09.30 Conference Desk, Chemistry Department Foyer

SUNDAY 15 JULY

15.00 - 20.30	Registration at Hugh Stewart Hall
16.00 - 17.30	Tea, Hugh Stewart Hall
19.00	Buffet/Reception, Hugh Stewart Hall
19.00 - 24.00	Cash bar in Hugh Stewart Hall

STATEMENT "A" per D. Tyrell
AFOSR/XOTD (400)
TELECON 2/16/90

CG



Accession For	
NTIS CRA&I	<input checked="" type="checkbox"/>
DTIC TAB	<input checked="" type="checkbox"/>
Unannounced	<input checked="" type="checkbox"/>
Justification	
By <i>per all</i>	
Distribution /	
Availability Codes	
Dist	Avail and/or Special
A-1	

MONDAY 16 JULY

Partial contents,

09.00 - 09.15 **Official Welcome by Dr. B. C. L. Weedon, FRS,**
Vice-Chancellor, University of Nottingham

SESSION I - THEORY: REACTIVE PROCESSES -

- 09.15 - 10.00 A1 **Transition states and trapped trajectories,** *pg. 11*
M. S. Child (Oxford)
- 10.00 - 10.20 A2 Dynamics of centrifugal barrier complexes close to
orbiting
K. Rynefors and N. Marković (Göteborg)
- 10.20 - 10.40 A3 An adiabatic theory of chemical reactions
V. Z. Kresin and W. A. Lester (Berkeley)
- 10.40 - 11.10 Coffee
- 11.10 - 11.30 A4 Vinylidene: potential energy surface and
unimolecular reaction dynamics
W. H. Miller (Berkeley)
- 11.30 - 11.50 A5 Calculations on the rates of neutral reactions
dominated by long range intermolecular forces.
D. C. Clary (Cambridge)
- 11.50 - 12.10 A6 Theoretical studies of state to state kinetics in
 $H + H_2O \rightarrow OH + H_2$, $H_2 + H_2^+ \rightarrow H_3^+ + H$ and $O + H_2$
 $\rightarrow OH + H$
G. C. Schatz (Northwestern)
- 12.10 - 12.30 A7 Photolysis quantum yields and recombination rate
coefficients in highly compressed gases and liquids
J. Troe and J. Schroeder (Göttingen)
- 13.00 Lunch

MONDAY 16 JULY

SESSION II - THE TRANSITION STATE

- 14.10 - 14.55 B1 **Understanding rate data for elementary processes**
D. M. Golden (SRI) *cont'd*
- 14.55 - 15.15 B2 Calculation of the thermodynamics of molecular reactions using the BAC - MP4 method: reactions of OH with C₂H₂, C₂H₄ and HCN*
C. F. Melius, J. S. Binkley and M. L. Koszykowski (Sandia) *pg. 1*
- 15.15 - 15.35 B3 Kinetic studies of OH - alkene reactions
F. P. Tully and J. E. M. Goldsmith (Sandia)
- 15.35 - 17.45 Poster Session I and Tea at Hugh Stewart Hall
(See list of poster titles below)
- 18.30 Dinner
- 20.00 - 21.30 Workshop - Transition State Theory - in Large Lecture Theatre, Department of Chemistry
Chairman: I. W. M. Smith (Cambridge)

POSTER SESSION I (Hugh Stewart Hall)

- C1 Reactions of wrong radicals
G. Ács, A. Péter and P. Huhn (Szeged)
- C2 Coupling schemes and hyperspherical expansions for elementary chemical reactions
V. Aquilanti, G. Grossi, S. Cavalli and A. Laganà (Perugia)
- C3 The extent of alkyl nitrate formation from the RO₂ + NO reaction
R. Atkinson, W. P. L. Carter, A. M. Winer and J. N. Pitts, Jr. (Riverside)
- C4 Pyrolysis of organic nitrates studied by MB-MS technique
L. Holmlid and E. Axelsson (Göteborg)
- C5 Weak collisional efficiencies in the thermal unimolecular dissociation of ethane
J.-R. Cao and M. H. Back (Ottawa)
- C6 Pressure dependence of the reaction OH + HO₂NO₂
I. Barnes, V. Bastian, K. H. Becker and E. H. Fink (Wuppertal)
- C7 Rate coefficients for the reaction
HS + NO + M → HSNO + M (M = He, Ar and N₂) over the temperature range 250-445 K
G. Black, R. Patrick, L. E. Jusinski and T. G. Slanger (SRI)
- C8 The temperature dependence of the Lewis-Rayleigh afterglow from atomic nitrogen
A. Billington, P. M. Borrell, P. Borrell and D. S. Richards (Keele)
- C9 Temperature dependence of simple ion-neutral clustering reactions
P. A. M. van Koppen, S. Liu, R. Derai and M. T. Bowers (Santa Barbara)

MONDAY 16 JULY

- C10 Energy disposal of the products of simple ion-molecule reactions
A. O'Keefe, D. C. Parent, W. Wagner-Redeker and M. T. Bowers (Santa Barbara)
- C11 Reduced dimensionality quantum rate constants for the $D + H_2$ ($v = 0$) and $D + H_2$ ($v = 1$) reactions on the LSTH surface
J. M. Bowman, K. Tung Lee (IIT) and R. B. Walker (Los Alamos)
- C12 'Polymode': A program to calculate vibrational energies of polyatomic molecules. I. Application to H_2O
H. Romanowski and J. M. Bowman (IIT)
- C13 A study of N_2O_5 and NO_3 chemistry and the photolysis of N_2O_5 mixtures
J. P. Burrows, G. S. Tyndall and G. K. Moortgat (MPI, Mainz)
- C14 The photolysis of $ClONO_2$ and the production of NO_3
J. P. Burrows, G. S. Tyndall, G. K. Moortgat and D. W. T. Griffith (MPI, Mainz)
- C15 Reactions of O atoms with alkanes
N. Cohen (Aerospace Corporation)
- C16 A computerised thermochemical data base of molecules and free radicals in the gas phase
C. Muller, J - M. David, G. Scacchi and G - M. Côme (Nancy)
- C17 Computer aided design of gas phase free radical reaction mechanisms
L. Haux-Vogin, G - M. Côme (Nancy), P. Y. Cunin (Dijon) and M. Griffiths (Marseille)
- C18 The reaction $H + D_2 \rightarrow HD + D$: Distorted wave calculations at 0.55 eV and 1.3 eV
J. N. L. Connor and W. J. E. Southall (Manchester)
- C19 Kinetics studies of the reactions of NO_3 with Cl and ClO
R. A. Cox, D. Stocker (AERE, Harwell), M. Fowles, D. Moulton, R. P. Wayne (Oxford) and E. Lungstrom (Gothenburg)
- C20 Effects of olefines on thermal decomposition of propane
A. Dombi and P. Huhn (Szeged)
- C21 Vibrational relaxation of highly excited HF and DF
L. S. Dzelzkalns and F. Kaufman (Pittsburgh)
- C22 A quasiclassical trajectory study of collisions of He with electronically, rotationally and vibrationally excited HD and H_2
S. C. Farantos (Athens)
- C23 Collisional energy transfer and macroscopic disequilibrium
W. Forst (Laval)
- C24 Study of the equilibrium $i - C_3H_7 + O_2 \rightleftharpoons i - C_3H_7O_2$
I. R. Slagle, E. Ratajczak, M. C. Heaven, D. Gutman (IIT) and A. F. Wagner (Argonne)
- C25 Vibrational induced dissociation of tetramethyl-dioxetane by overtone and infrared multiple photon absorption
S. Ruhman, O. Anner and Y. Haas (Jerusalem)
- C26 Separation of fluence and intensity effects in infrared multiple photon absorption
G. Hancock, A. J. MacRobert, K. G. McKendrick and J. H. Williams (Oxford)
- C27 Direct observation of collisional energy transfer of vibrationally highly excited CS_2 molecules
J. E. Dove, H. Hippler and J. Troe (Göttingen)


111

MONDAY 16 JULY

- C28 Crossed beam study of reaction of van der Waals molecules, $O + (NO)_2 \rightarrow NO_2^+ + NO$:
angle-resolved chemiluminescence detection
K. Honma and O. Kajimoto (Tokyo)
- C29 An optoacoustic study of infrared multiphoton absorption in polyatomic molecules
P. John, C. L. Wilson, R. G. Harrison and R. G. McGuire (Heriot-Watt)
- C30 The reaction of $NH(X^3\Sigma)$ with $O_2(^3\Sigma_g)$ and $O_2(^1\Delta_g)$
W. Hack, H. Kurzke and H. Gg. Wagner (MPI, Göttingen)
- C31 An improvement of the $Li + HF$ PES by means of quasiclassical calculations
E. Garcia, A. Laganà (Perugia), J. M. Alvarinho and M. L. Hernandez (Pais Vasco)
- C32 Kinetic study of the reactions of acetonitrile with OH and Cl radicals
G. Poulet, J. L. Jourdain, G. Laverdet and G. Le Bras (CNRS, Orleans)
- C33 Decomposition and collisional deactivation of chemically activated tetrahydrofuran
L. Zalotai, I. Szilágyi, T. Bérces and F. Márta (Budapest)
- C34 The thermal decomposition of acrylonitrile
E. Metcalfe, D. Booth, A. Harman, H. McAndrew (Newcastle Polytechnic) and
W. D. Woolley (Fire Research Station, Borehamwood)
- C35 Collision dynamics and the thermal rate coefficient for the reaction $O + OH \rightarrow O_2 + H$
J. A. Miller (Sandia)
- C36 A theoretical analysis of the photo-activated unimolecular dissociation of t-butyl
hydroperoxide
D. W. Chandler and J. A. Miller (Sandia)
- C37 Highly excited alkyl radicals produced by the addition of hot hydrogen atoms to alkenes
K. H. Al-Niami, P. L. Gould, K. A. Holbrook and G. A. Oldershaw (Hull)
- C38 Energy transfer dynamics and efficiency in reacting polyatomic molecules
E. Tzidoni and I. Oref (Technion Institute)
- C39 Rate coefficients of hydrogen abstraction reactions in the thermal decomposition of
azoethane and azoisopropane
A. Péter, G. Ács and P. Huhn (Szeged)
- C40 Rate constants for $H + C_2H_4$ and $H + C_2H_5$
P. D. Lightfoot, M. Brouard and M. J. Pilling (Oxford)
- C41 The pressure dependence of the rate constant for the $CH_3 + O_2$ reaction at 298 K
M. J. C. Smith, M. J. Pilling (Oxford) and K. D. Bayes (UCLA)
- C42 Decomposition of $B^2B_2 H_2O^+$ via conversion to lower lying electronic states
R. G. C. Blyth (Oxford), K. M. Johnson and I. Powis (Nottingham)
- C43 Direct measurement of unimolecular reaction rates for carbon-halogen bond cleavage
in IR MPD
D. M. Rayner and P. A. Hackett (NRC, Canada)
- C44 The onset of chaos in the classical motion of argon clusters
J. Santamaría (Complutense, Madrid)
- C45 Rotationally resolved competitive predissociation in SiH_2^+
M. C. Curtis, P. A. Jackson and P. J. Sarre (Nottingham)

iv

MONDAY 16 JULY

- C46 Time-dependent wave mechanical study of the wings in the Lyman - α absorption spectrum for $H + H_2$ collisions
P. M. Agrawal, V. Mohan and N. Sathyamurthy (Indian Institute of Technology)
- C47 HeH_2^+ - a case study in ab initio dynamics
T. Joseph and N. Sathyamurthy (Indian Institute of Technology)
- C48 DTBP-initiated reaction of 2-methylpropene: k_d/k_c ratios of some alkyl radicals
L. Seres and A. Nacs (Szeged)
- C49 Deductions from the master equation for chemical activation
N. Snider (Queens, Ontario)
- C50 Chemical reactions on clusters. The gas phase unimolecular decomposition of molecular ions in association with inert gas clusters
A. J. Stace (Sussex)
- C51 Reactive collision cross-sections from a quantal 3-D perturbation treatment
S. H. Suck Salk (Missouri-Rolla)
- C52 Nitrobenzene decomposition in a heated single pulse shock tube
W. Tsang and D. Robaugh (NBS)
- C53 On the collision energy dependence of the reaction cross-section. A microcanonical transition state model analysis
A. G. Ureña (Complutense, Madrid)
- C54 Infrared laser isotope separation in a van der Waals cluster beam
J. M. Zellweger, J - M. Philippoz, H. van den Bergh and R. Monot (Ecole Polytechnique, Lausanne)
- C55 Temperature jump measurements in gas kinetics
P. Gozel, B. Calpini and H. van den Bergh (Ecole Polytechnique, Lausanne)
- C56 Decomposition of 2, 3-dimethylbutane in the presence of O_2
R. R. Baldwin, G. R. Drewery and R. W. Walker (Hull)
- C57 Energy transfer from excited cyclooctatetraene produced by the thermal decomposition of cubane
H - D. Martin, T. Urbanek (Dusseldorf) and R. Walsh (Reading)
- C58 Metastable atomic reaction dynamics: angle resolved scattering, opacity functions and excitation functions for the interaction of $Xe (^3P_{2,0})$ with CH_3I , CH_3Br and CH_3Cl
J. P. Simons, K. Suzuki and C. Washington (Nottingham)
- 

TUESDAY 17 JULY

cont'd
SESSION III - HIGH VIBRATIONAL STATES -

- 09.00 - 09.45 D1 **Stimulated emission and quantum beat spectroscopy of formaldehyde and acetylene**
E. Abramson, H - L. Dai, R. W. Field, K. K. Innes, J. L. Kinsey, R. Sundberg and P. H. Vaccaro (MIT)
- 09.45 - 10.05 D2 **Vibrational mode specificity vs. vibrational mixing in small polyatomic molecules: SRL's of S_1 H_2CO**
E. C. Apel, Nancy L. Garland and E. K. C. Lee (Irvine)
- 10.05 - 10.25 D3 **Investigations of the nascent vibrational state of products from thermal dissociation reactions**
J. Buxton, R. Sohm and C. J. S. M. Simpson (Oxford)
- 10.25 - 10.45 D4 **Bimolecular reactions and energy transfer involving highly vibrationally excited molecules**
J. R. Barker (SRI), T. C. Brown and K. D. King (Adelaide)
- 10.45 - 11.15 Coffee

SESSION IV - COMPLEX REACTIONS

- cont'd
- 11.15 - 11.35 E1 **Reactions of the vinyl, butadienyl, and hexatrienyl radicals**
A. B. Callear and G. B. Smith (Cambridge)
- 11.35 - 11.55 E2 **Unimolecular rearrangements of organo-silicon intermediates**
I. M. T. Davidson, K. J. Hughes, S. Ijadi-Maghsoodi and R. J. Scampton (Leicester)
- 11.55 - 12.15 E3 **The reactions of O atoms with $(CH_3)_3SiH$ and $(CH_3)_3SiSi(CH_3)_3$**
H. Hoffmeyer, B. Reimann and P. Potzinger (MPI, Mülheim)
- 12.15 - 12.35 E4 **Kinetic studies of halomethane photo-oxidation**
F. Caralp, A. M. Dognon and R. Lesclaux (Bordeaux)
- 13.00 Lunch
- Vi

TUESDAY 17 JULY

SESSION V – COMPLEX REACTIONS II

- 14.15 - 14.35 F1 Excimer laser perturbation of methane-air flames: a novel method for studying high temperature radical reactions
M. S. Chou, A. M. Dean and D. Stern (Exxon)
- 14.35 - 14.55 F2 Oscillations, glow and ignition in carbon monoxide oxidation in an open system: experiments and interpretation of behaviour in a CSTR
P. Gray, J. F. Griffiths and S. K. Scott (Leeds)
- 14.55 - 15.15 F3 Sensitivity analysis techniques for estimation of reaction rate parameters and their uncertainties: evaluation of the rate constant and the branching ratio for the reaction of OH + H₂CO
R. A. Yetter, H. Rabitz (Princeton) and R. B. Klemm (Brookhaven National Laboratory)
- 15.15 - 15.35 F4 Sensitivity analysis of a methane oxidation mechanism
C - R. Yu and J - T. Hwang (Taiwan)
- 15.35 - 15.55 Tea *contd*

SESSION VI – MOLECULAR DISSOCIATION

- 15.55 - 16.40 G1 *V* **Vibrational predissociation in pristine environments: complete and precise product state distributions**
C. Wittig (Southern California)
- 16.40 - 17.00 G2 Predissociation dynamics of Rydberg states of H₂O (D₂O) and H₂S (D₂S)
M. N. R. Ashfold, J. M. Bayley, R. N. Dixon and J. D. Prince (Bristol)
- 17.00 - 17.20 G3 Quantum state selected photodissociation of H₂O and D₂O \tilde{C}^1B_1
A. Hodgson and J. P. Simons (Nottingham);
M. N. R. Ashfold, J. M. Bayley and R. N. Dixon (Bristol)

TUESDAY 17 JULY

17.20 - 17.40 G4 Photodissociation and intramolecular dynamics
M. Shapiro (Weizmann Institute)

17.40 - 18.00 G5 Photofragment spectroscopy of CH_3I
M. D. Barry and P. A. Gorry (Manchester)

18.30 Dinner

20.00 - 21.00 **POLANYI LECTURE** – Large Lecture Theatre,
Department of Chemistry
Old Problems Never Die
B. S. Rabinovitch (Washington)

21.00 University of Nottingham Wine Reception
at Hugh Stewart Hall

WEDNESDAY 18 JULY

09.00 - 09.45 HT **Dynamics of gas/surface reactions**
G. Ertl (Munich)

SESSION VII - KINETICS OF ATMOSPHERIC REACTIONS

09.45 - 10.30 H2 **Recent advances in hydrogen, sulphur, oxygen, nitrogen and halogen kinetics; their mechanistic and atmospheric implications**
J. G. Anderson (Harvard)

10.30 - 11.00 Coffee

11.00 - 11.20 H3 Rate parameters of radical-radical and radical-molecule reactions
F. Kaufman (Pittsburgh)

11.20 - 11.40 H4 Rate coefficient for the association reaction $\text{NO}_3 + \text{NO}_2 \xrightarrow{M} \text{N}_2\text{O}_5$ at low pressures
C. A. Smith, A. R. Ravishankara and P. H. Wine
(Georgia Institute of Technology)

11.40 - 12.00 H5 A FTIR spectroscopic study of the photo-oxidation of acetaldehyde in air
G. K. Moortgat and R. D. McQuigg (MPI, Mainz)

12.30 - 18.00 Excursions

19.00 Sherry at Hugh Stewart Hall

19.30 Conference Banquet at Hugh Stewart Hall

ix

THURSDAY 19 JULY

SESSION VIII - ELEMENTARY REACTIONS

- 09.00 - 09.45 I1 Kinetics of reactions of free radicals produced by infra-red multiple photon dissociation
G. Hancock (Oxford)
- 09.45 - 10.05 I2 Vibrational energy scrambling in infrared multiple photon dissociation of large molecules
S. Ruhman and Y. Haas (Jerusalem); J. Laukemper, M. Preuss, D. Feldmann and K. H. Welge (Bielefeld)
- 10.05 - 10.25 I3 State selected kinetic measurements of radical-molecule reactions in the 298-1300 K temperature range
S. L. Baughcum and R. C. Oldenberg (Los Alamos)
- 10.25 - 10.45 I4 LIF measurements of the bimolecular reactions of CN radicals
X. Li, N. Sayah and W. M. Jackson (Howard)
- 10.45 - 11.15 Coffee
- 11.15 - 11.35 I5 Studies of the reactions of alkyl and alkenyl radicals with molecular oxygen at elevated temperatures
D. Gutman (IIT)
- 11.35 - 11.55 I6 A direct measurement of the temperature and pressure dependence of the $H + CH_3$ reaction
M. Brouard, M. T. Macpherson, M. J. Pilling, J. M. Tulloch and A. P. Williamson (Oxford)
- 11.55 - 12.15 I7 Dynamical calculation of the $H + CH_3 \rightarrow CH_4$ bimolecular recombination rate constant
W. L. Hase and R. J. Duchovic (Wayne State)
- 13.00 Lunch

X

THURSDAY 19 JULY

SESSION IX – ELEMENTARY REACTIONS II

- 14.15 - 14.35 J1 Photoenhanced electron attachment processes in the gas phase
M. J. Rossi, H. P. Helm and D. C. Lorents (SRI)
- 14.35 - 14.55 J2 Slow unimolecular dissociation of polyatomic ions at near threshold energies
C. Lifshitz (Jerusalem)
- 14.55 - 15.15 J3 Collisional energy transfer in the very low-pressure pyrolysis of some tert-butyl halide systems
T. C. Brown and K. D. King (Adelaide) and R. G. Gilbert (Sydney)
- 15.15 - 15.35 J4 Quantitative intermolecular energy transfer efficiencies from thermal studies
C. D. Eley and H. M. Frey (Reading)
- 15.35 - 16.05 Tea
- 16.05 - 16.25 J5 LIF studies of methoxy and vinoxy radical reactions
B. Fritz, K. Lorenz, D. Rhäsa and R. Zellner (Göttingen)
- 16.25 - 16.45 J6 Termolecular reactions of the alkali elements Na and K with O₂ and OH at elevated temperatures determined by time-resolved spectroscopic methods
D. Husain, J. M. C. Plane and C. C. Xiang (Cambridge)
- 16.45 - 17.05 J7 Temperature and pressure dependence of the reaction of atomic chlorine with acetylene
L. J. Stief and J. Brunning (NASA)
- 17.05 - 17.25 J8 The pressure dependence of the recombination $2\text{NO}_2 \rightarrow \text{N}_2\text{O}_4$
P. Borrell (Keele), K. Luther and J. Troe (Göttingen)
- 18.30 Dinner
- 20.00 - 22.30 Poster Session II at Hugh Stewart Hall
(See list of poster titles below)
- 20.00 - 21.30 Informal Workshop – Association Reactions – at Hugh Stewart Hall
Chairman: R. A. Marcus (Caltech)

X i

THURSDAY 19 JULY

POSTER SESSION II (Hugh Stewart Hall)

- K1 Thermal reactions of ethylene induced by pulsed infrared laser radiation
L. Giroux, M. H. Back (Ottawa) and R. A. Back (NRC, Canada)
- K2 Comparison of the oxidation kinetics of acetone, methyl ethyl ketone and diethyl ketone
E. Le Roux, G. Scacchi and F. Baronnet (Nancy)
- K3 Unimolecular decomposition of methyl nitrite
L. Batt and P. H. Stewart (Aberdeen)
- K4 Unimolecular decomposition of the s-butoxy radical
L. Batt and M. McKay (Aberdeen)
- K5 Kinetic studies using a laser photolysis/atomic resonance absorption system. I Rate constants for $I^2P_{3/2}$ and $I^2P_{1/2} + F_2$ at room temperature
M. R. Berlan and D. P. Whitefield (McDonnell Douglas Research)
- K6 Pyrolysis of n-decane/steam mixtures in a high temperature micropilot furnace
F. Billaud and E. Freund (Nancy)
- K7 Model studies of atom and molecule diffusion on surfaces
S. C. Park and J. M. Bowman (IIT)
- K8 Kinetics and mechanism of the formation of alkyl nitro-compounds in flowing $H_2O_2 + NO_2 + N_2 + O_2$ + alkane vapour systems
D. L. Baulch, I. M. Campbell and J. M. Chappel (Leeds)
- K9 Study of the SO_2 influence on slow oxidation of hydrogen by a "semi-static" method
J. Chamboux, V. Viossat, F. Jorand and K. A. Sahetchian (Université P. et M. Curie)
- K10 Electronic branching ratio between $CN(A^2\Pi)$ and $CN(X^2\Sigma^+)$ produced from the reaction $C + N_2O \rightarrow CN + NO$ at 300 K
M. Costes, C. Naulin and G. Dorthe (Bordeaux)
- K11 $NO(B^2\Pi, A^2\Sigma^+)$ chemiluminescence from the reaction $C + NO_2 \rightarrow CO + NO$ at 300 K
G. Dorthe, J. Caille, Ph. Caubet and M. Costes (Bordeaux)
- K12 High temperature pyrolysis of 1,3-butadiene
R. J. Denning and R. Foon (New South Wales)
- K13 Multiphoton excitation of CS_2 with a narrow-band, tunable KrF laser
C. Fotakis, D. Zevgolts, P. Papagiannacopoulos and T. Efthimiopoulos (Crete)
- K14 Mobility of a platinum surface during the heterogeneous oxidation of carbon monoxide
A. K. Galwey (Belfast), J. F. Griffiths and S. M. Hasko (Leeds)
- K15 Photodissociation dynamics of cyanogen halides
S. Hay, F. Shokoohi, I. Nadler, H. Reisler and C. Wittig (Southern California)
- K16 A comparative study of the importance of different wall treatments on the decomposition of a dialkyl peroxide
A. Heiss, R. Rigny and K. A. Sahetchian (Université P. et M. Curie)
- K17 A crossed beam study of the collision induced dissociation of CS_2^+
D. M. Hirst, K. R. Jennings, J. A. Laramée and A. K. Shukla (Warwick)
- K18 The reaction of OH radicals with butadiyne
M. Bartels, P. Heinemann and K. Hoyer (Göttingen)
- K19 Study of a mechanism for the Fischer-Tropsch synthesis
Y. J. Lee, J. T. Hwang and K. J. Chao (Taiwan)

THURSDAY 19 JULY

- K20 Computational sensitivity study of oscillating chemical reaction systems – the overall temporal sensitivity behaviour of the Oregonator
J. - T. Hwang (Taiwan)
- K21 Kinetic modelling of high temperature, high pressure hydrocarbon oxidation in a well-stirred reactor
J. C. Boettner, M. Cathonnet, P. Dagaut, F. Gaillard, H. James and J. P. Rouan (CNRS, Orleans)
- K22 Kinetics of the addition reactions of $\text{Me}_2\text{Si} = \text{CH}_2$ with conjugated dienes
P. John, B. G. Gowenlock and P. Groome (Heriot-Watt)
- K23 Vibrational relaxation of XeX (B) ($\text{X} = \text{Br}, \text{I}, \text{Cl}$) by Ar
A. Kvaran, I. D. Sigurðadóttir (Iceland) and J. P. Simons (Nottingham)
- K24 Kinetics of the reactions of OH radicals with benzene, naphthalene and phenanthrene between 400 and 1000 K
K. Lorenz and R. Zellner (Göttingen)
- K25 Oscillatory continuum emission from I_2 and Br_2
M. MacDonald, K. P. Lawley, J. P. T. Wilkinson, R. J. Donovan (Edinburgh) and M. C. Gower (RAL)
- K26 Kinetics of the reaction $\text{O} + \text{ClO} \rightarrow \text{Cl} + \text{O}_2$
J. J. Margitan (JPL)
- K27 Non quasi-stationary state pyrolysis of ethane
S. Corbel, P. - M. Marquaire and G. - M. Côme (Nancy)
- K28 Detailed mechanism of neopentane pyrolysis around 700 C
P. Azay, P. M. Marquaire and G. - M. Côme (Nancy)
- K29 The thermal reaction of butene-2-cis in a stainless steel reactor or surface effects as a means to accelerate and orientate complex olefin reactions
C. Collongues, C. Richard and R. Martin (Nancy)
- K30 I. R. laser photo-oxidation of n-butane and carbon monoxide
J. Masanet, C. Lalo, F. Lempereur and J. Tardieu de Maleissye (Université P. et M. Curie)
- K31 Laser studies on the reaction of Mg with oxidants
B. Bourguignon, J. McCombie, J. Rostas and G. Taieb (Orsay)
- K32 Laser powered homogenous pyrolysis of nitroaromatics: the mechanism of homogeneous, gas phase decomposition of nitrotoluenes
D. F. McMillen, C. W. Larson, A. Gonzalez and D. M. Golden (SRI)
- K33 Pressure effects on some bimolecular reactions of the OH radical
L. T. Molina, M. J. Molina and R. Stachnik (JPL)
- K34 Spectrokinetic studies of HO_2 and OH involved in the chain reactions (2) $\text{H} + \text{O}_2 \rightarrow \text{HO}_2$; (3) $\text{H} + \text{HO}_2 \rightarrow 2\text{OH}$; and (4) $\text{OH} + \text{H}_2 \rightarrow \text{H} + \text{H}_2\text{O}$ under experimental conditions where (7) $\text{OH} + \text{HO}_2 \rightarrow \text{H}_2\text{O} + \text{O}_2$ is the predominant termination reaction for OH
J. Munk, O. J. Nielsen, A. Sillesen and P. Pagsberg (Rise)
- K35 The photophysics and photochemistry of NCNO
I. Nadler, M. Noble, J. Pfab, H. Reisler and C. Wittig (Southern California)
- K36 Temperature dependence of NH ($a^1\Delta$) reactions
J. W. Cox, H. H. Nelson and J. R. McDonald (NPL)
- K37 Classical trajectory calculations of the Br_2 - graphite surface scattering
G. Nyman and L. Holmlid (Göteborg)

XIII

THURSDAY 19 JULY

- K38 The reaction of methyl radicals with neopentane in flow photolysis at 607 - 823 K
H. Furue, K. C. Manthorne and P. D. Pacey (Dalhousie)
- K39 A study of the product states of the $\text{He}^+ + \text{CO}_2 \rightarrow \text{CO}^+ + \text{O} + \text{He}$ reaction
D. C. Parent, M. Chevrier, G. Mauclore, R. Marx (Orsay) and M. T. Bowers (Santa Barbara)
- K40 Absolute rate constants for the reaction of O (^3P) atoms with ethene, propene-d6, 1-butene, cis-2-butene, trans-2-butene and isobutene over the temperature range 260 - 860 K
R. A. Perry (Sandia)
- K41 A comprehensive study of the "wall effects" mechanism due to gas/surface reactions by use of high surface area particles
J. C. Petit, H. James (CNRS, Orleans)
- K42 Model calculations on the methane pyrolysis
M. H. Back (Ottawa), R. A. Back (NRC, Canada), J. M. Roscoe and M. J. Thompson (Acadia)
- K43 Laser induced fluorescence studies of the quenching kinetics of $\text{N}_2 \text{B}^3\Pi_g, v = 1 - 11$ and $\text{B}^3\Sigma_u^-, v = 4 - 6$
I. Bar, A. Rotem and S. Rosenwaks (Beer-Sheva)
- K44 Absolute rates of free radical reactions and their temperature dependence
N. Selamoglu, M. Rossi and D. M. Golden (SRI)
- K45 The reactivity of hydrogen and deuterium atoms trapped at a glass surface
G. McLeod and D. B. Sheen (Strathclyde)
- K46 Primary process in the photolysis of acetaldehyde
G. N. Bagnall and H. W. Sidebottom (University College, Dublin)
- K47 Reactions of polyaromatic molecules in gas and liquid phases
S. E. Stein (NBS, Washington)
- K48 Elementary reactions of the SO radical
J. Brunning and L. J. Stief (NASA)
- K49 Temperature dependence of O-atom reactions with olefins
R. Browarzik and F. Stuhl (Bochum)
- K50 Radiative lifetime and quenching of metastable NH ($b^1\Sigma^+$)
U. Blumenstein, F. Rohrer and F. Stuhl (Bochum)
- K51 The study of ion-molecule reactions in the gas phase using a triple quadrupole mass spectrometer
A. Mitchell, J. K. Conner and J. M. Tedder (St. Andrews)
- K52 Determination of the absolute rate constant for the reaction of OH with CO by cw uv-laser absorption at atmospheric conditions
A. Wahner (Bochum) and C. Zetzsch (Hannover)
- K53 OH internal state distributions from the reactions of O (^3P) with cyclic and aromatic hydrocarbons
N. J. Dutton, I. W. Fletcher and J. C. Whitehead (Manchester)
- K54 Visible chemiluminescence from the multiple collision reactions of F atoms with organic iodides
H. S. Braynis, D. Raybone and J. C. Whitehead (Manchester)

XIV

THURSDAY 19 JULY

- K55 A comprehensive mechanism for the oxidation of carbon monoxide
R. A. Yetter, F. L. Dryer and H. Rabitz (Princeton)
- K56 Evaluation of smog chamber experiments with dilution: rate constants for the reactions of OH with alkanes up to C₁₂
W. Behnke, F. Nolting and C. Zetzsch (Hannover)
- K57 A new theory for vibrational and rotational energy transfer in the collisions of symmetric top molecules with atoms
D. C. Clary (Cambridge)

FRIDAY 20 JULY

cont'd
SESSION X - STATE SELECTION -

- 09.00 - 09.45 L1 **Photodissociation dynamics of small cluster ions** (AW)
M. T. Bowers (Santa Barbara)
- 09.45 - 10.05 L2 Mode specificity in the reaction $C_2H_4^+ (v_2, v_4) + C_2H_4 \rightarrow C_3H_5^+ + CH_3$
K. Tanaka, T. Kato and I. Koyano (Okazaki)
- 10.05 - 10.25 L3 Comparison of the energy partitioning in charge transfer reactions of Ar^+ and N_2^+
**R. Marx, G. Mauclaire, R. Derai, D. C. Parent (Orsay);
A. O'Keefe and M. T. Bowers (Santa Barbara)**
- 10.25 - 10.45 L4 Product state distributions of thermal energy ion-molecule reactions
S. R. Leone (JILA, Boulder)
- 10.45 - 11.15 Coffee
- 11.15 - 11.35 L5 Spectroscopy and quenching behaviour of some excited states of iodine monobromide
**J. P. T. Wilkinson, M. A. Macdonald and
R. J. Donovan (Edinburgh)**
- 11.35 - 11.55 L6 Energy partitioning in the reaction of F atoms with formyl radicals
D. J. Donaldson and J. J. Sloan (NRC, Canada)
- 11.55 - 12.15 L7 Molecular beam studies of the interactions of P state atoms
V. Aquilanti (Perugia)
- 12.15 - 12.35 L8 The reaction and relaxation of vibrationally excited OH and OD with other radical species
M. J. Howard, I. W. M. Smith and M. D. Williams (Cambridge)
- 13.00 Lunch

CONFERENCE CLOSES
XVI

Transition states and trapped trajectoriesM.S. Child (University of Oxford)

It will be shown how the properties of trapped periodic trajectories or periodic orbit dividing surfaces (PODS) on collinear model potential surfaces can be used (a) to test the strengths and limitations of transition state theory (b) to determine the adiabatic translational kinetic energy thresholds for different reactant internal states and (c) to predict the energies of resonant features in the reaction probability.

The first argument, relevant to the occurrence of a single trapped trajectory, is that the path of this trajectory defines the exact transition state. Its periodic nature ensures that scattering trajectories will either fail to reach it or, having once crossed it, proceed to reaction. The beauty of this procedure is that the trajectory itself draws out the dividing surface between reactants and products which can otherwise be obtained only approximately, as in variational transition state theory. One must remember however that the variational method is more readily applied to true three-dimensional situations.

The second important point is that the single transition state regime typically gives way at energies greater than 0.1 - 0.2 eV above the reaction threshold, to normally three alternating 'repulsive' and 'attractive' trapped trajectories. The outer two, which are repulsive, constitute flux bottlenecks. The crossing of one by no means guarantees the crossing of the other. Hence any estimate of reaction probability based on a single transition state, whether variational or exact, may be seriously inaccurate. Three trapped trajectories each carry with them knowledge of associated fluxes, say F_1 and F_2 for the

repulsive PODS and F_x for the attractive one from which a strict lower bound on the microcanonical reactive flux F_r may be obtained

$$F_L = F_1 + F_2 - F_x,$$

while the larger of F_1 and F_2 gives by the variational argument a strict upper bound F_u . Test calculations for $H + H_2$, $F + H_2$ and $H + Cl_2$ confirm that $F_u > F_r > F_L$ with F_r normally much better estimated by F_L than by F_u .

The bottleneck character of the repulsive PODS closest to reactants may also be used to establish the adiabatic reaction thresholds for classical reactivity from the v th internal reaction state as the energy at which $F_i = (v + \frac{1}{2})h$. Calculations made on this basis account for a marked reduction in the activation barrier for $F + H_2(v = 1)$ compared with $F + H_2(v = 0)$, and for the relative success of reverse over forward quasiclassical simulations for $F + H_2(v = 0) \rightarrow HF(v = 3) + H$.

Finally the flux for a different type of 'resonant' trapped trajectory has proved to have remarkable predictive powers in relation to the positions of resonances in the reaction probability

DYNAMICS OF CENTRIFUGAL BARRIER COMPLEXES CLOSE TO ORBITING

Kjell Rynefors and Nikola Marković
 Department of Physical Chemistry, University of Göteborg
 and Chalmers University of Technology
 S-412 96 GÖTEBORG, Sweden

Trajectories close to orbiting have been studied for central and several noncentral potentials in atom-molecule reactions. The complex formation of $K + NaCl$ is considered as a prototype process. The potential consists of a harmonic oscillator and a long range dipole-induced dipole term, where the noncentral form depends on two parameters A and Δ . During the trajectory different quantities were followed. These included position R_m of the centrifugal barrier, distance R_c between the atom and the center of mass of the molecule, rotational L_{rot} and orbital L_{orb} angular momenta, rotational ϵ_r^+ and vibrational ϵ_v^+ energies of the diatomic molecule and centrifugal E_c and radial translational ϵ_t^+ energies.

To minimize Coriolis effects the minimum of the effective potential of the rotating harmonic oscillator was chosen as one of the initial conditions. The initial value of L_{orb} was chosen to give a value of ϵ_t^+ close to 0. All trajectories in this study were initiated close to an orbiting situation. An iterative procedure, with rapid convergence for finding this distance, has been developed.

In fig. 1 distances R_m and R_c are given for a strongly non-central potential and with the initial value of ϵ_r^+ equal to $4.5 \times E_B$. In fig. 2 the time development of L_{orb} , L_{rot} , E_c and ϵ_r^+ are given for the same trajectory. It is seen that these quantities show considerable variations. Despite the influence of strongly perturbing factors the trajectory remains close to orbiting for at least 360° .

From the present trajectory study, the following conclusions can be drawn.

1. The stability of nearly orbiting trajectories are not strongly influenced by the detailed form of the potential energy surface or the magnitude of the rotational energy.

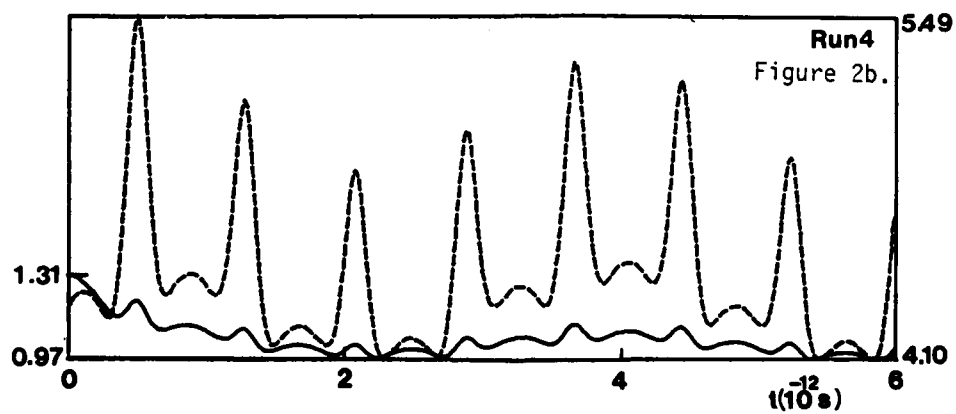
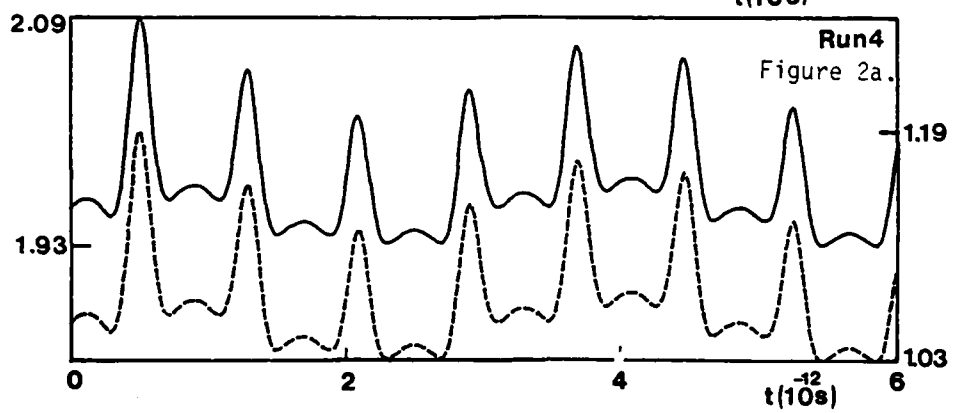
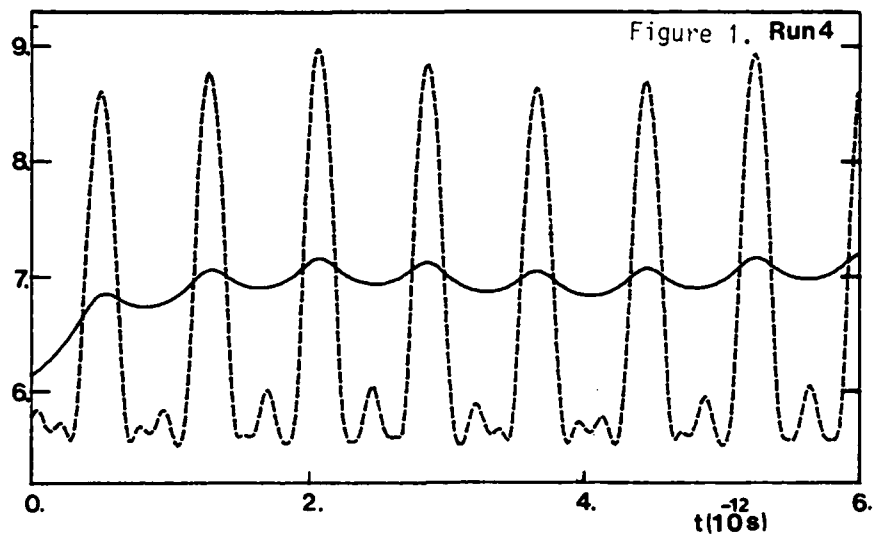
2. The detailed form of the noncentral potential has profound impact on the orbiting trajectory path, including the frequency of the oscillation.
3. For a physically realistic potential the distance R_c can vary up to 10% during a complete molecular rotation for low values of ϵ_r^+ . For increasing ϵ_r^+ the inner turning points increase until they converge with the outer turning points.
4. At low rotational energies distance R_c , angular momenta and rotational energies show very regular variations. At higher rotational energies the variations are less regular due to Coriolis effects.
5. The nearly orbiting trajectories, investigated in this paper, are closely analogous to trapped trajectories, which has been extensively investigated for binary processes.

FIGURE CAPTIONS

Fig. 1. Time dependence of separation distance R_c , solid curve, and barrier position R_m , broken curve, in units of \AA .

Fig. 2(a). Time dependence of L_{orb} , solid curve and left scale, and L_{rot} , dotted curve and right scale, in units of 10^{-32} Js .

(b). Time dependence of E_c , solid curve and left scale, and ϵ_r^+ , broken curve, right scale, in units of 10^{-20} J .



AN ADIABATIC THEORY OF CHEMICAL REACTIONS*

Vladimir Z. Kresin and William A. Lester, Jr.⁺
Materials and Molecular Research Division
Lawrence Berkeley Laboratory
University of California
Berkeley, California 94720

In this theory a chemical reaction is treated as a quantum transition from reactants to products. It leads to a Franck-Condon-like factor for the evaluation of production energy distributions. A specific adiabatic method is used to describe the dynamics of nuclear motion. The theory is applied to the reactions: $\text{HO} + \text{D} \rightarrow \text{H} + \text{OD}$ and $\text{ClI} + \text{D} \rightarrow \text{Cl} + \text{ID}$.

*This work was supported by the Director, Office of Energy Research, Office of Basic Energy Sciences, Chemical Sciences Division of the U. S. Department of Energy under Contract No. DE-AC03-76SF00098.

⁺Also, Department of Chemistry, University of California, Berkeley, California 94720.

Vinylidene: Potential Energy Surface and
Unimolecular Reaction Dynamics

William H. Miller

Department of Chemistry, and Materials and Molecular Research Division,
of the Lawrence Berkeley Laboratory, University of California,
Berkeley, California 94720

Abstract

New quantum chemistry calculations (with a triple zeta plus polarization basis set, and a single and double configuration interaction) have been carried out to determine the equilibrium points and the transition state for the vinylidene ($\text{H}_2\text{C}=\text{C}:$) \rightarrow acetylene ($\text{HC}\equiv\text{CH}$) isomerization. A classical barrier height (i.e., with no zero point energy effects) of 6.3 kcal/mole is obtained, and application of the Davidson correction for unlinked clusters reduce this to 5.4 kcal/mole. Our best estimate is that the true classical barrier lies in the range 2-4 kcal/mole. The dynamics of the vinylidene/acetylene isomerization has been described within the framework of the reaction path Hamiltonian. The lifetime of vinylidene (in its ground vibrational state) with respect to this process is calculated to be 0.24 to 4.6 psec for a classical barrier of 2 to 4 kcal/mole. This lifetime decreases by a factor of ~ 2 if one quantum of the CH_2 scissors mode of vinylidene is excited, but is predicted to increase somewhat if a quantum of the C-C stretch is excited. These results are all consistent with the recent experimental observation of vinylidene via photodetachment of C_2H_2^- .

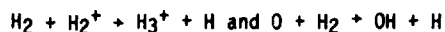
Calculations on the rates of neutral reactions dominated
by long-range intermolecular forces

D.C. Clary,
University Chemical Laboratory,
Lensfield Road,
Cambridge, CB2 1EW.

A series of calculations of rate constants have been performed for a variety of chemical reactions that have no barriers to reaction in the potential energy surface, and have reaction rate constants that are determined by long-range intermolecular forces. Two types of methods have been used. In the first, more accurate, approach¹ quantum-mechanical close-coupled equations are solved over the region of the entrance channel of the reaction which determines the reaction cross section. In the second, more approximate, approach the maximum value of the total angular momentum required for reaction to occur is determined from adiabatic potential energy curves labelled by the initial (V j) state, and obtained by application of the centrifugal sudden approximation. This yields a "capture" cross section for the reaction.

The two theories have been applied to the $O+OH \rightarrow O_2 + H$ reaction, and the calculated reaction cross sections compare very well. The more approximate method has been used in calculations on the reactions $NO + ClO$, $NO + BrO$, $SO + OH$, $CH + O_2$ and $CN + O_2$, which have dipole-dipole and dipole-quadrupole terms in the intermolecular potential. The overall rate constant for all these reactions is found to decrease with increasing temperature. However, the rate constants for fixed initial rotational j states increase with increasing temperature, but decrease strongly with increasing initial j for a given temperature. Thus it is the Boltzmann average of j states that produces the negative temperature dependence in the overall rate constants for reactions such as these.

¹ D.C. Clary, Molec.Phys., 1982, 48, 619.

Theoretical Studies of State to State Kinetics in $\text{H} + \text{H}_2\text{O} \rightarrow \text{OH} + \text{H}_2$,

George C. Schatz

Department of Chemistry, Northwestern University,
Evanston, IL 60201 USA

There are a growing number of bimolecular gas phase reactions for which theoretical methods may be used to calculate rate constants or cross sections at a level of accuracy which approaches (and at a level of detail which surpasses) that obtainable from experimental measurements. This paper describes three reactions which we have recently studied which fall into this category.

The reaction $\text{H} + \text{H}_2\text{O} \rightarrow \text{OH} + \text{H}_2$ and its reverse are reactions of significant interest in combustion and in state to state chemistry. The thermal rate constant is well known, and recently Wolfrum and Kleinermauns have measured the rate of formation of specific OH vibration/rotation states in hot $\text{H} + \text{H}_2\text{O}$ collisions (1). We have studied this system from several points of view (2) using the quasiclassical trajectory method and an analytical fit to an accurate ab initio surface. Our calculated thermal rate constants for both forward and reverse reactions are in good agreement with experiment, as are reagent state resolved rate constants for $\text{OH} + \text{H}_2$. Recently we have combined the quasiclassical trajectory procedure with methods for determining the semiclassical eigenstates of polyatomic molecules to study the state to state chemistry of $\text{H} + \text{H}_2\text{O}$. We find that excitation of any of the three H_2O vibrational modes leads to substantial rate constant enhancements, with the enhancement larger for symmetric stretch excitation than for comparable amounts

of asymmetric stretch excitation. We also find that the OH product in hot $H + H_2O$ is relatively cold in both its rotational and vibrational distributions. This agrees with the results of Ref. 1, and we further find that most of the energy available to the products ends up as relative translation, with a surprising amount also going to H_2 rotation.

We have also used trajectories to study the reaction $H_2^+ + H_2 \rightarrow H_3^+ + H$, with special emphasis on the state to state dynamics, and on the competition between (electronically adiabatic) charge transfer and reaction. The surface used for these studies is a diatomics in molecules (DIM) potential surface. The application of classical methods to the determination of the product H_3^+ vibration/rotation distributions has proved to be a real challenge because of the very high amounts of excitation resulting from this highly exoergic reaction. Recently we have discovered a method for quantizing the H_3^+ product states which uses fast Fourier methods to determine vibrational and rotational action variables from the normal coordinate power spectra (3). With this method we have determined that the dominant H_3^+ vibrational excitation is in the degenerate bend/asymmetric stretch modes, with lesser amounts in the symmetric stretch. We have also calculated total reaction cross sections, and find good correspondence with recent molecular beam results.

The reaction $O + H_2 \rightarrow OH + H$ is sufficiently simple that quantum mechanical methods can be used to calculate cross sections and rate constants. Recently we have developed a very accurate method for doing this based on coupled channel distorted wave theory. In applications to $H + H_2$, we found that this method gives cross sections which are exact as long as the reaction

proceeds mainly via tunnelling. We have now used this method to calculate rate constants for $O + H_2$, $O + D_2$, $O + HD$ and $O + DH$ using a LEPS surface. The resulting cross sections appear for all four systems to be accurate up to at least 0.5 eV translational energy. For $O + H_2$ in the 0.35 - 0.50 eV range where the classical trajectory cross section is nonzero and where quantum results are accurate, there is good agreement between the two. Tunneling plays an important role in the dynamics, however, and thus we find that the quantum rate constant is well above the classical value (factor of 2.5) at 300 K. Our applications to $O + D_2$, $O + HD$ and $O + DH$ emphasize the role of tunnelling in the low temperature isotope effects. The branching ratio between HD and DH shows strong sensitivity to reagent rotation, and to the different endoergicities of the different branches.

1. J. Wolfrum and K. Kleinermanns, Appl. Phys. B., in press.
2. (a) G.C. Schatz, J. Chem. Phys. 74, 1133 (1981);
 (b) G.C. Schatz, M.C. Colton and J.L. Grant, J. Phys. Chem., in press.
3. (a) C.W. Eaker, G.C. Schatz, N. DeLeon and E.J. Heller, to be published.
 (b) C.W. Eaker and G.C. Schatz, J. Chem. Phys., in press.
4. G.C. Schatz, L.M. Hubbard, P.S. Dardi and W.H. Miller, J. Chem. Phys., in press.

Photolysis Quantum Yields and Recombination Rate Coefficients
in Highly Compressed Gases and Liquids

J. Troe and J. Schroeder

Institut für Physikalische Chemie der Universität Göttingen
Tammannstraße 6, D-3400 Göttingen, Germany

In two recent articles we have described experimental investigations of photolysis quantum yields and atom recombination rate coefficients over very large ranges of "solvent" gas and liquid phase densities: Experiments with iodine¹⁾ were performed in the gas phase up to 1 kbar, in the liquid phase up to 5 kbar, experiments with bromine²⁾ were extended in the gas phase up to 7 kbar. These experiments reveal a complicated transition from low pressure gas phase into diffusion controlled liquid phase reaction behaviour. Since extensive theoretical calculations on these reactions are available, a comparison may be used as a test of our understanding of elementary reactive processes in dense environments.

Although many-body trajectory calculations under some conditions do reproduce the experiments quite well³⁾, the details of the complicated transition behaviour have not yet been demonstrated in theory. The present talk discusses a number of much simpler, intuitive models to "explain" the experimental observations. We separate a "cluster-mechanism" from

a model with competing diffusion out of a cage and energy relaxation in a cage. Whereas the "cluster mechanism" is characterized by marked wavelength dependences of quantum yields, in the "energy relaxation-diffusion mechanism" so far no such dependence was noticed indicating negligible primary cage break-out during photolysis at high densities. The density dependences of quantum yields and atom recombination rates generally showed an internally consistent behaviour.

-
- 1) B. Otto, J. Schroeder, and J. Troe, J. Chem. Phys.,
in the press.
 - 2) H. Hippler, V. Schubert, and J. Troe, J. Chem. Phys.,
in press.
 - 3) see, e. g., A. H. Lipkus, F. P. Buff, and M. G. Sceats,
J. Chem. Phys. 79, 4830 (1983).

NOTES

UNDERSTANDING RATE DATA FOR ELEMENTARY PROCESSES

David M. Golden
Department of Chemical Kinetics
SRI International
Menlo Park, CA 94025

This paper is presented from the viewpoint of the researcher who is motivated by the application of basic scientific understanding to the solution of practical problems. For the gas phase kineticist these problems have involved the chemistry of the atmosphere such as photochemical smog, stratospheric ozone balance and problems of ionic chemistry even as remote as interstellar cloud formation. Also receiving much attention has been the chemistry involved in combustion science. Various fuel-oxidizer systems in flames, as well as the problems associated with propellant and explosive uses have been dealt with extensively. (For purposes of this presentation only gas-phase processes will be considered.)

Understanding the types of complex systems mentioned above requires a chemical mechanism with rate constants assigned as functions of temperature and pressure (and colliding partners). This mechanism is then evaluated with an appropriate computer code to calculate concentration-time profiles of individual species and any other system observables that depend on them. Such a model combined with an appropriate sensitivity analysis will reveal those elementary rate steps for which experimental values are needed. Both the assignment of mechanism and of rate constant values necessitates a global view of chemical kinetics.

For sake of discussion it is convenient to divide all elementary processes into bimolecular and unimolecular reactions. It is then instructive to consider unimolecular processes according to whether only one simple

reaction is possible over the range of conditions of interest or whether multiple pathways must be considered. The intimate interaction of the problems of energy transfer and chemistry are best addressed here.

Bimolecular reactions can be subdivided also. The simple metathesis reaction is most well understood, but a surprising number of kinetic data compilations avoid the critical analysis of reported values that could be based on this understanding. Radical-radical disproportionation reactions are a type of metathesis reaction that may not be so well understood however.

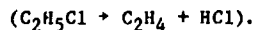
All other bimolecular reactions are really unimolecular reactions in disguise. Simple association reactions are the reverse of unimolecular dissociations and are subject to the same pressure and temperature dependences. Bimolecular reactions that proceed via a bound intermediate may be considered from the point of view of the multipath unimolecular process mentioned earlier.

Ion molecule interactions will be discussed within the same framework. It seems that an entire redundant theoretical literature has been developed in the community that studies ion-molecule interactions. This is particularly true with respect to association reactions where the "wheel" of thermal unimolecular reaction rate theory has been rediscovered by some workers.

Specific examples to be discussed are:

Unimolecular reactions:

One path-molecular dissociation-tight transition state



One path-bond scission-loose transition state

$(C_2H_6 \rightarrow CH_3 + CH_3; PhNO_2 \rightarrow Ph + NO_2; M(CO)_x \rightarrow M(CO)_{x-1} + CO, M \text{ is } Fe(x=5), Mo(x=6), W(x=6), Cr(x=6)).$

Two paths—one tight and one loose

$(HNNO \rightarrow NNOH \rightarrow N_2 + OH; HNNO \rightarrow NH + NO).$

Bimolecular reactions:

Simple metathesis $(O + NH_3 \rightarrow OH + NH_2).$

Radical disproportionation $(C_2H_5 + C_2H_5 \rightarrow C_2H_6 + C_2H_4).$

Simple association $(N_2^+ + N_2 \rightarrow N_4^+; CH_3^+ + H_2 \rightarrow CH_5^+;$

$M + O_2 \rightarrow MO_2, M \text{ is } Li, Na, K).$

Reaction via bound intermediate $(H + N_2O \rightarrow N_2 + OH; H + N_2O \rightarrow NH + NO;$

$HO_2 + HO_2 \rightarrow H_2O_2 + O_2).$

Calculation of the Thermodynamics of Molecular Reactions
Using the BAC-MP4 Method:
Reactions of OH with C₂H₂, C₂H₄ and HCN*

C. F. Melius, J. S. Binkley and M. L. Koszykowski
Sandia National Laboratories
Livermore, CA 94550

The understanding of molecular reactions requires knowledge of the energetics of the reaction mechanisms including the thermodynamic stabilities of the reactants, products and various intermediate complexes which can be formed during the reaction. Also of importance in describing chemical reactions is the topology of the reaction pathway, particularly the activation energy of the transition state along the reaction coordinate.

In order to study these problems theoretically, we have developed a new quantum chemical method (BAC-MP4) which can provide accurate heats of formation for H, C, N and O containing species. In particular, we have used this method to calculate heats of formation for radical species and unstable molecular complexes which are important in combustion systems. The thermochemical properties of many of these species have not been determined accurately by experimental means. In order to provide activation energies for reactions, we have recently extended this method to the calculation of heats of formation of transition state species.

The BAC-MP4 method involves the use of Hartree-Fock theory with a split-valence plus polarization basis set to determine the equilibrium geometry and zero-point vibrational energy of a given molecule. Determination of the zero-point energy is accomplished by calculation of the vibrational frequencies within the harmonic approximation. This information also serves to characterize the nature of the geometry (i.e. minimum or transition state structure). Using the geometry determined at the Hartree-Fock level, we calculate the total energy with fourth-order Møller-Plesset perturbation theory (MP4), which includes electron correlation beyond that of Hartree-Fock.

While the MP4 method represents one of the most sophisticated methods for calculating total energies of molecules of the type considered here, there are still limitations in the calculated energies. The principle deficiencies in calculations of this nature arise from basis set limitations and truncation of the wavefunction expansion. Thus, calculated bond dissociation energies, from which heats of formation are derived, are systematically underestimated.

These errors form a consistent trend which can be compensated for in a bond-wise additive manner. We therefore have developed Bond-Additivity-Corrections (BAC) which are added to the theoretically calculated energies. The BAC parameters were determined by a least-squares fit to ~50 stable molecules whose heats of formation have been fairly well established experimentally. The resulting BAC bond energies agree, on the average, to within one kcal/mole of the corresponding experimental values. The maximum energy difference obtained in this manner is less than three kcal/mole. For open shell species, additional energy corrections are included to compensate for contamination in the MP4 electronic wavefunction from states of higher spin multiplicity.

In Table 1 we present our calculated heats of formation (at 0 K) for molecular species which are of interest in combustion processes. Where available, experimental values are presented for comparison. Even for the unstable and radical species the agreement between the experimental and calculated values is very good. One advantage of using the BAC-MP4 method for determining thermochemical properties is that all the calculations are done in a consistent manner. Thus, BAC-MP4 provides a reliable approach for calculating accurate heats of formation of unstable or transient molecular species which would be difficult (or impossible) to determine experimentally.

The BAC-MP4 method is not limited to the study of minimum energy species and we have recently extended it to the calculation of transition state energies. We have applied this method to the reactions of OH with acetylene, ethylene and hydrogen cyanide. A representative potential energy diagram for the reaction of OH with C_2H_4 is shown in Figure 1. The energetics of the important intermediate and transition state species which are involved in addition, rearrangement, and elimination reactions have been investigated and compared with the direct hydrogen abstraction mechanism. We find that the activation energy for addition is generally less than that for rearrangement or for hydrogen abstraction. Thus, at low temperatures, the adduct can be formed but will not rearrange to form other products. At higher temperatures, hydrogen abstraction is found to be the dominant process.

*This work was supported by the U. S. Department of Energy.

Table 1. Calculated heats of formation ΔH_f° at 0 K for various molecular species using the BAC-MP4 method compared with experimental values (energy in kcal/mole).

Stable Molecules								
Molecule	Theor.	Exp.	Molecule	Theor.	Exp.	Molecule	Theor.	Exp.
CH ₄	-16.0	-16.0	CH ₃ CCH	45.2	45.9	CH ₂ (OH) ₂	-88.5	-89.9
NH ₃	-9.3	-9.3	Cyclopropene	68.4	68.0	HN ₃	72.7	72.0
H ₂ O	-57.1	-57.1	CH ₃ CHCH ₂	9.0	8.7	N ₂ O	20.0	20.4
C ₂ H ₂	55.0	54.3	Cyclopropane	16.5	16.6	NO ₂	7.2	8.6
C ₂ H ₄	15.1	14.6	CH ₃ CH ₂ CH ₃	-19.5	-19.2	HONO(CIS)	-18.4	-16.9
C ₂ H ₆	-16.4	-16.3	Ethylenimine	34.1	33.2	HONO(TRANS)	-17.0	-17.4
HCN	33.4	32.4	CH ₃ NHCH ₃	1.9	1.1	C ₂ H ₅ CHO	-38.9	-41.2
CH ₃ NH ₂	-1.3	-1.7	C ₂ H ₅ NH ₂	-6.6	-5.4	(CN) ₂	73.6	73.4
CO	-30.0	-27.2	CH ₃ CH ₂ OH	-51.4	-51.5	CH ₃ COCH ₃	-47.1	-48.0
H ₂ CO	-24.7	-25.0	H ₂ CCO	-12.5	-14.0	(CHO) ₂	-49.5	-48.7
CH ₃ OH	-44.9	-45.3	CH ₃ CHO	-36.4	-36.9	CH ₃ COOH	-99.9	-100.6
N ₂	1.4	0.0	Oxirane	-9.5	-9.6	CH ₃ NO ₂	-15.1	-14.3
H ₂ NNH ₂	25.1	26.2	CH ₃ OCH ₃	-38.6	-39.4	CH ₃ ONO	-10.1	-11.7
NO	21.1	21.4	CH ₃ NNH ₂	26.0	25.8	HONO ₂	-29.0	-29.9
HNO	26.7	24.5	NH ₂ CHO	-43.9	-41.7	CH ₃ CN	21.0	22.7
O ₂	-0.6	0.0	CO ₂	-92.7	-94.0	HNCO	-25.8	-23.6
H ₂ O ₂	-31.0	-31.1	HCOOH	-89.3	-88.8	CH ₃ NO	20.8	18.0
CH ₃ CCH ₂	46.5	47.8	CH ₃ OOH	-26.7	-27.7	HCOOCH ₃	-82.9	-80.0
HCCCH	105.0	112.9	CH ₃ CHCCH	70.7	74.6	CH ₃ CHCHCH ₂	30.9	30.0
CH ₃ CCCH ₃	36.1	38.2	CH ₃ CH ₂ CCH	42.5	43.0	Cyclobutene	44.4	34.2
Cyclobutane	14.1	12.4	n-Butane	-22.7	-23.1	iso-Butane	-24.3	-25.0
CH ₃ CHCHCH ₃	2.8	2.5	CH ₃ CH ₂ CHCH ₂	6.6	5.4	C ₆ H ₆	20.7	24.2
Radicals and Other Unstable Molecules								
Molecule	Theor.	Exp.	Molecule	Theor.	Exp.	Molecule	Theor.	Exp.
CH ₂	92.9	92.9	HCO	9.9	8.9	(CH ₃)CH	26.6	24.2
CH ₃	35.8	35.6	H ₂ CO	10.2	5.4	CH ₂ CHCH	43.4	41.9
NH	87.5	90.0	CH ₂ OH	-1.6	-4.3	HNNH	49.7	52.6
NH ₂	47.2	46.2	CCO	89.8	89.0	CH ₃ CH ₂ O	4.6	-0.3
OH	9.7	9.3	³ CO	112.9	112.0	H ₂ CNN	65.1	71.0
C ₂ H	130.0	127.0	³ HNO	46.6	43.5	HO ₂	4.5	1.2
C ₂ H ₃	72.2	70.5	H ₂ CNH	48.6	47.5	H ₂ NOH	-9.5	-6.3
C ₂ H ₅	32.6	31.3	H ₂ CNH ₂	39.4	36.0	CH ₃ OO	8.3	9.3
CN	101.9	103.2						

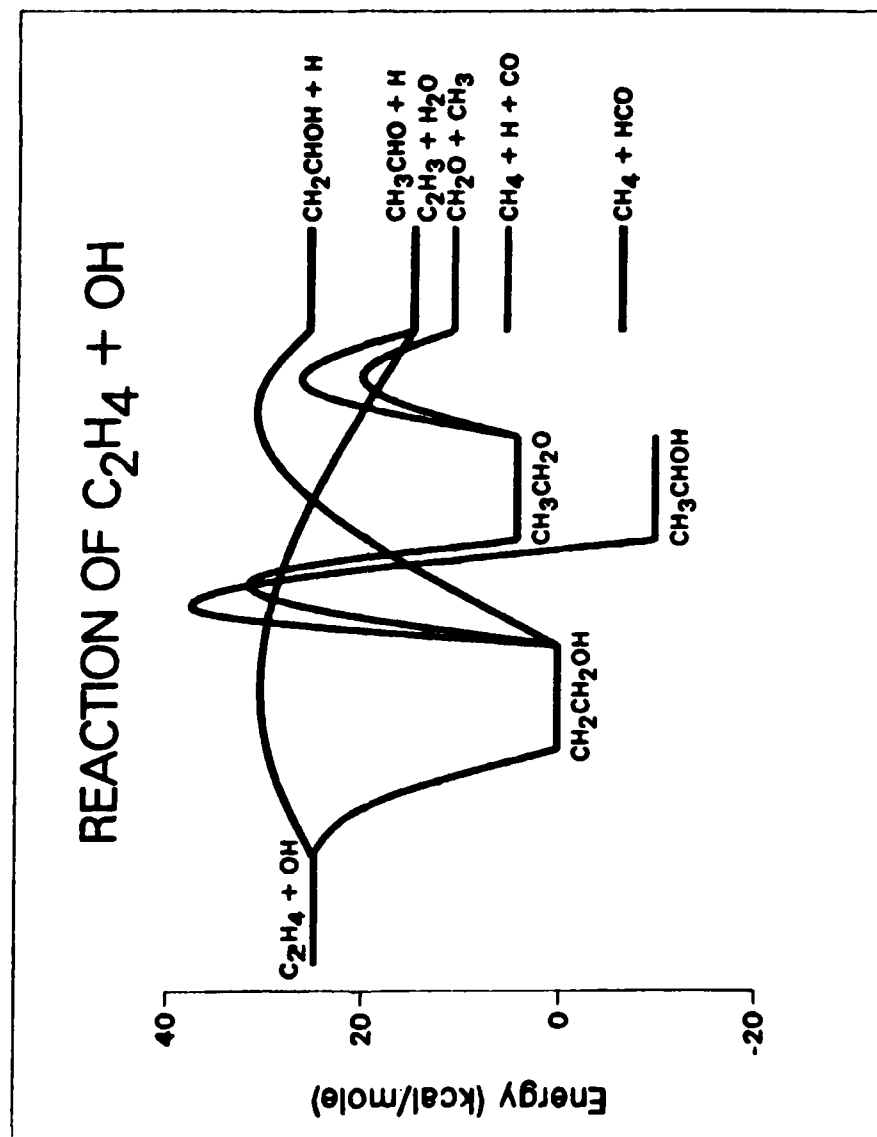


Fig. 1. Calculated reaction pathways for the reaction of $C_2H_4 + OH \rightarrow$ Products, based on BAC-MP4 heats of formation for stable and transition structure species.

KINETIC STUDIES OF OH-ALKENE REACTIONS

Frank P. Tully and John E. M. Goldsmith

Sandia National Laboratories

Livermore, CA 94550

U.S.A.

Detailed kinetic studies of the reactions between hydroxyl radicals and alkenes are in progress. The experiments are performed with a pulsed-laser photolysis/cw laser-induced fluorescence technique. OH radicals are formed by 193-nm photolysis of N_2O in N_2O/H_2O /alkene/helium gas mixtures, followed by the rapid reaction of the resulting $O(^1D)$ with H_2O . Time-resolved OH concentration profiles are measured as functions of alkene number density by laser-induced fluorescence. Excitation of the OH $A \leftarrow X$ $R_1(3)$ transition at 307 nm is accomplished with an intracavity frequency-doubled, single-mode, ring dye laser. Use of this diffraction-limited, narrowband excitation source ensures high signal/scattered light ratios and thus very precise OH concentration profile measurements.

In the reactions of OH with ethylene and propylene, both OH addition and H-atom abstraction reaction channels are observed. Our current results for the OH + propylene reaction are plotted in Arrhenius form in Fig. 1. At temperatures below 440 K, exponential $[OH]$ decay profiles are measured, as expected when operating under pseudo-first order kinetic conditions. At these temperatures, the reaction mechanism is dominated by electrophilic addition of OH to the propylene double bond, and the product adduct is stable with respect to decomposition back to reactants throughout the time scale of the experiment. No difference in reactivity is observed for C_3H_6

and C_3D_6 , demonstrating the lack of importance of H(D)-atom abstraction processes in the low-temperature mechanism.

The measured $[OH]$ profiles are complex between 440 K and 700 K, decaying quickly initially and then disappearing more slowly at longer times, as shown in Fig. 2. These profiles may be explained by OH reformation upon decomposition of the thermalized adduct HOC_3H_6 (HOC_3D_6) back to reactants during the time scale of the experiment. Correcting for molecular diffusion out of the observation volume (triangles in Fig. 2), $[OH]$ attains its constant chemical equilibrium concentration. The $[OH]$ profiles measured in this intermediate regime are being modelled and separation of the various reaction processes is in progress.

Above 700 K, adduct decomposition back to reactants becomes very fast and the addition channel effectively closes. At these temperatures, the diffusion-corrected $[OH]$ decays are again exponential, and the rate coefficients increase as the temperature is raised. H(D)-atom abstraction reaction channels dominate above 700 K, and the expected kinetic isotope effects are observed.

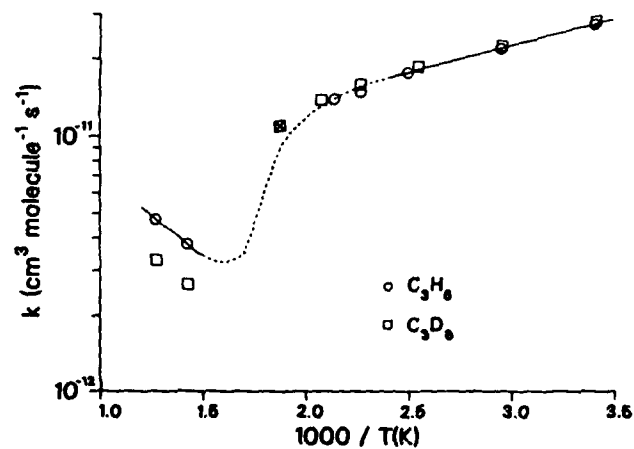


Fig. 1. Arrhenius plot for the reaction $\text{OH} + \text{C}_3\text{H}_6(\text{C}_3\text{D}_6) \rightarrow \text{products}$. The dashed curve represents the trend in the net reactivity through the region of complex OH decays.

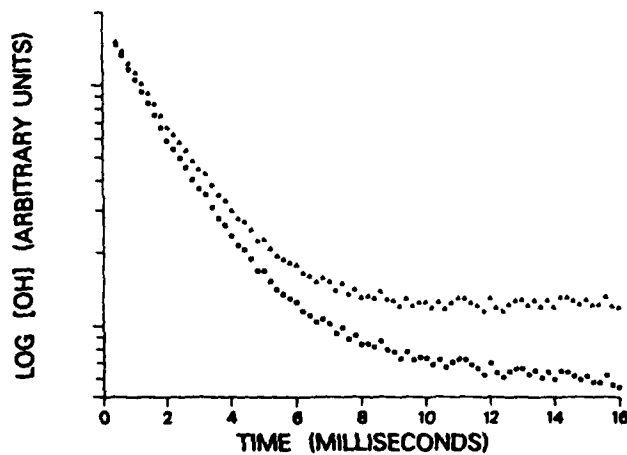


Fig. 2. OH concentration profiles obtained in kinetic measurements of the reaction $\text{OH} + \text{C}_3\text{D}_6 \rightarrow \text{products}$, $T = 533 \text{ K}$, $P = 400 \text{ torr He}$, and $[\text{C}_3\text{D}_6] = 4.73 \times 10^{13} \text{ molecule cm}^{-3}$. The upper curve (triangles) is produced from the raw data (lower curve, squares) by correcting for molecular diffusion out of the observation region.

NOTES

REACTIONS OF WRONG RADICALS

G. Ács, A. Péter and P. Huhn

Reaction-Kinetics Research Group of the Hungarian Academy of Sciences, Department of Inorganic and Analytical Chemistry, Attila József University, Szeged, Hungary

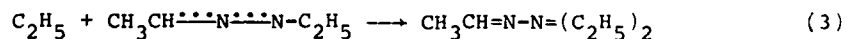
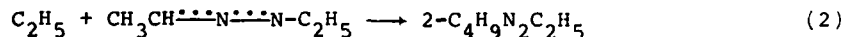
Wrong radicals are those which are not capable or only moderately capable of propagating a chain reaction. The thermal decomposition of azoalkanes is a typical example for the appearance of radicals like that. In azoalkanes the weakest C-H bond can be found on the carbon atom neighbouring the azo-nitrogen, thus the radical formed in the elementary step



- as a result of the interaction of the unpaired electron and the -N=N- double bond - is capable of resonance stabilization which appears in moderate reactivity. These radicals, however, play an important role in the formation of decomposition products in relatively large quantities.

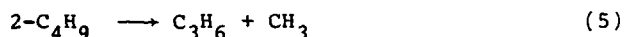
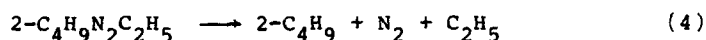
Investigating the thermal decomposition of azoethane (AE) and azoisopropane (AIP), some typical reactions of the formed radicals of less reactivity have been observed.

(i) As known from the literature data [1, 2, 3] in the case of AE it is directly proved that the μ -radical formed in the (1) reaction is capable of recombination reactions of two kinds with the ethyl radical:

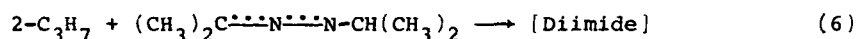


The ratio of the rates of accumulation (approximately k_2/k_3) of the products of nitrogen content has been determined and proved to be 1.3 ± 0.1 independent of the temperature and the

pressure. These compounds are not stable in the examined temperature range ($T = 509-598$ K), their decomposition results in the appearance of new products and new radicals capable of propagating chain reactions. E.g.

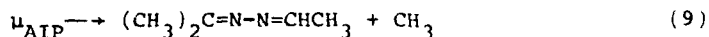
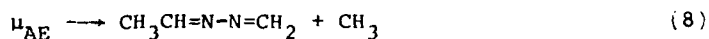


The $\beta + \mu$ radical-radical reaction corresponding to reactions (2) and (3) also takes part in the decomposition of AIP:



but the recombination products are not accumulated. By a mass spectrometer signs referring to hydrazone could be found, but the gas chromatographic method failed in the detection of diimide or hydrazone. The result is not surprising, because reactions (6) and (7) have large steric effects or the stability of products of large molecular weight is insignificant in the temperature range $T = 500-563$ K. The effect of the propylene additive on the thermal decomposition of AIP showed that the 2-methyl-2-butene, 2,3-dimethyl-1-butene and 2,3-dimethyl-2-butene secondary products were formed through reactions (6) and (7).

(ii) Another typical reaction of the two μ -radicals is the decomposition



which could be directly proved only in the case of the second radical by the identification of ethylidene-propylidene-azine.

In the case of both azo-compounds the formation of the methyl radical in that way is referred by the fact that methane is a primary product and other primary methyl radical sources can be hardly imagined.

After all, the μ -radicals (the concentration of which, moreover, can be compared with that of the ethyl or the 2-propyl radicals) contribute only slightly to the chain decomposition of azo-compounds.

- [1] H. S. Sandhu, J. Phys. Chem., 72, 1857 (1968)
- [2] O. P. Strausz, R. E. Berkly, and H. E. Gunning, Can. J. Chem., 47, 3470 (1969)
- [3] G. Martin and A. Maccoll, J. Chem. Soc. Perkin Trans, 2, 1887 (1977)

COUPLING SCHEMES AND HYPERSPHERICAL EXPANSIONS FOR ELEMENTARY
CHEMICAL REACTIONS

V.Aquilanti, G.Grossi, S.Cavalli and A.Lagarà - Dipartimento
di Chimica dell'Università, 06100 Perugia, Italy.

Expansions of potential energy surfaces for elementary chemical reactions in hyperspherical harmonics provide a tool for the description of dynamical features, such as interferences and resonances, within quantum and semiclassical frameworks. The introduction of alternative coupling schemes allows the search for approximately conserved quantities and the development of decoupling approximations. Several examples are considered.

THE EXTENT OF ALKYL NITRATE FORMATION FROM THE $RO_2 + NO$ REACTION

Roger Atkinson, William P. L. Carter, Arthur M. Winer and James N. Pitts, Jr., Statewide Air Pollution Research Center, University of California, Riverside, California 92521, U.S.A.

Organic peroxy (RO_2) radicals are important intermediates involved in the degradation of organics emitted into the troposphere. It has been assumed until recently in chemical computer models that the reaction with NO (their dominant reaction under polluted atmospheric conditions) proceeds via formation of NO_2 and an alkoxy radical



However, work in these laboratories has shown [1-3] that for alkyl peroxy radicals the reaction with NO to form alkyl nitrates also occurs to a significant extent



Indeed, for the alkyl peroxy radicals generated from the n-alkanes the fraction of the overall reaction forming $RONO_2$, $[k_2/(k_1 + k_2)]$, increases monotonically with the carbon number of the RO_2 radical from ≤ 0.014 for ethane to ~ 0.33 for n-octane at 299 K and atmospheric pressure [2]. Furthermore, the alkyl nitrate yields are temperature and pressure dependent, increasing with increasing pressure and decreasing temperature [3].

Recently we have extended these observations to branched and cyclic alkyl peroxy radicals generated from neopentane, cyclohexane, 2-methylbutane, 2-methylpentane and 3-methylpentane. The experimental technique used was as described previously [2]. Alkyl peroxy radicals were formed in the presence of NO by photolysis of CH_3ONO -NO-alkane-air mixtures at wavelengths ≥ 290 nm, with typical initial reactant concentrations of

CH_3ONO , NO , and the alkane of $\sim 2.4 \times 10^{13}$ molecule cm^{-3} . Irradiations were carried out in a 60 liter cylindrical Teflon reaction chamber at 298 ± 2 K and 735 torr total pressure. The alkane and alkyl nitrate concentrations were quantitatively monitored by gas chromatography prior to and during these irradiations.

As in our previous studies [2,3] the observed alkyl nitrate yields were corrected for their loss by reaction with the OH radical, using kinetic data obtained as an integral part of this study, and it was shown from a consideration of the chemistry occurring in these irradiations that these alkyl nitrates were formed essentially entirely from reaction (2). Using available kinetic data concerning the fraction of the overall OH radical reactions with the alkanes yielding the individual alkyl peroxy radicals [4,5], the rate constant ratios $k_2/(k_1 + k_2)$ for the individual RO_2 radicals given in Table 1 can be derived.

Table 1 shows that for the secondary alkyl peroxy radicals these rate constant ratios increase monotonically with the carbon number of the RO_2 radical and to a first approximation are reasonably consistent for a given set of alkyl peroxy radicals of the same carbon number. It is also apparent from Table 1 that the rate constant ratios for primary alkyl peroxy radicals are at least a factor of 2 lower than those for secondary alkyl peroxy radicals of the same carbon number and that the rate constant ratios $k_2/(k_1 + k_2)$ for tertiary alkyl peroxy radicals are also markedly lower, by factors of ~ 3 -5, than are those for the corresponding secondary alkyl peroxy radicals.

These data are important inputs into chemical computer models and allow approximate a priori estimates for alkyl nitrate yields from the various alkyl peroxy radicals involved in alkane degradation pathways to be made.

Table I. Rate constant ratios $k_2/(k_1 + k_2)$ for individual alkyl peroxy (RO_2) radicals at 299 ± 2 K and 735-740 torr total pressure of air.

Alkane	Primary	Secondary		Tertiary	
	$k_2/(k_1 + k_2)$	Isomer	$k_2/(k_1 + k_2)$	Isomer	$k_2/(k_1 + k_2)$
Ethane ^a	≤ 0.014				
Propane ^a	0.020 ± 0.009	2-	0.043 ± 0.003		
n-Butane ^a	≤ 0.040	2-	0.090 ± 0.009		
n-Pentane ^b		2-	0.129 ± 0.014		
		3-	0.118 ± 0.014		
Neopentane	0.0513 ± 0.0053				
2-Methylbutane		3-	0.109 ± 0.003	2-	0.0533 ± 0.0022
n-Hexane ^a		2-	0.220 ± 0.034		
		3-	0.219 ± 0.029		
Cyclohexane			0.160 ± 0.015		
2-Methylpentane		3-+4-	0.165 ± 0.016	2-	0.0350 ± 0.0096
3-Methylpentane		2-	0.140 ± 0.014		
n-Heptane ^b		2-	0.324 ± 0.044		
		3-	0.312 ± 0.041		
		4-	0.290 ± 0.037		
n-Octane ^a		2-	0.353 ± 0.027		
		3-	0.343 ± 0.031		
		4-	0.324 ± 0.032		

^aCalculated from the data of [2].

^bCalculated from the data of [2,3].

- [1] K. R. Darnall, W. P. L. Carter, A. M. Winer, A. C. Lloyd and J. N. Pitts, Jr., J. Phys. Chem., 80, 1948 (1976).
- [2] R. Atkinson, S. M. Aschmann, W. P. L. Carter, A. M. Winer and J. N. Pitts, Jr., J. Phys. Chem., 86, 4563 (1982).
- [3] R. Atkinson, W. P. L. Carter and A. M. Winer, J. Phys. Chem., 87, 2012 (1983).
- [4] R. Atkinson, S. M. Aschmann, W. P. L. Carter, A. M. Winer, and J. N. Pitts, Jr., Int. J. Chem. Kinet., 14, 781 (1982).
- [5] R. Atkinson, W. P. L. Carter, S. M. Aschmann, A. M. Winer, and J. N. Pitts, Jr., Int. J. Chem. Kinet., in press (1984).

Pyrolysis of organic nitrates studied by MB-MS technique

Leif Holmlid and Eva Axelsson

Department of Physical Chemistry

University of Göteborg and Chalmers University of Technology

S-412 96 Göteborg

Sweden

The pyrolysis of three organic nitrates; isopropyl nitrate (IPN), tetrahydrofurfuryl nitrate (THFN) and 2-ethylhexyl nitrate (2-EHN), has been studied in a molecular beam apparatus. These nitrates are used as ignition improvers in Diesel alcohol fuels and the experiments have been carried out to investigate their functions in the combustion process. We have also studied the reactions between methanol and such nitrates, to be published elsewhere [1].

The nitrate was diluted with He to a total pressure of about 200 mbar in a small reactor and the temperature was varied from 295 K to 550 K. The residence time in the reactor was 10-15 s. Decomposition of the nitrate and reactions of the intermediates were followed by molecular beam sampling from the reactor. The results show that all three nitrates initially dissociate by splitting off NO_2 . Depending on the radical formed, the following reactions produce more or less stable compounds. The ring of THFN remains relatively intact at these temperatures and dissociates only at a slow rate. Intermediates like large nitrites appear but decompose due to their low stability, giving maxima for some mass peaks at the same temperature as found for IPN (see below). 2-EHN forms large unsaturated compounds following the release of NO_2 . These appear quite stable and further reactions take place only at higher temperatures. In the case of IPN the major products are acetaldehyde and nitromethane, whose relatively low reactivity may explain the low efficiency of IPN as ignition improver.

Some experimental data for IPN are given in Fig. 1. The reaction mechanism deduced is shown in Table 1. Note the maxima of mass peaks $M=32$, 45, 58, 61 and 74 around 493 K. The signal increase below 493 K is probably due to the decreasing stability of methyl nitrite, which gives increased concentrations of NO and NO_2 . The signal decrease above 493 K is proposed to

be due to the appearance of another dissociation reaction (4c in Table 1).

References

1. E. Axelsson and L. Holmlid, to be submitted to Combust. Flame.
2. J.F. Griffiths, M.F. Gilligan and P. Gray, Combust. Flame 24(1975)11.

1.	$(CH_3)_2CHONO_2 \rightarrow (CH_3)_2CHO + NO_2$	*	
	105-43,46,20,41 59 46-46,30		
2.	$(CH_3)_2CHO \rightarrow CH_3CHO + CH_3$	*	
	44-29,44,43,15 15		
3.	$CH_3 + NO_2 \rightarrow CH_3NO_2$	*	
	61-30,61,15,46		
4a.	$CH_3 + NO_2 \rightarrow CH_3ONO$	*	
	61-30,29		
4b.	$CH_3ONO \rightarrow CH_3O + NO$	*	
	31-30 30		
4c.	$CH_3ONO \rightarrow HCHO + HNO$ or $CH_3O + NO \rightarrow HCHO + HNO$	*	
	30 31-30 30 31-30		
5.	$CH_3CHO + NO_2 \rightarrow CH_3CO + HNO_2$	(*)	
	43-43,41,27 47-46		
6.	$(CH_3)_2CHO + NO_2 \rightarrow (CH_3)_2CO + HNO_2$	*	
	58-43,58 47-46		
7.	$HNO_2 + CH_3CHO \rightarrow CH_3CO + H_2O + NO$	(*)	
	43-43,41,27 18 30		
8.	$CH_3 + NO \rightarrow CH_3NO$		
	45		
9.	$CH_3CHO + NO \rightarrow C_2H_4ONO$		
	74		
10.	$CH_3O + MH \rightarrow CH_3OH + M$		
	32		
11.	$(CH_3)_2CHO + NO \rightarrow (CH_3)_2CHONO$		
	89-74,59		
12.	$(CH_3)_2CHO + NO \rightarrow (CH_3)_2CO + HNO$		
	58-43,58 31-30		
13.	$(CH_3)_2CHO + MH \rightarrow (CH_3)_2CHOH + M$		
	60-45,43		
	M = NO ₂ , NO.		
14.	$CH_3NO \rightarrow HCN + H_2O$		
	27 18		

Table 1.
Pyrolysis of IPN.
Reactions proposed in
[2] are marked *. In-
dependently known and
here observed ions are
underlined.

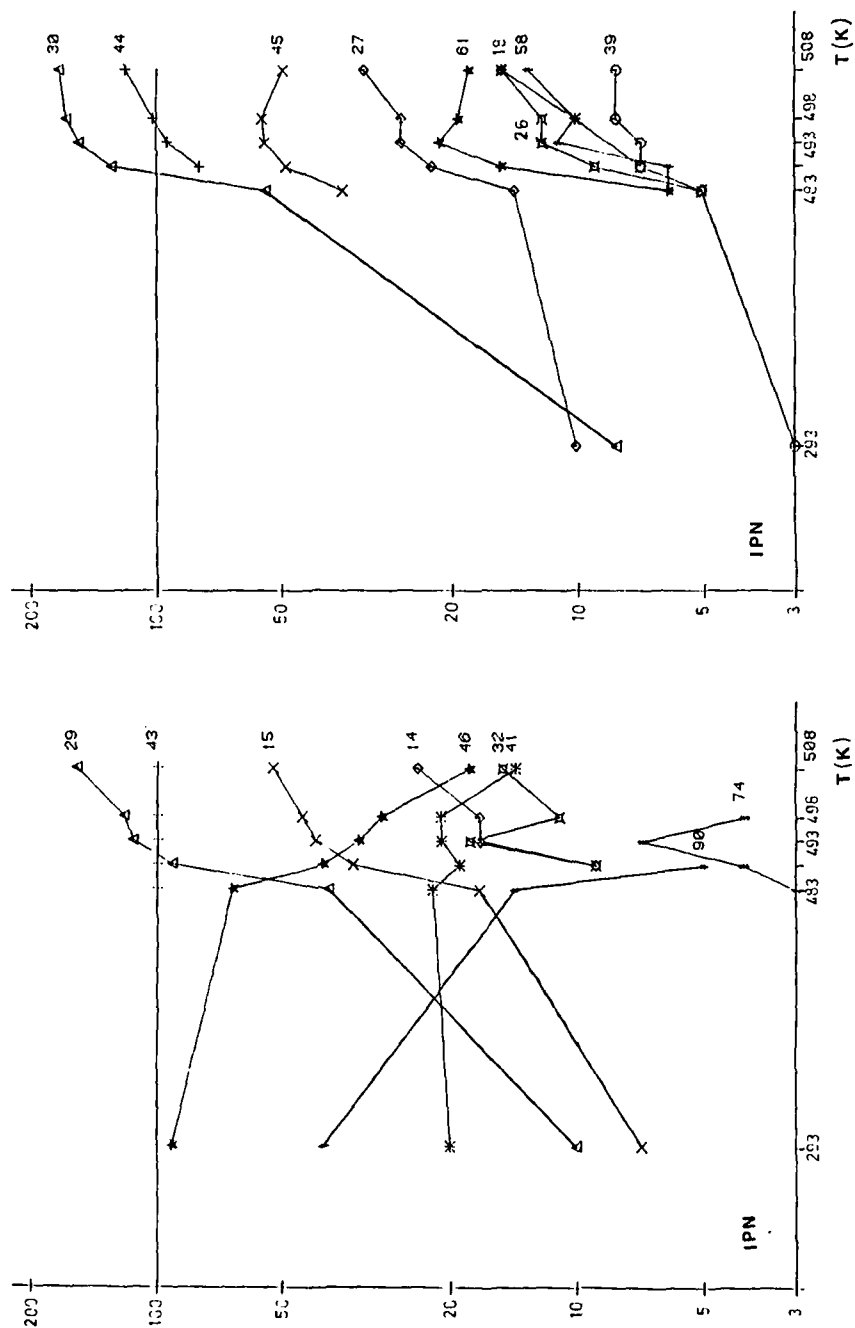


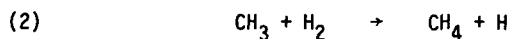
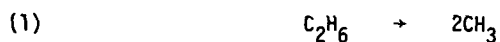
Fig. 1. Results for IPN pyrolysis, normalized to M=43 at each temperature.

Weak Collisional Efficiencies in the Thermal Unimolecular Dissociation
of Ethane

J.-R. CaO⁵ and M.H. Back

Ottawa-Carleton Institute for Research and Graduate Studies in Chemistry,
University of Ottawa Campus, Ottawa, Canada. K1N 9B4

The understanding of the process of collisional deactivation for molecules with energy near to the critical amount for reaction has important implications in many areas of chemical kinetics (1). Theories of collisional deactivation are based on measurements of collisional efficiency, β , from which is derived $\langle \Delta E \rangle$, the average energy transferred per collision. Of particular interest is the dependence of these parameters on temperature. The present work describes measurements of collisional efficiency in the thermal dissociation of ethane diluted with hydrogen and with mixtures of hydrogen and xenon. (2) In this system the chain reaction is suppressed and the methyl radicals formed by dissociation of ethane react quantitatively with hydrogen to form methane.



Analysis of the results showed that the yield of methane provided a direct measure of k_1 , which was calculated from the following equation:

$$\frac{d\text{CH}_4}{dt} = 2k_1 [\text{C}_2\text{H}_6]$$

Initial rates were measured at concentrations of ethane from 25 - 210 ppm in hydrogen and in mixtures of hydrogen and xenon. These mixtures were considered as infinitely dilute. Measurements were made at total pressures between 25 and 400 Torr over the temperature range 938 - 1038 K.

Values of k_1^∞ were obtained by extrapolation of k^{-1} as a function of $P^{-\frac{1}{2}}$.

Good agreement of these values with a recent evaluation of k_1^∞ (3) was obtained.

Values of k_1 at 958 K as a function of ω , the collision rate, are shown in Figure 1, which includes the measurements of k_1 in pure ethane at the same temperature by Lin and Back (4). From these results the integral collisional efficiency $\bar{\beta}_\omega$ was calculated in two ways.* (a) The ratio of collision rates $\omega_{C_2H_6}/\omega_{H_2}$ to produce the same rate constant for dissociation, $k_1[H_2] = k_1[C_2H_6]$, was calculated for values of k_1/k_1^∞ from 0.2 to 0.9. Over this range $\bar{\beta}_\omega^\infty$ varied from 0.05 to 0.02 at 958 K, while at 998 K values ranged from 0.02 to 0.01. The relative collisional efficiency for xenon was about twice the value for hydrogen and showed the same variations. Extrapolation gave a value for $\beta_0(H_2)$ of 0.025 and for $\beta_0(Xe)$ of 0.046.

(b) The ratio of rate constants, $k_1(H_2)/k_1(C_2H_6)$, for the same collision rate, $\omega(H_2) = \omega(C_2H_6)$, was obtained from results as in Figure 1 at 998 and 958 K and at other temperatures by interpolation. These values of $\bar{\beta}_\omega^T$ varied from 0.46 at 943 K to 0.24 at 1000 K. From these values E' was estimated from the "Universal" plots of Tardy and Rabinovitch (1) and $\langle\Delta E\rangle$, the energy transferred in a deactivating collision, was obtained from the relation

$$E' = \frac{\langle\Delta E\rangle}{E^+}$$

$\langle\Delta E\rangle$ varied from 1.7 kcal mol⁻¹ (480 cm⁻¹ mol⁻¹) at 943 K to 1.25 kcal mol⁻¹ (350 cm⁻¹ mol⁻¹) at 1000 K. The present results show that $\langle\Delta E\rangle$ decreases significantly over this temperature range.

*The symbols used are those defined by Tardy and Rabinovitch (1).

References

1. D.C. Tardy and B.S. Rabinovitch, Chem. Rev. 77 369 (1977)
2. J-R. Cao and M.H. Back, J. Phys. Chem. in press
3. D.L. Baulch and J. Duxbury, Comb. Flame 37 313 (1980)
4. M.C. Lin and M.H. Back, Can. J. Chem. 44 505, 2357 (1966)
5. J-R. Cao, Chemistry Department, Peking University, Peking, The People's Republic of China

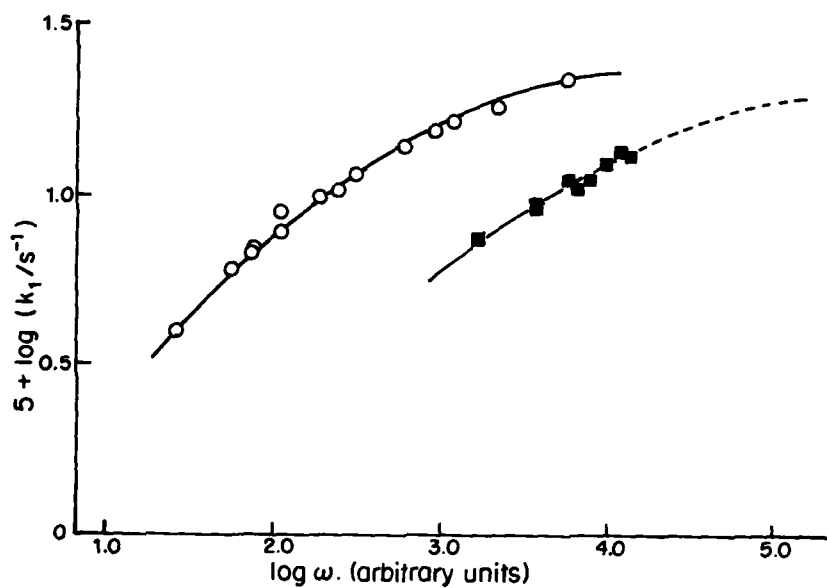


Figure 1. k_1 as a function of ω at 958 K

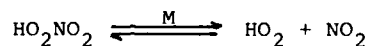
○ : pure ethane; ■ : $C_2H_6 + H_2$ (infinite dilution)
 ---- extrapolation from plots of k^{-1} against $P^{-1/2}$

PRESSURE DEPENDENCE OF THE REACTION $\text{OH} + \text{HO}_2\text{NO}_2$.

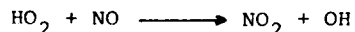
I. Barnes, V. Bastian, K.H. Becker and E.H. Fink.
Physikalische Chemie/FB 9, Bergische Universität-GH
Wuppertal, D-56 Wuppertal 1, W.Germany.

The reaction of OH radicals with peroxyntic acid (PNA), HO_2NO_2 , has been studied over the pressure range 1-760 Torr at 298 K using synthetic air, N_2 and He as diluent gases. The experiments were carried out in a temperature stabilized 420 l glass reaction chamber.

When PNA is admitted to the reactor it is subject to homogeneous and heterogeneous thermal decomposition



If NO is added to the system the HO_2 radicals are rapidly converted to OH via



The steady-state concentration of OH radicals in the system can be controlled by the addition of a hydrocarbon



Kinetic analysis of PNA/NO/propene/M reaction systems in which the propene concentration is greatly increased during the course of the reaction allows the determination of rate constants for the reaction of OH with PNA over the pressure range $M = 1$ to 750 Torr. The NO was either added directly, in excess, to the system or was produced indirectly by photolysis of NO_2 . The concentration-time behaviour of PNA was monitored by in-situ Fourier-Transform infrared absorption spectroscopy and that of propene by GC analysis.

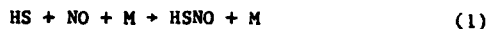
The measured rate constant for $\text{OH} + \text{PNA}$ shows a strong pressure dependence. The value obtained for 1 atm air is a factor 3-4 higher than the value of $4 \times 10^{-12} \text{ cm}^3/\text{s}$ obtained by a number of investigators at low pressure. Preliminary analysis indicates that H_2O_2 is one of the reaction products.

RATE COEFFICIENTS FOR THE REACTION $\text{HS} + \text{NO} + \text{M} \rightarrow \text{HSNO} + \text{M}$
($\text{M} = \text{He}, \text{Ar}$ and N_2) OVER THE TEMPERATURE RANGE 250-445 K

G. Black, R. Patrick, L. E. Jusinski, and T. G. Slanger
Chemical Physics Laboratory
SRI International
Menlo Park, California 94025

ABSTRACT

In a recent paper,¹ the reaction of HS with NO was found to involve a third body suggesting the formation of an adduct, HSNO



This observation of a pressure dependent reaction rate is in conflict with the conclusions of earlier work^{2,3} which suggested that the reaction was a simple two body process with a rate coefficient^{2,4} of $\approx 6 \times 10^{-13} \text{ cm}^3 \text{ molecule}^{-1} \text{ s}^{-1}$.

To further characterize the reaction of HS with NO, our earlier work, which was limited to 298 K, has been extended to cover the temperature range 250-445 K using He, Ar and N_2 as diluent gases.

The experiment involved the production of HS radicals by the photolysis of H_2S with ArF laser radiation at 193 nm. The radicals were detected by LIF spectroscopy. The (0,0) band of the $\text{A}^2\Sigma^+ \rightarrow \text{X}^2\Pi$ system of HS at 323.7 nm was used for excitation and emission was monitored from the (0,1) band at 354.5 nm so as to avoid problems from scattered laser light. The kinetics of the disappearance of HS radicals were determined by measuring the decrease in the LIF signal as a function of increasing time delay between the excimer and dye lasers. A slowly flowing system was used, giving a residence time of ~ 60 s for the gas in the cell.

In the absence of NO (that is, with only H₂S and buffer gas) the HS lifetime was very long (≈ 3 -10 msec) and appeared to be largely determined by diffusion from the ≈ 1 cm diameter cylindrical overlap region of the two laser beams. In the presence of 0.25-1.5 Torr NO the HS decay time was typically in the 10-100 μ sec range and the slope of semilog plots of LIF signal versus delay time was found to be a linear function of added NO. The resulting bimolecular rate coefficients (k_{bi}) were determined as functions of added He, Ar and N₂ over the temperature range 250 to 445 K. k_{bi} was then used in the expression suggested by Troe^{5,6} to describe the pressure dependence of a recombination reaction in its 'fall-off' region

$$k_{bi} = \frac{k_{\infty} k_0 [M]}{k_{\infty} + k_0 [M]} \cdot F \quad \{1 + (\log[k_0 [M]/k_{\infty}])^2\}^{-1} \quad (2)$$

where k_0 and k_{∞} are the low and high pressure limiting rate coefficients respectively, and F is a parameter describing the deviation of the fall-off curve from Lindemann behaviour.

As in our previous study, the experimental range was not high enough to reach more than $\sim 25\%$ of the high pressure limiting rate coefficient. Consequently, it was not possible to fit equation (3) to the experimental data with three adjustable parameters. Hence, F was calculated from the empirical prescription given by Troe^{5,6} and the fit used to obtain values of k_0 and k_{∞} . The results are shown in Table 1 and will be discussed in terms of unimolecular rate theory.

Table 1 Fall-Off Parameters for the Reaction $\text{HS} + \text{NO} + \text{M} \rightarrow \text{HSNO} + \text{M}$

T/K	M	F	$10^{31}k_0/\text{cm}^6\text{molecule}^{-2}\text{s}^{-1}$	$10^{11}k_\infty/\text{cm}^3\text{molecule}^{-1}\text{s}^{-1}$
250	He	0.54	4.17 ± 0.54	2.26 ± 0.60
	Ar	0.57	4.98 ± 0.92	
	N ₂	0.57	6.58 ± 1.50	
255	He	0.54	3.73 ± 0.60	2.65 ± 0.74
265	He	0.53	2.63 ± 0.30	2.63 ± 0.46
	Ar	0.56	2.95 ± 0.48	
	N ₂	0.56	3.40 ± 0.62	
298	He	0.51	2.18 ± 0.18	3.20 ± 0.54
	Ar	0.54	2.24 ± 0.22	
	N ₂	0.54	2.44 ± 0.44	
370	He	0.47	0.89 ± 0.14	4.07 ± 1.70
	Ar	0.50	1.21 ± 0.10	
	N ₂	0.50	1.52 ± 0.10	
445	He	0.44	0.60 ± 0.08	1.76 ± 0.26
	Ar	0.47	0.71 ± 0.09	
	N ₂	0.47	1.07 ± 0.08	

REFERENCES

1. G. Black, J. Chem. Phys. 80, 1103 (1984).
2. J. N. Bradley, S. P. Trueman, D. A. Whytock and T. A. Zaleski, JCS Faraday I, 69, 416 (1973).
3. J. J. Tjee, F. B. Wampler, R. C. Oldenborg and W. W. Rice, Chem. Phys. Lett. 82, 80 (1981).
4. D. L. Baulch, D. D. Drysdale, J. Duxbury and S. Grant, "Evaluated Kinetic Data for High Temperature Reactions," Vol. 3 (Butterworths, London, 1976).
5. J. Troe, Ber. Bunsenges Phys. Chem. 87, 161 (1983).
6. R. G. Gilbert, K. Luther and J. Troe, Ber. Bunsenges Phys. Chem. 87, 169 (1983).

The temperature dependence of the Lewis-Rayleigh
afterglow from atomic nitrogen

by

Andrew Billington, Patricia M. Borrell,

Peter Borrell and Donald S. Richards

Department of Chemistry, Keele University,
Staffordshire, England.

The yellow afterglow, which is a prominent and attractive feature of flowing discharges in nitrogen, has been studied extensively since its first discovery (1). In some careful work Campbell and Thrush (2) showed that the emitting $B(^3\Pi_g)$ state is formed by crossover at several specific vibrational levels from the $A(^3\Sigma_u^+)$ state which itself is formed by a three body combination reaction of the atoms. It was suggested that the A state can redissociate by a bimolecular process so that, overall, the luminescence depends simply on the square of the nitrogen atom concentration. The observed changes in luminescence intensity with added gas are accounted for by differing efficiencies of the additive in vibrationally deactivating the A state.

In our program to study the reactions of oxygen atoms at high temperatures we generate the atomic oxygen by first producing nitrogen atoms in a flowing discharge, reacting then with nitric oxide to form O, and then running a shock wave into the flow to raise the temperature. It seemed worthwhile therefore to make a brief study of the effect of temperature on the Lewis-Rayleigh emission itself.

Experimental.

The high temperature experiments were performed in a new discharge flow/shock tube apparatus similar to that used for the studies of $O_2(^1\Delta_g)$ and $O_2(b^1\Sigma_g^+)$ (3). Nitrogen atoms are produced by passing

$\sim 670 \mu\text{mol s}^{-1}$ of nitrogen at 5 torr pressure through a 2450 MHz discharge. The concentration of N atoms was measured by titration with NO and was found to be $\sim 1.5\%$ of the total at the inlet to the system.

The flow is passed into the test section of a 5 cm diameter shock tube 5 metres in length with a 1.5 metre driver section. Shock waves are generated by bursting aluminium diaphragms naturally using either helium or nitrogen as driver gases. The shock speed is measured with laser light screens.

The luminescence is observed with photomultipliers fitted with 579 nm interference filters.

The resulting traces are analysed by comparing the pre- and post-shock emission levels and concentration gradients in the tube to yield the emission efficiency at the shock front.

Measurements were also made at lower temperatures using a temperature controlled discharge flow tube. Nitrogen atoms were generated and estimated in a similar way and then passed along a jacketed flow tube the temperature of which could be varied from 200 to 400 K using various cooling or heating fluids. The emission efficiency was estimated by comparing the luminescence at the required temperature to that at room temperature.

Results.

The measurements made with the low temperature apparatus extend, and largely confirm the results of Campbell and Thrush (2) not only for the emission reaction but also for the overall 'dark' recombination reactions. The rate constants and surface efficiencies are essentially the same as theirs.

At high temperatures the emission does not rise as much as would be predicted from a simple consideration of the compression ratio; this is

in marked contrast to our work with $O_2(^1\Sigma_g^+)$ where large enhancements of the emission were observed. Thus the emission rate constant declines with temperature. Our results extrapolate to encompass those of Campbell and Thrush at lower temperature.

At the meeting the full results will be presented.

This work is generously supported by the SERC, the University of Keele, and the U.S. Air Force.

1. Lord Rayleigh (R.J. Strutt) Proc. R. Soc. Lond. A85 (1911) 219.
2. I.M. Campbell and B.A. Thrush, Proc. R. Soc. Lond. A296, (1967) 201.
3. P.M. Borrell, P. Borrell and K.R. Grant, J. Chem. Phys. 78 (1983) 748.
R. Boodaghians, P.M. Borrell, P. Borrell, J. Chem. Soc. Farad. Trans. 2 79 (1983) 907.

Temperature Dependence of Simple Ion-Neutral Clustering Reactions,
P.A.M. van Koppen, S. Liu, R. Deral and M.T. Bowers, Department of
Chemistry, University of California, Santa Barbara, California 93106 U.S.A.

The temperature dependence of the 3rd order association rate constant for a number of relatively simple ion-neutral reactions have been measured. These systems vary in complexity from N_2^+/N_2 to $C_6H_6^+/C_6H_6$. The temperature dependence can be relatively accurately fit using an empirical expression of the form $k = aT^{-m}$. The values of m obtained vary from ca. 1.7 ± 0.1 for N_2^+/N_2 to 9 ± 1 for $C_6H_6^+/C_6H_6$, and are found to roughly scale with the number of atoms in the molecule undergoing the clustering reaction. Both the absolute value of k and the temperature dependence are accurately fit using rigorous statistical phase space theory. Approximate statistical methods adequately fit the smaller systems but not the larger systems. The origin of the temperature dependence will be discussed.

Energy Disposal of the Products of Simple Ion-Molecule Reactions

A. O'Keefe, D.C. Parent, W. Wagner-Redeker and M.T. Bowers, Department
Department of Chemistry, University of California, Santa Barbara, CA 93106,
U.S.A.

Techniques have been recently developed [1,2] for accurately measuring kinetic energy distributions of products of exoergic, thermal ion-molecule reactions. Under favorable conditions these measurements allow determination of the partitioning of the energy in the products, including vibrational state distributions, and the dependence of this partitioning on the kinetic energy of the reactant ion.

The reaction of N^+ with CO is particularly interesting. Using the methods described above [1], the results in Table I have been obtained [2] for reaction (1);

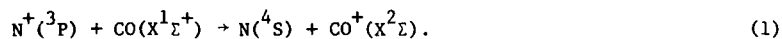


Table I. Product vibrational state distributions for reaction (1) as a function of $N^+(^3P)$ kinetic energy.

$\langle E_t(N^+) \rangle^a$, eV	$CO^+(X^2\Sigma^+)$ v=0	$CO^+(X^2\Sigma^+)$ v=1 and 2
Thermal (~ 0.025)	85 \pm 5	15 \pm 5
0.055	60 \pm 5	40 \pm 5
~ 0.10	40 \pm 5	60 \pm 5

^aApproximate average laboratory $N^+(^3P)$ kinetic energy.

The energy of the N^+ ion is changed by very mild cyclotron heating. Clearly this mild heating has a dramatic effect on the product vibrational state

distribution. Unfortunately it is impossible in the ICR experiment to go to low enough trapping voltages to distinguish between $v=1$ and $v=2$.

The energetics of the reaction are summarized below. In all cases ground state $N^+(^3P)$ and $CO(X^1\Sigma^+)$ reagents are assumed as is ground state $N(^4S)$ product.

$CO^+(X^2\Sigma)$	$\Delta E(eV)$
$v=0$	-0.53
$v=1$	-0.255
$v=2$	+0.02

The $v=2$ state is nearly energy resonant. Hence, one explanation for the very sharp dependence on $N^+(^3P)$ kinetic energy could be the opening up of this channel and preferential population of $CO^+(X^2\Sigma)$, $v=2$. A higher resolution technique, such as laser induced fluorescence is required to determine the answer.

LIF studies on this reaction have been reported. The results are summarized in Table II;

Table II. Vibrational distributions in the $CO^+(X^2\Sigma)$ product.

Method	$N^+(^3P)$ Kinetic Energy, eV	$CO^+(X^2\Sigma)$ % $v=0, 1, 2$	Reference
ICR	Thermal	85, 15 ^a	This work
LIF	0.39	>81, <15, 4	[3]
LIF	Thermal	83, 15, 2	[4]

^aThe sum of $v=1$ and $v=2$.

The thermal energy ICR results are consistent with both sets of LIF results. What is puzzling is why does the vibrational distribution in $CO^+(X^2\Sigma)$ change so dramatically when small amounts of kinetic energy are imparted to N^+ (Table I) yet seemingly are nearly unchanged for relatively

large values of N^+ kinetic energy as demonstrated by the LIF results above. It has been noted [2] that one possible reason could be the fact that 0.39 eV N^+ ions in the lab correspond to 0.13 eV N^+ ions in the N^+/CO center of mass. This energy would bring the N^+/CO reaction energy almost exactly between $v=2$ and $v=3$ in $CO^+(X^2\Sigma)$. Hence, the system is non-resonant and perhaps no enhancement of $v=2$ is attained.

In order to test the resonance notion we have examined reaction (1) using ^{13}CO and $C^{18}O$ isotopic variants. For both cases $v=2$ in the $CO^+(X^2\Sigma)$ product is almost exactly resonant. Final numbers are not yet available at the time of submission of this abstract, but preliminary results indicate a very large enhancement of $v=1$ and 2, somewhere around $80\pm 20\%$. This is a truly phenomenal result and suggests the dynamics of this reaction are very specific. In response to these ICR results, LIF experiments will soon be initiated [5]. The final results from both sets of data will hopefully be presented at the meeting.

- [1] G. Mauclaire, R. Deraï, S. Feinstein, R. Marx and R. Johnson, J. Chem. Phys. 70, 4023 (1979); G. Mauclaire, R. Deraï, S. Feinstein and R. Marx, J. Chem. Phys. 70, 4017 (1979).
- [2] A. O'Keefe, D. Parent, G. Mauclaire and M.T. Bowers, J. Chem. Phys. (in press).
- [3] D.R. Guyer, L. Huwei and S.R. Leone, J. Chem. Phys. 79, 1259 (1983).
- [4] C. Hamilton, V. Bierbaum and S.R. Leone (private communication).
- [5] V. Bierbaum, (private communication).

REDUCED DIMENSIONALITY QUANTUM RATE CONSTANTS FOR THE $D+H_2(v=0)$
AND $D+H_2(v=1)$ REACTIONS ON THE LSTH SURFACE

J.M. BOWMAN^{a)} and K.T. LEE^{a),b)}

Department of Chemistry, Illinois Institute of Technology, Chicago,
IL 60616, U.S.A.

and

R.B. WALKER

Theoretical Division, Los Alamos National Laboratory, Los Alamos,
New Mexico 87545, U.S.A.

Collinear exact quantum reaction probabilities for
the $D+H_2(v=0)$ and $D+H_2(v=1)$ reactions were calculated using the ab initio
surface of Liu and Siegbahn (as fit by Truhlar and Horowitz) with an
adiabatic treatment of the ground state bend. These probabilities
are used to obtain approximate three-dimensional thermal rate constants
which are compared with experiment and other calculations.

a) Supported by the Department of Energy, Division of Chemical Sciences,
Office of Basic Energy Sciences, under contract (DOEDE-AC02-91ER10900).

b) Present address: Dept. of Chemistry, University of Rochester

'POLYMODE': A PROGRAM TO CALCULATE VIBRATIONAL ENERGIES OF POLYATOMIC MOLECULES. I. APPLICATION TO H_2O

H. ROMANOWSKI* AND J.M. BOWMAN

Department of Chemistry, Illinois Institute of Technology, Chicago,
IL 60616, U.S.A.

A general code to calculate vibrational energies of polyatomic molecules based on the vibrational self-consistent field plus configuration interaction methods [K.M. Christoffel and J.M. Bowman, Chem. Phys. Lett., 85, 220 (1982)] is described. Energies of forty-six stretching/states of H_2O are calculated using the ab initio quartic force field of Bartlett et al. [J. Chem. Phys., 71, 281 (1979)], in both internal and normal coordinate representations. The constant G-matrix approximation in internal coordinates is tested and shown to lead to substantial errors. Finally the efficiency of the method is demonstrated by comparing an extensive CI mix with a much smaller all-singles CI mix in which states which differ from the vibrational SCF reference state by one quanta are mixed.

*Permanent address: Institute of Chemistry, The Wroclaw University,
50-383 Wroclaw, Poland

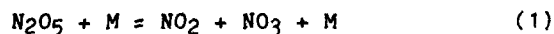
A Study of N₂O₅ and NO₃ Chemistry and the Photolysis of
N₂O₅ Mixtures

J.P.Burrows, G.S.Tyndall and G.K.Moortgat

Max Planck Institut für Chemie

Postfach 3060, D-6500 Mainz, F.R.G.

N₂O₅ exists in the gas phase in equilibrium with NO₂ and NO₃. This equilibrium is responsible for tying up a large part of the NO_x in the atmosphere during the night.

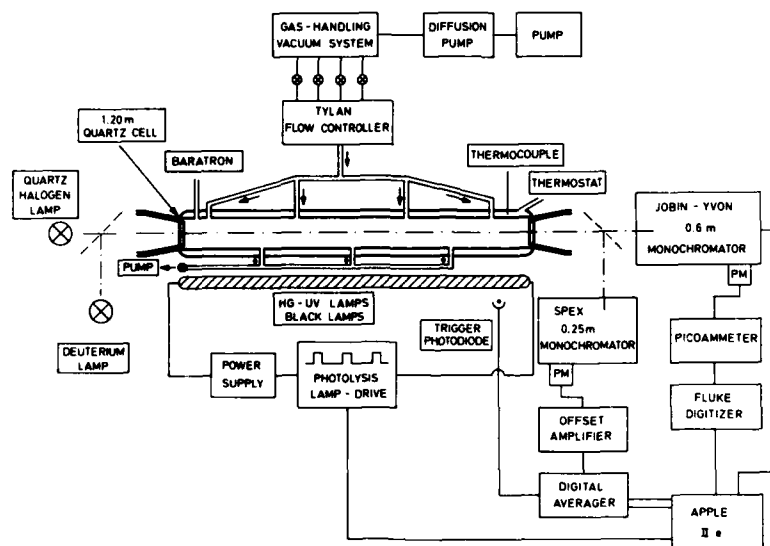


The equilibrium constant has been determined at 294K by flowing mixtures of N₂O₅ in N₂ through a 114cm long quartz photolysis cell and monitoring all components by their UV or visible absorptions. The measured value for the equilibrium constant

$$K_1 = \frac{[\text{NO}_3][\text{NO}_2]}{[\text{N}_2\text{O}_5]} = 6 \times 10^{10} \text{ molecule cm}^{-3}$$

is in good agreement with the literature value.

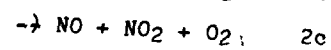
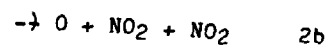
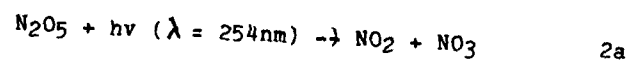
The recombination reaction (-1) has been studied directly in flowing mixtures of Cl₂-ClNO₃-NO₂-N₂ and F₂-HNO₃-NO₂-N₂ at pressures between 20 and 40 Torr. The mixtures were photolysed using blacklamps driven by a novel rectangular wave generator, in which the dark period could be lengthened to up to 10 times the light period. NO₃ modulations were monitored at 623nm and averaged over many cycles in a digital signal averager. The apparatus is shown in the figure.



UV-VIS ABSORPTION MODULATED PHOTOLYSIS APPARATUS

Analysis of the NO_3 decays yields $k_{-1} = (3.0 \pm 1) \times 10^{-13}$ and $(5.0 \pm 1.5) \times 10^{-13} \text{ cm}^3 \text{ molecule}^{-1} \text{ s}^{-1}$ at 20 and 40 Torr of N_2 respectively and 294K, consistent with values calculated from the equilibrium constant K_1 and the rate of thermal dissociation of N_2O_5 . From the observed stationary state concentration of NO_3 in these experiments a value of $1.17 \times 10^{-17} \text{ cm}^2 \text{ molecule}^{-1}$ is obtained for the absorption cross section at 623nm. By performing the experiments at different wavelengths a complete absorption spectrum could be built up point by point between 610 and 670nm.

Finally, flowing N_2O_5 mixtures in N_2 were photolysed using modulated low pressure mercury lamps. Possible photolysis pathways are:



By observing NO_3 and NO_2 modulations directly it was found that $k_{2a}/k_2 \gg 0.7$ for an N_2O_5 concentration of 4×10^{14} molecule cm^{-3} .

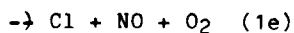
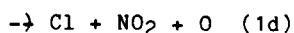
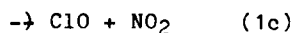
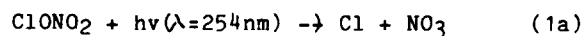
The Photolysis of ClONO₂ and the Production of NO₃

J.P.Burrows, G.S.Tyndall, G.K.Moortgat and

D.W.T.Griffith

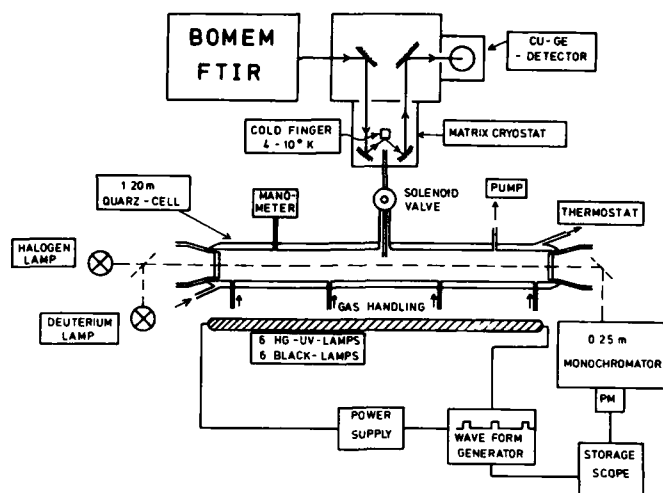
Max Planck Institut für Chemie, D6500 Mainz, F.R.G.

The photolysis of mixtures of ClONO₂ in N₂ by 254nm radiation has been studied in a stirred flow reactor. A rectangular waveform was applied to up to 6 low pressure Hg lamps, which surround the cell. The apparatus used here is shown schematically below. Both the period of the photolysis cycle and the relative lights on and off time are variable. ClONO₂ has several energetically feasible photolysis pathways:



The final products of the system were studied using matrix isolation Fourier transform infra red (FTIR) spectroscopy. The main product observed is N₂O₅, and an upper limit was obtained for the production of ClONO from pathway (1b). The production of any NO in the system was

investigated by photolysing mixtures of ClONO_2 and NO_2 and using a chemiluminescence detector. An upper limit has been determined for the production of NO by reaction (1e).
Figure 1.

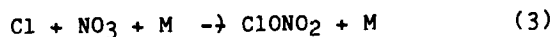
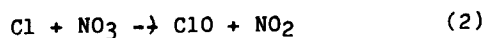


MATRIX ISOLATION FTIR, U.V.-VIS. ABSORPTION and MODULATED PHOTOLYSIS APPARATUS

The overall photolysis rate of ClONO_2 was determined in two ways. The photolysis rate, k_1 , could be calculated from a knowledge of the absorption cross-sections of ClONO_2 , NO_2 and H_2O_2 and measurements of the H_2O_2 and NO_2 photolysis rates. The photolysis rate of ClONO_2 was measured by monitoring the optical density changes at 220nm where both the reactant ClONO_2 and the final

product N_2O_5 absorb. However the apparent photolysis rate depends on the initial concentration of ClONO_2 . At higher concentrations of ClONO_2 the decay of optical density is slower than the calculated value. This somewhat surprising behaviour is unlikely to be due to self quenching and is better explained by secondary chemical reactions.

In order to understand the system better the concentration of NO_3 was monitored as a function of time in modulated photolysis experiments. In a study of the modulated photolysis of mixtures of Cl_2 , ClONO_2 and N_2 using blacklamps evidence has been found for a fast reaction between Cl and NO_3 . The most energetically favourable products of this reaction are NO_2 and ClO ; however ClONO_2 might also be produced:



These reactions may play a role in the photolysis of ClONO_2 .

The time dependent behaviour of NO_3 was monitored in the photolysis of ClONO_2 and the rate of production of NO_3 determined. A full analysis of the system enables a value for k_{1a}/k_1 to be estimated.

The results obtained in this laboratory will be compared with those obtained elsewhere and the consequences for stratospheric chemistry discussed.

REACTIONS OF O ATOMS WITH ALKANES*

N. CohenThe Aerospace Corporation
El Segundo, Calif., U.S.A.

Recently a study was published illustrating the use of conventional transition state theory for extrapolating rate coefficients for reactions of OH radicals with alkanes to temperatures above the range of experimental data. In this paper we present a follow-on study of reactions of O atoms with alkanes. Expressions are developed for estimating structural properties of the activated complex necessary for calculating enthalpies and entropies of activation. Particular attention is given to the problem of the effect of the O atom adduct on the internal rotations in the activated complex. Differences between primary, secondary, and tertiary attack are discussed, and the validity of representing the activated complexes of all O + alkane reactions by a fixed set of vibrational frequencies and other internal modes is evaluated. Experimental data for reactions of O atoms with fifteen different alkanes (CH_4 , C_2H_6 , C_3H_8 , C_4H_{10} , C_5H_{12} , C_6H_{14} , C_7H_{16} , C_8H_{18} , $i\text{-C}_4\text{H}_{10}$, $(\text{CH}_3)_4\text{C}$, $(\text{CH}_3)_2\text{CHCH}(\text{CH}_3)_2$, $(\text{CH}_3)_3\text{CC}(\text{CH}_3)_3$, $n\text{-C}_5\text{H}_{10}$, $n\text{-C}_6\text{H}_{12}$, $n\text{-C}_7\text{H}_{14}$) are reviewed and used as the basis for developing the models.

It is assumed that in the activated complex the C...H and H...O bond lengths are 1.36 and 1.20 Å, respectively, and the C...H...O bond angle is 180° , as calculated by Walch and Dunning for the reaction of O + CH_4 . Other bond lengths and angles are assumed to be the same as in the alkane itself. It is further assumed that the electronic multiplicity of the activated complex is 6, and that the O atom lowers the barriers to internal rotation about the $\alpha\text{-CC}$ bonds by approximately 1 kcal/mole. The following changes are made in the vibrational frequencies as compared with those of the alkane:

* Work supported by the National Bureau of Standards

Reaction	Frequencies removed	Frequencies added
O + methane	3000, 1530, 1300	1000(2), 700, 240(2)
O + primary H	3000, 1400, 800	1000, 700, 350, 240(2)
O + non-cyclic secondary H	2900, 1450, 1350, 1250, 750	1000, 700, 500(2), 300, 240(2)
O + cyclic secondary H	2900, 1450, 1350, 1250, 750, 500, 400	1000, 700, 500(2), 300, 250, 240(2), 200
O + tertiary H	3000, 1200(2)	700, 350(2), 240(2)

If a value for $k(300)$, which is required for the transition state theory calculation, is not available from experimental data, it can be estimated from the following approximate expressions for $\Delta S^\ddagger(300)$ and $E_a(300)$:

Reaction	$\Delta S^\ddagger(300)$, e.u.	$E_a(300)$, cal/mol
O + straight chain primary H	$-21.2 + R \ln(\sigma/n_C)$	7500 ± 500
O + branched chain primary H	$-21.2 + R \ln(\sigma/n_C)$	6300 ± 500
O + non-cyclic secondary H	$-21.2 + R \ln(\sigma/n_C)$	4000 ± 1000
O + cyclic secondary H	-19.0	4000 ± 1000
O + tertiary H	$-21.6 + R \ln(\sigma/n_C)$	2700 ± 500

where n_C = total number of carbon atoms in the alkane and σ = symmetry number (the number of "equivalent" H atoms). Using the expression, $k(300) = 10^{15.06} \exp(\Delta S^\ddagger/R) \exp(-E_a(300)/300R)$, one then obtains:

$\log k(300) = 5.0 + \log \sigma/n_C$	(primary H, unbranched)
$= 5.8 + \log \sigma/n_C$	(primary H, branched)
$= 7.5 + \log \sigma/n_C$	(secondary H, non-cyclic)
$= 8.0$	(secondary H, cyclic)
$= 8.4 + \log \sigma/n_C$	(tertiary H)

These expressions agree with experimental values within a factor of approximately 2 for alkanes larger than C_3H_8 .

The requirement for an experimental value of $k(300)$ to carry out the transition state theory calculations prompted a careful examination of available data for the reactions considered. In the case of $O + CH_4$, C_2H_6 , and $(CH_3)_4C$ --i.e., reactions involving only primary H abstraction--the experimental data, especially at low temperatures, need to be scrutinized carefully because of the possible errors introduced by olefinic impurities in the alkane

reagent or because of unaccounted for secondary reactions. Both of these complications are a result of the reactions of O atoms with primary alkanes being so slow at low temperatures.

A COMPUTERIZED THERMOCHEMICAL DATA BASE OF MOLECULES AND FREE RADICALS IN THE GAS PHASE

by Chantal MULLER^a, Jean-Marie DAVID^b, Gérard SCACCHI^a and Guy-Marie CÔME^a

^a Département de Chimie Physique des Réactions, L.A. C.N.R.S. 328, Université de Nancy I et Institut National Polytechnique de Lorraine, 1, rue Grandville, 54000 NANCY, FRANCE.

^b Centre de Recherches en Informatique de Nancy, L.A. C.N.R.S. 262, Nancy.

Two programs for the automatic computing of thermochemical properties of molecules and free radicals in the gas phase have been set up, based on the group additivity method of BENSON (¹). In this method, each thermochemical quantity of a molecule is considered as the sum of the similar quantities of the groups which compose the molecule, each of them being defined as an atom (ligancy > 2) and its ligands.

In the program relating to molecules (MOL-DATA) [Figure 1], the input of molecules is done by means of a linear notation (²). For a non-tabulated molecule the decomposition into groups is achieved and, if all the necessary incremental values are tabulated, we obtain ΔH_f° (300 K), S° (300 K) and C_p° (at different temperatures between 300 and 1500 K) for the molecule. If some of the incremental values are not known, a "by-pass" program is started. This program uses the additivity law of bond properties : each thermochemical quantity of the molecule is the sum of the contributions of its different bonds. If all the necessary bonds are tabulated we obtain ΔH_f° (300 K), S° (300 K) and C_p° (300 K only) for the molecule. If one of these values is missing the calculations are impossible with any of the two methods used.

But the ΔH_f° , S° and C_p° thus obtained are not correct. Some corrections are needed. For the three quantities, "ring correction", "cis correction" and "ortho correction" must be applied. Only ΔH_f° is concerned by "1-4 and 1-5 gauche correction", and "symmetry correction" and "optical isomer correction" must be done on S° . All these corrections are made automatically.

After these corrections the correct values of the three thermochemical quantities are obtained, at 300 K (and at other temperatures for C_p° if it has been evaluated by group additivity method). Simple calculations permit then to calculate ΔH_f° and S° at any temperature.

The linear notation is also used for the input of radicals $R\cdot$ in the corresponding program (RADICAL-DATA) [Figure 2]. All the calculations

are done, the molecule RH being considered as a model. Thus the thermochemical quantities of RH are needed. The previous program MOL-DATA provides these quantities at the chosen temperature T.

The estimation of $\Delta H_f^\circ (R\cdot)$ is achieved by considering the reaction : $RH \longrightarrow R\cdot + H\cdot$ whose ΔH° is given by a Table of bond-dissociation energies. For the calculation of $S^\circ (R\cdot)$ the evaluation of the differences between RH and $R\cdot$ is made. These differences include : the symmetries and optical isomers (given by previous subroutines in MOL-DATA program), the spin ($R \ln 2$), the three vibrational degrees of freedom of the additional H atom and the possible changes in the values of reduced moments of inertia and of potential barriers of some internal rotations. A differential vibrational analysis between $R\cdot$ and RH permits to evaluate the two last differences. In the same way this analysis provides $C_p^\circ (R\cdot)$ from $C_p^\circ (RH)$.

The mean accuracy of the group additivity method [for molecules] is the one claimed by BENSON : $\pm 0.5 \text{ kcal.mole}^{-1}$ in ΔH_f° and $\pm 1 \text{ e.u.}$ in S° and C_p° . For radicals the similar values are : ± 1 to 2 kcal.mole^{-1} and $\pm 2 \text{ e.u.}$. The limits of these methods are due to the limited number of groups (about 400), bonds (about 35) and to the unknown values of some corrections (in particular some "ring corrections").

Note : The QCPE Program n° 244 ⁽³⁾ also uses the group additivity method to calculate the thermochemical quantities of molecules but it is more limited than the present program MOL-DATA as it deals only with molecules containing C, H, O and N atoms.

REFERENCES

- (¹) S.W. BENSON - *Thermochemical Kinetics*, 2nd ed., Wiley (1976).
- (²) G.M. CÔME, P.Y. CUNIN, M. GRIFFITHS and C. MULLER - *Computers & Chemistry*, to appear.
- (³) M.R. MARTINEZ, QCPE 11,244 (1973).

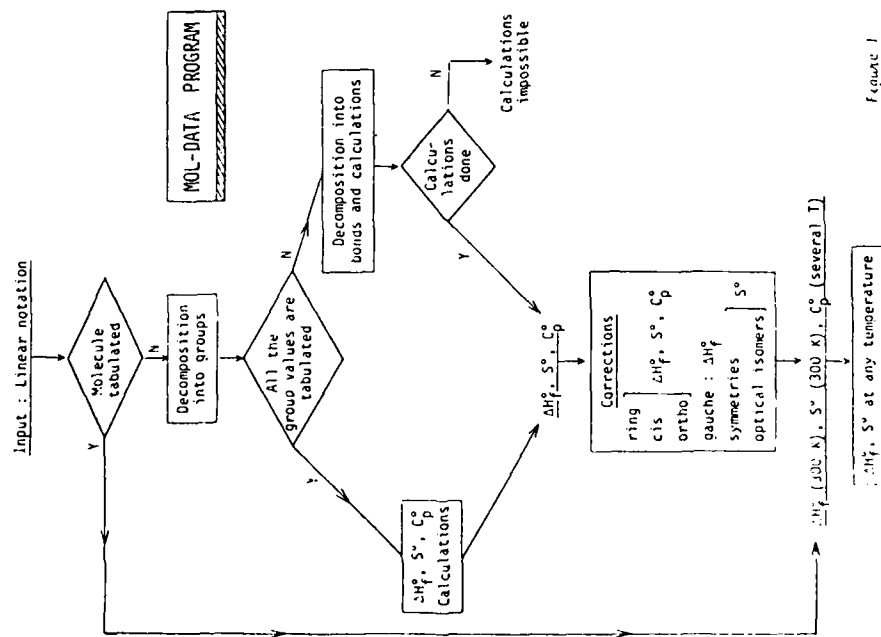


Figure 1

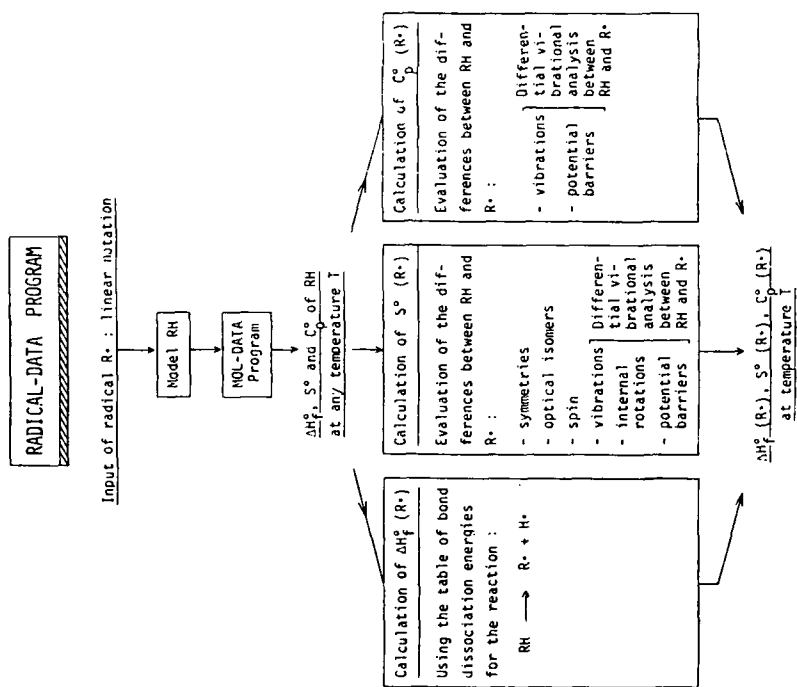


Figure 2

COMPUTER AIDED DESIGN
OF GAS PHASE FREE RADICAL REACTION MECHANISMS

by L. HAUX-VOGIN^a, P.Y. CUNIN^b, M. GRIFFITHS^c and G.M. CÔME^a

^a Département de Chimie Physique des Réactions, L.A. C.N.R.S. 328,
Université de Nancy I et Institut National Polytechnique de
Lorraine, 1, rue Grandville, 54000 Nancy, France

^b Laboratoire d'Informatique, Faculté des Sciences, Dijon

^c L.I.S.H., C.N.R.S., Marseille

A program has been written, which, from the list of the reactants, gives as output the primary reaction mechanism, i.e. a sequence of elementary processes, a list of intermediate free radicals and primary molecular reaction products. This program applies to gas phase free radical reactions.

The input of reactants is achieved by means of a linear notation, the grammar of which is very simple (¹). This notation is non-ambiguous, but non-canonical, because a reactant can have several input representations.

Therefore, an algorithm has been devised, which generates a canonical representation of chemical compounds, including free radicals. First, a focus is looked for. It is an atom or a bond having no equivalent in the compound. Equivalence is obtained by means of graph automorphisms. Moreover, a focus must minimize the number of parentheses in the external representation of the compound. After the focus has been found, a total order is defined on bonds, atoms and groups of atoms, allowing to get the final canonical representation. This representation brings equivalent atoms and bonds to light, so that the same elementary process will not be written several times. The theory made here cannot be applied to cyclic compounds.

The elementary processes which will be included in the mechanism are the following : unimolecular and bimolecular initiations, additions of free radicals on unsaturated molecules, unimolecular decompositions of free radicals, metatheses, combinations and disproportionations of free radicals. Some of these processes are considered in the program as the sum of two others, e.g. a bimolecular initiation can be formally considered as a unimolecular initiation followed by a free atom addition. An elementary process must not change the valency of an atom, thus excluding the process $\text{CHO} \cdot \longrightarrow \text{CO} + \text{H} \cdot$, for example

All these elementary processes are systematically applied to the reactants and to the corresponding free radicals. The molecular products of these steps, which are the primary reaction products, are supposed to be inert at this stage. The mechanism obtained is called primary. The corresponding algorithm has been devised in such a way that all the conceivable processes are written at least one time but also one time only, with the following limitation : there is an upper limit, chosen by the user, for the number of atoms in a free radical ; otherwise, free radical additions would create indefinitely growing polymeric radicals.

At this moment, the primary mechanism is confronted with the stoichiometric and kinetic experimental results. If needed, a secondary mechanism is generated by defining as reactants the initial ones plus some primary reaction products (e.g. the major ones), and so on. The final mechanism, being exhaustive, is generally too much complicated. It is simplified by means of thermochemical and kinetic considerations, using a computerized thermochemical data base ⁽²⁾ and a kinetic data base ⁽³⁾. A sensitivity analysis allows one to detect negligible, non-determining and determining processes of the mechanism ⁽⁴⁾. Negligible processes are eliminated, whereas the rate parameters of some determining processes can be determined from the experimental results by model identification techniques ⁽⁴⁾. This results in a fitted kinetic model, which is expected to explain, both qualitatively and quantitatively, the stoichiometric, thermodynamic and kinetic laws of the reaction under study.

In the future, we intend to generalize our program to reactions of cyclic molecules and to include all these features, plus some qualitative knowledges of gas phase kineticists, in an expert system.

REFERENCES

1. G.M. CÔME, P.Y. CUNIN, M. GRIFFITHS and C. MULLER - Computers & Chemistry, to appear.
2. C. MULLER, G. SCACCHI and G.M. CÔME - 9th International Codata Conference, Jerusalem, Israel, 24-28 June 1984.
3. S. DIAKHATE, O. FOUCAUT and G.M. CÔME - to be published.
4. G.M. CÔME - Comprehensive Chemical Kinetics, Vol. 24, Chapter 3, Elsevier (1983).

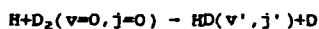
The reaction $\text{H}+\text{D}_2 \rightarrow \text{HD}+\text{D}$: Distorted wave calculations at

0.55 eV and 1.3 eV

J N L Connor and W J E Southall

Department of Chemistry,
University of Manchester,
MANCHESTER,
M13 9PL,
U.K.

Two important experiments have recently measured the vibrational-rotational product distributions of the $\text{H}+\text{D}_2 \rightarrow \text{HD}+\text{D}$ chemical reaction^{1,2}. We have carried out distorted wave calculations for the state selected reaction



at two translational energies, 0.55 eV and 1.3 eV, using an accurate ab initio potential energy surface³.

Two variants of the distorted wave approximation have been used: In the static-static distorted wave method (SSDW), the vibrational-rotational wavefunction of both the target and product molecules is unperturbed as the reactant or product atom approaches or recedes, whereas in the vibrationally adiabatic distorted wave (VADW) method, the vibrational wavefunctions of the reactant and product molecules are allowed to distort adiabatically during the collision⁴.

At 0.55 eV, the SSDW and VADW rotational distribution agree quite well with each other as well as with coupled states calculations⁵ and with quasiclassical (QC) trajectory results⁶. At 1.3 eV, the SSDW theory predicts less rotational excitation of the products than the QC method. The SSDW results are generally in better agreement with the experiments of Marinero et al¹ than with the measurements of Gerrity and Valentini².

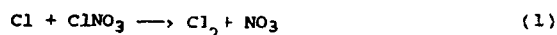
1. E.E. Marinero, C.T. Rettner and R.N. Zare J. Chem. Phys (in the press).
2. D.P. Gerrity and J.J. Valentini J. Chem. Phys. 1983, 79, 5202;
ibid (in the press).
3. P. Siegbahn and B. Liu, J. Chem. Phys. 1978, 68, 2457;
D.G. Truhlar and C.J. Horowitz J. Chem. Phys. 1978, 68, 2446;
erratum ibid 1979, 71, 1514.
4. D.C. Clary and J.N.L. Connor Chem. Phys. Lett. 1979, 66, 493;
Chem. Phys. 1980, 48, 175; Mol. Phys. 1980, 41, 689; J. Chem.
Phys. 1981, 74, 6991; Mol. Phys. 1981, 43, 621; J. Chem. Phys.
1981, 75, 3329.
5. G.C. Schatz J. Chem. Phys. (in the press).
6. N.C. Blais and D.G. Truhlar Chem. Phys. Lett. 1983, 102, 120.

Kinetics Studies of the reactions of NO_3 with Cl and ClO

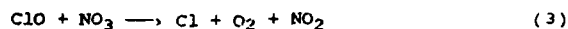
R.A. Cox, D. Stocker, AERE, Harwell
 M. Fowles, D. Moulton, R.P. Wayne, University of Oxford
 E. Lungstrom, Chalmers University, Gothenburg

Reactions of nitrate radicals are of interest in atmospheric chemistry, since NO_3 is produced by the thermal reaction of NO_2 with ozone and can initiate free radical chemistry at night when photochemical radical sources are absent. Until recently, most of the photochemical and kinetic data concerning NO_3 reactions were due to H. Johnston and co-workers who studied the $\text{NO}_3\text{-O}_3\text{-N}_2\text{O}_5$ system and obtained rate constants for elementary NO_3 reactions together with the absorption cross section, σ and, quantum yields for photodissociation of NO_3 in its broad, structured, visible absorption band. Recently, several new studies of NO_3 photochemistry and kinetics have been reported, including a preliminary report of our own work.

We have used the reaction of Cl atoms, produced by 350 nm photolysis of Cl_2 , with chlorine nitrate as a source of NO_3



NO_3 formation and decay was monitored in absorption at 662 nm and the observed kinetic behaviour of NO_3 indicated the occurrence of two novel reactions leading to NO_3 removal i.e.



The occurrence of these reactions was further indicated by observation of characteristic absorption due to ClO in the $A^2\Pi - X^2\Pi$ system near 277 nm. By monitoring ClO decay kinetics in the presence of excess NO_3 , a direct determination of k_3 was obtained. These experiments will be described and the results presented.

The experiments were performed in a quartz cell, 120 cm long which was illuminated by up to 6 fluorescent blacklights ($\lambda = 350$ nm). Absorption was monitored at selected wavelengths on a light beam passing along the cell, using a fast digital multichannel scaler. This device was timed synchronously with the operation of the photolysis lamps, which could be square wave modulated at frequencies between 0.02 and 10 Hz. The reaction cell was filled with mixtures of Cl_2 and ClONO_2 from a flow manifold at 1 atm pressure. The slow formation and decay of the NO_3 radical was investigated in photolysis of static mixtures whilst the faster reaction involving NO_3 with ClO was investigated using modulated photolysis of flowing mixtures.

During static photolysis NO_3 was observed to increase to a steady state concentration of $\sim (0.5 - 1.0) \times 10^{13}$ molecule cm^{-3} after $\sim 5\text{-}15$ s (based on a value of 1.63×10^{-17} cm^2 determined for σ_{NO_3}). The kinetics were consistent with a constant NO_3 production rate via reaction (1) and loss by reaction (2) provided the latter was pseudo first order i.e. $[\text{Cl}]$ remained essentially constant. Regeneration of Cl via reactions (2) and (3) has been postulated to account for the constancy of $[\text{Cl}]$. Further

evidence for this mechanism comes from positive identification of ClO as a reaction intermediate. Fig. 1 shows the modulated absorption spectrum near 277 nm observed in 0.5 Hz photolysis of a flowing Cl₂-ClONO₂ mixture. The characteristic bands of the A²Π - X²Π system of ClO are clearly visible. The kinetic behaviour of ClO was determined by monitoring at the 11-0 band head at 277.2 nm. Fig. 2 shows data obtained for a mixture containing Cl₂ and ClONO₂. ClO is seen to rise to a steady state during photolysis and fall to near zero in the dark. The half-times for rise and fall are approximately equal, suggesting first order kinetics for ClO removal. The rate coefficient from the relationship $t_{1/2} = \ln 2/k_1$ is 4.5 s⁻¹. The concentration-time behaviour of ClONO₂ and NO₃ shown in Fig. 2 has been corrected for components due to flow out and other slow loss processes. ClONO₂ decays steadily during photolysis but remains constant during the dark period, reflecting the proposed constant steady state concentration of [Cl] during illumination and rapid decay to zero in the dark. The behaviour of NO₃ is more complex showing a small concentration modulation with a similar time constant to that of ClO, superimposed on a large residual concentration resulting from the balance between production by reaction (1) and the slow removal processes.

The rate coefficient k₃ can be determined from the value of k₁ together with the mean [NO₃] present during the modulation cycle, assuming reaction (3) is responsible for ClO decay. k₂ can be determined from steady state analysis when $k_2[Cl] = k_3[ClO]$ and $[Cl] = -d[ClONO_2]/dt \times k[ClONO_2]^{-1}$. Preliminary analysis of 6 experiments gives the following values at 298K.

$$k_2 = 5.0 \times 10^{-11} \text{ cm}^3 \text{ molecule}^{-1} \text{ s}^{-1}$$

$$k_3 = 5.7 \times 10^{-13} \text{ cm}^3 \text{ molecule}^{-1} \text{ s}^{-1}$$

Results of a more detailed analysis using computer simulation of data at several temperatures in the range 278 - 343K will be presented at the conference.

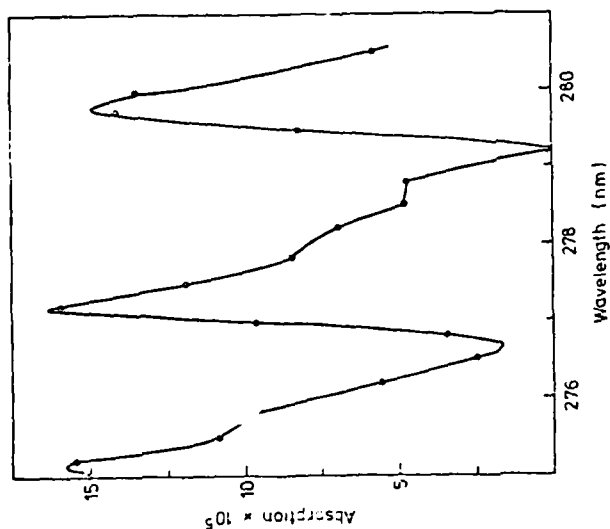


Fig. 1 Absorption Spectrum of ClO in the $A_2\Pi - X_2\Pi$ system recorded during 65 Hz modulated photolysis of $Cl_2-ClONO_2$ mixtures

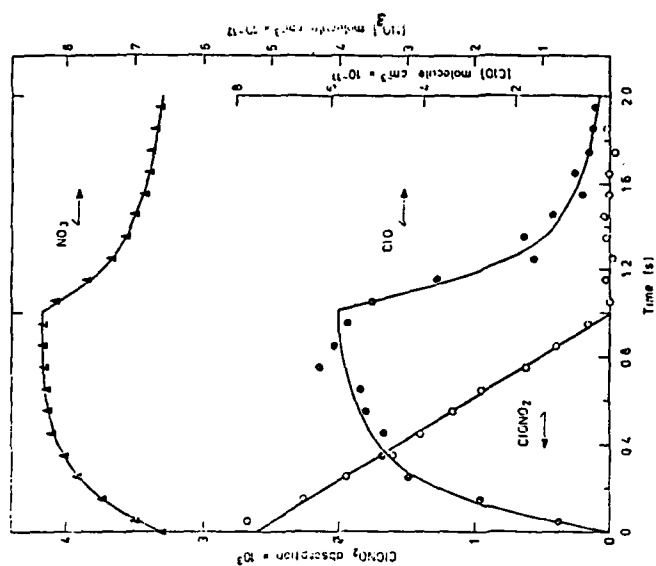


Fig. 2 Concentration-time behaviour of NO_2 , ClO and $ClONO_2$ during a single cycle of 0.5 Hz modulated photolysis of $Cl_2-ClONO_2$ mixtures at 1 atm, 298K. Lamp on: 0-1s.

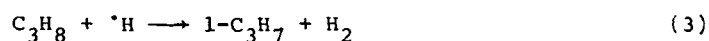
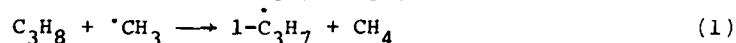
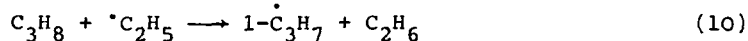
EFFECTS OF OLEFINS ON THERMAL DECOMPOSITION OF PROPANE

A. Dombi and P. Huhn

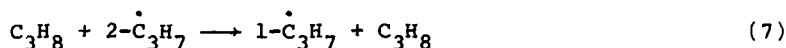
Institute of Inorganic and Analytical Chemistry University of Sciences, Szeged, Hungary

The decomposition of propane has been chosen as a model reaction for the study of the inhibiting effect of olefines. The decomposition of propane and the influence of olefines (ethylene, propylene and 2-butene) added in large quantities (0-100 v/v %) has been studied at a low extent of reaction (less than 0.2 %) in the temperature range 760-830 K and in the propane concentration range 10-175 torr.

The generally accepted decomposition mechanism of Rice-Herzfeld type for propane is as follows:



This mechanism does not give an explanation for the experienced change of the ratio $(v_{\text{CH}_4} + v_{\text{C}_2\text{H}_6} / v_{\text{H}_2} + v_{\text{C}_3\text{H}_6})$ describing the two channels belonging to the 1-C₃H₇ and 2-C₃H₇ radicals. For this purpose, it is enough to complete the mechanism with the intermolecular isomerization reaction:

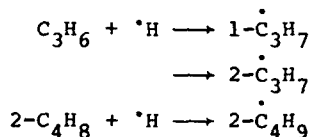


The added olefines inhibited the decomposition in different ways, the effect of ethylene was moderate, while a small amount (a few %) of propylene and 2-butene reduced the formation of products by about 10 %. The inhibiting effect of ethylene can be interpreted by

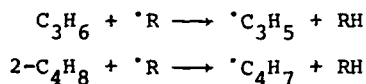


and reactions 9, 10 and 10* following it. (The ratio of the inhibiting and decomposition reactions has been determined from that of the formed ethane and the main decomposition products.) Further, it was stated that the relative formation rate of the 1-propyl and 2-propyl radicals was practically unchanged for the effect of ethylene, which can be interpreted by the fact that the selectivity of the H-atom, the methyl and ethyl radicals is the same in the hydrogen abstraction from the methyl and methylene groups of propane.

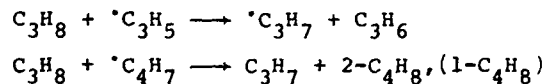
The inhibiting effect of propylene and 2-butene can be interpreted by addition reactions

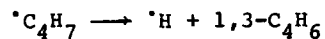


as well as by rapid reactions

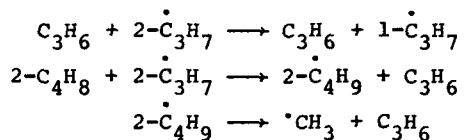


(where $\text{R} = \cdot\text{H}, \cdot\text{CH}_3, 2\text{-}\dot{\text{C}}_3\text{H}_7$). These radicals replace the chain cycle very slowly in reactions





The increase of the ratio $v_{\text{H}_2}/v_{\text{CH}_4}$ at small propylene concentration, then its rapid decrease by the increase of the amount of propylene, moreover, the characteristic change of the CH_4 and C_3H_6 excess formed on the effect of 2-butene requires the completion of the mechanism with reactions



The Arrhenius parameters of the rate constants and their ratio have been determined by the quasi-stationary treatment (allowed on the basis of our calculations) of the kinetically not so complex mechanism for the decomposition of propane and the inhibiting effect of ethylene.

The adequacy of the presented chemical mechanism of propylene and 2-butene is underlined by computer simulations, the description of which is not possible because of conciseness.

VIBRATIONAL RELAXATION OF HIGHLY
EXCITED HF AND DF

L. S. Dzelzkalns and F. Kaufman,
Department of Chemistry, University of
Pittsburgh, Pittsburgh, PA 15260, U. S. A.

The fast flow, infrared chemiluminescence method¹⁻³ is used to measure step-wise ($\Delta v = -1$) vibrational energy transfer rate constants for HF($v=5-7$) and DF($v=9-12$) at thermal ($T \sim 300$ K) rotational and translational temperature for the quencher molecules N_2 , CO, CO_2 , N_2O , HF, and DF. The excited HF(v), DF(v) molecules are prepared by the H , $D + F_2$ reactions in the field of view of a liquid nitrogen cooled circularly variable filter, InSb detector, spectrometer. The initial distributions, in the absence of added quencher, are vibrationally entirely unrelaxed. The vibrational energy disposal, $\langle f_v \rangle$ is 0.53 for HF and 0.64 for DF, as a consequence of the light atom anomaly. For DF(v), the distribution peaks at $v=9$ whereas Jonathan et al.'s⁴ peaked at $v=10$, but shows no sign of partial vibrational relaxation when reactant concentrations are varied.

The outstanding characteristic of the relaxation rate constants is their large magnitude, approaching and sometimes exceeding the Lennard-Jones collision frequency for the highest v -levels. Table 1 lists 42 quenching probabilities, P , per Lennard-Jones collision, $k_{LJ} = \pi d_{AB}^2 \bar{c} \Omega^{(2,2)}$, as well as the rotationless V-V energy gaps for six quenchers. For $Q=N_2$, there is a strong v -dependence for both HF(v) and DF(v), although for DF(v) the ΔE_{V-V} dependence is negative, i.e. the rate constant increases with increasing endothermicity. For $Q=CO$, CO_2 , and N_2O , DF(v) relaxation is somewhat faster than HF(v), probably because of its closeness to V-V energy resonance, but the ΔE_{V-V} dependence is still wrong for DF(v) when plotted as a Lambert-Salter diagram. The very fast relaxation of HF(v)

in spite of the large V-V energy gaps may be rationalized as being due to $v_2 + v_3$ excitation in CO_2 and N_2O , but this explanation obviously does not apply to Q=CO which is only a factor of two slower.

The four HF-DF energy transfer processes are clearly V-R,T, i.e. independent of the sign or magnitude of ΔE_{v-v} . They are extremely fast, ~ 0.5 to 1.7 times gas kinetic, and strongly v -dependent, $P \sim v^{2.5 \text{ to } 3}$. Although this may be ascribed to HF-HF dimer formation with binding energy of the order of 6 kcal/mol and is in rough agreement with the results of trajectory calculations,⁵ the same mechanism cannot be invoked for the other quenchers whose Q-HF binding energies are much lower, but whose P 's are almost as large. A generally applicable, physical model of the process is still lacking.

1. B. M. Berquist, J. W. Bozzelli, L. S. Dzelzkalns, L. G. Piper, and F. Kaufman, J. Chem. Phys. 76, 2972 (1982).
2. L. S. Dzelzkalns and F. Kaufman, J. Chem. Phys. 77, 3508 (1982).
3. L. S. Dzelzkalns and F. Kaufman, J. Chem. Phys., in press.
4. N. B. H. Jonathan, J. P. Liddy, P. V. Sellers, and A. J. Stace, Mol. Phys. 39, 615 (1980).
5. M. E. Coltrin and R. A. Marcus, J. Chem. Phys. 76, 2379 (1982).

TABLE 1
QUENCHING PROBABILITIES, P, PER LENNARD-JONES GAS KINETIC
COLLISION AND V-V ENERGY GAP, $\Delta E_{V-V}^{(a)}$.

		HF(v)			DF(v)			
		v = 5	6	7	9	10	11	12
Q = N ₂	P	0.002 ^b	0.010	0.039	0.02 ^b	0.049	0.074	0.13
	ΔE_{V-V}	970	814	660	-106	-186	-267	-347
CO	P	0.13	0.29	0.38	0.56 ^b	0.71	0.57	0.41
	ΔE_{V-V}	1156	1000	846	80	0	-81	-161
CO ₂	P	0.23	0.44	0.79	0.59 ^b	0.66	0.71	0.80
	ΔE_{V-V}	950	794	640	-126	-206	-287	-367
N ₂ O	P	0.34	0.49	0.81	0.97 ^b	0.74	0.73	0.69
	ΔE_{V-V}	1075	919	765	-1	-81	-162	-242
HF	P	0.47	0.96	1.45	0.86 ^b	1.17	1.44	1.72
	ΔE_{V-V}	-663	-819	-973	-1739	-1319	-1900	-1980
DF	P	0.51	0.84	1.24	0.67 ^b	0.79	1.07	1.37
	ΔE_{V-V}	392	236	82	-684	-764	-845	-925

(a) units cm⁻¹; positive ΔE_{V-V} means exoenergetic energy transfer; for CO₂ and N₂O, acceptor frequency is asymmetric stretch, ν_3 .

(b) less accurate due to cascade effect or low rate.

"A quasiclassical trajectory study of collisions of He with electronically, rotationally and vibrationally excited HD and H₂"

by

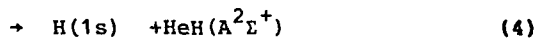
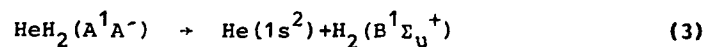
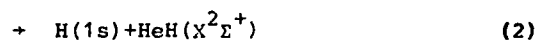
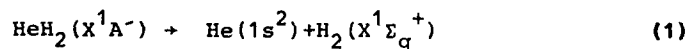
Stavros C. Farantos

Theoretical and Physical Chemistry Institute

National Hellenic Research Foundation

Vas. Constantinou 48 Ave., Athens 116/35, Greece

Extended ab initio MRD-CI [1] calculations on the ground and first singlet excited state (¹A⁻) of HeH₂ have been used to construct analytical potential energy surfaces with the Sorbie-Murrell method [2]. The functions describe correctly all dissociation channels of HeH₂:



The potential of the excited state reproduces the main characteristics of the surface. That is a well of 1.58 eV below the dissociation channel (3) on the entrance to which there is a barrier of 0.15 eV (figure 1).

Quasiclassical dynamics has been used to study electronic quenching and vibrational energy transfer cross sections in collisions of ^4He with $\text{H}_2(\text{B } ^1\Sigma_u^+)$ and its isotopic substitute HD. Non-adiabatic transitions from the excited to the ground state are treated within the Landau-Zener approximation. Making the assumption that trajectories which jump to the ground state will dissociate and never return to the excited surface, we find that the long lived complex results in an almost unit transition probability at least for room temperature collisions. The results of $^4\text{He}+\text{HD}(v=3, J=2)$ are in qualitative agreement with the experimental results of Fink et al [3]. The discrepancies should be attributed to strong tunnelling effects and to the inaccuracies of the potential energy surfaces. Another interesting outcome of these calculations is the following observation; the electronic quenching cross section decreases with increasing rotational energy of the diatom (figure 2). This behaviour is typical in reactive scattering when there is one favoured orientation. In the present case this is a 45° degree approach of He to $\text{HD}(\text{B } ^1\Sigma_u^+)$. Other results will be presented at the conference.

References

1. S.C.Farantos, G.Theodorakopoulos and C.A.Nicolaides, *Chem.Phys.Lett.* **100**, 263, 1983
2. K.S.Sorbie and J.N.Murrell, *Mol.Phys.*, **29**, 1387, 1975
3. E.H.Fink, D.L.Akins and C.B.Moore, *J.Chem.Phys.* **56**, 900, 1972.

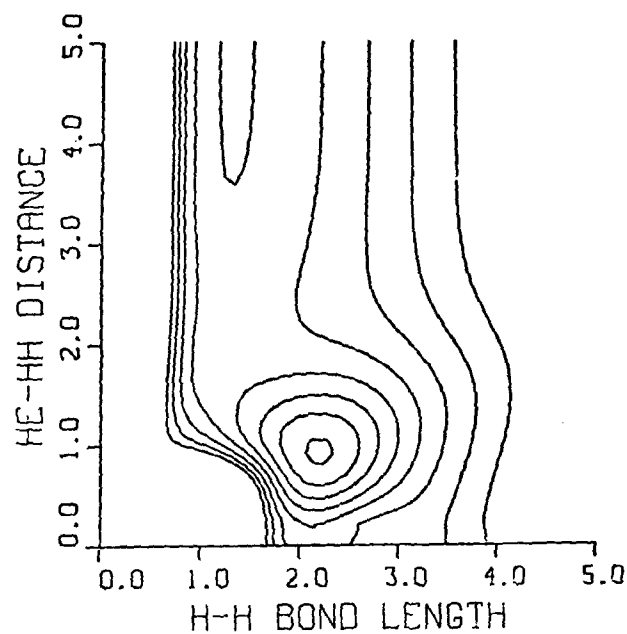


Fig.1 Contour diagram for the first singlet excited surface of HeH_2 . He approaches the middle of H_2 at the angle of 45° .

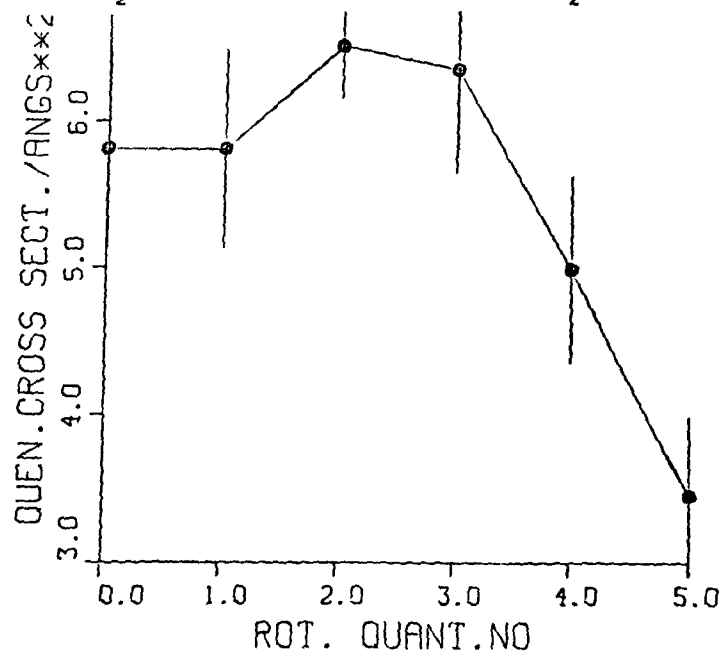


Fig.2 Electronic quenching cross section as a function of the initial rotational quantum number for room temperature collisions of $^4\text{He}+\text{HD}(\text{B}^1\Sigma_u^+, v_i=3, J_i)$

COLLISIONAL ENERGY TRANSFER AND MACROSCOPIC
DISEQUILIBRIUM

W. Forst, Department of Chemistry, Laval University, Quebec Canada
G1K 7P4

Relaxation of internal energy of a molecule (y) following laser (or any other) excitation in the presence of a heat bath is an experimental observable that represents a macroscopic (bulk) average (denoted by $\langle\langle \dots \rangle\rangle$), since it involves an average over the instantaneous (time-dependent) population distribution $c(y,t)$:

$$\langle\langle y \rangle\rangle = \int y c(y,t) dy \quad (1)$$

Here $c(y,t)$ is the fractional population of molecules of internal energy y at time t ; thus $\langle\langle y \rangle\rangle$ is time-dependent, and over the course of the time history of the system it decays from $\langle\langle y \rangle\rangle_0$ (initial average energy at $t=0$) to $\langle\langle y \rangle\rangle_\infty$, the final internal energy, which is the average energy of the molecule of interest at the temperature of the heat bath (a constant). Of particular interest in the present context is the bulk average energy transfer $\langle\langle \Delta E \rangle\rangle$ defined by

$$\langle\langle \Delta E \rangle\rangle = \int \langle \Delta E \rangle c(y,t) dy \quad (2)$$

i.e. the average of $\langle \Delta E \rangle$ over $c(y,t)$. $\langle \Delta E \rangle$ is the average energy transferred per collision, a microscopic property. Since measurements on a system in macroscopic disequilibrium can yield only bulk averages (e.g. $\langle\langle \Delta E \rangle\rangle$), $\langle \Delta E \rangle$ is not normally accessible to direct measurement.

From (1), the time derivative of $\langle\langle y \rangle\rangle$ is

$$\frac{d \langle\langle y \rangle\rangle}{dt} = \int y \frac{d c(y,t)}{dt} dy \quad (3)$$

It can be shown that in any non-reactive system

$$\frac{d \langle\langle y \rangle\rangle}{dt} = \omega \langle\langle \Delta E \rangle\rangle \quad (4)$$

where ω is the collision frequency. Since (in a laser system) $\langle\langle y \rangle\rangle$ decreases with time and ultimately decays to a constant,

$d\langle y \rangle / dt$ and $\langle \Delta E \rangle$ are both negative and time-dependent, and both must ultimately decay to zero. The result $\langle \Delta E \rangle = 0$ simply means that at equilibrium there is no net energy transfer in the bulk (macroscopic) system. On the microscopic level, of course, in any individual collision energy continues to be transferred up and down randomly. The time decay of $\langle y \rangle$ and $\langle \Delta E \rangle$ in an actual experimental system is shown in FIGS. 1 and 2.

The microscopic property $\langle \Delta E \rangle$ can be shown to be the first moment of the collisional transition probability $q(x,y)$:

$$\langle \Delta E \rangle = \int (x - y) q(x,y) dx \quad (5)$$

where $q(x,y)$ is the probability that if the internal energy of the molecule of interest before the collision was y , it shall be x after the collision. The usual procedure for analyzing experimental data on collisional energy transfer is to postulate some (hopefully reasonable) form of $q(x,y)$ and then, in effect, work one's way backward through $\langle \Delta E \rangle$ (eq. 5) to some bulk average directly related to an experimental observable. This will be illustrated using the exponential form¹ of $q(x,y)$ where it turns out that the system does not undergo simple exponential decay because the exponential transition probability does not satisfy the so-called "linear sum rule". The bulk average $\langle \Delta E \rangle$ is constrained to a maximum which is independent of the nature and the level of initial excitation, thus producing a bottleneck in the macroscopic relaxation process.

However if the initial distribution $c(y,0)$ is a delta function

$$c(y,0) = \delta(y_0 - y) \quad (6)$$

then, as $t \rightarrow 0$, $\langle \Delta E \rangle \rightarrow \langle \Delta E \rangle$, i.e. a direct connection exists between the macroscopic observable $\langle \Delta E \rangle$ and the microscopic property $\langle \Delta E \rangle$. For this approach to be successful, it is necessary, in addition to ensuring that the initial distribution is indeed a delta function, to obtain experimental data as close to $t = 0$ as possible.

Such is the case of azulene² (Fig. 1), in which the time decay of $\langle\langle y \rangle\rangle$ is obtained by monitoring the infrared fluorescence. From the time dependence of $\langle\langle y \rangle\rangle$ one then obtains the time dependence of $\langle\langle \Delta E \rangle\rangle$ (Fig. 2) via eq. (4) which, after a short extrapolation to $t = 0$ yields $\langle\langle \Delta E \rangle\rangle_0 = \langle \Delta E \rangle$, in this case 1400 cm^{-1} . Note that the microscopic property $\langle \Delta E \rangle$ (average energy transferred per collision) was obtained from the bulk average $\langle\langle \Delta E \rangle\rangle$ without any assumption as to the nature of the collisional transition probability. It is thus possible to make a model-independent connection between a macroscopic and microscopic property³.

1. W. Forst, J. Chem. Phys. 80 2504 (1984)
2. J. R. Barker, J. Phys. Chem. 88 11 (1984)
3. W. Forst and J. R. Barker, in preparation

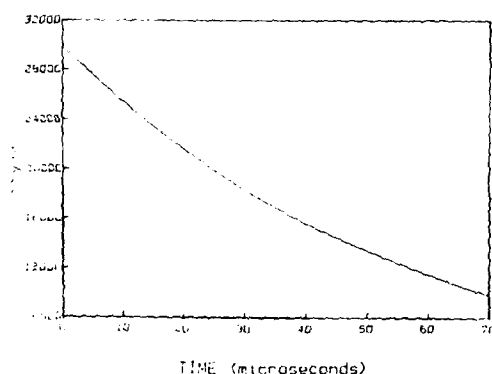


Fig. 1.
Time dependence of
 $\langle\langle y \rangle\rangle \text{ (cm}^{-1}\text{)}$
8.9 mtorr pure azulene
One-photon laser
excitation at 337 nm.
Initial energy 30644 cm^{-1}

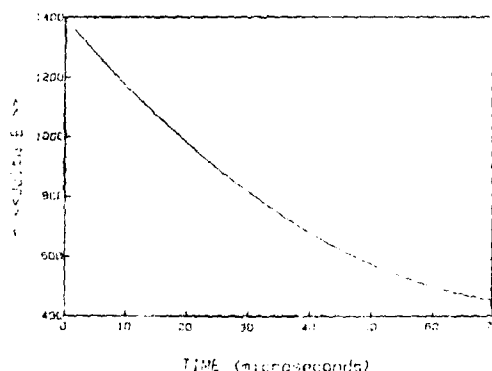


Fig. 2.
Time dependence of
 $\langle\langle \Delta E \rangle\rangle \text{ (cm}^{-1}\text{)}$
Same system as in Fig. 1.

STUDY OF THE EQUILIBRIUM $i\text{-C}_3\text{H}_7 + \text{O}_2 \rightleftharpoons i\text{-C}_3\text{H}_7\text{O}_2$

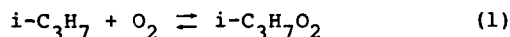
I. R. Slagle, E. Ratajczak, M. C. Heaven, and D. Gutman
 Department of Chemistry, Illinois Institute of Technology
 Chicago, Illinois 60616, U.S.A.

and

A. F. Wagner
 Chemistry Division, Argonne National Laboratory
 Argonne, Illinois 60439, U.S.A.

ABSTRACT

The reaction of $i\text{-C}_3\text{H}_7$ with molecular oxygen was studied in a temperature range in which the equilibrium,

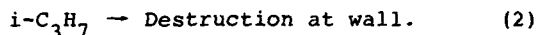


could be directly observed in time-resolved experiments. The equilibrium constant for Reaction 1 was measured at seven temperatures between 590 and 690K. These determinations were combined with Third-Law calculations of ΔS° for this equilibrium to obtain $\Delta H_{298}^\circ = -144(^{\pm}6)$ kJ for Reaction 1.

Studies were conducted in a heated tubular reactor coupled to a photoionization mass spectrometer.^{1,2} Pulsed 193nm radiation from a Lumonics TE-860-4 excimer laser was directed along the axis of the 35cm-long, 0.95cm i.d. Pyrex reactor to produce $i\text{-C}_3\text{H}_7$ radicals from the photolysis of $i\text{-C}_3\text{H}_7\text{Br}$. Gas was continuously sampled from an orifice in the side of the reactor, formed into a beam by a conical skimmer and continuously analyzed with a photoionization mass spectrometer.

Experiments were conducted under pseudo-first-order conditions ($[\text{O}_2] / [i\text{-C}_3\text{H}_7]_0 > 100$) and at O_2 concentrations that

placed the $[i\text{-C}_3\text{H}_7] / [i\text{-C}_3\text{H}_7\text{O}_2]$ ratio at equilibrium between 0.2 and 0.8 at each temperature. The $i\text{-C}_3\text{H}_7$ ion-signal profiles displayed the expected relaxation to equilibrium in the presence of a slower parallel heterogeneous reaction,



The ion-signal profiles were fitted to a function containing the sum of two exponentials,

$$I(i\text{-C}_3\text{H}_7^+) = C_1 \exp(-m_1 t) + C_2 \exp(-m_2 t).$$

The equilibrium constant for Reaction 1 was obtained from $R_{12} = C_1 / C_2$, m_1 , m_2 , and $[\text{O}_2]$. In the absence of Reaction 2, the equilibrium constant is $R_{12}[\text{O}_2]$.

The relatively small change in $\Delta G^\circ = -RT \ln K_p$ for Reaction 1 over the 100° temperature range of this study prevented the accurate determination of ΔH_{298}° for this reaction using data treatments based on the Second Law. Third Law determinations of ΔS° were therefore obtained using structural data or estimates and were also calculated using group-additivity procedures. These determinations of ΔS° were used to obtain the value of ΔH_{298}° for Reaction 1 from the direct determinations of ΔG° .

The experiments, the data analysis, a comparison of ΔS° determinations by the two methods mentioned, and a comparison of our determination of ΔH° with prior estimates will be presented.

-
1. I. R. Slagle, F. Yamada, and D. Gutman, J. am. Chem. Soc. 1981, 103,149-53.
 2. J.-Y. Park, M. C. Heaven, and D. Gutman, Chem. Phys. Lett. 1984,104,469-74.

VIBRATIONAL INDUCED DISSOCIATION OF TETRAMETHYLDIOXETANE
BY OVERTONE AND INFRARED MULTIPLE PHOTON ABSORPTION

S. Ruhman, O. Anner and Y. Haas
Department of Physical Chemistry and
The Fritz Haber Center for Molecular Dynamics
The Hebrew University, Jerusalem, Israel

Tetramethyldioxetane (TMD) undergoes facile dissociation following either overtone¹ (OT) or infrared multiple absorption² (IRMPA) excitation. The reaction can be followed in real time by monitoring the resulting chemiluminescence. In this paper we report quantitative comparison of the reaction rates and absolute dissociation yields obtained by these two methods. Assuming rapid intramolecular energy scrambling, the OT data are used to estimate the energy distribution of IRMPA-excited molecules at different fluence levels. The quantum yield of the OT experiments can be estimated from the absorption coefficients and dissociation rate constants. Those obtained following IRMPA are then derived by comparing the signal intensity registered under identical experimental conditions. The results are interpreted in terms of a rate equation model, which takes into account the changes in the IR absorption cross section and the spatial form of the TEM₀₀ CO₂ laser beam. A partial mapping of the energy distribution of the molecules following IRMPA is obtained.

The nature of the emitting species is probed by monitoring the emission of acetone following UV excitation at the $n\pi^*$ transition at low pressure (10^{-3} - 10^{-2} Torr). The results indicate that vibrationally excited singlet and triplet acetone states are involved. The nature of the emitting species formed by the chemiluminescent reaction, and the validity of the spin discriminating approximation is discussed.

-
- ¹ S. Ruhman, O. Anner and Y. Haas, Chem. Phys. Lett. 99, 281 (1983).
² B.D. Cannon and F.F. Crim, J. Chem. Phys. 75, 1752 (1981), J. Am. Chem. Soc. 103, 6722 (1981).

Separation of fluence and intensity effects in infrared
multiple photon absorption

G. Hancock, A.J. MacRobert, K.G. McKendrick and J.H. Williams

Physical Chemistry Laboratory, Oxford University, Oxford OX1 3QZ, U.K.

Summary

Recent experimental evidence has shown that processes induced by multiple photon absorption (MPA) of ir radiation depend not only upon the laser fluence (J cm^{-2}) but also upon the laser intensity (W cm^{-2}). Quantitative determination of such effects however requires ir laser pulses of particularly well defined spatial and temporal profiles, far removed from the standard TEA multimode CO_2 pulses used in the vast majority of infrared photochemistry experiments. We have used such 'shaped' pulses to determine quantitative and separate intensity and fluence effects in several molecules, including MPA in SF_6 .

Pulses were formed by slicing a constant power section from the output of a single transverse and longitudinal mode CO_2 laser oscillator by means of an electrooptic crystal switch, and subsequently amplifying these. The temporal form of each pulse was rectangular, with fast ($< 5 \text{ ns}$) rise and fall times, and constant power (to within 10%) between these for durations ranging from 50-1000 ns; their spatial profile was Gaussian. True dependences of quantities such as MPA cross sections upon fluence (at constant intensity) and intensity (at constant fluence) can be found straightforwardly from measurements with these shaped pulses.

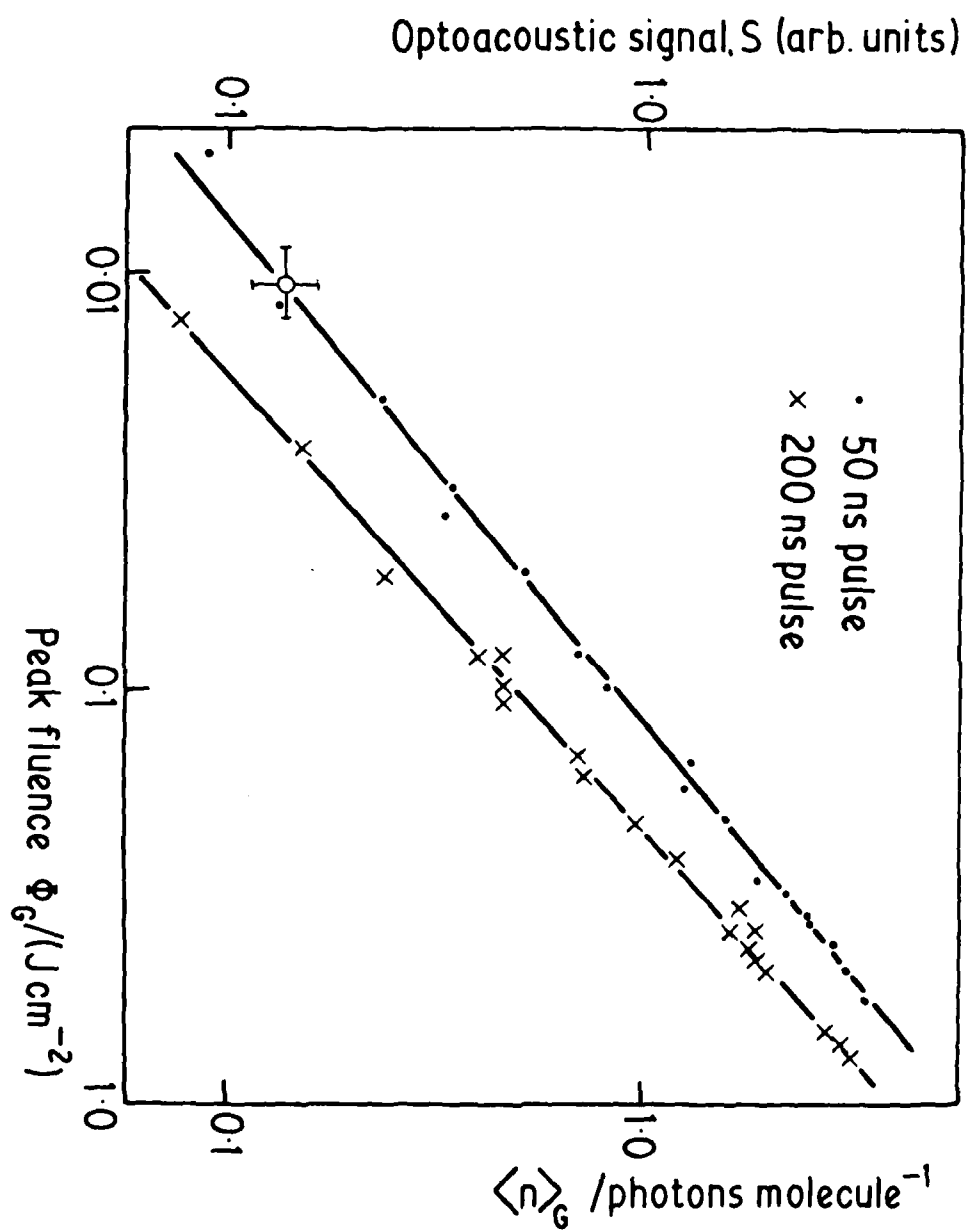
As an example, Fig. 1 shows the optoacoustic signal resulting from energy absorbed by SF_6 (100 m Torr) at 944.2 cm^{-1} as a function of peak

'Separation of fluence and intensity effects

G. Hancock et al., Oxford.

fluence (the value at the Gaussian beam centre) for pulses of length 50 and 200 ns. Collisional effects are negligible in these experiments, and the increase in signal with decrease in pulse length is due to the increased laser intensity. Long path absorption experiments put the data on an absolute basis, and deconvolution allows the fluence ϕ and intensity I dependences to be found. For example, the cross section σ varies as $I^{0.4}$ for $0.5 < I < 2 \text{ MW cm}^{-2}$ at a constant fluence of 100 mJ cm^{-2} , and as $\phi^{-0.5}$ for $50 < \phi < 200 \text{ mJ cm}^{-2}$ at a constant intensity of 1 MW cm^{-2} . Other intensity dependences (and their separation from fluence effects) have been found with these shaped pulses, and it is hoped that quantitative data of this kind will enable theoretical estimates of the experimental results to be made.

Figure 1. Measured optoacoustic signal S (arbitrary units) as a function of peak fluence ϕ_G for 50 and 200 ns pulses absorbed in SF_6 (100 mTorr) at 944.2 cm^{-1} . These data are put on an absolute scale of $\langle n \rangle_G$, the number of photons absorbed per SF_6 molecule averaged over the Gaussian profile by a long path absorption measurement (open circle). The absolute scale is shown on the right hand side of the figure. Clearly at a given fluence $\langle n \rangle_G$ is larger when that fluence is delivered in a shorter time, i.e. a higher laser energy.



Direct Observation of Collisional Energy Transfer of
Vibrationally Highly Excited CS₂ Molecules

J. E. Dove, H. Hippler, and J. Troe

Institut für Physikalische Chemie der Universität Göttingen,
Tammannstraße 6, D-3400 Göttingen, Germany

Vibrationally highly excited CS₂ molecules in the electronic ground state have been prepared by absorption of laser pulses at 308 and 351 nm and subsequent fast electronic transition. Collisional deactivation of these molecules is followed directly by observation of hot UV spectra of CS₂ at various wavelengths in the range 220 - 380 nm. A calibration of these spectra at various excitation energies has been made by laser measurements and by separate studies in shock waves. Experiments in a large variety of bath gases show markedly different collisional deenergization properties. The average energies transferred per collision vary strongly with CS₂ excitation energy. Energy transfer becomes increasingly less efficient with decreasing CS₂ energy.

To be presented as an oral contribution in the topic area D.

Crossed beam study of reaction of van der Waals molecule $O + (NO)_2 \longrightarrow NO_2^* + NO$: Angle-resolved chemiluminescence detection.

Kenji Honma and Okitsugu Kajimoto

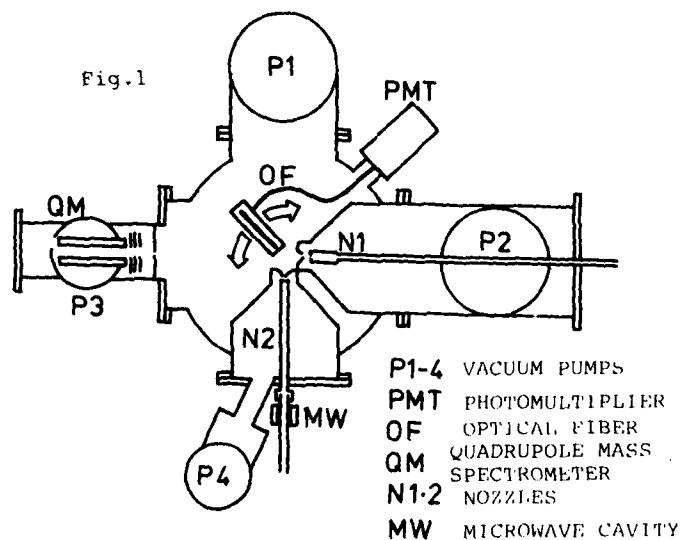
Department of Pure and Applied Sciences, University of Tokyo,
3-8-1 Komaba, Meguro, Tokyo, JAPAN 153

Chemiluminescence of NO_2^* from the reaction, $O + NO + M$, has been widely studied and the rate constants for various third body M have been well established.¹⁾ We studied the bimolecular reaction of NO dimer with O atom,



by use of a crossed beam apparatus together with an angle-resolved chemiluminescence detector. Since one of the NO molecules of dimer plays a role of "build-in" third body in this case, this is a good opportunity to study the details about the role of the third body in the recombination reactions.

The apparatus used in this research is shown in Fig.1. NO dimer was generated by supersonic expansion of the gas mixture of 12% NO with He through



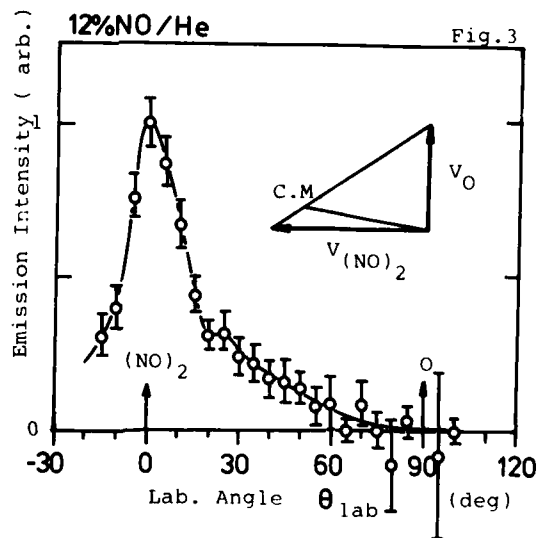
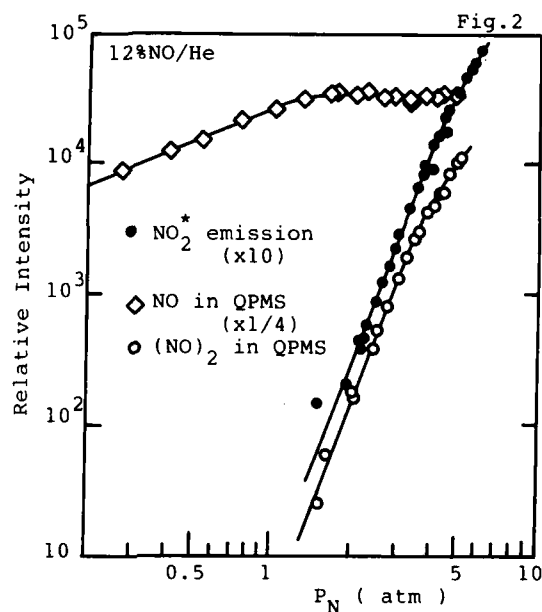
a 0.03 mm diameter nozzle and collimated by a skimmer. Oxygen atom, generated by the 2.45 GHz microwave discharge in the mixture of O_2 with Ar, issued effusively from a 1.0 mm Teflon nozzle. This beam was also collimated by a skimmer and crossed with $(NO)_2$ beam at right angles. The emission from NO_2^* scattered to a certain angle was focused by cylindrical lens onto an optical fiber bundle, guided out of the chamber and detected with a photon-counting device. The lens-fiber system can be rotated around the crossing center and enable us to measure the NO_2^* emission intensity as a function of the scattering angle (θ_{lab}).

The relative concentration of NO and $(NO)_2$ were measured with a quadrupole mass filter as a function of the nozzle pressure. NO_2^* chemiluminescence intensity was observed to change with the nozzle pressure in completely the same manner as the $(NO)_2$ as given in Fig.2. This indicates that the $(NO)_2$ is the only reactant to produce NO_2^* . Evidently, the cross section of producing NO_2^* from $O + (NO)_2$ is much larger than that of the two-body reaction $O + NO \rightarrow NO_2^*$.

The observed angular distribution is shown in Fig.3. It is quite anisotropic and peaking around $\theta_{lab}=0$ with respect to the $(NO)_2$ incidence. The Newton diagram is also shown in this figure. The velocity of $(NO)_2$ was determined by the time-of-flight method. For the velocity of O atom, the most probable velocity at 300 K is displayed. It is apparent from this Newton diagram that the product NO_2^* is scattered mainly toward sideway or backward with respect to the O atom incidence within the center-of-mass frame. This fact may suggest that O atom approaches toward the nitrogen bonding of $cis-(NO)_2^{2)}$ and rebound

as an electronically excited NO_2 molecule within one rotational period of the complex $\text{O}---(\text{NO})_2$.

- 1) See for example M. Sutoh, Y. Morioka, and M. Nakamura, J. Chem. Phys. 72, 20 (1980) and reference cited therein.
- 2) S. G. Kukolich, J. Am. Chem. Soc. 104, 4715 (1982); C. E. Dinerman and G. E. Ewing, J. Chem. Phys. 53, 626 (1970); J. Billingsley and A. B. Callear, Trans. Faraday Soc. 67, 589 (1971); J. P. Ritchie, J. Phys. Chem. 87, 2466 (1983).



An Optoacoustic Study of Infrared
Multiphoton Absorption in Polyatomic
Molecules

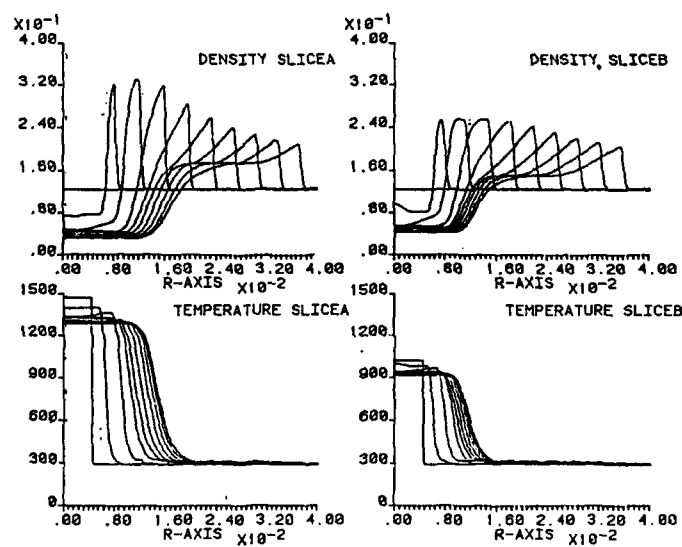
P. John and C.L. Wilson,
Department of Chemistry,
R.G. Harrison,
Department of Physics,
R.G. McGuire,
Department of Mathematics,
Heriot-Watt University, Riccarton, Currie,
Edinburgh EH14 4AS, UK.

Optoacoustic detection, o/a, is a highly sensitive method for determining the characteristics of infrared multiphoton absorption. Despite the increasing *empirical* use of optoacoustic detection, progress in describing the phenomena using pulsed laser excitation is limited. The fundamental mechanism for o/a detection is similar for both pulsed and cw excitation modes. An acoustic wave is generated after conversion of vibrational energy into translational degrees of freedom. The travelling acoustic wave can be detected by a suitable transducer e.g. a microphone.

The o/a signal comprises oscillatory structure ascribed to acoustic resonances within the cell and microphone diaphragm. The intensities and time evolution of the o/a peaks depend, in a complex fashion, on the cell dimensions and geometry and the relative positioning of the laser beam. We demonstrate that the propagation time of the initial o/a

peak is related to the absorbed fluence via the dependence of sound speed on temperature.

Calculations based on the method of characteristics have been performed which numerically solve the gas dynamic conservation equations, namely, mass, momentum and energy. An example of the results of such calculations is shown in the figure below.



Dependence of the gas density and temperature of SiF_4 (5 torr) as a function of radial distance after irradiation with TEA CO_2 pulse ($\sim 1 \text{ J cm}^{-2}$). Attenuation of the absorbed fluence is indicated by the data for the front (A) and back (B) of a 10 cm optical path length cell.

In this figure, the pressure and temperature radial distributions in a cylindrical cell are plotted at successive intervals of 20 μ s after the TEA CO₂ laser pulse. Propagation time measurements for the CO₂ laser excitation of SiF₄ and cyclobutanone will be compared with the results of gas dynamic calculations.

The reaction of $\text{NH}(\text{X } ^3\Sigma^-)$ with $\text{O}_2(^3\Sigma_g^-)$ and $\text{O}_2(^1\Delta_g)$

W. Hack, H. Kurzke, and H. Gg. Wagner

Max-Planck-Institut für Strömungsforschung,

Böttingerstraße 4-8, D-3400 Göttingen, Fed. Rep. of Germany

The formation of NH-radicals is known to be a major photochemical process in the photolysis of ammonia at wavelengths below 147 nm. Therefore it is of significant importance for many NH_3 containing photolytic systems. In combustion processes it is one of the species in the reaction scheme that determines whether fuel-nitrogen is converted to nitric oxide or to molecular nitrogen.

In this work the reaction of NH with $\text{O}_2(^3\Sigma_g^-)$ and $\text{O}_2(^1\Delta_g)$ was studied in an isothermal discharge-flow reactor, in the pressure range $1.3 \leq P/\text{mbar} \leq 10.7$ with He as the main carrier gas. NH-radicals were produced in the reaction $\text{NH}_3 + 2 \text{F} \rightarrow \text{NH} + 2 \text{HF}$ at ratios of ammonia over fluorine between $0.7 \leq [\text{NH}_3]/[\text{F}_2] \leq 3$. The decay of $\text{NH}(\text{X } ^3\Sigma^-)$ was measured under pseudo first order conditions by means of the highly sensitive and specific laserinduced fluorescence technique at $\lambda = 336 \text{ nm}$. $\text{O}_2(^1\Delta_g)$ has been produced either in a chemical generator or in a microwave discharge in oxygen.

For the reaction



the Arrhenius-expression

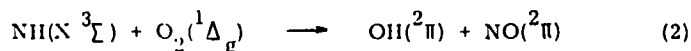
$$k_1(T) = 7.6 \times 10^{10} \exp(-6.4 \text{ kJ mol}^{-1}/R \cdot T) \text{ cm}^3/\text{mol s}$$

was obtained in the temperature range 268 to 543 K. In the pressure

range given above no dependence of the rate of reaction (1) upon this parameter was observed.

Under the experimental conditions used for the determination of the rate-constant of reaction (1), the concentration profiles of OH-radicals were recorded. The absolute concentration of OH-radicals together with the rate-constant gathered from the slope of the profiles indicate that OH is a main product of reaction (1) at these experimental conditions. No H- or O-atoms could be detected as a product of this reaction by means of atomic resonance absorption.

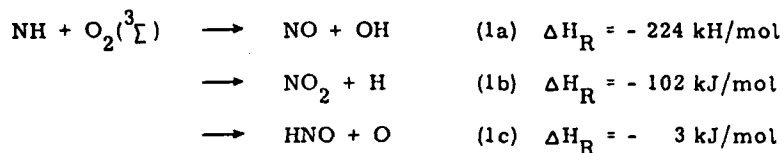
The reaction



has been investigated in separate experiments. Under the similar experimental conditions as for the measurement of reaction (1), no change in the rate of the reaction within an error limit of $\pm 10\%$ was detected. Upon addition of $\text{O}_2(^1\Delta_g)$ to the reaction system the profiles of OH-radicals did not differ significantly from those obtained in the absence of $\text{O}_2(^1\Delta_g)$. No other products than those for reaction (1) have been found. Therefore we concluded the following upper limit for reaction (2)

$$k_2(295\text{ K}) \leq 6 \times 10^{-9} \text{ cm}^3/\text{mol s.}$$

The room-temperature rate constant of reaction (1) measured in this work is in quite good agreement with that obtained by Zetzsch et al.¹⁾ in a flash-photolysis-system, the only direct investigation published so far. From the reaction paths of reaction (1), which are energetically possible:



(1b) can be ruled out since no H-atoms have been detected as a product of reaction (1). Ab initio electronic structure calculations of Binkley and Melius²⁾ indicate that there is a small energy barrier between the adduct of NH and $\text{O}_2(^3\Sigma)$ and the products of channel (1c) via a triplet surface through the metastable $\text{HNOO}(^3A')$ intermediate. This channel is supposed to have an activation energy exceeding 10 kJ/mol and a preexponential factor in the order of $10^{13} \text{ cm}^3/\text{mol s}$.

The direct formation of NO and OH is possible by a series of rearrangements of the different atoms involved into the complex on a singlet surface. This complex can be formed without a significant barrier.

The results of these calculations are consistent with our measurements, where an activation energy of 6.4 kJ/mol has been measured together with a preexponential factor far less than collision number.

Reaction (2) should occur on a triplet surface, thus favouring HNO and O-atoms as products. The addition of $\text{O}_2(^1\Delta_g)$ seems to have no influence, neither on the observed rate-constant nor on the product distribution, i.e. the effects measured upon addition of $\text{O}_2(^1\Delta_g)$ are not significant. The rate constant for reaction (2) at room temperature should not exceed that of reaction (1), resulting in the upper limit given above.

Literature

- 1) Zetzsch, C. and I. Hansen; Ber. Bunsenges. Phys. Chem. 82, 830 - 833 (1978)
- 2) Binkley, J. S. and C. F. Melius; paper WSS/CI 82-96, Fall Meeting of the Western States Section of the Combustion Institute, Livermore, CA (1982)

Figure captions

figure 1 Experimental arrangement

Fast discharge flow system with LIF and resonance absorption detection device.

figure 2 Production of NH- and NH₂-radicals v.s. the ratio of ammonia over fluorine

$$[F_2]_0 = 1.6 \times 10^{-12} \text{ mol/cm}^3 \quad t_n = 40 \text{ ms}$$

figure 3 First order plot of the decay of NH(X ³Σ_g⁻)-radicals in the presence and absence of O₂(³Σ_g⁻)

$$T = 464 \text{ K} \quad P = 2.6 \text{ mbar}$$

$$[O_2] \text{ [mol/cm}^3]$$

$$\circ \quad 0$$

$$\bullet \quad 1.9 \times 10^{-9}$$

$$\blacktriangle \quad 3.5 \times 10^{-9}$$

$$\blacksquare \quad 4.9 \times 10^{-9}$$

figure 4 Production of OH-radicals in reaction (1)

$$T = 295 \text{ K} \quad P = 2.6 \text{ mbar}$$

$$[O_2] \text{ [mol/cm}^3]$$

$$\circ \quad 1.9 \times 10^{-9}$$

$$\Delta \quad 4.1 \times 10^{-9}$$

$$\blacksquare \quad 8.1 \times 10^{-9}$$

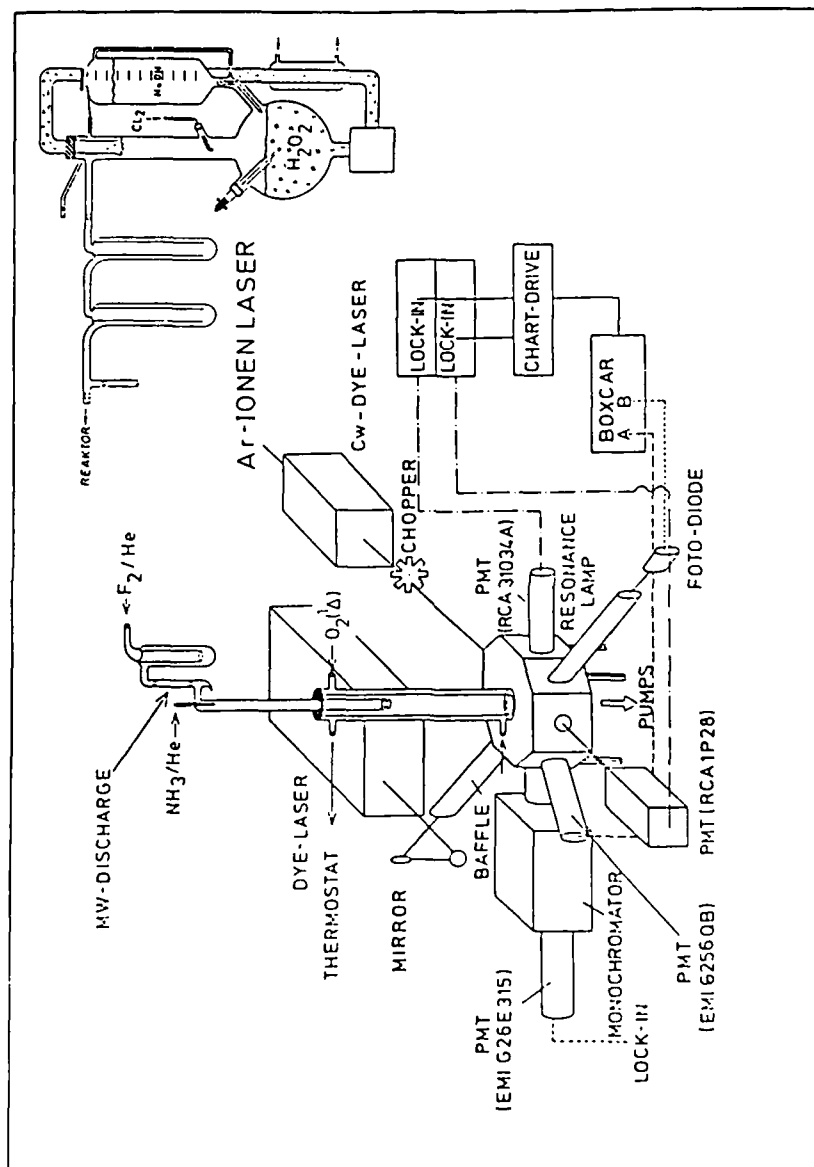
figure 5 Pseudo first-order rates for reaction (1) v.s. O₂(³Σ_g⁻)-concentration

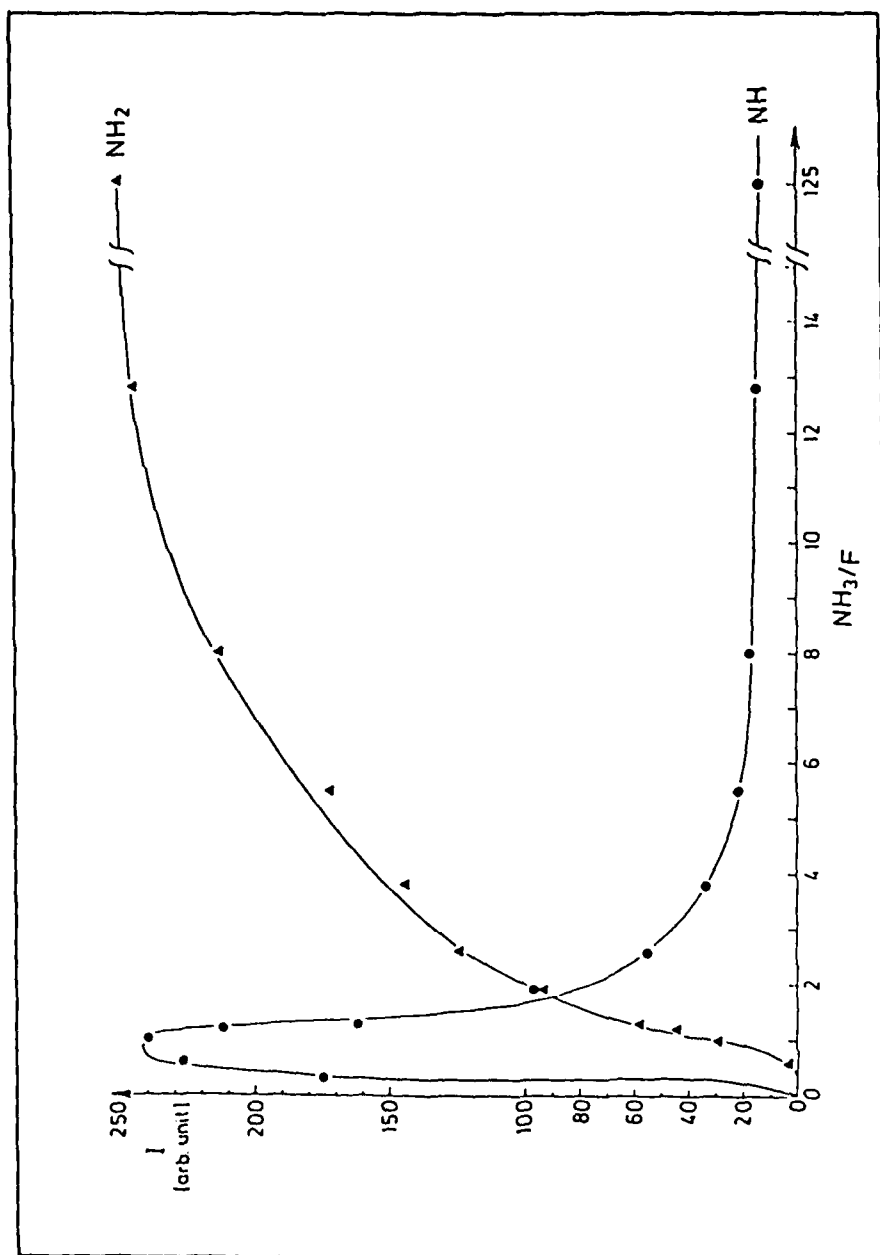
$$T \text{ [K]}$$

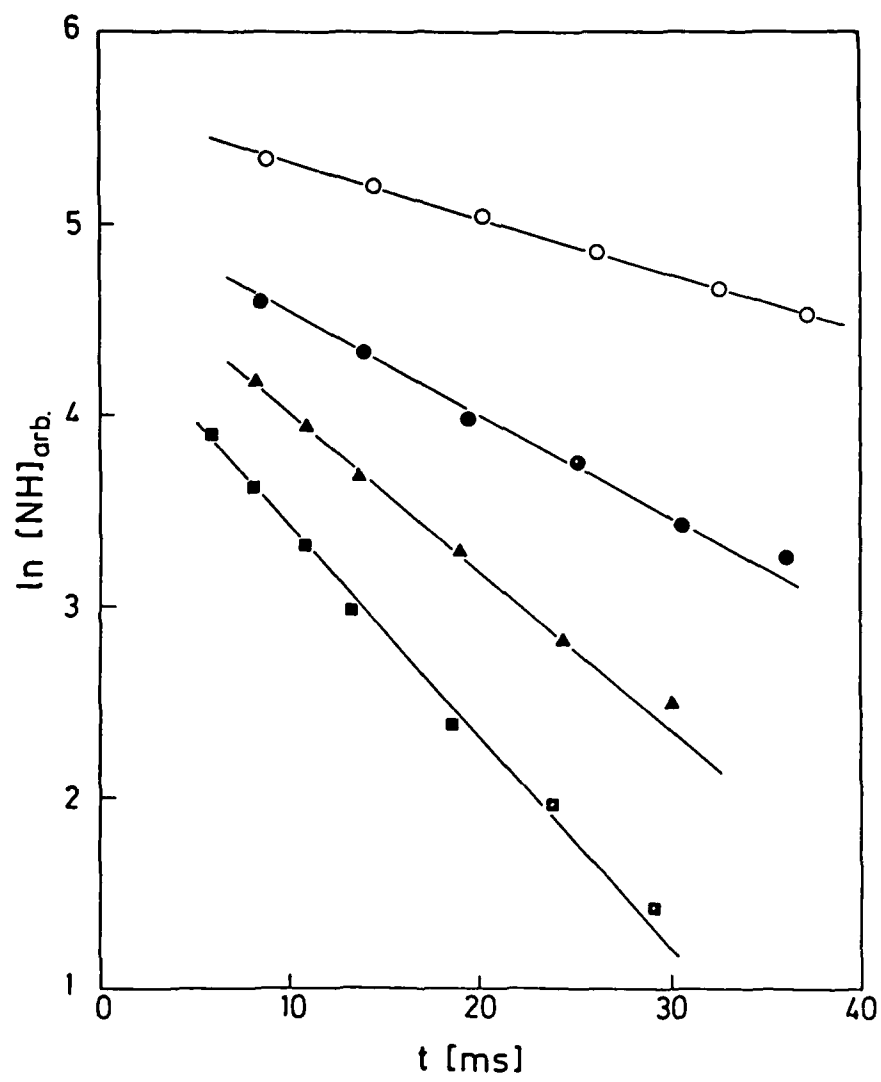
$$\bullet \quad 268, \quad \circ \quad 295, \quad \blacktriangle \quad 353, \quad \nabla \quad 398, \quad \blacksquare \quad 464, \quad \times \quad 543$$

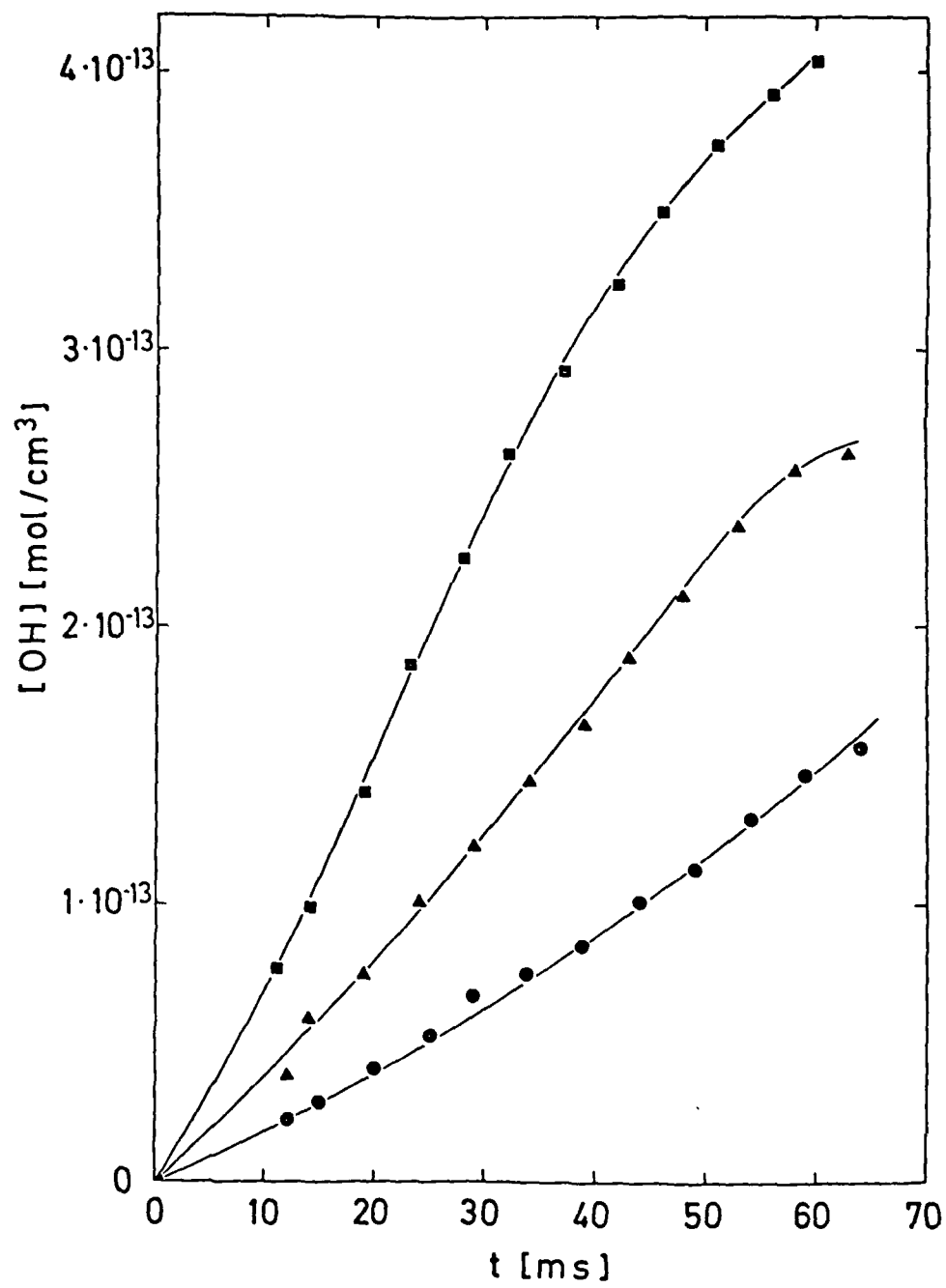
figure 6 Arrhenius-plot for reaction (1a)

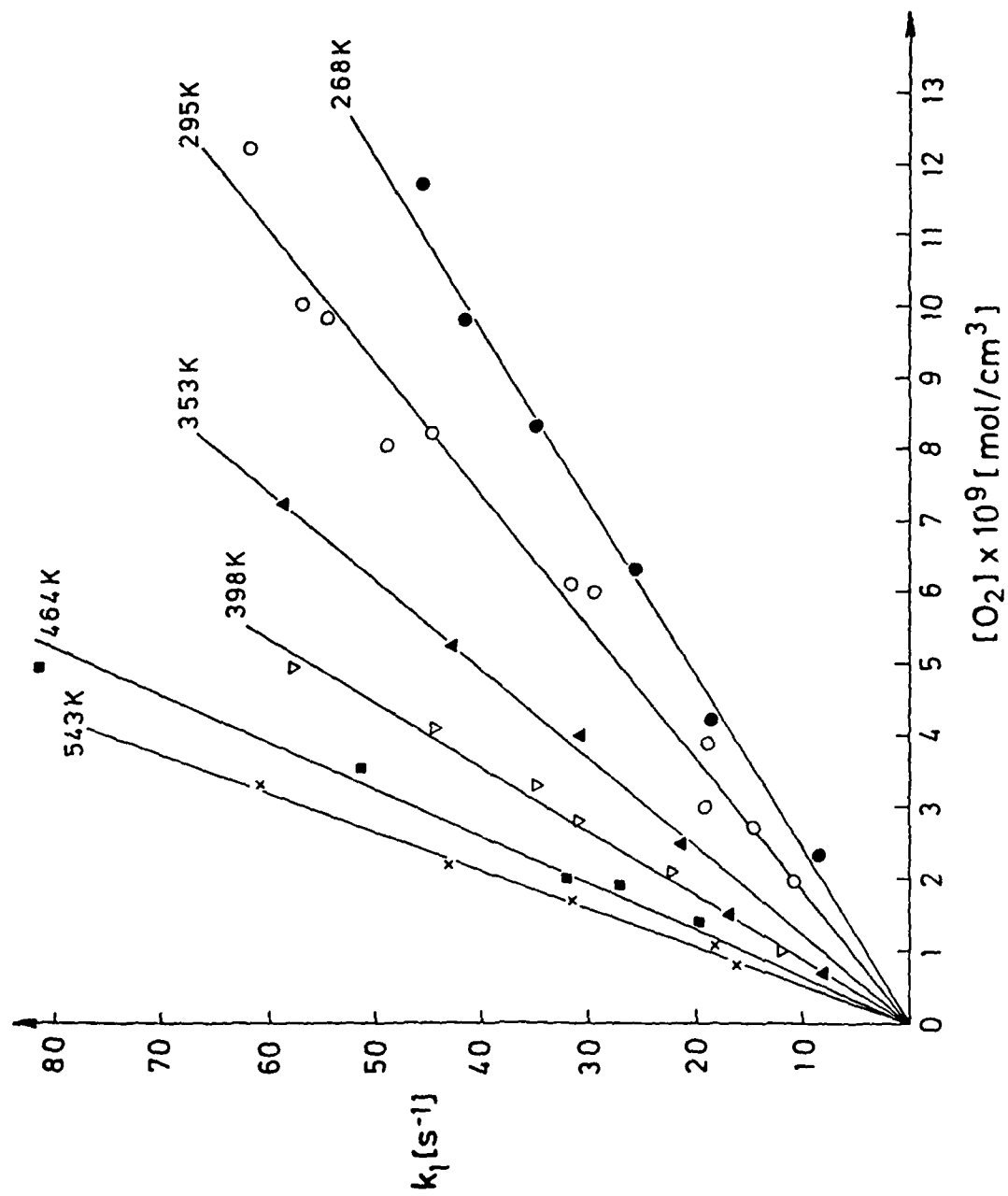
figure 7 Calculated energies of possible intermediates and products
for the reaction of $\text{NH} + \text{O}_2$
(Binkley and Melius, 1983)

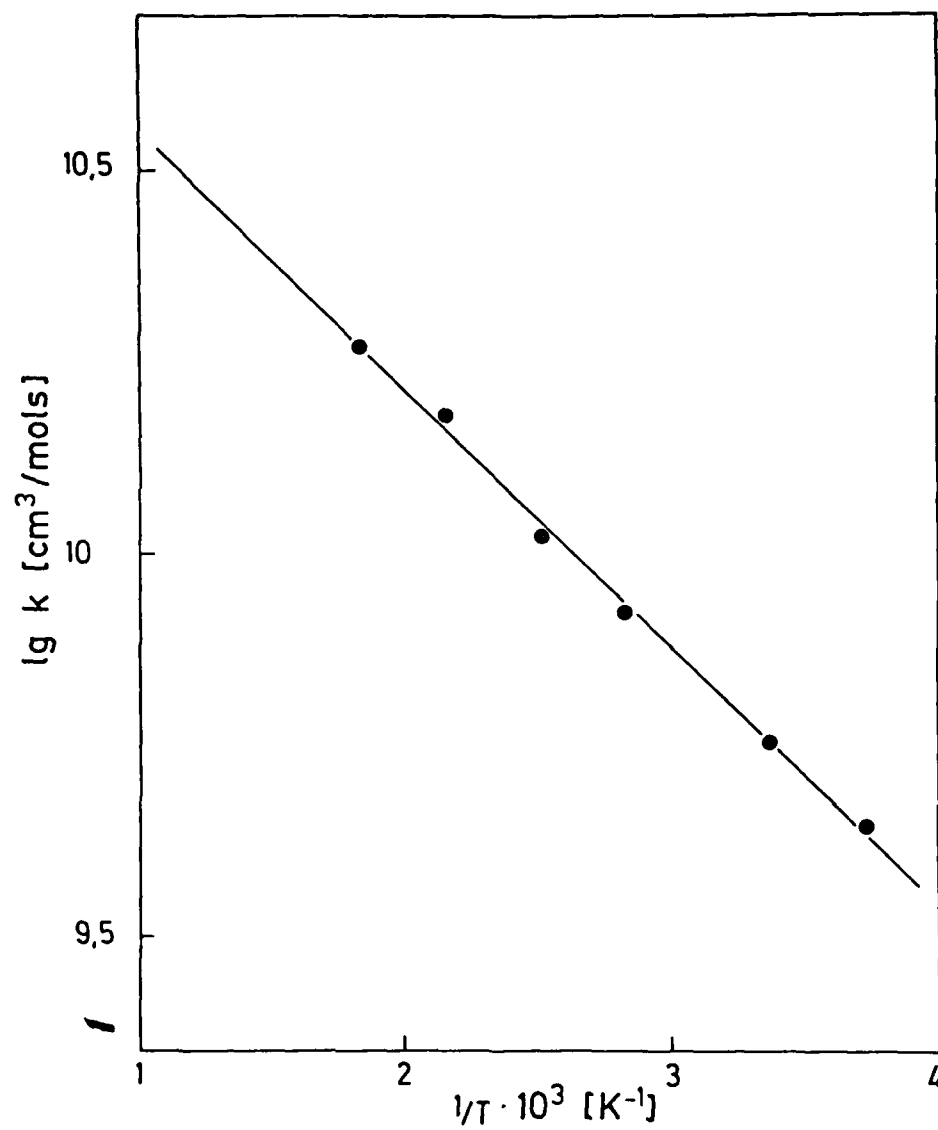


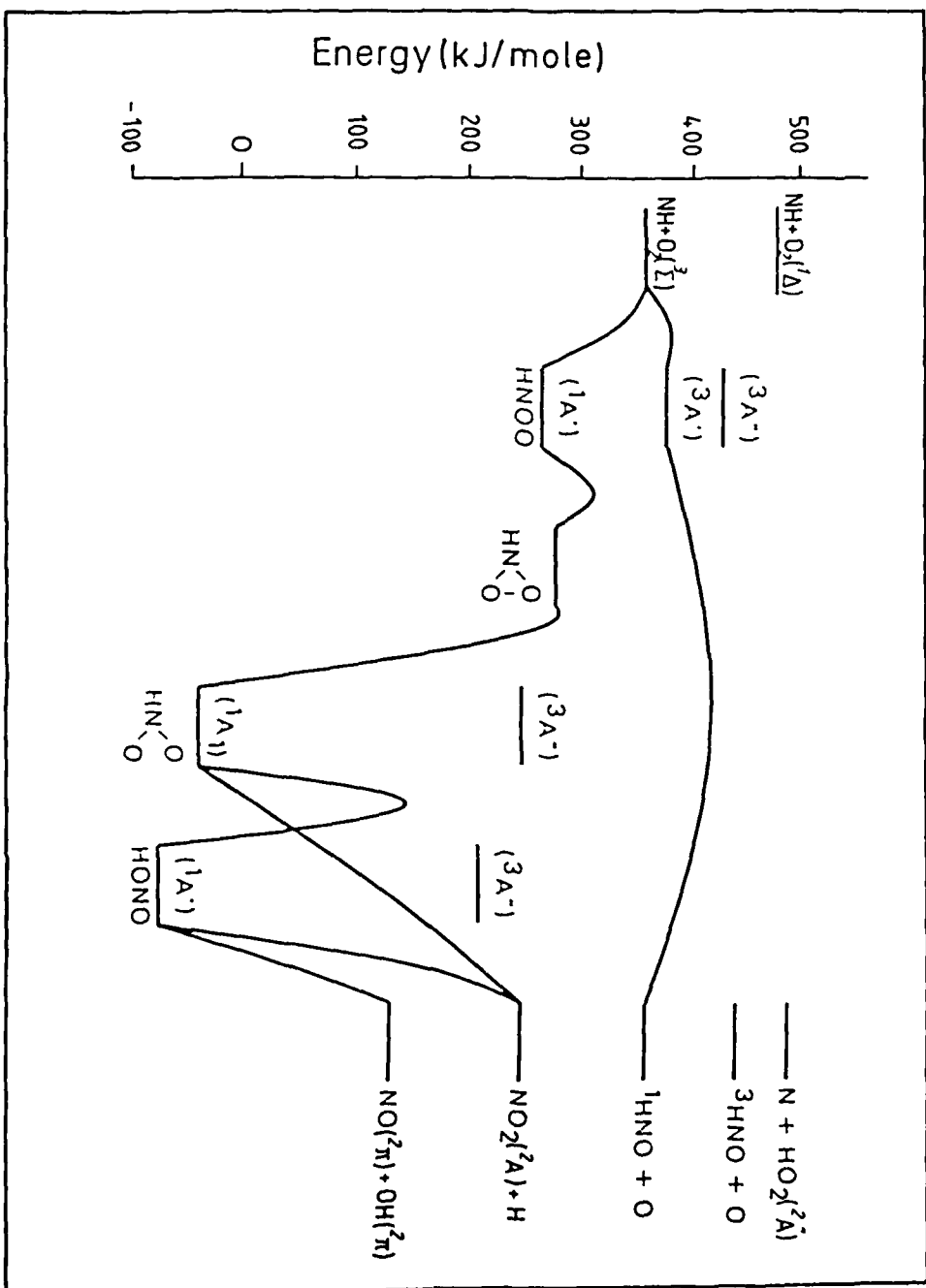












AN IMPROVEMENT OF THE Li+HF PES BY MEANS OF QUASICLASSICAL CALCULATIONS

E.GARCIA and A.LAGANA', Dipartimento di Chimica, Università di Perugia (Italy)
J.M.ALVARINO and M.L. HERNANDEZ, Departamento de Química Física, Facultad de Ciencias, Universidad del País Vasco (Spain)

Our previous 3D quasiclassical investigation of the Li + HF reaction¹ performed on the PES of Carter and Murrell² lead to contrasting results. On one side the reactive integral cross section (S_R) and the product angular distribution calculated at a translational energy of $8.7 \text{ kcal.mol}^{-1}$ were in excellent agreement with experimental findings.³ On the other side the product translational energy distribution and the energy dependence of S_R (as shown by the figure) deviated quite significantly from the experimental data. A comparison of collinear quantum and quasiclassical results showed several interesting effects.⁴ On this basis it could be concluded that quasiclassical calculations tend to overestimate the probability of getting products having low translational energy. As a consequence, the fact that the low energy side of the experimental product translational distribution is underestimated in quasiclassical results was attributed to the 3D shape of the PES. Therefore it is extremely important that the function fitting the ab initio points does not introduce spurious features in the entrance channel.

Unfortunately, the functional form adopted for fitting the LiHF

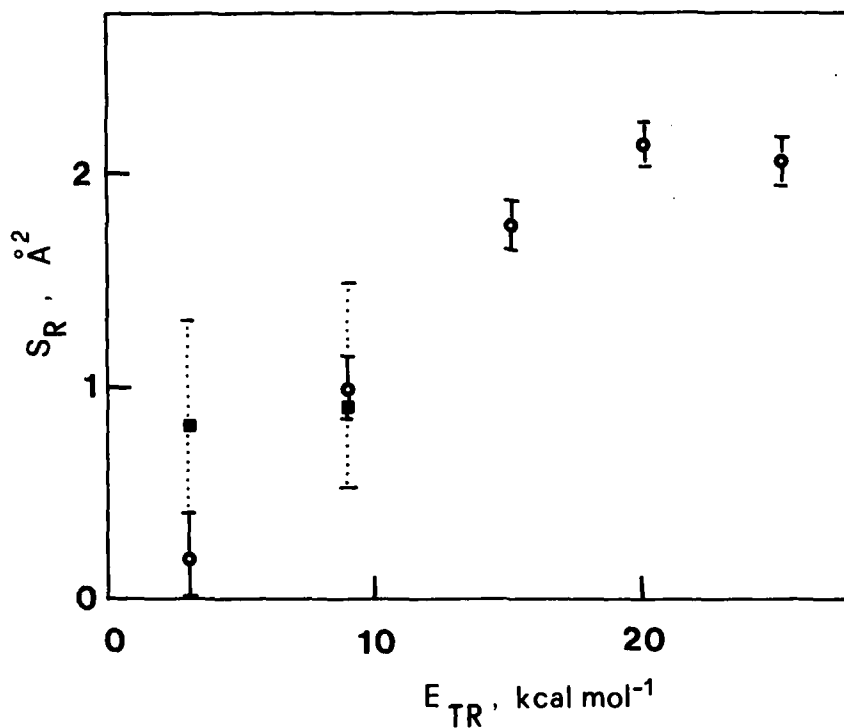


Fig.1 - Experimental³ () and calculated () integral cross section as a function of the reactant translational energy.

PES was found to add undesired structures at long range. In particular it was noticed that at the approaching angle of the lowest saddle to reaction there is early in the entrance channel a barrier higher than the saddle itself. Early barriers are known to introduce severe limitations on the efficiency of translational energy in promoting reaction. For this reason we suggested to eliminate these spurious features by connecting interaction and asymptotic re

gions in a smooth way. Therefore we adopted independent functional forms for inner and outer regions and connected them by means of a sinusoidal switching function.⁵ More in detail we adopted in the interaction region a polynomial of the nuclear distances, meanwhile at large distances a diatomic-like function was adopted. However, this PES turned out to be scarcely reactive probably because too much attractive in the long range. Using the large flexibility of the suggested functional form we varied the large distance shape of the surface. In this way we were able to get more accurate estimate of scattering properties.

REFERENCES

- 1) J.M.Alvarifo, O.Gervasi, P.Casavecchia and A.Laganà - J.Chem.Phys. 77,6341(1982)
- 2) S.Carter and J.N.Murrell- Mol. Phys. 41,567(1980)
- 3) C.H.Becker, P.Casavecchia, P.W.Tiedemann, J.J.Valentini and Y.T.Lee - J.Chem. Phys. 73,2833(1980)
- 4) A.Laganà, M.L.Hernandez and J.M.Alvarifo - Chem. Phys. Letters (in press)
- 5) E. Garcia and A. Laganà - Molecular Physics (in press)
- 6) J.M.Alvarifo, E.Garcia, M.L.Hernandez and A.Laganà (unpublished results)

KINETIC STUDY OF THE REACTIONS OF ACETONITRILE
WITH OH AND Cl RADICALS

G. Poulet, J.L. Jourdain, G. Laverdet and G. Le Bras

(Centre de Recherches sur la Chimie de la Combustion et
des Hautes Températures, C.N.R.S. - 45045 ORLEANS CEDEX, FRANCE)

Rate parameters for reactions of OH and Cl with CH_3CN have been determined in relation with their possible occurrence in atmospheric chemistry.

The method used and previously described (1)(2) was the discharge flow -EPR for OH + CH_3CN and the discharge flow-mass spectrometry for Cl + CH_3CN . The rate constants were measured under the pseudo first order conditions using a large excess of CH_3CN and Cl over OH and CH_3CN respectively. In both experiments the reactor was made of quartz. The pressure in the reactor was 1.2 Torr for reaction OH + CH_3CN and in the range 0.47 - 2.06 Torr for reaction Cl + CH_3CN .

Reaction OH + CH_3CN \rightarrow products (1)

The rate constant obtained at 295 K is :

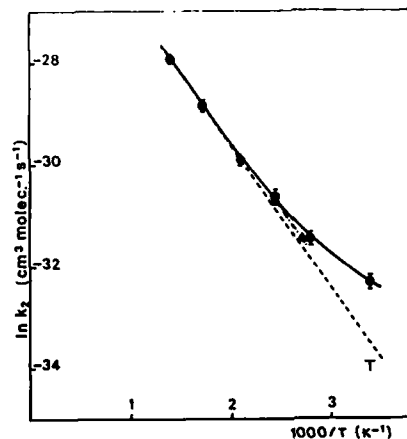
$$k_1 = (2.1 \pm 0.3) \times 10^{-14} \text{ cm}^3 \text{ molecule}^{-1} \text{ s}^{-1}$$

It was observed that heterogeneous reaction of OH with CH_3CN was negligible at this temperature.

This k_1 determination is in good agreement with data of references (3, 4, 5) obtained at 7, 100 - 300 and 20 - 50 Torr respectively. Then, the present value obtained at 1.2 Torr would indicate that k_1 is pressure independent, which confirms the combined data of references (3) and (5), rather than those of reference (4) which showed a decrease of k_1 with decreasing pressure, down to 0.8×10^{-14} at 7 Torr. This pressure independence of k_1 confirms the assumption that reaction (1) would proceed via an H atom transfer.

Reaction Cl + CH_3CN \rightarrow products (2)

The rate constant k_2 has been measured at six temperatures between 295 and 723 K. The Arrhenius T dependence of k_2 is shown in the figure below.



Reaction $\text{Cl} + \text{CH}_3\text{CN}$ (2) = Arrhenius plot of k_2 values.

● : this work ($\pm 2\sigma$), ▲ ref. 6 △ upper limit of ref. 5

The linear dependence observed at the highest temperatures (478 - 723 K) led to the following value :

$$k_2 = (3.46 \pm 0.70) \times 10^{-11} \exp [(-2785 \pm 115)/T].$$

A curvature of the Arrhenius plot was observed at the lowest temperatures and $k_2 = (8.89 \pm 1.24) \times 10^{-15}$ at 295 K.

Our data fairly agree with very recent measurements made at 370 and 413 K (6), but our k_2 value at 295 K is higher than the upper limit of 2×10^{-15} recently determined at room temperature, using the flash photolysis method (5). A wall reaction between Cl and CH_3CN in the flow tube could explain this discrepancy and the curvature of the Arrhenius plot. However this has not been experimentally established since similar values of k_2 were obtained when the quartz reactor was uncoated or coated with an halocarbon wax. Another tentative explanation of the curvature would be a change in mechanism. At the lowest temperatures an addition step, leading to the CH_3CNCl adduct, might occur in addition to the H atom transfer mechanism which is dominant at the highest temperatures. Besides, the low reactivity observed for this reaction cannot be explained from a correlation between activation energy and C - H bond strength, as for similar reactions of Cl with CH_4 , CH_3Cl and CH_3OH . Other arguments such as the large dipole of CH_3CN coupled with the strong electron affinity of Cl should be considered.

For atmospheric applications, the present results show that CH_3CN cannot be a sink for Cl atoms and also that reaction $\text{Cl} + \text{CH}_3\text{CN}$ is a negligible sink of CH_3CN compared to reaction $\text{OH} + \text{CH}_3\text{CN}$.

References :

- (1) J.L. JOURDAIN, G. LE BRAS and J. COMBOURIEU. J. Phys. Chem. (1981), 85, 655.
- (2) G. POULET, G. LE BRAS and J. COMBOURIEU. J. Chem. Phys. (1978), 69, 767.
- (3) B. FRITZ, K. LORENZ, W. STEINERT and R. ZELLNER. Proceedings of the 2nd Europ. Symp. on Physico-Chemical Behaviour of Atmospheric Pollutants. Reidel Pub. Comp. (1981) p. 192.
- (4) C. ZETZSCH, Bunsenkolloquium. Battelle Institut. Frankfurt (1983).
- (5) M. KURYLO and G. KNABLE. J. Phys. Chem. in press.
- (6) J. OLBREGTS, G. BRASSEUR and E. ARIJS. J. Photochem. in press.

Decomposition and Collisional Deactivation of Chemically
Activated Tetrahydrofuran

L.Zalotai, I.Szilágyi, T.Bérces and F.Márta

Central Research Institute for Chemistry, Hungarian Academy
of Sciences, Budapest, Hungary

Ketene and diazomethane were photolized at 334 nm and 366 nm, respectively, in the presence of excess oxetan and small amounts of oxygen. Singlet methylene produced in the photolysis reacted with oxetan forming chemically activated tetrahydrofuran, 2- and 3-methyloxetan. At 10-15 kPa pressure, where vibrational relaxation is significant, the stabilization product ratio was found to be tetrahydrofuran: 2-methyloxetan: 3-methyloxetan = 1.0 : 0.1 : 0.02.

Apparent first order rate coefficients were determined for the decomposition of the chemically activated molecules from $\langle k_a \rangle = \omega R^D / R^S$, where ω is the collision frequency, R^D and R^S are the rates of decomposition and stabilization, respectively. R^D / R^S was obtained using the internal standard method. The high pressure $\langle k_a \rangle$ values determined in the ketene photolysis system at room temperature were $1.2 \times 10^8 \text{ s}^{-1}$ and $3 \times 10^9 \text{ s}^{-1}$ for tetrahydrofuran and 2-methyloxetan decomposition, respectively. As expected, the latter value could be rationalized by assuming a biradical mechanism for the decomposition of the oxetan ring. However, various reacti-

on mechanisms had to be considered for tetrahydrofuran decomposition. Transition state calculations showed that tetrahydrofuran decomposes to formaldehyde and cyclopropane through a concerted reaction channel.

The first order rate coefficient for tetrahydrofuran decomposition was studied as a function of pressure in the range from 0.1 to 22 kPa. Results obtained in both ketene and diazomethane systems indicated that collisional deactivation occurs as a multistep process. Using RRKM theory and assuming a stepladder deactivation model, the average amount of vibrational energy transferred per collision was found to be small, around 10-15 kJ mol⁻¹. Similarly small step sizes were reported recently by H.M. Frey and I.M. Pidgeon [1] for 2-methyloxetan deactivation in collision with oxetan.

A pressure dependence of the first order rate coefficient is apparent also at the high pressure end of our pressure range. The turn up of $\langle k_a \rangle$ at high pressures is interpreted to be the results of the wide vibrational energy distribution of tetrahydrofuran at the time of formation in the diazomethane photolysis system. This is in full agreement with our previous results obtained with chemically activated dimethylcyclopropane[2].

[1] H.M. Frey and I.M. Pidgeon, J.C.S. Faraday Trans. I., 79, 1237 /1983/

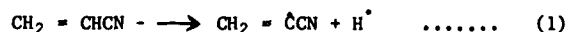
[2] I.Szilágyi, L.Zalotai, T.Bérces and F.Márta, J.Phys. Chem., 87, 3694 /1983/

The Thermal Decomposition of AcrylonitrileE Metcalfe, D Booth, A Harman and H McAndrew*School of Chemical and Life Sciences
Newcastle Polytechnic, UK.*and*W D Woolley**Fire Research Station
Borehamwood, UK.*

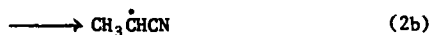
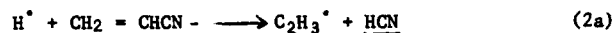
In fires involving nitrogen-containing polymers such as polyurethane and polyacrylonitrile, both hydrogen cyanide and a variety of organic nitriles may be produced. Hydrogen cyanide is known to be a contributory factor in some domestic fire fatalities, and may well be an important factor in the incapacitation of victims during the early stages of fires.^{1,2} Acrylonitrile is one of the major products obtained on the thermal degradation of nitrogen-containing polymers, yet little is known about the reactions of acrylonitrile under conditions relevant to fire atmospheres. This study forms part of an investigation into the relationship between organic nitrile and hydrogen cyanide production in fires.³

The thermal decomposition of acrylonitrile was studied using a flow reactor in nitrogen diluent at atmospheric pressure and temperatures of 728 to 1055 K. Flow rates of 3-200 ml min⁻¹ were used and analysis was by gas chromatography.

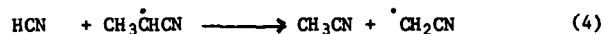
The major reaction products are hydrogen cyanide, acetonitrile and ethene. In addition, moderate quantities of methane, ethyne, propene and benzonitrile are produced and a black thermally stable polymeric residue is deposited on the walls of the reactor. Since the 1C - 2C bond in acrylonitrile is very strong owing to delocalisation, initiation will involve rupture of the weaker C-H bond to form a resonance stabilised α -cyano radical.



The major products are readily accounted for by two competing reactions between the hydrogen atoms and acrylonitrile

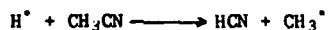


followed by the reactions



The relative rates of formation of these products do not vary considerably with temperature and average values $r(\text{C}_2\text{H}_4) : r(\text{HCN}) : r(\text{CH}_3\text{CN})$ of 1.00 : 2.46 : 1.34 are obtained, which cannot be accounted for on the above simple scheme which necessarily predicts $r(\text{C}_2\text{H}_4) > r(\text{HCN})$. This discrepancy arises largely from the presence of further reactions forming benzonitrile, presumably by reaction of ethene with the $\text{CH}_2 = \dot{\text{C}}\text{CN}$ radical, and mass balance data can be explained by assuming that two moles of ethene are consumed in the formation of each mole of benzonitrile. A ratio for k_{2a}/k_{2b} of 4.6 then predicts the following values of α ($= [\text{Product}]/\text{formed} / [\text{Acrylonitrile}]/\text{reacted}$): $\alpha(\text{HCN}) = 0.32$, $\alpha(\text{CH}_3\text{CN}) = 0.18$ and $[2\alpha(\text{C}_6\text{H}_5\text{CN}) + \alpha(\text{C}_2\text{H}_4)] = 0.41$ which are in good agreement with the experimental data obtained at the highest temperatures studied.

Methane is only formed at long reaction times and almost certainly arises from reactions of acetonitrile

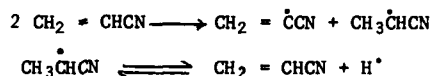


where RH is $\text{CH}_2 = \text{CHCN}$, CH_3CN or C_2H_4 . Propene is also formed in secondary reactions, such as the $\text{CH}_3^\bullet + \text{C}_2\text{H}_4$ metathesis reaction, and ethyne is probably formed by decomposition of vinyl radicals.

The polymeric residue on the reactor walls is formed in much larger quantities than are observed during the pyrolysis of other nitriles such as acetonitrile or propionitrile, and is resistant to thermal decomposition at temperatures up to 760°C . The residue is soluble in polar solvents such as

DMSO and elemental analysis ($C_1H_{0.74}N_{0.33}$) and infra-red analysis indicate that the residue arises from the recombination of $CH_2 = \dot{C}CN$ radicals to form dicyanobutadiene which polymerises and then undergoes a cyclisation process analogous to that observed during polyacrylonitrile pyrolysis.

The concentration-time curves of the major products all exhibit curvature indicating autocatalysis, which suggests that bimolecular initiation reactions involving one acrylonitrile molecule and one product molecule are important at longer reaction times. Indeed the low activation energy (200 kJ mol^{-1}) and low A-factor for the initial reaction rates indicate that bimolecular initiation



is dominant over unimolecular initiation during the initial stages of the reaction. The observed activation energy is very similar to that for the analogous reaction of propene ($2C_3H_6 \longrightarrow C_3H_5^\bullet + C_3H_7^\bullet$).

References

1. R A Anderson, A A Watson and W A Harland,
Med. Sci. Law 21 288 (1981).
2. D A Purser and W D Woolley,
J. Fire Sciences 1 118 (1983).
3. E Metcalfe, D Booth, H McAndrew and W D Woolley,
Fire and Materials 7 185 (1983).

COLLISION DYNAMICS AND THE THERMAL RATE COEFFICIENT FOR THE REACTION

$O + OH \rightarrow O_2 + H$ -- James A. Miller, Sandia National Laboratories,
Livermore, CA 94550, U.S.A.

ABSTRACT

The title reaction is of particular interest for two reasons. First, the reverse reaction is the single most important chemical reaction in combustion. It is primarily responsible for the chain-branching character of all flame oxidation processes. Second, the title reaction itself is a good example of a neutral-neutral reaction that has no intrinsic energy barrier. Both reactions have been studied extensively in the laboratory, and there is very little doubt about the correct thermal rate coefficient values.

In two previous papers^{1,2} we have computed quasi-classical trajectory values of k_{-1} and its deuterated analog as a function of temperature using the Melius-Blint³ potential.



The theoretical results were compared to experimental results for k_{-1} at high temperature and to experimental values of k_1



at low T , where k_1 was determined from k_{-1} and the equilibrium constant.

The trajectory results so obtained are in excellent agreement with experiments at high temperature and differ (too high) from the Howard-Smith⁴ low temperature results by less than a factor of two. In Refs. 1 and 2, the low temperature discrepancies were attributed to the crude

handling of quantum effects near threshold, and it was felt that trajectories in the (+1) direction would give results in better agreement with experiment. Subsequently, Rai and Truhlar⁵ have performed variational transition-state theory calculations of k_1 using the Melius-Blint potential. Their results were in poor agreement with experiment at all temperatures, but were only slightly higher than the trajectory results in the $T = 250\text{-}300\text{K}$ range. They attributed the low temperature discrepancies to errors in the Melius-Blint potential (the same for both trajectories and transition-state theory) and the high temperature differences to "recrossing" effects.

The present investigation was initiated to see if indeed the trajectory results could be improved by computing trajectories in the (+1) direction or if the Melius-Blint potential was the primary culprit. The following is a table of rate coefficients obtained by the two different trajectory methods (uncertainty from Monte Carlo samples $\pm 10\%$).

T(K)	k_1 (from (-1) Trajectories) ($\text{cm}^3/\text{mole-sec}$)	k_1 (from (+1) Trajectories) ($\text{cm}^3/\text{mole-sec}$)
250	7.3×10^{13}	8.2×10^{13}
300	5.1×10^{13}	8.7×10^{13}
500	2.4×10^{13}	7.2×10^{13}
1000	1.2×10^{13}	5.7×10^{13}
2500	6.3×10^{12}	3.8×10^{13}

The two methods are in reasonably good agreement at low temperature, but differ by about a factor of 6 at 2500K. The (+1) trajectory method gives results that are in good agreement with the variational TST calculations at all temperatures. The (-1) trajectory results are in excellent agreement

with experiment above $\sim 500\text{K}$.

Although quasi-classical trajectory methods do not necessarily satisfy balance, the large difference between results from the two methods at 2500K is somewhat surprising. Detailed analysis of the trajectories shows that the "bottlenecks" to reaction in the two different cases occur in different regions of the potential surface. For the (+1) trajectories the bottlenecks occur along the high energy portion of the reaction path at relatively large O-O separations of roughly 2.5\AA to 5.0\AA . These locations are in good agreement with the variationally located transition states and lie in the region where the Melius-Blint potential is in error, as pointed out by Rai and Truhlar. By contrast the reaction bottleneck in the (-1) direction lies in the HO_2 well region of the potential at O-O separations less than 1.95\AA , even near threshold¹. In this region Melius and Blint computed a large number of ab initio points, and the potential apparently is accurate there. Consequently, the (-1) trajectories give rate constants that are in good agreement with experiment, whereas the (+1) trajectories do not.

References

1. J. A. Miller, J. Chem. Phys. 74, 5120 (1981)
2. J. A. Miller, J. Chem. Phys. 75, 5349 (1981)
3. C. F. Melius and P. J. Blint, Chem. Phys. Lett. 64, 183 (1979)
4. M. J. Howard and I. W. M. Smith, J. Chem. Soc. Faraday Trans. 2 77, 997 (1981)
5. S. N. Rai and D. G. Truhlar, J. Chem. Phys. 79, 6046 (1983)

A THEORETICAL ANALYSIS OF THE PHOTO-ACTIVATED UNIMOLECULAR DISSOCIATION
OF T-BUTYL HYDROPEROXIDE -- David W. Chandler and James A. Miller,
Sandia National Laboratories, Livermore, CA 94550

ABSTRACT

Collisional energy transfer in highly vibrationally excited polyatomic molecules is a subject of intense theoretical and experimental investigation. In nonreacting systems various schemes have been developed in order to determine the average energy transferred per deactivating collision. In reacting systems both average energy transferred and the specific rate constant, $k(E)$, are the quantities of interest. In order to obtain these quantities experimentally it is necessary to produce an ensemble of vibrationally excited molecules with a narrow distribution of internal energy and then to monitor an observable that reflects this internal distribution of energy.

Recently the method of high vibrational overtone excitation, above a reaction barrier, followed by product detection has been used obtain $k(E)$ data on highly excited ground state systems. Final product detection as a function of pressure along with a Stern-Volmer like analysis has been used recently by various groups⁽¹⁻⁶⁾ in an effort to determine $k(E)$. Crim and co-workers have used real time product detection following overtone excitation in an effort to measure $k(E)$.

In the present paper, realistic descriptions of the collisional activation, collisional deactivation, and unimolecular dissociation are incorporated into a master equation formalism to produce an overall scheme for the pressure dependence of the dissociation rate and yield of the product. We have chosen the photo-activated dissociation of t- Butyl Hydroperoxide(tBuOOH) to analyze since there are both final product and real time product detection experiments performed on this system.

We compare our results to the experimental results of Chandler, Farneth, and Zare and of Chuang, et al. We find that the curvature in their Stern-Volmer plots cannot be explained by a collisional energy transfer mechanism. At high pressure, the theoretical Stern-Volmer plots are linear, independent of the collisional energy transfer properties. This linearity is related to the existence of a limiting high pressure "reactive distribution". We identify three different pressure regimes that exist in photoactivated unimolecular reaction experiments, and we relate these regimes to the properties of the reactive distribution. In particular, we find that, when a Stern-Volmer analysis is used, curvature at very low pressure can result in systematic errors in determining the unimolecular rate constants. In addition, we have successfully analyzed the real-time experiments of Rizzo and Crim⁽⁷⁾ using the same molecular model and parameters necessary to predict the experiments of Chandler, et al.

References

1. K. V. Reddy and M. J. Berry, Chem. Phys. Lett. **52**, 111 (1977).

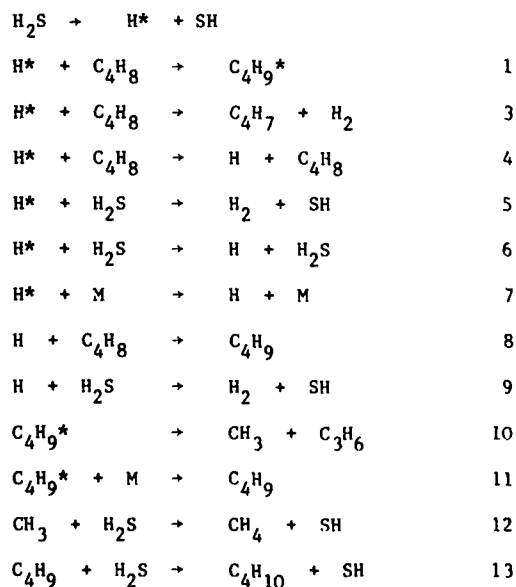
2. K. V. Reddy and M. J. Berry, Chem. Phys. Lett. 66, 223 (1979).
3. D. W. Chandler, W. E. Farneth, and R. N. Zare, J. Chem. Phys. 77, 4447 (1982).
4. M. C. Chuang, J. E. Baggott, D. W. Chandler, W. E. Farneth, and R. N. Zare, Faraday Discuss. 75/17 (1982).
5. J. M. Jasinski, J. K. Frisoli, and C. B. Moore, J. Phys. Chem., 87, 2209 (1983).
6. J. M. Jasinski, J. K. Frisoli, and C. B. Moore, J. Chem. Phys., 79, 1312 (1983).
7. T. R. Rizzo and F. F. Crim, J. Chem. Phys. 76, 2754 (1982).

Highly excited alkyl radicals produced by the addition
of hot hydrogen atoms to alkenes

K.H. Al-Niami, P.L. Gould, K.A. Holbrook, and G.A. Oldershaw

'Chemically activated' alkyl radicals produced by the exothermic addition of thermal hydrogen atoms to alkenes have been widely studied, particularly in order to compare rates of their unimolecular decomposition with those predicted theoretically [1].

Hydrogen atoms with substantial translational energy are produced by photolysis of gaseous H_2S with ultraviolet light [2]. In the addition of H to an alkene, most of the translational energy of the hydrogen atom appears as internal energy of the radical adduct, so that alkyl radicals produced by the use of 'hot' H atoms have enhanced internal energy. The reaction of photochemically generated hot hydrogen atoms with cis but-2-ene has been studied in order to establish the reaction mechanism and to examine the lifetimes of the radicals produced. H_2S was used as the source of hot atoms. The reaction mechanism is as follows:



where H^* is a 'hot' atom and H a 'thermalized' atom. At pressures above about 15 kPa the product ratio $[C_4H_{10}]/[CH_4]$ is found to be a linear function of pressure with positive intercept, as required by this mechanism. We shall discuss the cross section for reaction (1) and the lifetimes of the $C_4H_9^*$ radicals, as compared with lifetimes calculated using RRKM theory. Work with isobutene and 1-butene may also be discussed.

1. B.S. Rabinovitch and D.W. Setzer, Adv. Photochem. 3, 1 (1964)
2. G.A. Oldershaw, D.A. Porter and A. Smith, J. Chem. Soc. Faraday Trans. I, 68, 2218 (1972)

ENERGY TRANSFER DYNAMICS AND EFFICIENCY
IN REACTING POLYATOMIC MOLECULES

by

E. Tzidoni and I. Oref

Department of Chemistry

Technion--Israel Institute of Technology

Haifa 32000, Israel

ABSTRACT

The temporal evolution of the population, the average vibrational energy transferred in a collision, and the collisional efficiency are determined for a variety of temperatures, pressures, and chaperon molecule sizes by using strong and weak collision transition probabilities. The time dependent population distribution of a reactive polyatomic system is evaluated by solving for the eigenvalues and eigenvectors of the master equation. It is found that steady state is obtained up to ca. 700K. At higher temperatures the population distributions and the reaction rate coefficients vary with time and therefore no steady state solution to the master equation applies. In the steady state region the efficiency declines with the temperature and decreasing size of bath molecules.

RATE COEFFICIENTS OF HYDROGEN ABSTRACTION REACTIONS IN THE THERMAL DECOMPOSITION OF AZOETHANE AND AZOISOPROPANE

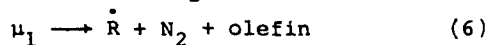
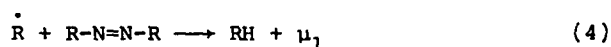
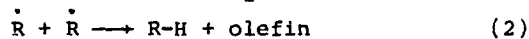
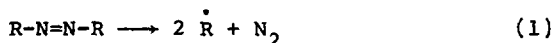
A. Péter, G. Ács, P. Huhn

Reaction-Kinetics Research Group of the Hungarian Academy of Sciences, Department of Inorganic and Analytical Chemistry, Attila József University, Szeged, Hungary

Azoalkanes are often applied as alkyl radical sources in kinetical investigations. Besides the recombination of alkyl radicals formed in the initiation step, hydrogen abstraction reactions can be also observed. These cause the complexity of the decomposition mechanism.

The hydrogen abstraction reactions are treated uniformly in the literature without distinction in respect to whether the hydrogen abstraction takes place from the primary, secondary or tertiary carbon atoms of azoalkane. Thus, it is not clear either which elementary reaction can the rate coefficients obtained for the hydrogen abstraction be coordinated to [1, 2].

In the thermal decomposition of azoethane and azoisopropane the different hydrogen abstraction reactions were managed to be separated by a detailed product analysis. It was stated that the mechanism of their decomposition could be described by the next way:



where in the case of azoethane: $R: C_2H_5$; $\mu_1: \dot{C}H_2-CH_2-N_2-C_2H_5$;

μ_2 : $\text{CH}_3-\dot{\text{C}}\text{H}-\text{N}-\text{N}-\text{C}_2\text{H}_5$; olefin: C_2H_4 ; and in the case of azo-
isopropane: R: $2-\text{C}_3\text{H}_7$; μ_1 : $\text{CH}_2-\text{CH}(\text{CH}_3)-\text{N}_2-\text{CH}(\text{CH}_3)_2$;
 μ_2 : $(\text{CH}_3)_2\dot{\text{C}}-\text{N}-\text{N}-\text{CH}(\text{CH}_3)_2$; olefin: C_3H_6 .

The new element of the mechanism is that two abstraction reactions can be distinguished. Although reaction (5) is more advantageous energetically, it is of less reactivity as a result of the resonance stability of the μ_2 -radical formed in the reaction. By process (4) and through steps (4) and (6) a short chain cycle is formed. This is proved by our experience that in the case of azoethane, the ratio of ethylene and butane, and in the case of azoisopropane, that of propylene and 2,3-dimethyl-butane is greater than that of the corresponding rate coefficients (k_2/k_3) and it changes with the temperature and the pressure. The olefine, therefore, is formed in the disproportionation reaction(2) as well, and the most obvious way of the formation is chain cycle (4) and (5). This chain cycle makes the distinction between abstraction steps (4) and (5) and the determination of the rate constants in these steps possible, for the olefine formed in the chain is the degree of the hydrogen abstraction reaction taking place from the primary carbon atom. In the case of azoethane, on the basis of the mechanism the next correlations can be found:

$$\begin{aligned} R_{\text{C}_2\text{H}_4} &= (k_2/k_3)R_{\text{C}_4\text{H}_{10}} + k_4[\dot{\text{C}}_2\text{H}_5][\text{AE}] \\ R_{\text{C}_2\text{H}_6} &= (k_2/k_3)R_{\text{C}_4\text{H}_{10}} + (k_4 + k_5)[\dot{\text{C}}_2\text{H}_5][\text{AE}] \\ R_{\text{C}_4\text{H}_{10}} &= k_3[\dot{\text{C}}_2\text{H}_5]^2 \end{aligned}$$

From these for the quotients of the coefficients

$$k_4/k_3^{1/2} = [R_{C_2H_4} - (k_2/k_3)R_{C_4H_{10}}] / R_{C_4H_{10}}^{1/2} [AE]$$

$$k_5/k_3^{1/2} = [R_{C_2H_6} - R_{C_2H_4}] / R_{C_4H_{10}}^{1/2} [AE]$$

can be obtained. From our measurements the next values were calculated for the temperature dependence:

$$\lg(k_4/k_3^{1/2} \text{ dm}^{3/2} \text{ mol}^{-1/2} \text{ s}^{-1/2}) = (3,3+0,1) - (54,3+1) \cdot \text{kJmol}^{-1/2, 303RT}$$

$$\lg(k_5/k_3^{1/2} \text{ dm}^{3/2} \text{ mol}^{-1/2} \text{ s}^{-1/2}) = (3,0+0,1) - (33,7+1,4) \cdot \text{kJmol}^{-1/2, 303RT}$$

By a similar method, the values for the rate coefficients of the hydrogen abstraction taking place from the methyl or methyne group of azoisopropane by the isopropyl radical proved to be the following:

$$\lg(k_4/k_3^{1/2} \text{ dm}^{3/2} \text{ mol}^{-1/2} \text{ s}^{-1/2}) = (4,1+0,3) - (52,5+3,0) \cdot \text{kJmol}^{-1/2, 303RT}$$

$$\lg(k_5/k_3^{1/2} \text{ dm}^{3/2} \text{ mol}^{-1/2} \text{ s}^{-1/2}) = (2,4+0,1) - (27,6+1,3) \cdot \text{kJmol}^{-1/2, 303RT}$$

In the case of both azoethane and azoisopropane no values can be found in the literature for the rate coefficients of reactions (4). The comparison of the rate coefficients of reactions (5) with the reference data shows that the latter refer to the hydrogen split taking place from the methylene group, in the case of azoethane [1], and from the methyne group, in the case of azoisopropane [2].

[1] H. CERFONTAIN, K. O. KUTSCHKE, *Canad. J. Chem.*, **36**, 344 (1958) and references cited

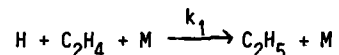
[2] L. SZIROVICZA, *Acta Phys. et. Chem. Szegediensis* **25**, 147 (1979) and references cited

Rate constants for $\text{H} + \text{C}_2\text{H}_4$ and $\text{H} + \text{C}_2\text{H}_5$

P.D. Lightfoot, M. Brouard and M.J. Pilling

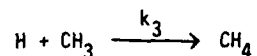
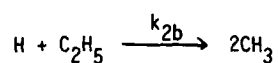
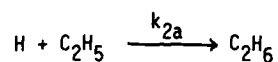
Physical Chemistry Laboratory, South Parks Road,
Oxford, OX1 3QZ.

The reaction

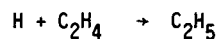
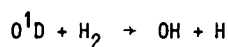
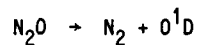


was the first to be studied by flash photolysis/resonance fluorescence.¹ Since then, its pressure dependence at room temperature² and the temperature dependence³ of k_∞ have been determined, although there has been no systematic study of its pressure dependence at elevated temperatures. The importance of both the forward and reverse reactions in hydrocarbon cracking, and interest in the reaction as a model system for unimolecular rate theory⁴ encourage further investigation.

Analysis of the atom decay profiles is complicated at higher atom concentrations because of contributions from the reactions



In the present experiments we overcome these problems by operating at low, constant, initial atom concentrations, $[\text{H}]_0$, using the carefully controlled output of an ArF excimer laser. The source of H is N_2O photolysis in the presence of H_2 and in a helium diluent;



The H atom decay is monitored by Lyman α resonance fluorescence.

Table 1 shows the slopes and intercepts obtained from plots of the first order rate constant, k , for H atom decay vs $[\text{C}_2\text{H}_4]$, for different concentrations of N_2O and, therefore, for different values of $[\text{H}]_0$. k increases with $[\text{N}_2\text{O}]$, because of contributions from $\text{H} + \text{C}_2\text{H}_5$ and $\text{H} + \text{C}_2\text{H}_4\text{OH}$. Table 1 shows that the slopes of the plots of k vs $[\text{C}_2\text{H}_4]$ are independent of $[\text{N}_2\text{O}]$ and that the increase in k with $[\text{H}]_0$ is reflected solely in the intercept. This observation is supported by simulations, which demonstrate that the slope is equal to k_1 . Thus accurate values for k_1 may be obtained directly from the experimental data, without extrapolation or numerical integration, provided the laser power is carefully controlled.

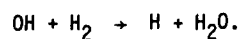
Table 1

Slopes and Intercepts of plots of k vs $[\text{C}_2\text{H}_4]$ at a total pressure of
100 Torr (He) and at 285K.

$[\text{N}_2\text{O}]/10^{15}$ molecule cm^{-3}	Slope/ cm^3 molecule $^{-1}\text{s}^{-1}$	Intercept/ s^{-1}
0.67	6.82 ± 0.54	52 ± 30
1.33	6.73 ± 0.21	76 ± 12
2.67	6.95 ± 0.06	113 ± 4
5.33	6.77 ± 0.20	144 ± 9

(The quoted errors refer to 95.5% confidence limits.)

For $T > 400\text{K}$, OH may be converted into H at short times by using H_2 as the diluent gas:-



Thus, at higher temperatures, the dependence of k on $[\text{H}]_0$ may be analysed numerically to provide estimates of k_2 .

References

1. W. Braun and M. Lenzi, Disc. Faraday Soc., 1967, 44, 252.
2. M.J. Kurylo, N.C. Peterson & W. Braun, J. Chem. Phys., 53, 2776 (1970).
3. J.W. Lee, J.V. Michael, W.A. Payne & L.J. Stief, J. Chem. Phys., 68, 1817 (1978).
4. W.L. Hase & H.B. Schlegel, J. Phys. Chem., 86, 3901 (1982).

The pressure dependence of the rate constant for the $\text{CH}_3 + \text{O}_2$ reaction at 298K.

M.J.C. Smith and M.J. Pilling

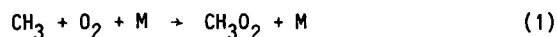
Physical Chemistry Laboratory, South Parks Rd, Oxford, OX1 3QZ, U.K.

and

K.D. Bayes

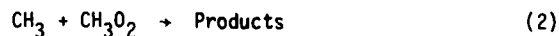
Dept. Chemistry, University of California, Los Angeles,
California 90024, U.S.A.

The reaction between CH_3 and O_2 :-



has been investigated in several laboratories over a wide range of pressure conditions. At low pressures, two recent studies^{1,2} are in reasonable agreement and demonstrate that an earlier suggestion,³ that the reaction had a second-order component, is erroneous. At higher pressures the agreement is less satisfactory.⁴⁻⁸ Selzer and Bayes¹ pointed out that accurate values of $k_{i\infty}$ are needed if an unambiguous fit is to be made to the low pressure data. The present work was undertaken to obtain more accurate data at higher pressures, so that $k_{i\infty}$ can be estimated, and to examine the fall-off behaviour over a wide range of pressures.

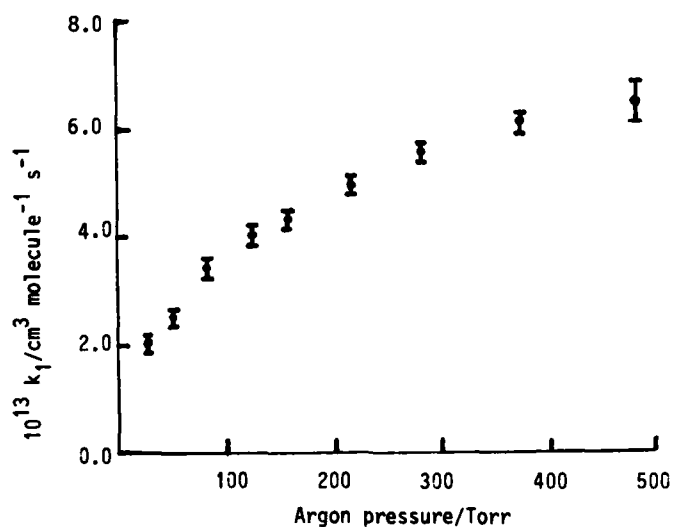
Most of the high pressure data⁴⁻⁷ have been obtained using flash photolysis with absorption spectroscopy, where comparatively high radical densities are required. It is now accepted⁸ that the reaction



can compete with reaction (1) under these circumstances. Even in Parkes' molecular modulation experiments,⁸ reaction (2) is important and corrections

must be made because the steady state concentration of CH_3O_2 builds up to substantial levels.

Reaction (2) decreases in importance as $[\text{O}_2]/[\text{CH}_3]_{t=0} (= R)$ increases. In the present work, excimer laser flash photolysis was employed enabling reaction (1) to be studied on short time-scales under conditions of high oxygen concentration. Signal averaging permitted radical decay signals to be obtained with good signal to noise ratios (> 10) at low radical concentrations ($2 \times 10^{13} \text{ molecule cm}^{-3}$). At low values of R the apparent rate constant (k_{app}) decreases as R increases but eventually k_{app} approaches a limiting value corresponding to k_1 . Fig. 1 shows a plot of k_1 vs pressure over the pressure range 30-500 Torr for argon as third body.



The dependence of k_{app} on R has been studied over a $2\frac{1}{2}$ orders of magnitude variation in R . A numerical analysis of these data will be presented which enables k_2 to be evaluated.

The relationship of the present data to those of Selzer and Bayes and Plumb and Ryan and an analysis of the pressure dependence will be discussed.

References

1. E.A. Selzer and K.D. Bayes, J. Phys. Chem. (1983) 87, 392.
2. I.C. Plumb and K.R. Ryan, Int. J. Chem. Kinet. (1982) 14, 861.
3. N. Washida and K.D. Bayes, Int. J. Chem. Kinet. (1976) 8, 777.
4. H.E. van den Bergh and A.B. Callear, Trans. Faraday Soc., (1971) 67, 2017.
5. N. Basco, D.G.L. James and F.C. James, Int. J. Chem. Kinet (1972), 4, 129.
6. A.H. Laufer and A.M. Bass, Int. J. Chem. Kinet. (1975), 7, 639.
7. C.J. Hochenadel, J.A. Ghormley, J.W. Boyle and P.J. Ogren, J. Phys. Chem. (1977), 81, 3.
8. D.V. Parkes, Int. J. Chem. Kinet. (1977), 9, 451.

DECOMPOSITION OF \tilde{B}^2B_2 H_2O^+ VIA CONVERSION TO LOWER LYING ELECTRONIC STATES

R.G.C. Blyth

Physical Chemistry Laboratory, South Parks Road, Oxford OX1 3QZ, United Kingdom

K.M. Johnson and I. Powis

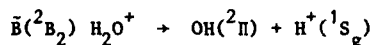
Department of Chemistry, The University, Nottingham NG7 2RD, United Kingdom

The predissociation of water ions prepared in selected vibronic levels of the \tilde{B}^2B_2 state has been investigated by a photoelectron-photoion coincidence technique (PEPICO), and the product H^+/OH^+ branching ratios determined. Also recorded were product translational energies which permit deductions as to the diatomic fragment's rotational excitation.

An early suggestion¹ was that the bent \tilde{B} state is predissociated by a repulsive 4B_1 state giving OH^+ via spin-orbit coupling whereas a repulsive $^2A''$ state leads to H^+ fragments via both spin-orbit and Coriolis interactions. However, a previous PEPICO study of D_2O^+ has pointed out that predissociation to OH^+ and H^+ is also possible via the \tilde{X} and \tilde{A} states respectively of the parent ion. The unexpectedly high proportion of D^+ produced was taken to indicate a significant role for the \tilde{A} state, whereas the OD^+ kinetic energy data were held to indicate a vibrational type predissociation from the \tilde{X} ground state surface.²

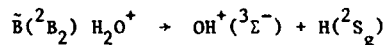
There remains a considerable uncertainty as to the involvement of different electronic surfaces in experimental studies of this system. In the meantime a number of theoretical studies of the \tilde{B} ionic state^{3,4,5} have focussed attention on a conical intersection between the \tilde{B} and \tilde{A} surfaces which thereby provides a mechanism for transition between these adiabatic states. A dynamical study⁵ shows this to be a highly efficient mechanism for connecting the \tilde{A} and \tilde{B} states.

The present experimental results for the channel



demonstrate that the OH fragment is formed rotationally hot in its ground vibrational state. This is consistent with the involvement of the conical intersection since its effect is to "funnel" the initial \tilde{B} state population into a localised region of the \tilde{A} state surface where the H-O-H angle is highly distorted from its equilibrium value. The consequent high degree of excitation of the bending mode on this lower surface is expected to correlate with product rotational excitation. This correlation is demonstrated by calculations of the product translational energy distributions using statistical adiabatic channel theory.⁶ No significant dependence on initial vibronic level is evident in the experimental data.

For the channel,



a greater proportion of the excess energy is proportioned into product translation (viz. ~50%). Two models are considered:

- (a) predissociation by the 4B state. Since this is repulsive in the reaction coordinate and is expected to be linear it could favour partitioning between rotation and translation.
- (b) a vibrational predissociation mechanism following conversion to the \tilde{X} surface as suggested by Eland.²

Neither model can be unambiguously rejected at present. Calculations of the 4B_1 surface would permit a comparison of its topography with that of the \tilde{A}^2A_1 surface and would aid understanding of this second channel.

References

1. A.J. Lorquet and J.C. Lorquet, Chem. Phys., 4 (1974) 353.
2. J.H.D. Eland, Chem. Phys., 11 (1975) 41.
3. G.G. Balint-Kurti and R.N. Yardley, Chem. Phys. Lett., 30 (1975) 342.
4. C.F. Jackels, J. Chem. Phys., 72 (1980) 4873.
5. D. Dehareng, X. Chapuisat, J.C. Lorquet, C. Galloy and G. Raseev,
J. Chem. Phys., 78 (1983) 1246.
6. M. Quack and J. Troe, Ber.Bunsenges. Phys. Chem., 78 (1974) 240;
74 (1975) 170;
79 (1975) 469.

Direct Measurement of Unimolecular Reaction Rates for Carbon-Halogen Bond
Cleavage in IR MPD.

D.M. Rayner and P.A. Hackett

Laser Chemistry Group, Division of Chemistry, National Research Council Canada,
100 Sussex Drive, Ottawa, Ontario K1A 0R6 Canada.

In principle infrared multiphoton excitation offers a general method for the preparation of vibrationally excited ground state molecules in experiments designed to measure unimolecular reaction rates, $k(E)$. However, in practice, the long pulse length of most CO_2 lasers limits this approach to slow dissociation times. The use of a plasma shutter to terminate the CO_2 pulse is an elegant solution to this problem. However the high time resolution of this technique, determined by the ~ 30 ps shutter speed, can only be realized if the termination point can be precisely located with respect to the experimental product evolution curve. Multiphoton ionization, MPI, of iodine atoms is a precise actinometer for IR MPD of perfluoroalkyl iodides. In addition the 485.5 nm iodine atom MPI peak, which is resonant at both the three and four photon levels, is ac-Stark shifted by intense infrared laser fields offering an ideal method to locate the infrared pulse termination point. Here we have combined these techniques to study the collision free dissociation dynamics of CF_3I and $\text{C}_6\text{F}_{13}\text{I}$ following infrared multiphoton excitation by the 9R20 output of a TEM₀₀, SLM, pulse terminated CO_2 laser. The colinear dye laser pulse used to detect iodine atoms by MPI probed only the centre of the Gaussian profile of the infrared beam, a uniform, defined, constant intensity region.

Iodine atom appearance curves, constructed by varying the delay between the photolysis and probe pulses, were obtained as a function of infrared fluence

for both compounds. In the case of CF_3I these curves exhibit the effect of the Stark shift and subsequently rise at a rate corresponding to the upper limit of the experiment ($5 \times 10^8 \text{ s}^{-1}$) even at the lowest fluences studied. This rapid rise is consistent with RRKM calculations and with previous measurements of translational energy release. In the case of $\text{C}_6\text{F}_{13}\text{I}$ the Stark shift effect is also observed and the subsequent rise, which is less rapid and fluence dependant, can be attributed to unimolecular dissociation of the ensemble of vibrationally-excited molecules prepared by the foregoing IR pulse. Average appearance rates were estimated by fitting the rises to single exponentials. Equating the appearance rate with $k(E)$, the specific internal energy, E , and hence the optical pumping rates, α were estimated through RRKM modelling of $\text{C}_6\text{F}_{13}\text{I}$ dissociation.

Simple modelling of the IR multiphoton adsorption process using levels equally spaced at the IR photon energy, α independent of level and time and the RRKM predicted level specific dissociation rate gives a consistent picture for the IR MPD of $\text{C}_6\text{F}_{13}\text{I}$. At the highest intensities the yield saturates at unity with the probability distribution for the internal energy of the reacting molecules determined by intensity. At lower intensities the yield is not saturated and the average degree of excitation is determined by fluence.

THE ONSET OF CHAOS IN THE CLASSICAL MOTION OF ARGON CLUSTERS.

Jesús Santamaría

Departamento de Química Física, Facultad de C. Químicas.
Universidad Complutense. MADRID-3. SPAIN.

A detailed study of the classical motion of Argon clusters (Ar_4, Ar_3), where the energy is located initially in selected vibrational modes and/or rotational degrees of freedom, has been initiated. The onset of chaos has been followed estimating the maximum Lyapunov characteristic exponent, which is related to the K entropy. Different patterns for vibrational and rotational motions have been observed. In particular, the threshold energy for the onset of chaos is much lower for vibration than for rotation. A full study of the several ergodic components is under way.

ROTATIONALLY RESOLVED COMPETITIVE PREDISSOCIATION IN SiH_2^+ M.C. Curtis, P.A. Jackson and P.J. SarreDepartment of Chemistry, University of Nottingham, Nottingham NG7 2RD,
United Kingdom

The first spectrum of the SiH_2^+ molecule has been recorded between 580 nm and 610 nm in a laser/ion beam experiment. Transitions in the $\tilde{A}^2B_1 + \tilde{X}^2A_1$ system are detected by monitoring the appearance of Si^+ or SiH^+ fragment ions which arise from predissociation of rovibronic levels of the \tilde{A} state. It is found that predissociation of individual rovibronic levels occurs competitively into the two dissociation channels, $\text{Si}^+ + \text{H}_2$ and $\text{SiH}^+ + \text{H}$.

A mass-selected beam of SiH_2^+ ions is generated following electron impact ionisation of SiH_4 , and is irradiated coaxially by a c.w. tunable laser operating with a linewidth of ca. 30 GHz. Laser induced transitions populate predissociated rovibronic levels which lie above the two dissociation limits. The resultant Si^+ or SiH^+ fragment ions are then separated from the parent SiH_2^+ ion beam with a low resolution electromagnet and are detected on an electron multiplier.

The \tilde{X}^2A_1 and \tilde{A}^2B_1 states of SiH_2^+ are expected to be bent and linear respectively, and are derived from a hypothetical linear $^2\Pi$ state, which is split by static Renner-Teller interaction. On the basis of calculated potential energy curves [1], the $\tilde{A}^2B_1 - \tilde{X}^2A_1$ absorption spectrum is expected to lie in the visible part of the spectrum and this is confirmed in our work. The isoelectronic molecule AlH_2 exhibits a strong absorption band at 658 nm [2], and has also been

analysed in terms of a linear-bent transition. In SiH_2^+ we have so far identified and assigned the three rotational branches of a Σ sub-band ($K' = 0$) near 600 nm, but interestingly this sub-band appears only in the $\text{Si}^+ + \text{H}_2$ dissociation channel. However, many other rotational lines which must arise from sub-bands with $K' > 0$, appear in both dissociation channels. The spectrum is being studied further with a single mode dye laser, which should permit a full spectroscopic analysis, measurement of predissociation lifetimes from spectral line broadening, and a detailed study of the competitive predissociation. Measurement of the fragment translational energy will provide information on the disposal of the available energy between translational and internal degrees of freedom of the fragments.

- [1] Bruna, P.J., Hirsch, G., Buenker, R.J. and Peyerimhoff, S.D., in "Molecular Ions", ed. Berkowitz, J. and Groeneveld, K.-O., Plenum (1983), p.323.
- [2] Herzberg, G., in "Molecular Spectra and Molecular Structure" III, Electronic Spectra of Polyatomic Molecules, Van Nostrand (1966), p.583.

TIME-DEPENDENT WAVE MECHANICAL STUDY OF THE WINGS IN THE LYMAN- α
ABSORPTION SPECTRUM FOR $H + H_2$ COLLISIONS

P.M. AGRAWAL, V. MOHAN AND N. SATHYAMURTHY

Department of Chemistry, Indian Institute of Technology, Kanpur 208 016,
India

It has become possible to monitor the spectrum of a transition state, for example by monitoring the wings of the D-line emission from a sodium atom retreating from a freshly formed NaF molecule in the reaction $Na_2 + F \rightarrow Na^* + NaF$. It is of fundamental interest to predict and observe the wings (if any) to the Lyman- α absorption (emission) line in $H + H_2$ collisions. We have therefore followed the time-evolution of a wavepacket on the chemically accurate potential-energy surface for the H_3 system. By obtaining the probability density function by summing up $\psi^*\psi$ as a function of time over the configuration space and by assuming vertical transitions and reliable transition moments for transitions from $2pE'$ (1) to the low lying electronic excited states, we predict the absorption spectrum for the H_3 systems. Complementary emission studies are also planned.

HeH_2^+ - A CASE STUDY IN AB INITIO DYNAMICST. JOSEPH AND N. SATHYAMURTHYDepartment of Chemistry, Indian Institute of Technology, Kanpur 208 016,
India

We report the first successful analytic fit of the ab initio potential-energy surface of near configuration-interaction level of accuracy for the HeH_2^+ system published by McLaughlin and Thompson. Using three dimensional quasiclassical trajectory method, we have computed the reaction cross section for the exchange reaction $\text{He} + \text{H}_2^+ \rightarrow \text{HeH}^+ + \text{H}$ and the collision-induced dissociation $\text{He} + \text{H}_2^+ \rightarrow \text{He} + \text{H} + \text{H}^+$ for different vibrational states of H_2^+ over a wide range of relative translational energies. The results, including the vibrational enhancement are in near-quantitative agreement with the available state-selected experimental data. We have also computed the product energy and angular distributions and compared with the available experimental results.

We have also carried out collinear quantum mechanical calculations for the exchange reaction using the R-matrix of Walker and Light. The results confirm the overall validity of the QCT method to the title reaction. The oscillations in the quantum mechanical reaction probabilities as a function of energy are identified as the scattering resonances.

DTBP-initiated reaction of 2-methylpropene;
 k_d/k_c ratios of some alkyl radicals

L. Sere and A. Nacea

Institute of General and Physical Chemistry
 Attila József University, Szeged, Hungary.

The initial rate of formation of 17 products from the di-*t*-butyl peroxide (DTBP)-initiated reaction of 2-methylpropene (B) has been determined in a static system from gas-chromatographic measurements over the temperature range 395.2-442.6 K.

The 2-methyl-2-butyl (MB) and 2,4,4-trimethyl-2-hexyl (MBB) radicals were generated in the oligomerization reaction of methyl radical (M) and B

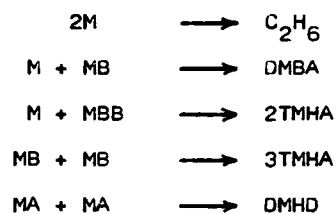


Thermochemical calculations indicate that the concentration of the C_{12} radical formed in the next step of oligomerization



is negligible.

We assume that ethane, 2,2-dimethylbutane (DMBA), 2,2,4,4-tetramethylhexane (2TMHA), 3,3,4,4-tetramethylhexane (3TMHA) and 2,5-dimethylhexadiene (DMHD) are formed solely in the following reactions



where $MA \equiv i-C_4H_7$.

In order to evaluate the rate constants of some selected reactions the concentrations of different radicals were expressed from the initial rates of formation of the above products.

The kinetic quantities calculated from the initial rates are

- a) $M + MBB \longrightarrow CH_4 + TMHE1$
 $\Delta(M, MBB) = 2.5 \pm 0.9$
- b) $MB + MBB \longrightarrow 2MBA + TMHE1$
 $\Delta(MB, MBB) = 5.8 \pm 0.8$
- c) $M + MB \longrightarrow CH_4 + 2MB2$
 $\Delta(M, MB) = 0.094 \pm 0.041$
- d) $MB + MB \longrightarrow 2MBA + 2MB2$
 $\Delta(MB, MB) = 0.70 \pm 0.04$

where $2MBA \equiv$ 2-methylbutane

$TMHE1 \equiv$ 2,4,4-trimethyl-1-hexene

$2MB2 \equiv$ 2-methyl-2-butene and

$$\Delta = \frac{k_d}{k_c}$$

Deductions from the Master Equation for Chemical Activation

Neil Snider

Department of Chemistry, Queen's University at Kingston, Ontario, Canada

The theory¹⁻³ of competing rates of gas phase decomposition and stabilization of a highly vibrationally excited molecule A is based on a master equation,

$$\frac{dc_n}{dt} = \sum_{\substack{m=1 \\ m \neq n}}^N (k_{nm} c_m - k_{mn} c_n) c_M - \kappa_n c_n + F_n \omega_A c_A \quad (1)$$

where n refers to an interval of energy, c_n to the concentration of A molecules in the n th interval, k_{mn} to the rate constant for collisional transitions to interval m from interval n , c_M to the concentration of a chemically inert collider gas present in large excess, κ_n to the rate constant for unimolecular decomposition of A molecules in interval n , F_n to the fraction of A molecules newly formed in interval n , c_A to the total concentration of A and $\omega_A c_A$ to the total rate of formation of A. It is to be understood that κ_n and F_n are zero for intervals with energy less than ϵ_d , the threshold energy for decomposition.

The solution of Eq. (1) is well known³ to be expressible in terms of the eigenvalues λ_1 and the normalized eigenvectors $|u_1\rangle$ of the matrix with m th element given by

$$\begin{aligned} & (k_{mn} k_{nm})^{1/2} && \text{for } m \neq n, \\ & - \sum_{j=1}^N k_{jn} - \kappa_n c_M^{-1} && \text{for } m=n. \end{aligned}$$

1. M. Hoare, J. Chem. Phys. 38, 1630 (1963).

2. G.H. Kohlmaier and B.S. Rabinovitch, J.Chem.Phys.38, 1692, 1709 (1963).

3. R.V. Serauskas and E.W. Schlag, J.Chem.Phys.42, 3009 (1965);

43, 898 (1965).

Frequently, one may assume $|\lambda_1| \ll |\lambda_\ell|$ ($2 \leq \ell \leq N$). There is then a considerable period during which the time evolution is determined by an exponential, $\exp(\lambda_1 c_M t)$. During this period the system is said to be in a pseudo steady state.

It has been argued⁴ that experimental measurements of the rates of decomposition and stabilization, denoted D and S respectively, are measured at the beginning of the pseudo steady state when $\lambda_1 t$ is nearly zero. One then obtains D and S in terms of $|u_1\rangle$. An accurate approximation to this eigenvector has been found⁴, and it can be evaluated in closed form for the stepladder model.^{4,5}

In calculations of collision frequency ω times the ratio D/S, hereafter denoted $\kappa_A(\omega)$, a number of approximations have been employed. All of these are low temperature approximations. In all calculations the steady state approximation has been used. This approximation can be shown⁴⁻⁶ to be quite accurate provided kT is small compared to ϵ_d . Other approximations, which become accurate only at considerably lower temperatures are neglect of all upward transitions and neglect of just those upward transitions to intervals with energy greater than ϵ_d from intervals with energy less than ϵ_d .

The steady state approximation yields formulas for $\kappa_A(\omega)$ at large and small ω for the stepladder model and for the separable model.^{4,6} Such expressions are of use in the interpretation of numerical results. For example, one can derive criteria for the validity of the approximations involving neglect of upward transitions. These approximations give κ_A 's which are too small at high temperatures.²

4. N. Snider, J. Chem. Phys. 80, 1885 (1984).

5. N. Snider, J. Chem. Phys., 77, 789 (1982).

6. N. Snider, unpublished.

In the large ω limit the steady state approximation gives for the separable exponential model

$$\kappa_a(\omega) = \bar{\kappa}_a(\omega) \{1 - [I_-(\epsilon_a - \epsilon_d) + I_+ kT] \langle \Delta \epsilon \rangle^{-1}\} \quad (2)$$

where $\bar{\kappa}_a(\omega)$ is the strong collision limit of $\kappa_a(\omega)$, I_- and I_+ are independent of the k_{mn} 's, $\langle \Delta \epsilon \rangle$ is the average energy change in A-M collisions and ϵ_a is the average energy of nascent A molecules. Numerical values of I_- and I_+ lie in the neighborhoods of 0.1 and 1 respectively. A similar expression is obtained for the stepladder model, the difference being that I_- and I_+ are replaced by quantities which depend on the k_{mn} 's and which approach I_- and I_+ from below as $\langle \Delta \epsilon \rangle$ goes to zero.

Neglect of all upward transitions leads to an equation for $\kappa_a(\omega)$ for the separable exponential model which differs from Eq. (2) in that the term $I_+ kT$ is missing and in that $-\langle \Delta \epsilon \rangle$ is replaced by $\langle \Delta \epsilon_- \rangle$, the average energy loss in deactivating collisions. Neglect of all upward transitions leads to an underestimate of $\kappa_a(\omega)$ which is about the same for all ω . However, when this approximation is used in the fitting of experimental data, it gives $\langle \Delta \epsilon_- \rangle$'s which are fairly accurate at small ω even when κ_a is considerably underestimated. Such is not the case in the large ω limit.⁴

Neglect of just those upward transitions to intervals with energies greater than ϵ_d from intervals with energies less than ϵ_d gives κ_a 's much more accurately at large ω than it does at small ω .

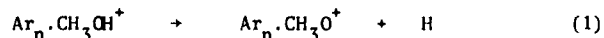
Chemical reactions on clusters. The gas phase unimolecular decomposition of molecular ions in association with inert gas clusters.

A.J. Stace, School of Molecular Sciences, University of Sussex, Falmer, Brighton, Sussex, BN1 9QJ, U.K.

By carefully controlling the nozzle conditions in an adiabatic expansion of gas mixtures it is possible to form clusters of the type $\text{Ar}_n \cdot \text{X}$ and $(\text{CO}_2)_n \cdot \text{X}$, where X ranges from I_2 to $(\text{CH}_3\text{CH}_2)_2\text{CO}$. Despite the apparent fragile nature of these mixed clusters, it is observed that upon electron impact ionization X undergoes unimolecular decomposition without significantly disrupting the inert gas component. Approximately 20 examples of this type of behaviour have now been observed; in some cases the critical energies of reaction are as high as 2 eV and several molecular ions display three or more parallel decomposition routes. Reactions on clusters as large as $\text{Ar}_{40} \cdot (\text{CD}_3)_2\text{CO}^+$ have been observed with no significant decrease in the relative intensities of the product ions.

From a detailed study of a number of these systems{1-3} the following conclusions have been drawn:

(1) in large clusters the excitation of X appears to proceed via a charge transfer mechanism. No reactions are observed when $\text{I.P.}(\text{inert gas cluster}) - \text{I.P.}(\text{X}) - \epsilon_0 < 0$, where ϵ_0 is the critical energy of reaction. As an example, ions of the type $\text{Ar}_n \cdot \text{CH}_3\text{OH}^+$ undergo the reaction



whereas $(\text{CO}_2)_n \cdot \text{CH}_3\text{OH}^+$ ions can easily be produced but do not appear to

give any reaction products associated with decomposition of the methanol ion.

(2) the molecular ion decomposes because of the comparatively slow rate of intermolecular energy transfer between it and the inert gas component. The charge transfer mechanism means that each molecular ion receives a fixed amount of internal energy. Hence it is possible to calculate the lifetime of an ion with respect to each of the observed decomposition routes. In all the examples studied so far these lifetimes are of the order 10^{-12} - 10^{-11} s. By comparison the vibrational predissociation times for van der Waals molecules are approximately 10^{-9} s. Those unimolecular reactions which, although energetically allowed, are calculated to occur on a timescale less than approximately 10^{-9} s are not observed.

(3) the molecular ion appears to 'sit on' rather than 'within' the ion cluster. Evidence for this comes mainly from the types of chemical reactions displayed by the cluster-bound molecular ions, compared to their behaviour as isolated ions.

(4) individual clusters appear to exhibit behaviour which could be associated with their undergoing a phase transition.

{1} A.J. Stace, J. Phys. Chem., 87,2286(1983).

{2} A.J. Stace, Chem. Phys. Letts., 99,470(1983).

{3} A.J. Stace, J. Am. Chem. Soc., in print.

Quantum Selected Kinetics

REACTIVE COLLISION CROSS SECTIONS FROM

A QUANTAL 3-D PERTURBATION TREATMENT

S.H. Suck Salk

Department of Physics
and Graduate Center for Cloud Physics Research
University of Missouri-Rolla
Rolla, Missouri 65401

Presently the validity of DWBA methods for the study of cross sections for elementary reactions has been largely unchecked with respect to exact methods. In the present study, direct comparison between the very computationally economical (a few minutes) DWBA and exact close-coupling calculations is made by examining the integrate cross sections and angular distributions of $H + H_2 \rightarrow H_2 + H$ for the same range of collision energy as Schatz and Kuppermann chose. We have found from the DWBA study that:

- 1) the structures of angular distributions between these two methods are remarkably similar at most collision energies;
- 2) the effect of coupling strongly affects the absolute magnitude of cross-sections but not the structures of normalized angular distributions;
- 3) kinematics associated with impact parameters (orbital angular momenta) plays a major role in determining the structure of the normalized angular distributions; and
- 4) the DWBA predicted state-to-state integrated (total) cross-sections σ_{DWBA} are much smaller than the exact close-coupling results σ_{EXACT} , due to the dominant effect of coupling which is found to rapidly increase with collision energy

E_K , observing the relationship of

$$\sigma_{\text{EXACT}} \propto E_K^{2/3} \sigma_{\text{DWBA}}^{-1}$$

Finally, we would like to stress that the present perturbation treatment will prove highly useful for revealing the knowledge of direct reaction mechanisms in elementary chemical reactions and that the finding of proper scaling laws will be needed for obtaining chemically important reaction rates. Judging from the satisfactory relation¹ above, such study of finding scaling laws is expected to be within our reach.

NITROBENZENE DECOMPOSITION IN A HEATED SINGLE PULSE SHOCK TUBE

W. TSANG AND D. ROBAUGH

Chemical Kinetics Division, National Bureau of Standards, Washington DC
20234, U.S.A.

A heated single pulse shock tube has been constructed in order to study the high temperature stability of low volatility organic compounds. We have used the instrument to study nitrobenzene decomposition in the temperature range of 950 - 1050 K and at three atmospheres pressure. Nitrobenzene concentration was near 1000 ppm and experiments were carried out in the presence and absence of a chemical inhibitor (cyclopentane). In the absence of an inhibitor and with gas chromatographic analysis, the reaction products included ethylene, acetylene, vinylacetylene, benzene, phenol, biphenyl and diphenyl ether. Material balance was not satisfactory since only about 60% of the products were recovered. This may be due to the failure to search for the nitrobiphenyls and other high boiling compounds. In the presence of 10% cyclopentane the reaction products in relative order of importance were, ethylene, benzene, propylene and phenol. The ratio of ethylene to benzene was of the order of 3 to 1, while that of benzene to phenol was of the order of 7 to 1. A very satisfactory mass balance was obtained in terms of nitrobenzene disappeared and phenol and benzene concentration. It is clear that the main initial process in nitrobenzene decomposition is the cleavage of the C-N bond. The secondary chemistry is dominated by the reactions of NO_2 with the radicals present in the system. These are phenyl for the uninhibited reaction and allyl (or perhaps cyclopentyl) for the inhibited system. Quantitative kinetic data on the initial bond breaking process and the reactions of allyl and phenyl radicals with various substrates will be presented.

ON THE COLLISION ENERGY DEPENDENCE OF THE REACTION CROSS-SECTION. A
MICROANONICAL TRANSITION STATE MODEL ANALYSIS

A. Gonzalez Ureña

Departamento de Química Física, Facultad de Química, Universidad Complutense,
Madrid-3, Spain

A microanonical transition state model calculation is presented to account for the kinetic energy dependence of the reaction cross section $\sigma_R(E_T)$. An atom-diatom reaction scheme was used to obtain different expressions for the reaction cross section as a function of the internal density of states of the transition state and, on the other hand, of the adiabatic character of the rotational and vibrational motion of the diatomic. The model was applied to the $M + RX \rightarrow MX + R$, $M + X_2O \rightarrow MO + X_2$, etc., where M = alkali, X = halogen or nitrogen and R = alkyl group. The model seems to explain satisfactorily the shape of these excitation functions and shows that the shape evolution of σ_R with E_T is a direct consequence of the collision energy dependence of the transition state location. Indeed, it is shown that for several exoergic reactions the maximum in $\sigma_R(E_T)$ can be originated by the shift of the transition state from an early location (at the entrance channel) towards the products' valley as E_T increases.

INFRARED LASER ISOTOPE SEPARATION IN A VAN DER WAALS CLUSTER BEAM

J.M. ZELLWEGER, J-M. PHILIPPOZ, H. VAN DEN BERGHInstitut de Chimie-Physique, Ecole Polytechnique Fédérale, Lausanne,
Switzerland

and

R. MONOT

Institut de Physique Expérimentale, Ecole Polytechnique Fédérale, Lausanne,
Switzerland

Efficient laser isotope separation is demonstrated in two distinct schemes. In the first, termed "laser enhanced gas dynamic isotope separation", irradiation of the collisional zone of the gas expansion provokes an isotopically selective condensation, as well as changes in the velocity distributions of the free jet. The resulting large changes in particle mass and/or changes in beam geometry, lead to separation of $^{32}\text{SF}_6$, $^{33}\text{SF}_6$ and $^{34}\text{SF}_6$ in an SF_6/Ar mixture and enrichment factors in excess of 2.0. In similar experiments we have separated bromine isotopes in $\text{CF}_3\text{Br}/\text{Ar}$ mixtures and silicon isotopes in SiF_4/Ar mixtures. In the second scheme, irradiation of the collision free part of the free jet induces single photon infrared vibrational predissociation of van der Waals clusters. Thus, at selected wavelengths clusters containing one isotopomer can be made to recoil out of the beam preferentially, resulting in the separation of isotopes. In both schemes a tunable IR laser of only a few watts is used.

TEMPERATURE JUMP MEASUREMENTS IN GAS KINETICS

P. GOZEL, B. CALPINI AND H. VAN DEN BERGHInstitut de Chimie-Physique, Ecole Polytechnique Fédérale, CH-1015
Lausanne, Switzerland

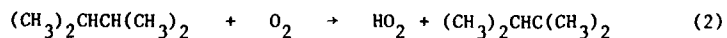
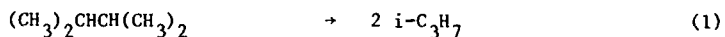
The temperature jump relaxation method is applied to kinetic measurements in the gas phase for the first time. The system $\text{N}_2\text{O}_4 \rightleftharpoons 2\text{NO}_2$ is studied. Fast T-jumps are induced by IR absorption from a TEA CO_2 laser. Temperature jumps of less than 1 K lead to readily detectable concentration changes which are monitored by UV absorption in a simple single shot experiment, $k_{\text{rec}}(\text{Ar})$ is found to be $1.05 \times 10^{10} \text{ cm}^3 \text{ mol}^{-1} \text{ s}^{-1}$ at $p_{\text{Ar}} = 1 \text{ bar}$ and $T = 258 \text{ K}$, in agreement with recent findings.

DECOMPOSITION OF 2,3-DIMETHYLBUTANE IN THE PRESENCE OF O_2 by R.R. Baldwin, G.R. Drewery, and R.W. Walker

Chemistry Department, University of Hull, Hull, HU6 7RX

As part of a long-term study of the elementary reactions involved in combustion, the decomposition of 2,3-dimethylbutane (DMB) in the presence of O_2 has been investigated using KCl-coated vessels between 480° and $540^\circ C$ over a wide range of mixture composition. The major initial products are propene, 2-methylbutene-2, methane, and formaldehyde, with smaller amounts of 2,3-dimethylbutene-2, 2,3-dimethylbutene-1, 3-methylbutene-1, and butene-2. Small amounts of tetramethyloxirane are observed as an initial product at high (ca 100 Torr) O_2 pressures. In this presentation attention will be focussed on results of general interest to gas kinetics.

At low pressures of O_2 , (1) is the main initiation reaction, but (2) becomes dominant at the higher pressures of O_2 used. From measurements of the initial amounts of propene, formed in 99% yield from $i-C_3H_7$ radicals, accurate values of k_1 are obtained after extrapolation to zero time to remove secondary formation, to zero DMB to remove any chain contribution, and to zero O_2 to eliminate reaction (2).



Combination with Tsang's high temperature values gives an excellent Arrhenius plot over the range 750 - 1200 K, from which $\log_{10}(A_1/s^{-1}) = 16.42 \pm 0.10$ and $E_1 = 319.1 \pm 1.5 \text{ kJ mol}^{-1}$. These parameters fit in well with analogous values for C - C homolysis in symmetrical alkanes, and the very simple reaction (i) predicts accurately to within $\pm 3 \text{ kJ mol}^{-1}$ the activation energy for C - C homolysis in alkanes and alkenes generally.

$$E_R - R' = (E_{R'} - R' + E_R - R)/2 \quad (i)$$

By use of the published values of k_{-1} and an assumed internal rotational energy barrier in the $i\text{-C}_3\text{H}_7$ radical of 8.5 kJ mol^{-1} , values of the entropy and heat of formation of the radical have been calculated at 926 and 298 K. A self-consistent set of data is now available for the heats of formation of the prototypical alkyl radicals, ethyl, i -propyl, and t -butyl.

Table 1 Heats of Formation of Alkyl Radicals ¹		
R	$\Delta_f H_{298}^{\circ}(\text{R})/\text{kJ mol}^{-1}$	$D_{298}^{\circ}(\text{R} - \text{H})/\text{kJ mol}^{-1}$
CH_3	145.6 ± 1.0	438.4 ± 1.0
C_2H_5	118.0 ± 4.0	420.5 ± 4.0
$i\text{-C}_3\text{H}_7$	79.6 ± 2.0	401.3 ± 2.0
$t\text{-C}_4\text{H}_9$	37.6 ± 2.0	390.2 ± 2.0

In the absence of a chain contribution to the removal of DMB, values for k_1 and k_2 may be obtained by use of equation (ii), the value of $-d[\text{DMB}]/dt$ being determined from the total yield of products.

$$R_o = -d[\text{DMB}]/dt = (k_1 + k_2[\text{O}_2])[\text{DMB}] \quad (ii)$$

Extrapolation to zero time and $[\text{DMB}]$ to obtain initial yields and to remove chain contributions, as above, gives R_o . Then a plot of $R_o/[\text{DMB}]$ against $[\text{O}_2]$ gives k_1 from the intercept and k_2 from the gradient. The values of k_1 are in good agreement (ca 10%) with those obtained from the propene yields, which are more accurate because less extrapolation is required. Table 2 gives the values for k_2 at 500 and 540°C . No other values of k_2 are available for DMB or any analogous reaction involving a hydrocarbon, despite the importance of this type of reaction in combustion and in O_2 -sensitised pyrolyses. The only other related rate constants available are for the HCHO and $\text{C}_2\text{H}_5\text{CHO}$ reactions².

Table 2 Rate Constants for RH + O₂ Reactions*

Reaction	A	E	k	T/°C	k ₅₄₀ (per C - H bond)
HCHO + O ₂	2.04 x 10 ¹⁰	163±6	-	-	0.346
C ₂ H ₅ CHO + O ₂	-	-	0.076	440	2.24
DMB + O ₂	-	-	0.163	540	0.082**
			0.0211	500	-
* Units, dm ³ mol ⁻¹ s ⁻¹ and kJ mol ⁻¹ .					
**Reaction involving the primary C - H bonds will be negligible.					

Reliable Arrhenius parameters for reaction (2) cannot be obtained due to the restricted temperature range, but if A₂ is equal to the A factor for the HCHO + O₂ reaction, then E₂ = 173 ± 4 kJ mol⁻¹. As E₋₂ is effectively zero, then E₂ = ΔH₂ and the value gives the tertiary C - H bond dissociation energy in DMB as 387 ± 4 kJ mol⁻¹ which is indistinguishable from the value of 390.0 ± 2.0 for the tertiary bond in i-butane given in Table 1.

With the reasonable assumption of equal A factors per C - H bond for HCHO + O₂ and C₂H₅CHO + O₂, and zero activation energies for the reverse reactions, then from the rate constants in Table 2, D(HCO - H) - D(C₂H₅CO - H) = 11 kJ mol⁻¹ in contrast to the current view that the difference is zero. A significantly stronger bond in HCHO is also consistent with the difference in the rate constants (per C - H bond) for H abstraction from the aldehydic position in HCHO, C₂H₅CHO and i-C₃H₇CHO by the selective HO₂ radical, the values being 2.9 x 10⁵, 1.52 x 10⁶, and 1.8 x 10⁶ dm³ mol⁻¹ s⁻¹, respectively at 440°C.³

References

1. R.R. Baldwin, G.R. Drewery, and R.W. Walker, J.C.S. Faraday Trans. I (in press).
2. R.W. Walker, in Reaction Kinetics (Specialist Periodical Report, The Chemical Society, London, 1975), vol 1, p 161.
3. R.R. Baldwin and R.W. Walker, 17th Int. Symp. Combustion (The Combustion Institute, Pittsburgh), 1979, p 525.

Energy transfer from excited cyclooctatetraene produced by the
thermal decomposition of cubane

by

H. -D. Martin and T. Urbanek

Institut für Organische Chemie I, Universität Düsseldorf,
4000-Düsseldorf, W.Germany

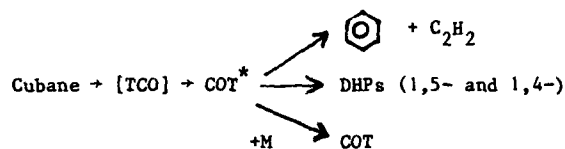
and

R. Walsh

Chemistry Dept., University of Reading, Whiteknights,
Reading RG6 2AD

A kinetic and mechanistic investigation of the thermal decomposition of cubane and related C_8H_8 hydrocarbons has been carried out in the gas phase. Cubane decomposes at 250°C in a clean first order process ($\log(k/s^{-1}) = (14.7 \pm 0.4) - (180 \pm 4 \text{ kJ mol}^{-1})/RT \ln 10$) to give benzene and acetylene, cyclooctatetraene (COT) and various isomeric dihydropentalenes (DHPs). The product ratios were pressure dependent (added gases N_2 and cyclo- C_4F_8) such that at the lowest pressure, benzene (with C_2H_2) was the major product pathway, while at the highest pressure COT predominated. The DHP's were minor products, amounting in total to ca 30% of benzene and, like benzene, decreasing in importance with pressure. An independent thermal study ($400\text{--}440^\circ\text{C}$) indicated that COT itself decomposed to give the same products as cubane (DHPs (now the major products) and benzene with acetylene) although in this case the products were not pressure dependent. The reaction is first order ($\log(k/s^{-1}) = (14.7 \pm 0.1) - (233.0 \pm 0.5 \text{ kJ mol}^{-1})/RT \ln 10$).

The cubane decomposition may be modelled by a reaction scheme based on the formation of vibrationally excited COT, viz



where TCO represents syn-tricyclo[4.2.0.0^{2,5}]octa-3,7-diene.

From the known strain energy in cubane (688 kJ mol⁻¹) and other available thermochemistry, COT* is estimated to contain an average energy of ca 540 kJ mol⁻¹. RRKM calculations have been carried out using transition state assignments for COT rearrangement (two channels) based on thermal data, together with a multistep collisional deactivation model. These calculations indicate that the average energy removed per down collision (stepladder model), <ΔE>, is ca 30 kJ mol⁻¹ for c-C₄F₈. The dependence of this figure on uncertainties in the calculations (initial energy distribution of COT*, transition state models for COT decomposition, etc.) will be discussed.

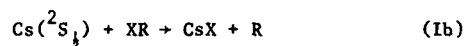
This system with its high excitation energy and dual decomposition channel would appear to offer good opportunities to probe energy transfer from (and by) polyatomics. The results and further *measurements* with N₂ as collider gas will be compared with the work from other laboratories on similar systems in an effort to clarify the currently confusing scene regarding such energy transfer.

METASTABLE ATOMIC REACTION DYNAMICS: ANGLE RESOLVED SCATTERING, OPACITY
FUNCTIONS AND EXCITATION FUNCTIONS FOR THE INTERACTION OF $\text{Xe}(^3\text{P}_{2,0})$ WITH
 CH_3I AND CH_3Br

J.P. Simons, K. Suzuki and C. Washington

Chemistry Department, The University, Nottingham NG7 2RD, United Kingdom

Similarities between the reactive scattering of alkali metal atoms and metastable electronically excited rare gas atoms are well documented [1] and are illustrated for example, by their reaction with halogen donors,



The dynamics of the reactive scattering (Ib) can be examined through measurements of differential cross-sections for product formation but in (Ia) the excited rare gas halide product is too short-lived and the product channels can only be monitored through spectral analysis of their fluorescence. An alternative approach focusses on the differential cross-sections for the elastic scattering of the incident atoms and their modification by the competing inelastic channels [2]. When the atoms are electronically excited, the competing channels may also include excitation transfer (Ic),



For $\text{XR} \equiv \text{CH}_3\text{I}$, CH_3Br the reactive channel (Ia) accounts for 1% of the scattering at thermal collision energies [1].

CH_3I ^[3]

There are both similarities and clear contrasts between the collision dynamics for the interaction of CH_3I with Cs and $\text{Xe}(^3\text{P}_{2,0})$. Collisions with Cs lead to reactive scattering into the backward hemisphere with

integral cross sections, $\sigma \leq 35 \text{ \AA}^2$ [4]. The reaction probability at zero impact parameter $P(b=0) < 1$, implies a collisional anisotropy - preferential attack at the iodine end of the target. Collisions with $\text{Xe}(^3\text{P}_{2,0})$ atoms lead predominantly to inelastic scattering in the forward hemisphere with integral cross-sections, $\sigma \leq 75 \text{ \AA}^2$. $P(b=0) = 1$ at all collision energies, implying an absence of any significant anisotropy for excitation transfer. Both the inelastic and/or reactive cross-sections fall with increasing collision energy; in the case of $\text{Xe}(^3\text{P}_{2,0})$ the two excitation functions follow the same dependence $\sigma(E_{\text{CM}}) \propto 1/E_{\text{CM}}^{1/2}$ (See Figure 1), implying passage over an orbiting barrier lying outside the ionic-covalent curve crossing region and branching on the ionic surface.

CH_3Br

In contrast to CH_3I , the excitation functions for both reactive (alkali metals, $\text{Xe}(^3\text{P}_{2,0})$) and inelastic ($\text{Xe}(^3\text{P}_{2,0})$) scattering show threshold behaviour, but once again the two competing channels in the $\text{Xe}^*/\text{CH}_3\text{Br}$ system show the same energy dependence (see Figure 2). Here the barrier to reaction is thought to involve stretching of the C-Br bond; the branching, as before, must occur inside this common barrier. The limiting reaction probability $P(b=0) \rightarrow 1$. New data for the $\text{Xe}(^3\text{P}_{2,0})/\text{HBr}$ system will be presented at the Conference.

Support from the SERC and from the Japanese Ministry of Education, Science and Culture (KS) is gratefully acknowledged.

- [1] D.W. Setser et.al., Faraday Discussions Chem. Soc., 67, 255 (1979).
- [2] J.L. Fraites and D.H. Winicur, J. Chem. Phys., 64, 89 (1976).
- [3] J.P. Simons, K. Suzuki and C. Washington, Mol. Phys., in press.
- [4] J.L. Kinsey, G.H. Kwei and D.R. Herschbach, J. Chem. Phys., 64, 1914 (1976).

FIGURE 1

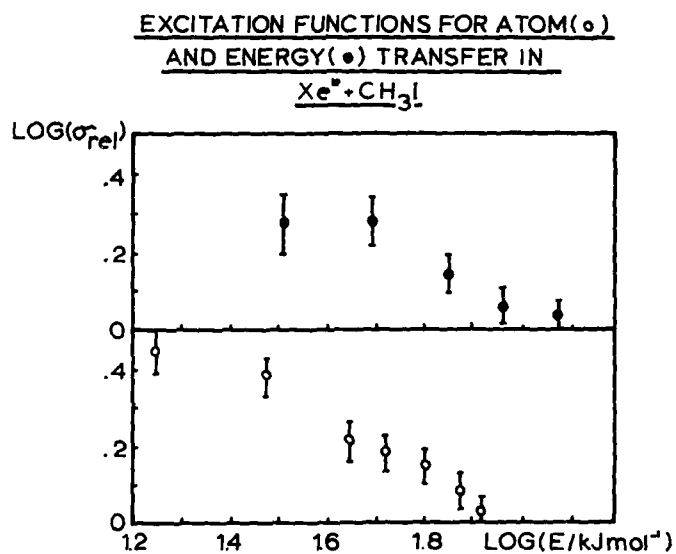
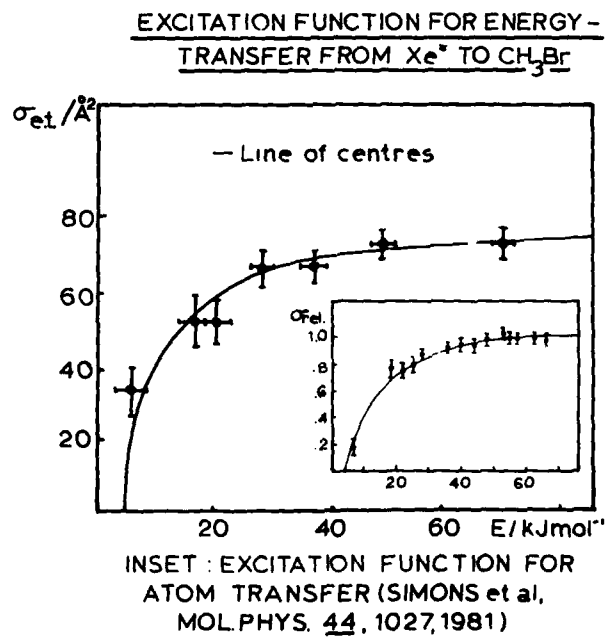


FIGURE 2



STIMULATED EMISSION AND QUANTUM BEAT SPECTROSCOPY
OF FORMALDEHYDE AND ACETYLENE

E. Abramson, H.-L. Dai, R. W. Field, K. K. Innes, J. L. Kinsey,
R. Sundberg and P. H. Vaccaro

Department of Chemistry
Massachusetts Institute of Technology
Cambridge, Massachusetts 02139, USA

Stimulated Emission Pumping is a new technique that permits study of previously inaccessible classes of moderately to extremely highly excited vibrational levels in polyatomic molecules[1]. Two pulsed lasers are used. The first (PUMP) excites the molecule to an excited electronic state, in practice to a ro-vibrational level already studied and characterized by absorption spectroscopy. A time-delayed pulse from the second laser (DUMP) stimulates emission into a selected ro-vibrational level of the electronic ground state. The PUMP-laser frequency is set at a value chosen to select a particular intermediate level, and the DUMP laser's frequency is scanned. This provides spectroscopic access, at a resolution limited by laser linewidth, to ground-state levels having up to several eV of energy. Since there is a single intermediate level with definite J , K_a values from which all final levels are reached, there is no rotational congestion in SEP spectra. SEP can be used as a preparative as well as a spectroscopic tool. We have demonstrated transfer of $\sim 10^{-4}$ of the total thermal population of H_2CO to a single ro-vibrational level with energy up to $\sim 10000\text{ cm}^{-1}$ [2].

We have studied two polyatomic species using SEP: formaldehyde (H_2CO) [2,3,4] and acetylene (C_2H_2) [5]. In both molecules, there was a relatively low energy "simple" spectrum which allowed normal-mode vibrational assignments and a higher energy "complex" spectrum. Up to this point, the

simple part of the H_2CO spectrum and the complex part of the C_2H_2 spectrum have received most attention. Over 50 assignable vibrational levels of H_2CO ranging in energy from ~ 4500 - 9500 cm^{-1} were identified in SEP. From these and other spectroscopic data a complete set of experimentally determined vibrational constants ($27\ \omega_i^0$ and X_{ij} values) were obtained [4]. Only a few low-energy vibrational levels near 9500 cm^{-1} in C_2H_2 have as yet been carefully studied. These have nonetheless provided a useful test of existing vibration-rotation constants at higher energies than had previously been reached, and they further permitted determination of the higher order constants Y_{244} and Y_{224} .

At the high end of the "simple" spectroscopic region in H_2CO ($\sim 9500\text{ cm}^{-1}$), multiple features are seen in some regions for which only a single vibrational state is expected to show spectroscopic activity. Exploration of the number and character of the "extra" features as a function of the J , K_a values of the intermediate SEP level proves quite instructive towards understanding the role of Coriolis coupling in the breakdown of simple normal-mode behavior. An analysis in terms of the fraction of available phase-space actually covered reveals an interesting paradox.

Studies of the C_2H_2 spectrum near 28000 cm^{-1} with broad-band SEP scans (resolution $\sim .3\text{ cm}^{-1}$) at a density of about 1 per 10 cm^{-1} . High resolution scans (resolution $\sim .03\text{ cm}^{-1}$) shows each of these to be a "clump" of closely spaced lines whose density is ~ 30 per cm^{-1} . The energies corresponding to the centers of these clumps vary with J as $B_J(J+1)$, with B -values indicative of large bending excitations. No discernable pattern in the substructure of clumps persists as J varies. These spectra have been analyzed using a variety of statistical parameters obtained in theoretical treatments of quantum chaotic behavior.

Non-SEP studies have also been carried out on both H_2CO and C_2H_2 . Stark-tuned anticrossing spectroscopy of interacting S_0 and S_1 levels lead to a determination of S_0 tunnelling lifetimes and hence the height of the S_0 barrier to the reaction $\text{H}_2\text{CO} + \text{H}_2 + \text{CO}$. Rotational relaxation of selected H_2CO S_1 (\tilde{A}^1A_2) levels has also been studied by transient gain spectroscopy, and dipole moments in the out-of-plane bending levels of S_1 H_2CO and D_2CO have been determined. In acetylene, Zeeman-tuned anticrossing spectroscopy of S_1 levels interacting with a dense manifold of triplet levels has been studied.

References

1. C. Kittrell, E. Abramson, J. L. Kinsey, S. A. McDonald, D. E. Reisner, R. W. Field and D. H. Katayama, J. Chem. Phys. 75, 2056 (1981).
2. D. E. Reisner, P. H. Vaccaro, C. Kittrell, R. W. Field, J. L. Kinsey, and H.-L. Dai, J. Chem. Phys. 77, 573 (1982).
3. P. H. Vaccaro, J. L. Kinsey, R. W. Field and H.-L. Dai, J. Chem. Phys. 78, 3659 (1983).
4. D. E. Reisner, R. W. Field, J. L. Kinsey and H.-L. Dai, J. Chem. Phys., in press.
5. E. Abramson, R. W. Field, D. Imre, K. K. Innes and J. L. Kinsey, J. Chem. Phys. 80, 2298 (1984).

"Vibrational Mode Specificity vs. Vibrational Mixing in Small
Polyatomic Molecules: SRL's of S_1 H_2CO "^a

Eric C. Apel, Nancy L. Garland, and Edward K.C. Lee

Department of Chemistry

University of California, Irvine, CA 92717

ABSTRACT^b

Recent experimental studies from our laboratory¹⁻² and elsewhere³⁻⁵ have demonstrated the importance of rotation-vibration interaction in radiationless transitions and vibrational mixing of polyatomic molecules. A strong Coriolis interaction can induce not only an extensive mixing of vibrational states but also cause the destruction of K quantum numbers in the cases of high J's. These rotational effects should increase the number of final states capable of communicating with the initial state and lead to a more efficient vibrational redistribution. Therefore, a systematic study of Coriolis-induced vibrational mixing at various ranges of vibrational and rotation quantum numbers, energies, and level densities of relatively simple, model polyatomic molecules can provide important information, both qualitative and quantitative, on intramolecular vibrational redistribution (IVR). One such molecular parameter is the mixing coefficient for each zero-order vibrational state composing the eigenstate whose magnitude is determined by the Coriolis coupling constant, the preperturbed energy level gap and the interaction matrix element. The magnitude of the mixing coefficients can be calculated from the degree of anomaly observed in the observed size of vibronic intensity

(a) The support of this research by the Petroleum Research Fund of the American Chemical Society is gratefully acknowledged.

(b) To be presented at the 8th International Symposium on Gas Kinetics, Nottingham, Great Britain, July 16-20, 1984.

borrowing,² the rotational line intensity distribution,^{2,4} and the magnitude of the perturbed energy level shifts.³ Each of the three methods are complementary.

Our initial study of the extent of vibrational mixing involves two different vibrational energy regions² of S_1 H_2CO (\tilde{A}^1A_2), $E'_{vib} = 2200$ and 3000 cm^{-1} , where the average level separations are approximately 50 and 20 cm^{-1} , respectively, as shown in Figures 1 and 2. It involves the measurements of rotationally resolved fluorescence emission spectra from a single rotational level excitation under collision-free conditions.² In the $E'_{vib} = 2200\text{ cm}^{-1}$ region,^{2c} an extensive vibrational mixing for $\Delta J' = 0$ and $\Delta K'_a = \pm 1$ has been observed between two zero-order states, $\underline{2}^1\underline{4}^1\underline{6}^1$ and $\underline{2}^1\underline{6}^1$ by b-axis Coriolis coupling, and $\underline{2}^1\underline{4}^3$ and $\underline{2}^1\underline{4}^1\underline{6}^1$ by c-axis Coriolis coupling. The a-axis Coriolis mixing (for $\Delta J' = 0$ and $\Delta K'_a = 0$) between $\underline{2}^1\underline{4}^3$ and $\underline{2}^1\underline{6}^1$ was observed to be small due to an unfavorably large vibrational energy difference. In the $E'_{vib} = 3000\text{ cm}^{-1}$ region,^{2b} an extensive vibrational mixing among three zero-order states has been observed: Between $\underline{1}^1\underline{4}^1$ and $\underline{5}^1$ by a-axis coupling due to a favorable vibrational energy gap ($\approx 2.7\text{ cm}^{-1}$), between $\underline{1}^1\underline{4}^1$ and $\underline{1}^1$ by b-axis coupling, and between $\underline{5}^1$ and $\underline{1}^1$ by c-axis coupling. A further study of H_2CO at higher values of E'_{vib} should reveal even greater degrees of vibrational mixing.

References

1. K.Y. Tang, P.W. Fairchild, and E.K.C. Lee, J. Chem. Phys., **66**, 3303 (1977).
2. N.L. Garland and E.K.C. Lee, (a) Faraday Discuss. Chem. Soc., **75**, 377, 1983; (b) Chem. Phys. Lett., **101**, 573 (1983); (c) E.C. Apel and E.K.C. Lee, J. Phys. Chem., **88**, 1283 (1984).
3. C.M.L. Kerr and D.A. Ramsay, J. Mol. Spectrosc., **87**, 575 (1981).
4. (a) P.H. Vaccaro, J.L. Kinsey, R.W. Field, and H.-L. Dai, J. Chem. Phys., **78**, 3659 (1983); (b) D.E. Reisner, R.W. Field, J.L. Kinsey, and H.-L. Dai, J. Chem. Phys., to be published.
5. E. Riedle, H.J. Neusser, and E.W. Schlag, J. Phys. Chem., **86**, 4847 (1982).

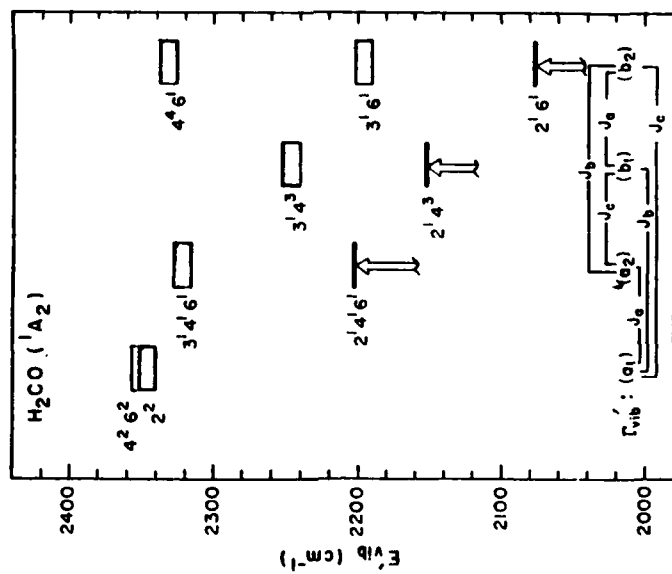


Figure 1.

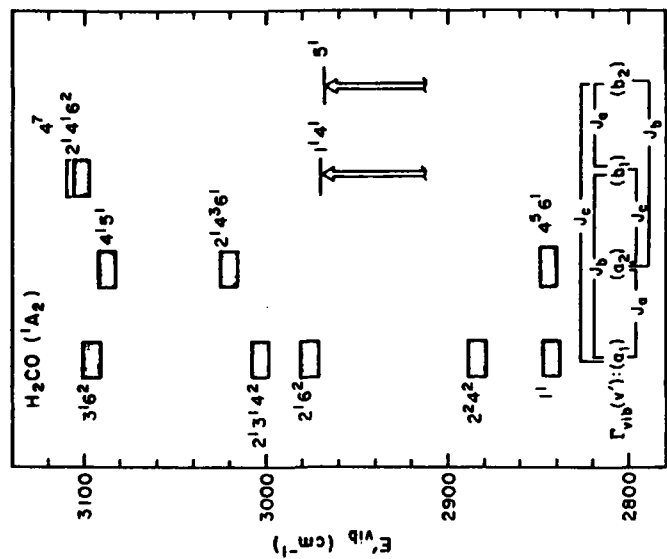


Figure 2.

Investigations of the nascent vibrational state
of products from thermal dissociation reactions

John Buxton, Rupert Sohm and Stephen Simpson
Physical Chemistry Laboratory, South Parks Road, Oxford

1. Introduction

The unimolecular decomposition of norbornenone has been investigated in the gas phase in the temperature range 675 to 3,000 K and the pressure range 140 to 1,600 torr. Mixtures containing $\leq 0.2\%$ of norbornenone in Ar were shock heated to the desired temperature. The reaction was carried out under nearly isothermal conditions. The production of CO and the nascent vibrational state of the CO(V) were monitored using a C.W. CO laser. The apparatus has been described in previous papers [1,2,3]. The present work follows on from the study of the nascent vibrational distribution in the decomposition of OCS in the temperature range 2,000 to 4,000 K [3].

2. Kinetic measurements

The rate of the reaction has been measured by monitoring the production of CO($v=0$) by measuring the gain on the $v=1 \rightarrow 0$ P(9) line of the C.W. CO laser. In the temperature range 675 to 850 K at thermal equilibrium there is 1.0% to 2.5% in the $v=1$ level so to a good approximation the change in intensity of the CO laser line directly monitors the production of CO($v=0$). It was found that the number density of CO($v=0$) molecules grows exponentially with time and rate constants could be calculated readily. A series of shocks was run at 150 torr in the temperature range 675 to 850 K to determine rate constants for the dissociation and a second series at 300 torr. The slope of the $\log k - 1/T$ plots are the same to within 10%, but the rate constants are higher by 36% for the series at 300 torr. A third series of shocks was run at 600 torr. The rate constants for the 300 torr and the 600 torr series are identical to within 7% showing that the

reaction is dominated by first order kinetics. The fact that the energy of activation for the higher pressure series is the same as that measured by Clarke and Johnson [4] in solution is further evidence that the high pressure limit has been reached in the gas phase. The energies of activation measured at 150, 300 and 600 torr are 112, 124 and 120 kJ mole⁻¹ respectively. Clarke and Johnson obtained the value 129 kJ mole⁻¹ in the temperature range 400 to 410 K.

The nascent vibrational state of the product CO molecules

(a) The temperature range 675 to 850 K

At 675 K there is 1% of CO(v=1) at equilibrium and at 850 K there is 2.5% hence it is very difficult for us to distinguish between the CO(v) being born with the Boltzmann distribution appropriate to the translational temperature and being born vibrationally cold. The population in the v=0 level grows exponentially with time from the base line and there is no sign of population in higher levels at short times. It is thus very improbable that the CO is born vibrationally hot and relaxes to a Boltzmann distribution before it can be detected. This possibility is eliminated by the experiments at higher temperatures in which the rate constants for the relaxation of the CO(v) by product molecules have been measured. Thus from these experiments we are left with the possibilities that the CO(v) is either born in Boltzmann equilibrium, or vibrationally cold.

(b) The temperature range 1,600 to 2,300 K

At these temperatures under our conditions the norbornene is dissociated in less than 1 μ s and its rate of decomposition cannot be measured. The CO(v) is relaxed very slowly by Ar on our time scale, however it is relaxed rapidly by the product molecule cyclohexadiene. We have measured the rate constant for this process using CO, cyclohexadiene, Ar mixtures. The relaxation is fast enough to ensure that the CO(v) is relaxed

to the Boltzmann equilibrium condition in our experimental observation time.

Our measurements of the laser gain for $v=1 \rightarrow 0$ and the $v=2 \rightarrow 1$ laser lines show that the CO(V) is born with an excess of population in ($v=0$). This is relaxed down to the equilibrium condition while the population in $v=1$ increases from a low nascent value up to the equilibrium condition. The CO is born vibrationally cold both in the fall off region and at the high pressure limit for unimolecular decomposition.

Conclusion

We have measured the energy of activation for the unimolecular decomposition of norbornene over a range of pressures near the high pressure limit and have shown that the product CO molecules are born vibrationally cold. This implies that the barrier to the reaction occurs very late in the reaction coordinate and suggests a concerted mechanism for dissociation. This conclusion appears to be at variance with that reached by Dewar and collaborator [5] on the basis of theoretical calculations.

References

1. J.P. Martin, M.R. Buckingham, J.A. Chenery and C.J.S.M. Simpson, Chem. Phys. 74 15 (1983).
2. A.J. Aherne, J.P. Buxton, J.A. Chenery, A. Fakhr and C.J.S.M. Simpson, Chem. Phys. Lett. 98 93 (1983).
3. J.A. Chenery, A. Fakhr, M.I. Wood and C.J.S.M. Simpson, Chem. Phys. Lett. 96 143 (1983).
4. S.C. Clarke and B.L. Johnson, Tetrahedron 27 3555 (1971).
5. Michael J.S. Dewar and Lek Chantarnupong, J. Am. Chem. Soc. 501 7161 (1983).

BIMOLECULAR REACTIONS AND ENERGY-TRANSFER
INVOLVING HIGHLY VIBRATIONALLY EXCITED MOLECULES

John R. Barker,^{*} Trevor C. Brown,[†] and Keith D. King[†]

^{*}SRI International, Menlo Park, CA 94025 U.S.A.

[†]University of Adelaide, S.A., Australia 5001

A new program is underway at SRI to investigate bimolecular reactions and energy-transfer involving highly excited species. Infrared multiphoton absorption is used to prepare an ensemble of vibrationally excited molecules. The first task of the experimental program is to characterize the initial population distribution of this ensemble. Once the population distribution has been characterized, energy-transfer data and data on bimolecular reactions can be interpreted in terms of the vibrational energy content of the excited molecules.

In the initial experiments, 1,1,2-trifluoroethane is excited at 1079.9 cm^{-1} with a CO_2 TEA laser. Data on the collision-free multiphoton decomposition (MPD) yield as a function of laser fluence was obtained using the very low-pressure photolysis technique (VLP Φ).¹ The results show fairly linear behavior on a log-normal plot,² and the maximum yield obtained with a collimated laser beam was $\sim 30\%$ at a fluence of $\sim 2 \text{ J cm}^{-2}$.

In a separate series of experiments, infrared fluorescence (IRF) from the excited molecules was monitored to determine energy-transfer rates;³ in addition, the initial IRF intensity is related to the ensemble average energy. In the same cell, optoacoustic measurements and Beer's Law absorption measurements were performed to determine the average number of photons absorbed per molecule.⁴

These three sets of experiments are complementary because they are sensitive to three overlapping ranges of vibrational excitation. Specifically, the MPD experiments probe molecules excited above the reaction threshold, the IRF experiments probe molecules having sufficient energy to emit light at $3.3\text{ }\mu\text{m}$, and the absorption/optoacoustic experiments are sensitive to absorbed energy over the whole range.

To interpret these data and infer the ensemble population distributions, a Master Equation treatment⁵ is employed which predicts MPD yields, IRF intensities, and average absorbed energy for various sets of assumed parameters. Our objective is to simultaneously simulate all three sets of experimental data using a single unified model of the system. At present, the experimental phase is nearly complete and the status of the effort will be reported at the meeting.

Depending on progress with the Master Equation simulations, experimental results on both homogeneous and heterogeneous energy transfer involving 1,1,2-trifluoroethane will be reported.

Acknowledgement: Support from the U.S. Army Research Office is gratefully acknowledged.

References

1. M. J. Rossi, J. R. Barker, and D. M. Golden, J. Chem. Phys., 76, 406 (1982), and references cited therein.
2. J. R. Barker, J. Chem. Phys., 72, 3686 (1980); A. C. Baldwin and J. R. Barker, J. Chem. Phys., 74, 3813, 3823 (1981).
3. J. R. Barker, J. Phys. Chem., 88, 11 (1984), and references cited therein.
4. N. Presser, J. R. Barker, and R. J. Gordon, J. Chem. Phys., 78, 2163 (1983), and references cited therein.
5. J. R. Barker, Chem. Phys., 77, 301 (1983).

NOTES

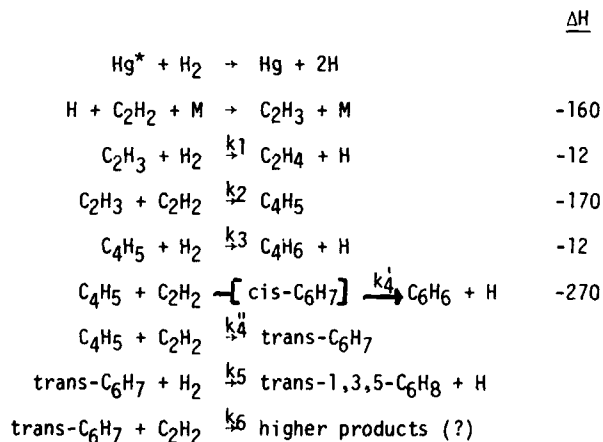
Reactions of the vinyl, butadienyl,
and hexatrienyl radicals

A.B. Callear and G.B. Smith,
Physical Chemistry Department,
University of Cambridge,
U.K.

The chemistry of the little known vinyl radical is being investigated by means of product analysis. The C_2H_3 is prepared by addition of atomic hydrogen to C_2H_2 ; reaction is initiated by mercury photosensitization. An account of the preliminary results has been published (1). The discovery of an electronic system of C_2H_3 has also been reported recently (2).

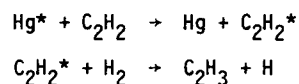
The main reaction products are C_2H_4 , 1, 3- C_4H_6 , benzene and trans-1,3,5-hexatriene, the formation rates all exhibiting a square root dependence on the light intensity. The rates of formation of higher hydrocarbons are comparatively very small.

We now have a good outline of the mechanism (ΔH in $J\ mol^{-1}$ are approximate)



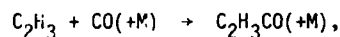
The k_1 is of the order of $10^{-17}\ cm^3\ molecule^{-1}\ s^{-1}$ at 300 K, with $E_1 = 23(\pm 5)\ kJ\ mol^{-1}$. The k_2/k_1 ratio is ~ 33 at 300 K. Considerable

uncertainty remains concerning the relative roles of the cis and trans hexatrienyl radicals. It is clear that part of the reaction of C_4H_5 with C_2H_2 goes 'directly' through to benzene, as shown, and is unaffected by addition of high pressures of N_2 . With trace quantities of H_2 added to excess C_2H_2 , reaction seems to be initiated by triplet C_2H_2 (3):



At this extreme high yields of benzene are found, with negligible trans hexatriene. At the other extreme, with $(H_2) \gg (C_2H_2)$, the rates of formation of benzene and trans hexatriene are approximately equal, though their quantum yields become very small in this limit.

It has been proposed that C_2H_3 , or its adduct, if any, with CO, has a role in carbon deposition in CO_2 gas cooled nuclear reactors. We have shown that addition of CO does inhibit C_2H_4 formation. At 300°K, the coefficient of the reaction,



is $\sim 2.5 \times 10^{-15} \text{ cm}^3 \text{ molecule}^{-1} \text{ s}^{-1}$ (600 Torr total pressure). At elevated temperatures, the reaction goes to equilibrium.

References.

- (1) A.B. Callear and G.B. Smith, Chem. Phys. Letters, 105 (1984) 119.
- (2) H.E. Hunziker, H. Knepe, A.D. McLean, P. Siegbahn and H.R. Wendt, Can. J. Chem., 61 (1983) 993.
- (3) C.S. Burton and H.E. Hunziker, J. Chem. Phys., 57 (1972) 339.
- (4) D.J. Norfolk, R.F. Skinner and W.J. Williams, in: Gas chemistry in nuclear reactors and large industrial plant, ed. A. Dyer (Heydon, London, 1980).

This research is supported by the United Kingdom Atomic Energy Authority.

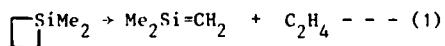
UNIMOLECULAR REARRANGEMENTS OF ORGANOSILICON INTERMEDIATES

I.M.T. Davidson, K.J. Hughes, S. Ijadi-Maghsoodi and R.J. Scampton

Department of Chemistry, The University, Leicester LE1 7RH, United Kingdom

A rich variety of intermediates results from pyrolysis of organosilicon compounds in the gas phase. Organosilyl radicals ($R_3Si\cdot$) may be produced by σ -bond homolysis, silylenes ($R_2Si:$) may be formed thermally under quite mild conditions from suitable precursors, as may silene intermediates ($R_2Si=CH_2$). Silenes are also formed by dissociation of larger organosilyl radicals. Certain silylenes and silenes interconvert by reversible unimolecular isomerisation, while organosilicon radicals may undergo unimolecular rearrangement. Consequently, pyrolyses of apparently simple organosilicon compounds often proceed by complex mechanisms involving several interdependent intermediates. In these circumstances, there are intriguing mechanistic complexities to be unravelled, in which gas kinetic experiments and estimates have played a prominent part and continue to do so, as illustrated by the following recent examples.

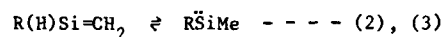
A long-established method of generating silenes is by pyrolysis of siletanes.^[1]



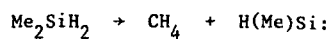
Formation of hydridosilenes $R(H)Si=CH_2$ ($R=H, Me$) by analogous routes^[2] and otherwise^[3] in non-kinetic experiments, with intermediates trapped by butadiene, gave apparently conflicting results. Silene-to-silylene isomerisation by a 1,2-hydrogen shift, $R(H)Si=CH_2 \rightarrow R(Me)Si:$, appeared

to go to completion in some cases^[2], but not at all in others^[3].

We shall describe experiments and calculations^[4] which extend earlier suggestions^[5], resolving these problems in terms of a reversible silene \rightleftharpoons silylene isomerisation, as expected theoretically^[6].



Likewise, the isomerisation of $\text{Me}_2\text{Si=SiMe}_2$ and $\text{Me}_3\text{Si}\ddot{\text{Si}}\text{Me}$ to 1,3-disiletanes will be interpreted by a mechanism involving intramolecular silylene insertions, a silene \rightleftharpoons silylene isomerisation, and a 1,2-silyl shift. Our quantitative model can also explain a remarkably specific isomerisation^[7] of $(\text{Me}_3\text{Si})_2\text{Si:}$. It is known^[8] that pyrolysis of hydridomonosilanes gives silylenes, thus:



The relevance of this type of reaction to the mechanism of pyrolysis of hydridosiletanes [which is much more complex than reaction (1)] will be discussed, as will some kinetic evidence for a 1,2-hydrogen shift in an α -silyl methyl radical: $\text{Me}_2(\text{H})\text{SiCH}_2\cdot \rightarrow \text{Me}_3\text{Si}\cdot$.

References

1. M.C. Flowers and L.E. Gusel'nikov, J.C.S. (B), 1968, 419.
2. R.T. Conlin and D.L. Wood, J.A.C.S., 1981, 103, 1843; R.T. Conlin and R.S. Gill, J.A.C.S., 1983, 105, 618.
3. T.J. Barton, S.A. Burns and G.T. Burns, Organometallics, 1982, 1, 210.
4. I.M.T. Davidson, S. Ijadi-Maghsoodi, T.J. Barton and N. Tillman, J.C.S. Chem. Comm., 1984, 478.
5. R. Walsh, J.C.S. Chem. Comm., 1982, 1415.
6. H.F. Schaefer III, Acc. Chem. Res., 1982, 15, 283.

7. Y.S. Chen, B.H. Cohen and P.P. Gaspar, J. Organometallic Chem., 1980,
195, C1.

8. M.A. Ring, H.E. O'Neal, S.F. Rickborn and B.A. Sawrey, Organometallics,
1983, 2, 1891.

The reactions of O atoms with $(\text{CH}_3)_3\text{SiH}$ and $(\text{CH}_3)_3\text{SiSi}(\text{CH}_3)_3$.

H. Hoffmeyer, B. Reimann, and P. Potzinger

Max-Planck-Institut für Strahlenchemie, D-4330 Mülheim/Ruhr W.-Germany

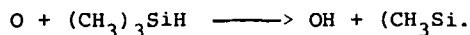
The reactions of $\text{O}(^3\text{P})$ with $(\text{CH}_3)_3\text{SiH}$ and $(\text{CH}_3)_3\text{SiSi}(\text{CH}_3)_3$ were investigated in a fast flow system and by stationary photolysis. For the primary steps the following rate constants were obtained:

$$k(\text{O} + (\text{CH}_3)_3\text{SiH}) = (1.5 \pm 0.3) \cdot 10^{-12} \text{ cm}^3 \text{ molecule}^{-1} \text{ s}^{-1}$$

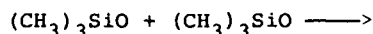
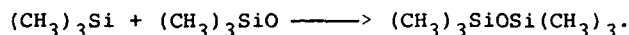
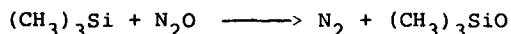
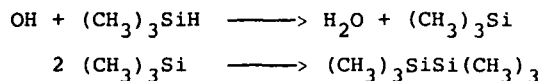
$$k(\text{O} + (\text{CH}_3)_6\text{Si}_2) = (1.8 \pm 0.4) \cdot 10^{-13} \text{ cm}^3 \text{ molecule}^{-1} \text{ s}^{-1}$$

The mechanistic pathways can be deduced from end-product analyses.

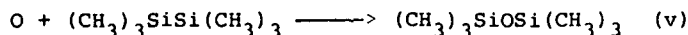
In the $\text{O}/(\text{CH}_3)_3\text{SiH}$ system, H_2O was produced in the flow experiment while in stationary photolysis, where the O atoms were generated by Hg sensitized photolysis of N_2O the main products were N_2 , $(\text{CH}_3)_3\text{SiOSi}(\text{CH}_3)_3$, and $(\text{CH}_3)_3\text{SiSi}(\text{CH}_3)_3$. The quantum yield of N_2 had a limiting value of three. These products are consistent with an initial simple abstraction reaction



In the case of the stationary photolysis this is followed by:



With hexamethyldisilane no water was observed, however methyl radicals and methane were detected. The product spectrum in the stationary photolysis of hexamethyldisilane is similar to that observed in the vacuum UV photolysis of hexamethyldisiloxane. It is suggested that the primary process consists of an insertion of the O atom in the SiSi bond



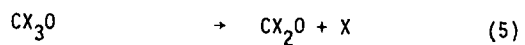
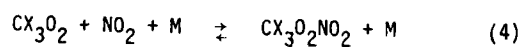
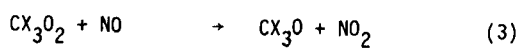
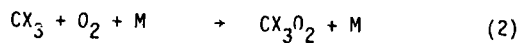
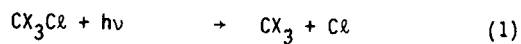
followed by unimolecular decomposition of the highly excited disiloxane molecule.

KINETIC STUDIES OF HALOMETHANE PHOTOOXIDATION

F. CARALP, A.M. DOGNON and R. LESCLAUX

Laboratoire de Chimie Physique A - Université
de Bordeaux I - 33405 Talence - France

The photooxidation mechanism of chlorofluoromethanes in the atmosphere is now fairly well understood. It can be summarized as follows :



where X = F or Cl.

It is generally assumed in stratospheric modelling that all the chlorine atoms are converted into ClO_x in a negligible delay after the initial photolysis (1). However, almost no kinetic data are available concerning the radical elementary reactions that would allow to verify this assumption.

Using pulsed laser photolysis and time resolved mass spectrometry, absolute rate constants were measured for reactions (2), (3) and (4).

These kinetic measurements were performed by monitoring the concentration of the CX_3O_2 radical at the m/e value of the corresponding $CX_2O_2^+$ ion.

Rate constants for the termolecular reactions (2) and (4) were determined for $CX_3 = CFC l_2$ in the pressure range 0-10 Torr, using either N_2 or O_2 as third bodies. The results are the following, taking $F_c = 0.6$ in TROE's rate expression :

$$k_2(0) = (5.0 \pm 0.8) \times 10^{-30} \text{ cm}^6 \cdot \text{molecule}^{-2} \text{ s}^{-1}$$

$$k_2(\infty) = (6.0 \pm 1.0) \times 10^{-12} \text{ cm}^3 \cdot \text{molecule}^{-1} \text{ s}^{-1}$$

$$k_4(0) = (3.5 \pm 0.5) \times 10^{-29} \text{ cm}^6 \cdot \text{molecule}^{-2} \text{ s}^{-1}$$

$$k_4(\infty) = (6.0 \pm 1.0) \times 10^{-12} \text{ cm}^3 \cdot \text{molecule}^{-2} \text{ s}^{-1}$$

The rate constants for reactions (3) were measured for $CX_3 = CF_3, CF_2Cl, CFC l_2$ and CCl_3 . The obtained values are all in the range $1.6 - 1.9 \times 10^{-11} \text{ cm}^3 \cdot \text{molecule}^{-1} \text{ s}^{-1}$ and therefore do not exhibit significant differences, taking into account the experimental uncertainties.

Measurements of the temperature dependences are in progress.

Preliminary results for the reaction $CFC l_2O_2 + NO$ give :

$$k = 1.6 \times 10^{-11} (T/298)^{-1.35} \text{ cm}^3 \cdot \text{molecule}^{-1} \text{ s}^{-1}.$$

NOTES

Excimer Laser Perturbation of Methane-Air
Flames: A Novel Method for Studying
High Temperature Radical Reactions

M. S. Chou, A. M. Dean and D. Stern

Corporate Research Science Laboratories
Exxon Research and Engineering Company
Annandale, New Jersey 08801 USA

Using the experimental arrangement shown in Figure 1, we have employed an ArF excimer laser to perturb the radical concentrations and a tunable dye laser to follow the rise and decay of the OH, NH, CN, CH and NO concentrations in rich ($\phi = 1.6 - 1.8$) atmospheric pressure methane air flames. The OH concentration was observed to increase over an order of magnitude immediately following the excimer laser pulse. This increase is due to the direct photolysis of H_2O in these flames. The excimer beam is only slightly focussed (2 m focal length lens) so as to excite a relatively large area and minimize temperature excursions ($\Delta T < 10$ K). The large excitation area also assures that the measured changes in radical concentrations are kinetic in origin, as changes due to convection or diffusion would require longer times. The observed decay in OH concentration (cf Figure 2 for typical data) depends only weakly upon distance above the burner, but increases at higher fuel equivalence ratios (ϕ). Such kinetic behavior is qualitatively consistent with the major channels for OH decay being the reactions $OH + H_2$, $OH + CH_4$, and $OH + CO$, since all of these species are present at various heights above the burner and increase in concentration in the richer flames. A quantitative comparison of predicted and observed OH decay is shown in Figure 2. The quality of this fit is particularly encouraging in that it was obtained using consensus high temperature rate constants for the main OH reactions. Since the OH profiles in rich flames are also reasonably well predicted, this fit can be taken to show that the perturbation approach is a

valuable new tool for analysis of complex high temperature systems. The real power of the techniques comes to bear for those radicals where the calculated profiles are not in good agreement with those observed, and the relaxation kinetics can be used for more explicit analysis of the radical decay channels.

Examples will be presented of detailed comparisons as functions of both distance above the burner and equivalence ratio for the species observed, with particular emphasis upon reconciling the observed radical decay kinetics to the overall profiles observed in these flames.

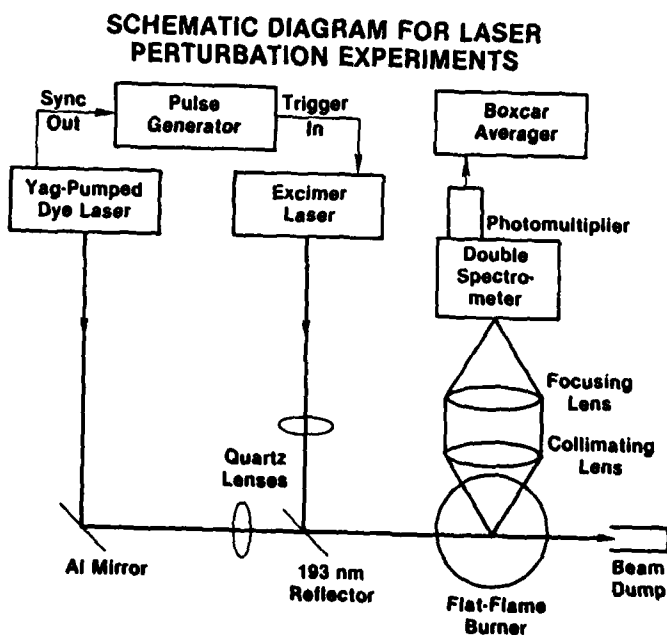


FIG. 1

OH DECAY IN EXCIMER PERTURBED RICH METHANE FLAME

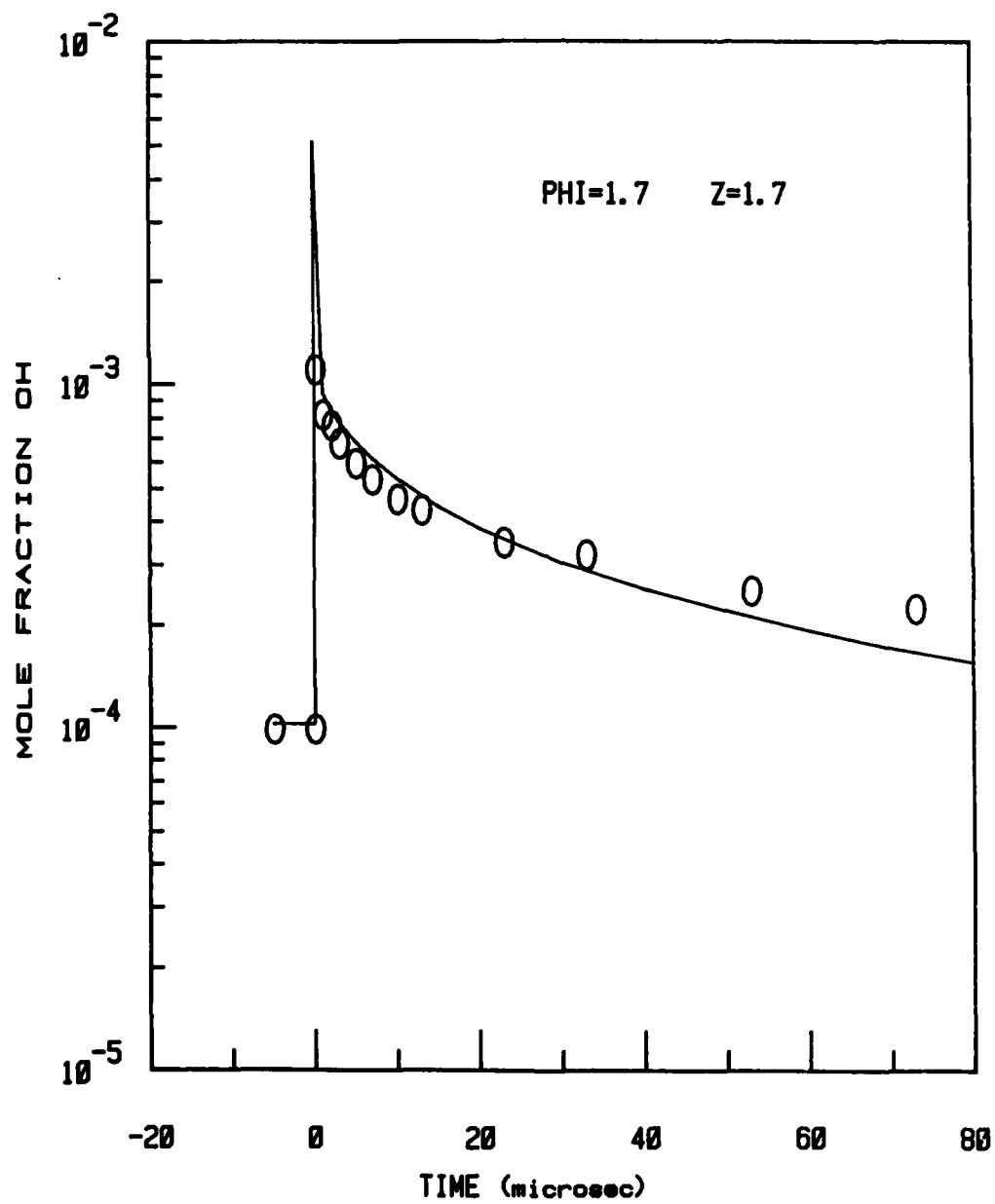


FIG. 2

Oscillations, glow and ignition in carbon monoxide
oxidation in an open system (a CSTR): experiments and
interpretation

P. Gray, J.F. Griffiths and S.K. Scott

School of Chemistry, University of Leeds, Leeds LS2 9JT, UK

Introduction

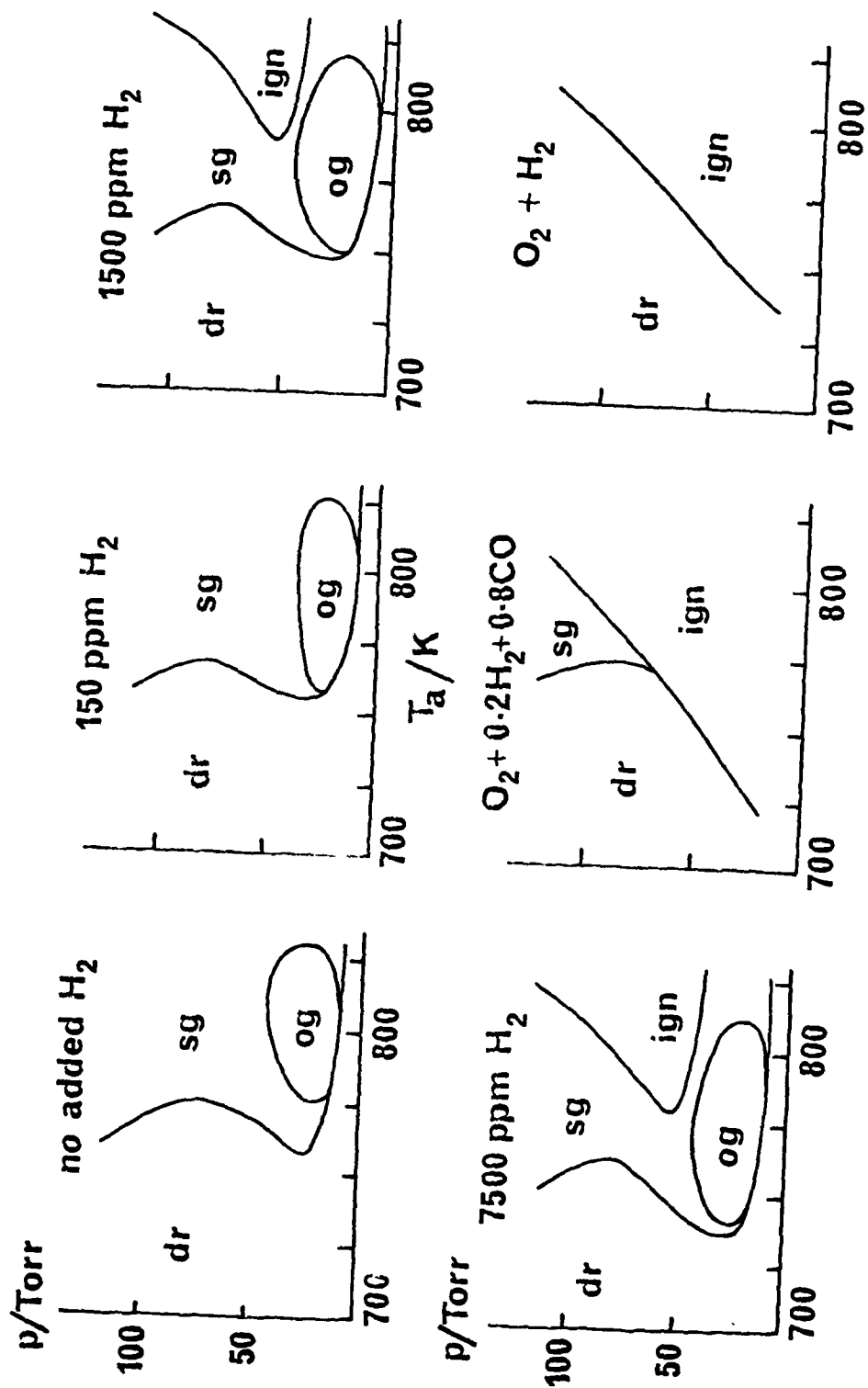
Although the oxidation of carbon monoxide can show oscillatory behaviour even in closed vessels, all investigators have encountered extraordinary difficulties in obtaining reproducible behaviour. To succeed in an open system offers important advantages but makes additional demands.

Experimental

We report such studies. The reaction vessel (0.5 dm^3 Pyrex glass) is mechanically stirred. Temperatures range from 740 to 840 K and pressures up to 100 Torr. Light emission, temperature excesses and reactant concentrations are monitored continuously. The influence of added hydrogen is studied by introducing metered amounts into the CO feed. Some difficulties have turned out to be less severe than in a closed system, results proving utterly reproducible over two years and from one reactor to another.

Results

Four different patterns of behaviour have been observed. Conditions for their occurrence are displayed in the figure, which covers the range of hydrogen additions from nil through ppm regions to the system abundant in H_2 .



Results (continued)

The four different types of reaction are:

- I steady dark reaction (dr) with moderate reaction rates and small temperature-excesses ($\Delta T < 5$ K)
- II steady glow (sg) with moderate reaction rates, small temperature-excesses and a steady emission of chemiluminescence
- III oscillatory glow (og) sustained pulses of chemiluminescence separated by dark interval periods only. If H_2 is added to the system is there measurable change in the reactant concentrations and reactant temperature during each pulse
- IV oscillatory ignition (ign) fully-fledged ignitions with large temperature excursions ($>> 400$ K) and complete reactant consumption. Only realizable in presence of added hydrogen.

Interpretation

Kinetic schemes in detail or in outline for the onset in open systems of oscillatory ignition and oscillatory luminescence can be set out, and their key factors can be highlighted even by the simplest of schemes. Oscillatory ignition is stressed in this paper.

References

- Bond, Gray & Griffiths (1981) Proc.Roy.Soc.Lond. A 375 43-64.
Bond, Gray, Griffiths & Scott (1982) Proc.Roy.Soc.Lond. A 381.
Scott (1982) Ph.D. diss. University of Leeds.
Gray & Scott in "Oscillatory Reactions" ed. Field & Burger J. Wiley 1984.

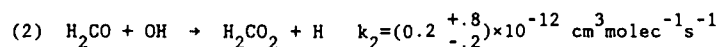
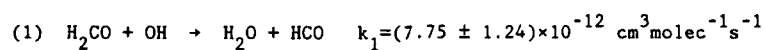
SENSITIVITY ANALYSIS TECHNIQUES FOR ESTIMATION OF REACTION RATE
PARAMETERS AND THEIR UNCERTAINTIES: EVALUATION OF THE RATE
CONSTANT AND THE BRANCHING RATIO FOR THE REACTION $\text{OH} + \text{H}_2\text{CO}$

by
R.A. Yetter and H. Rabitz
Princeton University, Princeton, New Jersey
and
R.B. Klemm
Brookhaven National Laboratory, Upton, New York

ABSTRACT

This paper discusses the simultaneous use of sensitivity analysis techniques and real experimental data for estimation of reaction rate parameters and their *uncertainties*. The techniques are then applied in an analysis of an ambient temperature-low pressure (1-3 torr) kinetic system to evaluate the rate constant, branching ratio, and corresponding uncertainties for the elementary reaction of hydroxyl radical with formaldehyde. Rate parameters are determined using weighted least squares methods based on minimizing differences between a set of experimentally measured observables and a corresponding set of calculated observables from a reaction model. The weighting function and actual experimental data used for fitting the model to experiment are selected with the aid of elementary and derived sensitivity coefficients. Both *experimental* sensitivity coefficients (i.e., the partial derivatives of the inferred rate parameters with respect to experimental observables) and *model* sensitivity coefficients (i.e., the partial derivatives of inferred rate parameters with respect to known model input parameters such as initial conditions, other rate parameters in the model, etc.) are derived from the least squares relationship. These fundamental quantities show *quantitatively* how the uncertainties in experimental data and model parameters are

converted into uncertainties in inferred rate parameters. The actual deviations of inferred rate parameters are determined based on a linear analysis using both *experimental* and *model* sensitivity coefficients. The validity of the linear analysis is examined with higher order derivatives of *experimental* and *model* sensitivity coefficients. For the analysis of the OH + H₂CO reaction, rate parameter values are determined by fitting OH concentrations calculated from a detailed kinetic model consisting of 15 chemical species and 17 elementary reactions to corresponding OH experimental data obtained from flow tube experiments. The rate parameters and parameter uncertainties obtained are:



These results demonstrate that the major reaction path, route (1), dominates in this reaction. Applying the range in derived uncertainties in k_1 and k_2 , the major branch accounts for 87% to 100% of the total reaction, while the most likely estimates yield a value of 97% for $k_1/(k_1+k_2)$. The stated parameter deviations account for *all* uncertainties in and discrepancies between model and measured observables (without cancellations) and therefore represent the maximum deviations possible. The uncertainties in k_1 and k_2 result mainly from uncertainties in the initial concentrations of H₂CO and OH and the total flow rate. In particular, 89% of the total deviation in k_1 results from uncertainties in the initial species concentrations, 10% to uncertainties in the rate constants of other reactions in the model, and *only* 1% to uncertainties in the experimental measurements of OH concentrations. In contrast, 56% of the total deviation in k_2 results from uncertainties in the initial species concentrations, 25% to uncertainties in experimental OH measurements, and 19% to uncertainties in the rate constants of secondary reactions.

Sensitivity Analysis of a Methane Oxidation Mechanism

Ching-Ren Yu and Jenn-Tai Hwang

Department of Chemistry

National Tsing Hua University

Hsinchu, Taiwan 300

Republic of China

The newly developed Polynomial Approximation Method¹ (PAM) of sensitivity analysis was applied to a 190-step mechanism of CH₄ oxidation kinetics proposed recently by Hidaka, Gardiner and Eubank.² Sensitivity profiles were obtained throughout the entire reaction process. On the average, the PAM took ca. 3 sec CP execution time for each sensitivity profile on a CDC-CYBER-172 computer. This should be compared with the computation time of ca. 200 CP sec required in solving the coupled rate equations for 31 species concentration profiles (ODE solver: GEAR³, relative error tolerance: 10⁻⁵). The sensitivity profiles were extremely useful in generating information concerning kinetic importance of the elementary steps, reaction pathways of chemical species, and functional dependence of chemical species upon rate coefficients. For example, by means of time averaged sensitivity coefficients

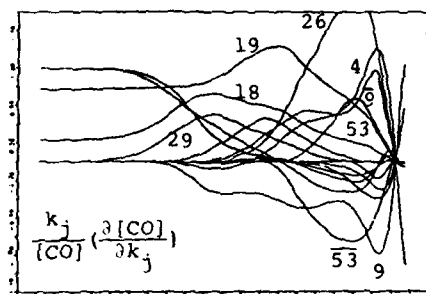
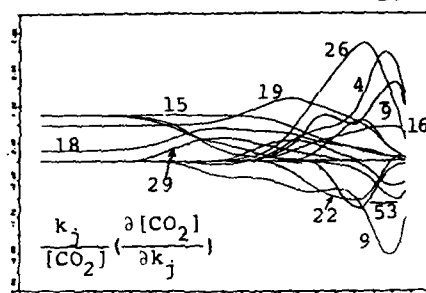
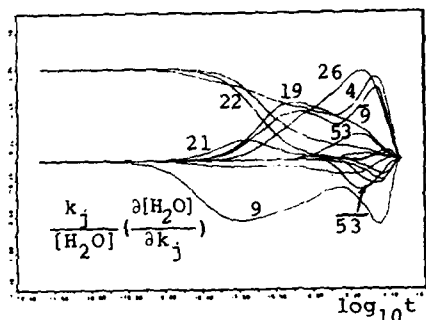
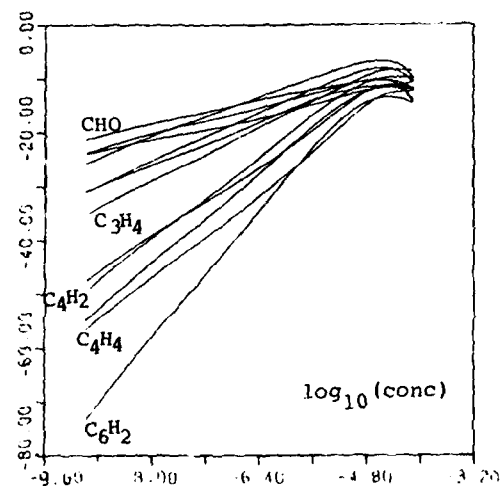
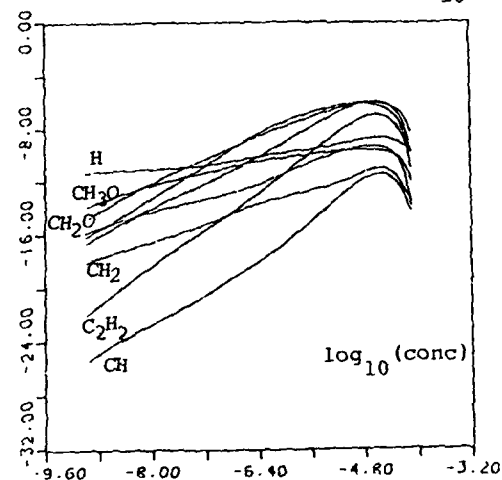
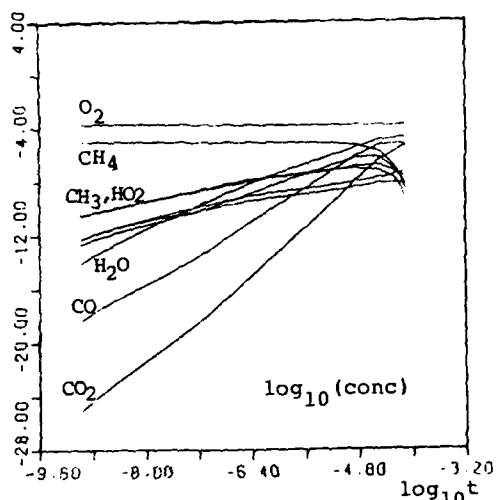
$$\frac{1}{t_2 - t_1} \int_{t_1}^{t_2} d\tau \left| \left(\frac{k_l}{c_i} \right) \left(\frac{\partial c_i}{\partial k_l} \right) \right|,$$

one could easily rank the elementary steps and simplify the mechanism. One could also use sensitivity coefficients in the form of

$$\left(\frac{\partial c_i}{\partial \xi} \right)_{c_l(0)+c_m(0)=\text{const}} = \frac{c_l(0)+c_m(0)}{(1+\xi)^2} \left[\left(\frac{\partial c_i}{\partial c_l(0)} \right) - \left(\frac{\partial c_i}{\partial c_m(0)} \right) \right],$$

where $\xi = c_l(0)/c_m(0)$, to study the influence of initial CH₄ to O₂ concentration ratio on the system behavior. Functional dependences of species concentration upon rate coefficients in the form of k_l^α/k_m^β , $k_l^\alpha k_m^\beta$, or $k_l^\alpha + k_m^\beta$ could be easily discerned from the "peculiar" temporal behavior of sensitivity coefficients:^{1,4}

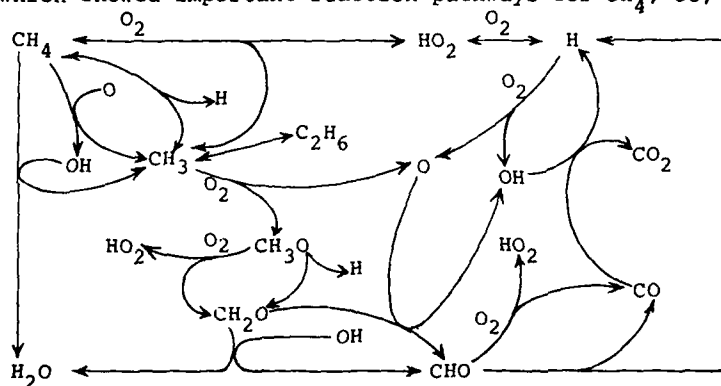
$$\frac{k_l}{\alpha} \left(\frac{\partial c}{\partial k_l} \right) = \pm \frac{k_m}{\beta} \left(\frac{\partial c}{\partial k_m} \right), \text{ or } \frac{1}{\alpha k_l^{\alpha-1}} \left(\frac{\partial c}{\partial k_l} \right) = \pm \frac{1}{\beta k_m^{\beta-1}} \left(\frac{\partial c}{\partial k_m} \right)$$



1	CH ₃ OH	32	CH ₃ OH + CH ₃ OH	64	CH ₃ OH + CH ₃ OH
2	CH ₃ OH + H ₂ O	33	CH ₃ OH + H ₂ O	65	CH ₃ OH + CH ₃ OH
3	CH ₃ OH + CH ₃ OH	34	CH ₃ OH + CH ₃ OH	66	CH ₃ OH + CH ₃ OH
4	CH ₃ OH + H ₂ O	35	CH ₃ OH + H ₂ O	67	CH ₃ OH + CH ₃ OH
5	CH ₃ OH + CH ₃ OH	36	CH ₃ OH + CH ₃ OH	68	CH ₃ OH + CH ₃ OH
6	CH ₃ OH + H ₂ O	37	CH ₃ OH + H ₂ O	69	CH ₃ OH + CH ₃ OH
7	CH ₃ OH + CH ₃ OH	38	CH ₃ OH + CH ₃ OH	70	CH ₃ OH + CH ₃ OH
8	CH ₃ OH + H ₂ O	39	CH ₃ OH + H ₂ O	71	CH ₃ OH + CH ₃ OH
9	CH ₃ OH + CH ₃ OH	40	CH ₃ OH + CH ₃ OH	72	CH ₃ OH + CH ₃ OH
10	CH ₃ OH + H ₂ O	41	CH ₃ OH + H ₂ O	73	CH ₃ OH + CH ₃ OH
11	CH ₃ OH + CH ₃ OH	42	CH ₃ OH + CH ₃ OH	74	CH ₃ OH + CH ₃ OH
12	CH ₃ OH + H ₂ O	43	CH ₃ OH + H ₂ O	75	CH ₃ OH + CH ₃ OH
13	CH ₃ OH + CH ₃ OH	44	CH ₃ OH + CH ₃ OH	76	CH ₃ OH + CH ₃ OH
14	CH ₃ OH + H ₂ O	45	CH ₃ OH + H ₂ O	77	CH ₃ OH + CH ₃ OH
15	CH ₃ OH + CH ₃ OH	46	CH ₃ OH + CH ₃ OH	78	CH ₃ OH + CH ₃ OH
16	CH ₃ OH + H ₂ O	47	CH ₃ OH + H ₂ O	79	CH ₃ OH + CH ₃ OH
17	CH ₃ OH + CH ₃ OH	48	CH ₃ OH + CH ₃ OH	80	CH ₃ OH + CH ₃ OH
18	CH ₃ OH + H ₂ O	49	CH ₃ OH + H ₂ O	81	CH ₃ OH + CH ₃ OH
19	CH ₃ OH + CH ₃ OH	50	CH ₃ OH + CH ₃ OH	82	CH ₃ OH + CH ₃ OH
20	CH ₃ OH + H ₂ O	51	CH ₃ OH + H ₂ O	83	CH ₃ OH + CH ₃ OH
21	CH ₃ OH + CH ₃ OH	52	CH ₃ OH + CH ₃ OH	84	CH ₃ OH + CH ₃ OH
22	CH ₃ OH + H ₂ O	53	CH ₃ OH + H ₂ O	85	CH ₃ OH + CH ₃ OH
23	CH ₃ OH + CH ₃ OH	54	CH ₃ OH + CH ₃ OH	86	CH ₃ OH + CH ₃ OH
24	CH ₃ OH + H ₂ O	55	CH ₃ OH + H ₂ O	87	CH ₃ OH + CH ₃ OH
25	CH ₃ OH + CH ₃ OH	56	CH ₃ OH + CH ₃ OH	88	CH ₃ OH + CH ₃ OH
26	CH ₃ OH + H ₂ O	57	CH ₃ OH + H ₂ O	89	CH ₃ OH + CH ₃ OH
27	CH ₃ OH + CH ₃ OH	58	CH ₃ OH + CH ₃ OH	90	CH ₃ OH + CH ₃ OH
28	CH ₃ OH + H ₂ O	59	CH ₃ OH + H ₂ O	91	CH ₃ OH + CH ₃ OH
29	CH ₃ OH + CH ₃ OH	60	CH ₃ OH + CH ₃ OH	92	CH ₃ OH + CH ₃ OH
30	CH ₃ OH + H ₂ O	61	CH ₃ OH + H ₂ O	93	CH ₃ OH + CH ₃ OH
31	CH ₃ OH + CH ₃ OH	62	CH ₃ OH + CH ₃ OH	94	CH ₃ OH + CH ₃ OH
32	CH ₃ OH + H ₂ O	63	CH ₃ OH + H ₂ O	95	CH ₃ OH + CH ₃ OH

For a particular chemical species, influence of other species at any instant could be unravelled readily from initial concentration sensitivity coefficients by a proper selection of time subdomains.

With the help of sensitivity analysis, the 190-step mechanism of Hidaka, Gardiner and Eubank was reduced to 62 steps (maximum deviation in concentration profiles <15%). The dynamical details of the reaction system were summarized by diagrams like the one below, which showed important reaction pathways for CH_4 , CO , CO_2 and H_2O .



We have also developed a generalized PAM⁵ for sensitivity study of non-uniform reaction systems. Work on the sensitivity analysis of the simplified 62-step mechanism with coupling to hydrodynamics is in progress and will be reported in a future publication.⁶

1. J.-T. Hwang, Int. J. Chem. Kinet., 15, 959 (1983)
2. Y. Hidaka, W. C. Gardiner, Jr. and C. S. Eubank, Comm. in J. of Mol. Sci., 2, 141 (1982)
3. A. C. Hindmarsh, Lawrence Livermore Lab. UCID-3001 (Rev. 3), Dec. 1974.
4. J.-T. Hwang, Proc. Nat'l Sci. Council, Rep. of China, 6B, 270 (1982).
5. J.-T. Hwang, "Sensitivity Analysis of Non-uniform Chemical Reaction Systems. Method of Polynomial Approximation", to be submitted.
6. C.-R. Yu and J.-T. Hwang, unpublished.

NOTES

G1

VIBRATIONAL PREDISSOCIATION IN PRISTINE ENVIRONMENTS:
COMPLETE AND PRECISE PRODUCT STATE DISTRIBUTIONS

C. Wittig

SSC 404, University of Southern California, University Park,
Los Angeles, CA 90089, U.S.A.

Rydberg State Predissociation Dynamics in $\text{H}_2\text{S}(\text{D}_2\text{S})$ and $\text{H}_2\text{O}(\text{D}_2\text{O})$

M.N.R. Ashfold, J.M. Bayley, R.N. Dixon and J.D. Prince

School of Chemistry, University of Bristol, Bristol BS8 1TS

The technique of multiphoton ionisation spectroscopy has been used to provide a uniquely detailed picture of the predissociation dynamics operating in various of the excited electronic states of $\text{H}_2\text{S}(\text{D}_2\text{S})$ and $\text{H}_2\text{O}(\text{D}_2\text{O})$. In each case, Rydberg states of these molecules are identified as three photon resonances in four photon ionisation spectra, and analysed through use of the appropriate three-photon rotational linestrength theory.

The most important conclusion to emerge from these studies is the recognition that, in many instances, parent rotational angular momentum will strongly influence the excited state predissociation dynamics, rates and (as shown in the succeeding presentation) even the resulting photo-products. More specific conclusions include:

1. Two predissociation routes are available to H_2O and D_2O molecules in their $\tilde{\text{C}}^1\text{B}_1(000)$ levels. One, homogeneous, mechanism (presumably involving high vibronic levels of the lower lying, dissociative $\tilde{\text{A}}^1\text{B}_1$ state) is more effective in H_2O than in D_2O , but affects all parent excited state rotational levels. The other, a heterogeneous mechanism, arises as a result of Coriolis coupling (via a-axis molecular rotation) with levels of the dissociative $\tilde{\text{B}}^1\text{A}_1$ state. The efficiency of this route scales with $\langle J_a^2 \rangle$ (i.e. with the expectation value of the square of the a-axis rotational angular momentum of the excited state level) and is thus not available to excited state levels having $\langle J_a^2 \rangle = 0$.
2. The higher ($\tilde{\text{D}}'$) electronic state of B_1 symmetry similarly shows evidence for predissociation via both homogeneous and heterogeneous

pathways. The homogeneous channel exhibits a dramatic kinetic isotope effect: $\text{H}_2\text{O}(\text{D}')$ vibronic levels predissociate homogeneously about two orders of magnitude faster than the corresponding levels in D_2O . In contrast, D_2O provides the most dramatic and illustrative examples of the effects of the heterogeneous predissociation route. Once again, Coriolis coupling (via a-axis rotation) to the dissociative $\tilde{\text{B}}^1\text{A}_1$ state can account for the observed $\langle J_a^2 \rangle$ dependence of the predissociation efficiency. However, this efficiency shows a striking, and irregular, vibronic level dependence, which can be rationalised by recognising the intercessional rôle of accidentally near resonant vibronic levels of the heavily predissociated $\tilde{\text{D}}^1\text{A}_1$ Rydberg state.

3. Multiphoton excitation enables population of excited electronic states forbidden (by electric dipole selection rules) to conventional one photon spectroscopy. By way of demonstration we present 3+1 MPI spectra involving hitherto unobserved $^1\text{A}_2$ Rydberg states in $\text{H}_2\text{O}(\text{D}_2\text{O})$ and $\text{H}_2\text{S}(\text{D}_2\text{S})$. Analyses of the intensities of individual rovibronic features displayed in these spectra has revealed a variety of predissociative behaviours. For example, in the case of $\text{H}_2\text{S}(\text{D}_2\text{S})$, the $^1\text{A}_2$ Rydberg states arising from the electronic promotion $\text{n}p_{b_2} + 2b_1$ are also found to exhibit both homogeneous and heterogeneous (Coriolis induced) predissociation mechanisms. The relative efficiencies of these two predissociation channels shows a marked sensitivity to n , the principal quantum number. Over the range $n=4$ to 7 the former decreases, whilst the latter (heterogeneous) predissociation mechanism rapidly gains in importance. Once again, the observations are interpretable through consideration of the likely forms of the relevant excited state potential energy surfaces.

QUANTUM STATE SELECTED PHOTODISSOCIATION OF $\text{H}_2\text{O}/\text{D}_2\text{O } \tilde{\text{C}}^1\text{B}_1$ A. Hodgson and J.P. Simons

Chemistry Department, The University, Nottingham NG7 2RD, United Kingdom

M.N.R. Ashfold, J.M. Bayley and R.N. Dixon

School of Chemistry, The University, Bristol BS8 1TS, United Kingdom

Photodissociation of small (triatomic) molecules provides an opportunity for studying "half-collisions" between two simple fragments in which the initial excited molecular state is prepared, and the final fragment detected, with resolution of the electronic, vibrational, rotational and translational energies. Ideally, if experimental data are to be readily understood and compared with theoretical predictions, then quantum state resolution in both the entry and exit channels is desirable.

Various elegant experiments have been performed in which photofragment alignment, and internal and translational energy distributions have been measured (either by L.I.F. or by resolved photofragment fluorescence) revealing details of the dissociation dynamics. Generally the selection of the initial molecular level has been limited to a knowledge of the alignment, the total energy and the electronic state populated. Sometimes the initial rotational state distribution has been narrowed by jet-cooling, but individual rotational state selection has not been possible. This work [1] describes the first fully quantum state selected photodissociation experiment based on excitation of the rotationally structured, but predissociated origin band in the $\tilde{\text{C}}^1\text{B}_1 \leftarrow \tilde{\text{X}}^1\text{A}_1$ Rydberg transition of H_2O and D_2O (cf. preceding presentation). This band, which lies near 124 nm can readily be excited by two photon absorption of KrF laser radiation at 248 nm. Rotational resolution is achieved by using a tunable, narrow line

($\sim 0.3 \text{ cm}^{-1}$) injection locked KrF laser to record the two photon OH/OD(A \rightarrow X) photofragment fluorescence excitation spectrum from $\text{H}_2\text{O}/\text{D}_2\text{O}$ in the region $80,400 - 80,650 \text{ cm}^{-1}$. Strong fluorescence can be recorded at pressures as low as 1 mtorr; the excitation spectra display well-defined rotational structure with little interference from underlying continua associated with the (2-photon allowed) ${}^1\text{A}_2 \leftarrow \tilde{\text{X}}$ or $\tilde{\text{B}}{}^1\text{A}_1 \leftarrow \tilde{\text{X}}{}^1\text{A}_1$ systems. The rotational lines are broadened by predissociation and the linewidths agree with those measured in the 3+1 MPI experiments (preceding abstract). However, we find that lines with $K_a' = 0$ (or strictly $\langle J_a'^2 \rangle = 0$ for an asymmetric top) are absent from the spectrum; OH/OD($\text{A}^2\Sigma^+$) fragments are only produced when predissociation involves Coriolis coupling with the neighbouring $\tilde{\text{B}}{}^1\text{A}_1$ continuum. The homogeneous predissociation pathway has to involve either the lower lying $\tilde{\text{A}}{}^1\text{B}_1$ continuum or a B_1 vibronic component of the ${}^1\text{A}_2$ level and each of these states correlate with different products. Parent molecular rotation influences the branching into alternative product electronic states as well as the excited state dissociation dynamics.

In a separate series of experiments, fully resolved OH/OD(A \rightarrow X) fluorescence spectra have been recorded following selection of individual J'_a, K'_c levels. The photofragment energy distributions are vibrationally cold but rotationally inverted with maximum populations at $N' = 15$ (OH) or 20 (OD) similar to those reported earlier by Donovan et.al. using broad-band KrF radiation [2]. Single photon excitation at 123.6 nm which generates maximum populations at the highest accessible levels $N' = 20$ or 26, is probably dominated by direct excitation into the $\tilde{\text{B}}{}^1\text{A}_1$ continuum. Differences in P and Q branch line intensities indicate strong alignment of the OH/OD products despite the (known) picosecond lifetime of the excited parent molecule. Finally, comparison of the calculated intensities of the 2-photon absorption spectra with those observed in the OH/OD(A)-photodissociation

spectra should allow estimates of the state selected branching ratios into competing channels.

- [1] A. Hodgson, J.P. Simons, M.N.R. Ashfold, J.M. Bayley and R.N. Dixon,
Chem. Phys. Lett., in press.
- [2] C. Fotakis, C.B. McKendrick and R.J. Donovan, Chem. Phys. Lett., 80,
598 (1981);
R.J. Donovan, C. Fotakis, A. Hopkirk, C.M. McKendrick and A. Torr,
Can. J. Chem., 61, 1023 (1983).

G4

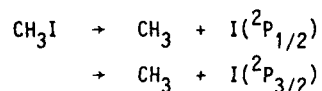
PHOTODISSOCIATION AND INTRAMOLECULAR DYNAMICS

M. Shapiro

Department of Chemical Physics, The Weizmann Institute,
76100 Rehovot, Israel

PHOTOFRAGMENT SPECTROSCOPY OF CH₃IM.D. BARRY and P.A. GORRYChemistry Department, University of Manchester, Manchester,
M13 9PL, UK

Using a newly completed, pulsed molecular beam, high resolution photo-fragment spectrometer we have performed angular and energy distribution measurements on the photodissociation of CH₃I at 248 nm.



The iodine atom fragment is produced in both spin orbit states with ~ 70% in the excited state I(²P_{1/2}) and 30% in the ground state I(²P_{3/2}). The angular scattering, shown in figure 1, is extremely anisotropic indicating direct photodissociation and can be used to provide an upper bound to the lifetime of the dissociating complex. The lifetime of the excited state is found to be very short, $(1.0 \pm 0.2) \times 10^{-13}$ s. It also reveals that the same parallel (³Q₀ + N) transition is responsible for both pathways.

Figure 2 shows the LAB time-of-flight distribution for the I fragment and the best fit from the forward convolution analysis method used to obtain the centre-of-mass distribution. Figure 3 shows the vibrational populations of the CH₃ ν₂ mode obtained from the analysis along with other experimental and theoretical determinations.

It is clear from the results that the photodissociation geometry is linear and excites only the 'umbrella' vibrational mode of the CH₃ group which is found to peak strongly at v = 2 for both pathways with ~ 88% of the available energy being disposed into translation. The ground state Iodine results from a

vibronically induced non-adiabatic crossing to an E electronic state and an analysis of the e vibrational modes of the CH₃I molecule and CH₃ fragment shows that it must involve the CH₃I methyl rocking (ν_6) mode.

References

1. S.C. Yang, A. Freedman, M. Kawasaki and R. Bersohn, J. Chem. Phys. 72, 4058 (1980).
2. J.E. Butler, W.S. Drozdowski and J.R. McDonald, Chem. Phys. 50, 413 (1980).
3. M.C. Addison, R.J. Donovan and C. Fotakis, Chem. Phys. Lett. 74, 58 (1980).
4. R.K. Sparks, K. Shobatake, L.R. Carlson and Y.T. Lee, J. Chem. Phys. 75, 3838 (1981).
5. M. Shapiro and R. Bersohn, J. Chem. Phys. 73, 3810 (1980).
6. S. Lee and E.J. Heller, J. Chem. Phys. 76, 3035 (1982).
7. G.N.A. van Veen, T. Baller, A.E. de Vries and N.J.A. van Veen, Chem. Phys. (in press).

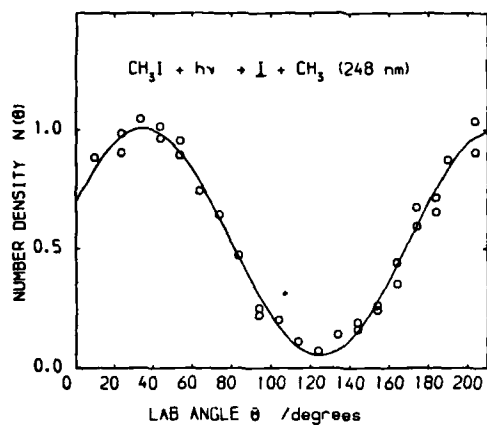


Figure 1

Angular distribution

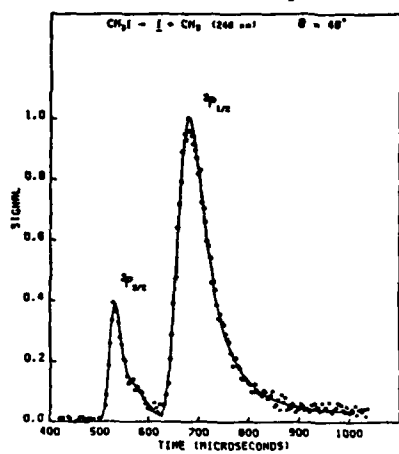


Figure 2

T.O.F. distribution

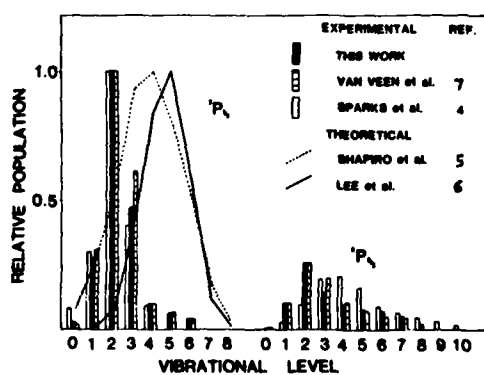


Figure 3

CH₃ v₂ vibrational
populations

POLANYI LECTURE

'OLD PROBLEMS NEVER DIE'

B.S. Rabinovitch

Department of Chemistry, University of Washington, Seattle,
WA 98195, U.S.A.

NOTES

Dynamics of gas/surface reactionsG. Ertl

Institut für Physikalische Chemie, Universität München, FRG

A molecule striking the surface of a solid may undergo elastic or inelastic collision-type scattering or is trapped in a potential well representing the formation of an adsorption bond. The latter process may involve the breaking of bonds within the molecule (dissociative chemisorption) or not. During its lifetime on the surface the particle migrates across the surface and eventually returns into the gas phase by excitation through phonons, probably preceded by recombination with another surface species. These processes form the basis for heterogeneous catalysis.

Experiments with clean surfaces require ultra high vacuum conditions and electron spectroscopic techniques. Kinetic parameters can most directly be determined by a molecular beam method. Laser induced fluorescence serves for probing the internal state population of molecules coming off the surface. This contribution will give an overview of the accessible information by means of a few selected examples: H_2 , NO, CO, O_2 , NO_2 interacting with Pt, Ni and Ge surfaces.

H2

RECENT ADVANCES IN HYDROGEN, SULPHUR, OXYGEN,
NITROGEN AND HALOGEN KINETICS; THEIR MECHANISTIC
AND ATMOSPHERIC IMPLICATIONS

J.G. Anderson

Department of Chemistry and Center for Earth and Planetary
Physics, Harvard university, Cambridge, MA 02138, U.S.A.

RATE PARAMETERS OF RADICAL-RADICAL AND
RADICAL MOLECULE REACTIONS

F. Kaufman, Department of Chemistry,
University of Pittsburgh, Pittsburgh, PA 15260

Recent examples are presented of rate measurements of two different reactions, in two flow reactor systems, and of their interpretation in terms of simple rate theory. The first, $\text{OH} + \text{HO}_2 \rightarrow \text{H}_2\text{O} + \text{O}_2$, (1), continues to be difficult to rationalize. Its rate was measured by laser induced fluorescence (LIF) and vacuum u.v. resonance fluorescence (VUVRF) in an apparatus (Fig. 1) in which HO_2 is prepared by the $\text{F} + \text{H}_2\text{O}_2$ pre-reaction in a movable, concentric double injector. With $[\text{HO}_2]$ in large excess over $[\text{OH}]$, which is produced independently in the flow tube, the pseudo-first-order decay of OH due to (1) was measured directly. The results,^{1,2} over the T-range 252 to 420 K, show k_1 to be very large, about 30 times larger than its two symmetrical counterparts, $\text{OH} + \text{OH}$ and $\text{HO}_2 + \text{HO}_2$, and to have a negative T-dependence corresponding to $\exp(416/T)$ or $T^{-1.3}$.

The interpretation is complicated by persistent reports of a pressure dependence, i.e. an increase from about 7×10^{-11} at a few torr to about $12 \times 10^{-11} \text{ cm}^3 \text{ s}^{-1}$ at 1 atm of N_2 which requires an inordinately long lifetime of $\sim 10^{-8} \text{ s}$ for the energy-rich ($\sim 70 \text{ kcal/mol}$) H_2O_3 adduct. In any event, the high-pressure rate constant of adduct formation must be about $1 \times 10^{-10} \text{ cm}^3 \text{ s}^{-1}$, much larger than corresponding estimates for $\text{HO}_2 + \text{HO}_2$.³ The reaction path, viz. H-abstraction vs. adduct formation plus rearrangement, as well as the transition states and energetics of this and related elementary radical-radical processes are still poorly understood.

The $\text{CH}_3\text{O} + \text{NO}_2$ reaction is being investigated by LIF of CH_3O and mass spectrometry in another apparatus (Fig. 2) where precursor CH_3 radicals are produced by IR laser multiphoton dissociation of $\text{C}_6\text{F}_5\text{OCH}_3$. The reaction has so far been studied over the temperature range 250 to 473 K and pressure range 0.6 to 4 Torr of He. It seems to be dominated by CH_3ONO_2 recombination at low temperatures, but shows an increasing component of a pressure-independent reaction channel, presumably $\text{CH}_2\text{O} + \text{HONO}$ at higher temperatures. The rate parameters of both reactions will be presented and discussed.

¹U. C. Sridharan, L. X. Qiu, and F. Kaufman, J. Phys. Chem. 85, 3361 (1981).

²U. C. Sridharan, L. X. Qiu, and F. Kaufman, J. Phys. Chem. 88, 1281 (1984)

³R. Patrick, J. R. Barker, and D. M. Golden, J. Phys. Chem. 88, 128 (1984).

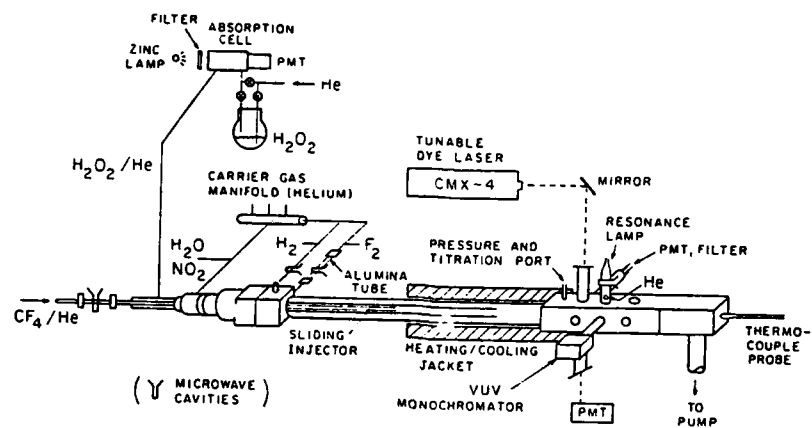


Figure 1.

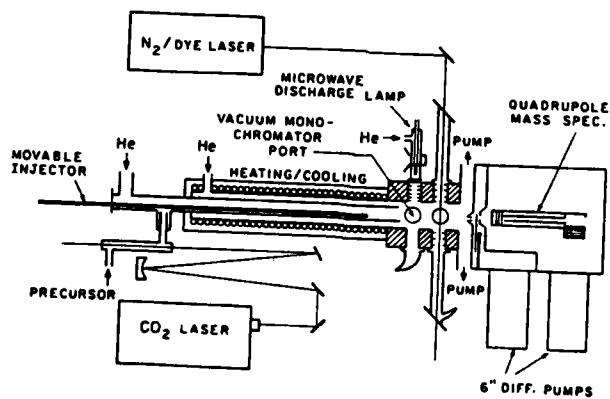


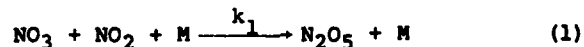
FIGURE 2

RATE COEFFICIENT FOR THE ASSOCIATION REACTION



C. A. Smith, A. R. Ravishankara and P. H. Wine
Molecular Sciences Branch
Engineering Experiment Station
Georgia Institute of Technology
Atlanta, Georgia 30332 USA

Oxides of nitrogen play very important roles in the chemistry of the earth's atmosphere. The NO_3 free radical is one of the nitrogen oxides which has been observed both in the stratosphere and the troposphere. Until recently, however, its reactions with most other atmospheric species have not been directly measured. Of the many reactions of NO_3 , one which controls its concentration (especially in the absence of sunlight) is the reversible addition of NO_3 to NO_2 to form N_2O_5 .



Even though the reverse reaction, i.e. the thermal decomposition of N_2O_5 , was studied many years ago, direct measurement of k_1 has not been carried out until very recently. During the past year k_1 has been measured in the pressure range of 1 torr to 200 atms. (2 to 100 atms. by Croce de Cobos¹ et al., 20 to 760 torr by Kircher et al.², and 0.5 to 8 torr by us). Our low pressure results will be presented here.

The availability of k_1 as a function of pressure over nearly six orders of magnitude can provide a nice data set for checking association reaction rate theories. This is especially true since k_1 is in the fall-off range over nearly four orders of magnitude in pressure and the structure (and spectroscopy) of all involved species are known.

A schematic diagram of the discharge flow apparatus used to measure k_1 is shown in Figure 1. NO_3 free radicals were generated by the reaction of F atoms (produced via microwave discharge of F_2/He mixtures) with HNO_3 . We have previously determined this to be a clean source of NO_3 ³. The concentration of NO_3 was measured by taking advantage of its strong absorption at 662 nm. The 662

nm laser beam was multipassed approximately 150 times through a small (4.5 cm long) absorption cell transverse to the gas flow direction to generate path lengths of the order of 7m while keeping the extent of reaction inside the detection zone to less than 3% even at the highest rate constants that were measured. Initial NO_3 concentrations in the range of 0.5 to $1 \times 10^{13} \text{ cm}^{-3}$ were used. The concentration of NO_2 was always much greater than that of NO_3 ($10 < [\text{NO}_2]/[\text{NO}_3]_0 < 100$) such that the NO_3 reaction time profile always followed first order kinetics. Typical plots of the pseudo first order rate coefficient ($d[\text{NO}_3]/dt = k'$) vs. $[\text{NO}_2]$ are shown in Figure 2. Both He and N_2 were utilized as diluent gases. Table I lists the rate coefficients measured at various pressures ranging from 0.5 to 8 torr.

The measured value of k_1 increases monotonically with the pressure of the bath gas. However, it is clear that even for He there is a significant fall off from the third order linear dependence of k_1 on bath gas pressure. Our data, in conjunction with those of Kircher et al., and Croce de Cobos et al., provides k_1 from 1 torr to 200 atms. of N_2 . A fit of all the data to a Troe formalism,⁴ by using a non-linear least squares fitting procedure, yields $k_0^{\text{N}_2} = 2.12 \times 10^{-30} \text{ cm}^6 \text{ molecule}^{-2} \text{ s}^{-1}$, $k_\infty^{\text{N}_2} = 1.85 \times 10^{-12} \text{ cm}^3 \text{ molecule}^{-1} \text{ s}^{-1}$, and $F_c = 0.47$ for N_2 . In addition, a slightly different value for $\Delta H_f^\circ(\text{NO}_3)$ is calculated when the results of Viggiano et al.⁵ for the thermal decomposition of N_2O_5 is used in conjunction with the recent direct studies of k_1 . Using this value of $\Delta H_f^\circ(\text{NO}_3)$, k_0^{SC} and F_c have been calculated and will be presented.

Acknowledgement: We thank Dr. Sander and Prof. Troe for providing us their results before publication. We gratefully acknowledge the financial support for this work by the Chemical Manufacturers Association.

References:

1. A. E. Croce de Cobos, H. Hippler, and J. Troe, J. Phys. Chem. (submitted).
2. C. C. Kircher, J. J. Margitan, and S. Sander, J. Phys. Chem., (submitted).

3. A. R. Ravishankara and P. H. Wine, Chem. Phys. Letts., **101**, 73 (1983).
4. J. Troe, J. Chem. Phys., **66**, 4745 (1977).
5. A. A. Viggiano, J. A. Davidson, F. C. Fehsenfeld, and E. E. Ferguson, J. Chem. Phys., **74**, 6113 (1981).

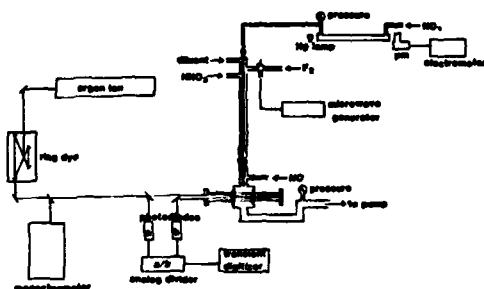


Figure 1: Schematic Diagram of the discharge flow - long path laser absorption apparatus used to measure k_1 .

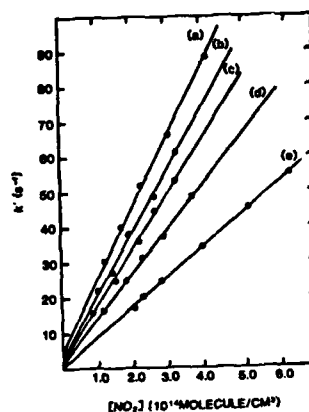


Figure 2: A plot of $k' = (-d[NO_3])/dt$ vs. $[NO_2]$ at various pressures of N_2 , at 298K: a- 6 torr, b- 5 torr, c - 4 torr, d - 3 torr, e - 2 torr.

Table I: Rate Coefficient k_1 for the Reaction $NO_3 + NO_2 + M \rightarrow N_2O_5 + M$ at 298 K

Pressure, Torr	$k_1, 10^{-14} \text{ cm}^3 \text{ molecule}^{-1} \text{ s}^{-1a}$	
	He	N_2
0.5	--	3.6 ± 2.0^b
1.0	2.58 ± 0.70^b	4.5 ± 1.0
2.0	5.43 ± 0.38	8.8 ± 1.3
3.0	7.2 ± 1.4	12.5 ± 2.4
4.0	8.6 ± 1.4	15.6 ± 3.4
5.0	9.5 ± 1.8	16.8 ± 3.6
6.0	--	20.0 ± 3.2
7.1	11.9 ± 0.4	--
8.0	12.7 ± 1.8	--

a: The quoted errors are 2 σ and include estimated systematic errors.

b: The effect of NO_2 itself as a bath gas was significant in these measurements. The value shown are corrected for quenching by NO_2 .

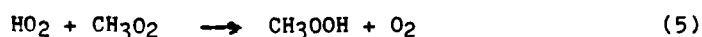
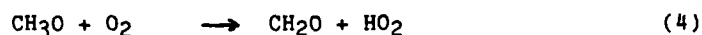
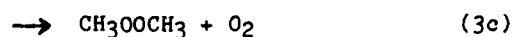
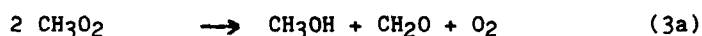
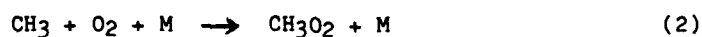
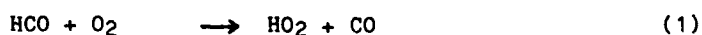
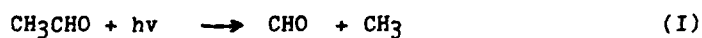
A FTIR SPECTROSCOPIC STUDY OF THE PHOTOOXIDATION OF
ACETALDEHYDE IN AIR.

Geert K. MOORTGAT and Robert D. McQUIGG.¹

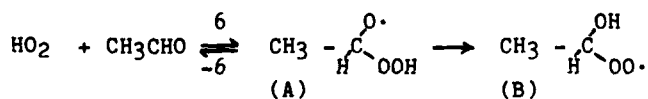
Max-Planck-Institut für Chemie, Air Chemistry Division
Saarstrasse 23, D-6500 Mainz, FGR.

Long path, Fourier transform infrared spectroscopy has been employed to study the mechanism of the acetaldehyde photooxidation in dilute gaseous mixtures of CH_3CHO (ppm level) in air at 700 torr and 25 °C. The concentrations of the products (CO , CO_2 , H_2CO , HCOOH , CH_3OH , CH_3OOH , CH_3COOH , etc...) were studied as function of irradiation intensity, time and ratio of reactants. Up to 24 UVB fluorescent lamps (280 - 360 nm, λ_{max} 315 nm), mounted around a quartz cell (1.2 m long, 12 cm diameter), were used as irradiation source. The experimental data were computer simulated, based on earlier quantum yield measurements, and currently accepted reaction rate constants of elementary reactions.

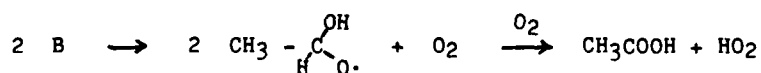
Figure 1 represents the concentration-time profile of the identified products of the photolysis of 57 ppm CH_3CHO in air. The mechanism leading to the formation of the products is initiated by the photolysis path I, leading to the formation of CO , HO_2 and CH_3O_2 , followed by the reaction sequence (3) to (5), producing mainly CH_3OH and CH_2O and CH_3OOH .



Recent studies of the photooxidation of CH_2O have shown that the formation of HCOOH occurs via a chain reaction initiated by the addition of HO_2 to CH_2O .^{2,3} Using an analogous mechanism, the formation of CH_3COOH can be explained by the reaction of HO_2 radicals with CH_3CHO via an adduct complex A, which can rearrange intramolecularly to form a peroxy radical B



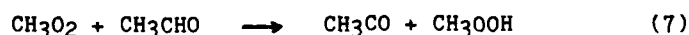
Two B radicals recombine to oxy radicals, which upon reaction with O_2 form CH_3COOH and HO_2 :



Rate constants $k_6 = 1 \times 10^{-15} \text{ cm}^3 \cdot \text{molec}^{-1} \cdot \text{s}^{-1}$ and $k_{-6} = 1.5 \text{ s}^{-1}$ are obtained by computer simulation.

The high CO_2 yield in the CH_3CHO photooxidation system is surprising. It is generally accepted that the oxidation of CH_3CO radicals leads to CH_3 and CO_2 , but although CH_3CO is produced as a primary photolysis product, its yield is only a few percent⁴, and cannot account for the high CO_2 yield.

On the other hand, many radicals may abstract an H-atom from CH_3CHO to produce CH_3CO . Suggested by the formation of relatively large amounts of CH_3OOH , it was found with the aid of computer simulation that the reaction

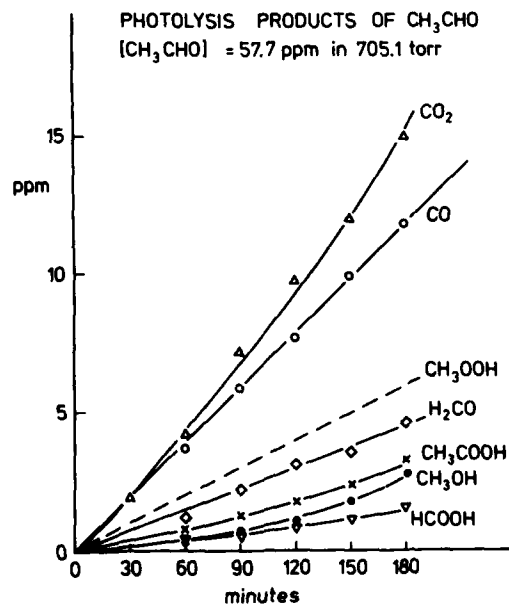


is responsible for the CH_3CO , and consequently for the high CO_2 formation. A reaction rate constant of $k_7 = 3.4 \times 10^{-16} \text{ cm}^3 \cdot \text{molec}^{-1} \cdot \text{s}^{-1}$ was deduced.

References

- 1) Fulbright Visiting Scientist (1982-83) from Ohio Wesleyan University, Delaware, Ohio 43015 USA.
- 2) F.Su, J.G.Calvert, J.H.Shaw, J.Phys.Chem., 83, 3185 (1979)
- 3) B.Veyret, J.C Rayez, R.Lesclaux, J.Phys.Chem., 86, 3424 (1982).
- 4) A.Horowitz, and J.G.Calvert, J.Phys.Chem., 86, 3105 (1982)

Figure 1
Concentration-time
profile of the pro-
ducts of the photo-
lysis of CH_3CHO .



NOTES

Kinetics of free radicals produced by infrared
multiple photon dissociation

G. Hancock

Physical Chemistry Laboratory, Oxford University, Oxford UK

Infrared multiple photon dissociation has proved to be a useful method for pulsed formation of gas phase free radicals in their ground electronic states. Time resolved laser induced fluorescence detection of these species can be used to determine both the kinetics of their decay in the presence of added reactants and can in some cases be of use in determining pathways for the multiple photon dissociation (MPD) process itself. This contribution describes three sets of measurements on triatomic radicals using the combination of these techniques.

a) Reactions of CHF (\tilde{X}^1A')

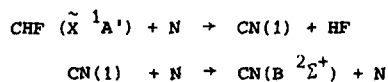
Bimolecular reactions of ground state CHF (\tilde{X}^1A') with NO, NO₂, O₂, N and O have been studied, and rate constants at 298K are given in Table 1.

Table 1 Bimolecular rate constants k for room temperature reactions of CHF (\tilde{X}^1A')

Reactant	$k/\text{cm}^3 \text{ molecule}^{-1} \text{ s}^{-1}$
NO	$(7.0 \pm 0.4) \times 10^{-12}$
NO ₂	$(8.6 \pm 0.5) \times 10^{-12}$
O ₂	$< 5 \times 10^{-16}$
N	$(2.5 \pm 0.5) \times 10^{-11}$
O	$(1.5 \pm 0.2) \times 10^{-10}$

The mechanisms of several of these processes have been investigated. For example, in the CHF + N reaction, strong B $^2\Sigma^+ \rightarrow X^2\Sigma^+$ emission from CN is observed, but its kinetic behaviour shows that it is not formed directly in the excited state. A two stage process is consistent with the

experimental results:



On energetic grounds the intermediate state $\text{CN}(1)$ could be $X^2\Sigma^+$, $A^2\Pi_1$ or $a^4\Sigma^+$, and experiments testing these possibilities will be discussed.

b) Reactions of $\text{NCO}(\tilde{X}^2\Pi_1)$

Ground state $\text{NCO}(\tilde{X}^2\Pi_1)$ can readily be detected by laser induced fluorescence as a primary product of the reaction between $\text{CHF}(\tilde{X}^1A')$ and NO :



NCO is rapidly removed by chemical reaction with NO in this system ($k \sim 2 \times 10^{-11} \text{ cm}^3 \text{ molecule}^{-1} \text{ s}^{-1}$) and to study this reaction quantitatively, MPD of $\text{C}_6\text{H}_5\text{NCO}$ has been used as a direct source of the ground state radical. The infrared dissociation technique generally has an advantage over single photon uv dissociation in that fragments are formed with relatively low internal energies, and thus problems of cascading of population into the probed level by vibrational relaxation from higher states can be avoided. This, surprisingly, is not the case for $\text{C}_6\text{H}_5\text{NCO}$, as appreciable quantities of $\text{NCO}(\tilde{X}^2\Pi_1(O,n,0))$ $n \leq 2$ is formed in the MPD process. The kinetic behaviour has been studied in the presence of N_2O , which was found to relax these levels without chemical removal of the NCO ground vibrational state.

c) MPD of $\text{C}_2\text{F}_2\text{Cl}_2$

MPD of either $\text{CF}_2 = \text{CCl}_2$ or $\text{CFCl} = \text{CFCl}$ under collision free conditions produces all three triatomic carbene radicals CF_2 , CCl_2 and CFCl in their ground electronic states (in addition to the major dissociation process, which is the loss of Cl atoms). Intramolecular rearrangements involving migration of both Cl and F atoms must take place before dissociation in order to explain the cross products observed. The measured ratios of the $\text{CF}_2 : \text{CFCl} : \text{CCl}_2$ channels are different for the two precursors, and show that dissociation after equilibration to a common $\text{C}_2\text{F}_2\text{Cl}_2$ intermediate cannot explain the results.

VIBRATIONAL ENERGY SCRAMBLING IN
INFRARED MULTIPLE PHOTON DISSOCIATION OF LARGE MOLECULES

S. Ruhman and Y. Haas

Department of Physical Chemistry and
The Fritz Haber Center for Molecular Dynamics
The Hebrew University, Jerusalem, Israel

J. Laukemper, M. Preuss, D. Feldmann and K.H. Welge,
Department of Physics, The University, Bielefeld, FRG

Infrared multiple photon absorption (IRMPA) is a convenient technique for exciting isolated polyatomic molecules to beyond their dissociation limit while in their electronic ground state. Considerable circumstantial evidence has been forwarded supporting the hypothesis of complete intramolecular energy randomization among all vibrational degrees of freedom in molecules excited by IRMPA. In this paper we discuss a direct experimental test of this hypothesis, and the possibility of selective IR excitation.

A major difficulty arising in interpreting past experiments directed at observing selective excitation was the lack of information on the energy distribution of excited molecules following IRMPA. Changes in the reaction pattern observed upon changing the excitation frequency could be accounted for, within the statistical theory, by assuming different initial vibrational population distributions. A direct probe of these distributions is not yet available, making this assumption tentative. In the present work the nature of the distribution is immaterial, as the molecule displays two kinetically identical reaction pathways that are spectroscopically distinguishable. The substrate, 1,5-dithia-hex-3-yne (DTH, $\text{CH}_3\text{SCCSCD}_3$) can be excited by absorption initially associated with either the CH_3 or the CD_3 group. The reaction is fission of the S-methyl bond, and the resulting CH_3/CD_3 ratio is monitored by VUV laser single photon ionization. One reason for choosing this molecule was the estimate that the presence of a relatively heavy atom (sulfur) in combination with the triple bond might hinder fast intramolecular vibrational redistribution.

In the experiments reported, a large number of CO_2 laser lines were used to excite the molecule. Probing was done in real time using 10.47 eV photons obtained by tripling the 355 nm radiation of a Nd:YAG laser. A time of flight (TOF) mass spectrometer was used to identify the products. Considerable fragmentation was observed at all irradiation wavelengths. Methyl radicals were observed to appear at higher fluence levels than other ions. In contrast with larger ionic fragments that are due to dissociative ionization of the parent, the methyl ions re-

STATE SELECTED KINETIC MEASUREMENTS OF
 RADICAL-MOLECULE REACTIONS IN THE
 298-1300 K TEMPERATURE RANGE

Steven L. Baughcum and Richard C. Oldenborg
 Chemistry Division, Los Alamos National Laboratory
 Los Alamos, NM 87545 USA

The reaction rate constants of electronically and vibrationally state selected radical-molecule reactions as a function of temperature are vital for assessing the importance of various reactions in combustion and similar high temperature processes and provide important insight into the details of the potential energy surfaces involved. We have constructed an apparatus for studying radical-molecule reactions over the 298-1300 K temperature range using state-of-the-art laser techniques. Radicals are produced by pulsed excimer laser photolysis of suitable precursor molecules. The disappearance rate of the radicals in the presence of a reactant gas is then measured under pseudo-first order conditions by varying the time delay between the excimer laser and a laser-induced fluorescence (LIF) probe laser. An optical-optical double resonance laser induced fluorescence probe has been developed for studying some radicals of interest at high temperatures where conventional LIF probes are unsuitable, as is the case for $C_2(X^1\Sigma_g^+)$. The results of a study of the reaction kinetics and intersystem crossing rates of the $C_2 + O_2$ system are reported over the 298-1300 K temperature range for $C_2(X^1\Sigma_g^+, v = 0)$ and $C_2(a^3\Pi_u, v = 0, 1, \text{ and } 2)$. The implications of these results on the reaction potential surface will be discussed. More recent results of high temperature studies of other radical-molecule reactions will be presented.

sult from ionization of methyl radicals formed by neutral dissociation. This conclusion is based on independent photoionization fragmentation spectra, (T. Baer, private communication), on the analysis of the temporal behaviour of the different fragments, and on calculated reaction rates.

In all the experiments, the yield of CH_3 was identical with that of CD_3 . It is concluded that in this case initial selective excitation of one part of the molecule is not maintained up to beyond the dissociation limit. Energy scrambling occurs either during the sequential multiple photon absorption process or during the finite lifetime of the metastable molecules excited beyond the dissociation energy. The $\text{SC}\equiv\text{CS}$ group is thus not a barrier to vibrational energy randomization on the time scale of the experiment — 10^{-7} - 10^{-6} second.

LIF Measurements of the Bimolecular Reactions of CN Radicals
Xuechu Li, Nahid Sayah and William M. Jackson, Laser Chemistry
Division, Department of Chemistry, Howard University
Washington, D.C. 20059

Abstract

ArF laser photolysis of CN compounds has been used as a source of CN radicals to measure the rate constants for its reactions with stable molecules. The quantum state distributions of CN radicals are measured as a function of time using the laser induced fluorescence technique (LIF).

The experimental apparatus has been previously described¹. Vibrational enhancement of the rate constant for the reaction of CN with O₂, CH₄, and H₂ was observed when C₂N₂ was used as a source for the vibrationally excited CN radicals¹. To extend this work to higher vibrational levels the use of BrCN as a source of vibrationally excited CN has been investigated. Earlier work² showed that the nascent internal distribution of CN radicals produced in the photolysis at 193 nm consist of rotationally hot radicals with few radicals produced in the upper vibrational levels. Heavens³ et al. saw higher vibrational levels and a different rotational distribution in the photolysis of BrCN in a supersonic molecular beam. Fig.1 shows that this apparent

1. Xuechu Li, Nahid Sayah, and William M. Jackson, to appear in J. Chem. Phys. July 15, (1984)

2. J. B. Halpern and W. M. Jackson, J. Phys. Chem. 86, 3528 (1982)

3. M. Heavens, T. A. Miller, and V. E. Bondybey, Chem. Phys. Letters, 84, 1 (1981)

discrepancy is caused by collisions of the nascent radicals in the molecular beam. The spectrum on the right, is essentially the same as Heavens³ et al., but it occurred only after CN collided.

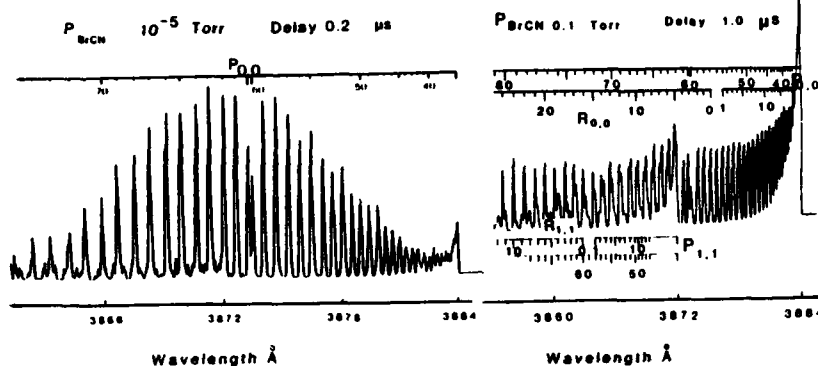


Fig. 1

To explain these observations an energy transfer mechanism has been proposed where CN radicals in states with $v''=0$ and a large rotational quantum numbers, N'' , are mixed by collision with a state of large v'' and lower N'' . After the collision some of the radicals are left in this new state with the overall result that T-V transfer has occurred with a high probability.

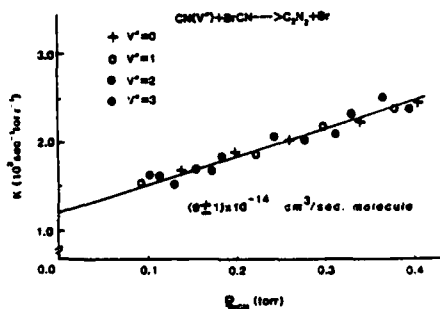


Fig. 2

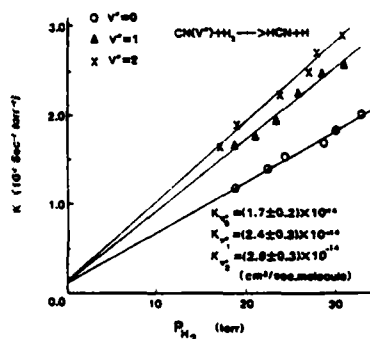


Fig. 3

CN radicals produced from the photodissociation of BrCN are rotationally and translationally equilibrated, and the rate constants for the reaction of vibrationally excited CN with BrCN and H₂ were measured. The results that were obtained are shown in Figs. 2 and 3.

The reaction of CN radicals with BrCN is independent of the vibrational energy in the CN radical, implying that quenching is not important for this system and that chemical reaction is occurring. The most likely path is the exothermic reaction shown in the figure, which must have an early barrier on its potential energy surface.

The rate constant for the reaction of H₂ varies with the vibrational energy, but the increase is less than one would expect. The activation energy for this reaction has been reported⁴ to be 5.3 Kcal/mole so that if vibrational energy was as effective as translational energy these rate constants would be much higher. Again this suggests that the potential surface has an early barrier, which agrees with the theoretical potential surface that has been reported for the reverse reaction⁵.

The authors wish to thank Drs. Hideo Okabe and Joshua B. Halpern for their many helpful comments during the course of this work. X. Li and N. Sayah gratefully acknowledge the support of the Department of Energy under grant number AS05-76ER05056.

4. Von H. Schacke, H. Gg. Wager and J. Wolfrum, Ber. Bunsenges Physik Chem. 81, 670 (1977)

5. Raymond A. Bauer and Thomas Dunning to be published.

"Studies of the Reactions of Alkyl and Alkenyl Radicals
with Molecular Oxygen at Elevated Temperatures".

Irene R. Slagle, Jong-Yoon Park, and David Gutman.
Department of Chemistry
Illinois Institute of Technology
Chicago, Illinois 60616, U.S.A.

The reactions of C_2H_5 , $n-C_3H_7$, $i-C_3H_7$ and C_3H_3 with molecular oxygen have been studied as a function of both temperature (up to 900K) and pressure (0.4 to 12 torr) to better understand the changing mechanisms of these elementary reactions as temperature increases.

Rate constants were measured in real-time experiments using homogeneous laser photolysis to generate the polyatomic free radical of interest and photoionization mass spectrometry to monitor free-radical decay profiles.

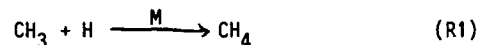
The results clearly indicate that these reactions do not proceed by parallel paths, an addition route that dominates at low temperatures, and an H-atom metathesis reaction that is the major route at high temperatures. The reactive route $R+O_2 \rightarrow R(-H)+HO_2$ proceeds via decomposition of the RO_2^* adduct. The temperature and pressure dependencies of the measured rate constants, as well as product yields have been modeled using the mechanism described above using RRKM theory. Extrapolations of our results to still higher temperatures are in the opposite sense (i.e. the reaction continues to become slower) than those previously presumed based on the results of more indirect studies.

A direct measurement of the pressure and temperature dependence of the rate constant for $\text{CH}_3 + \text{H}$.

M. Brouard, M.T. Macpherson, M.J. Pilling, J.M. Tulloch and A.P. Williamson

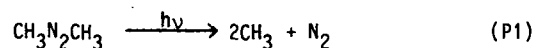
Physical Chemistry Laboratory, South Parks Road, Oxford, OX1 3QZ

The reaction between CH_3 and H

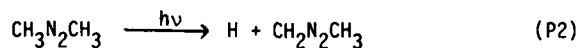


has been studied by observing the time dependence of CH_3 (by absorption spectroscopy) and H (by resonance fluorescence) in a two channel experiment following ArF laser photolysis of azomethane.

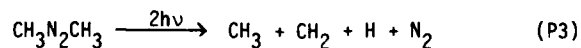
The major primary photolysis process is



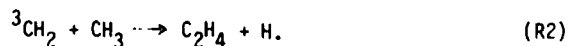
but H atoms are also produced in a yield of $(0.6 \pm 0.4)\%$ of that of CH_3 :-



High laser powers must be avoided because of the two photon process

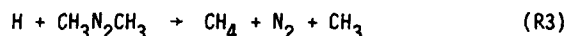


which probably proceeds via vibrationally excited CH_3 . The effects of this channel are readily observed at high laser powers and low total pressures, when an initial rise in $[\text{H}]$ may be observed, resulting from



Independent g.c. experiments¹ have established the dependence of photolysis channel (P3), and hence the yield of $^3\text{CH}_2$, on the percentage photolysis and simulations are performed for each set of experimental conditions to ensure that there is no significant contribution from reaction (R2).

A further complication is provided by the reaction



which is surprisingly rapid and can account for up to 50% of the total H atom decay on the time scale of interest. The reaction has been studied in detail and its rate constant determined to high precision ($k = (3.4 \pm 0.2) \times 10^{-12} \text{ cm}^3 \text{ molecule}^{-1} \text{ s}^{-1}$ [95% confidence limits] at 290K) so that (R3) can be incorporated in the analysis with little increase in uncertainty.

Under the experimental conditions, $[\text{CH}_3] \gg [\text{H}]$ so that CH_3 reacts primarily by recombination

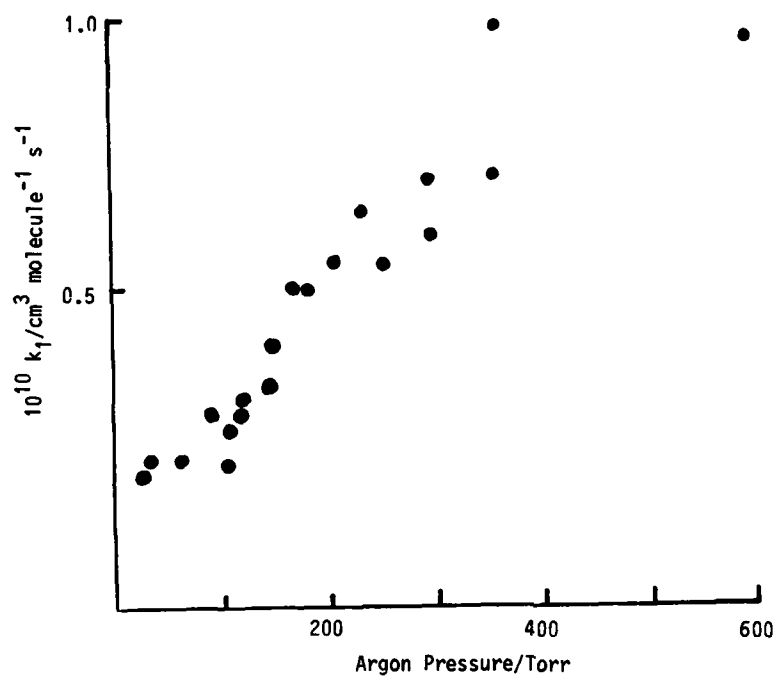


whilst H reacts via (R1) and (R3); there is also a small diffusive contribution which is effectively first-order in H (rate constant k_{diff}). We have shown that the most satisfactory method of analysis involves fitting the CH_3 decay to a second order profile, using the known values of $k_4^{2,3}$, to obtain $[\text{CH}_3]_0$, the methyl radical concentration at zero time. The H atom decay is then fitted to

$$[\text{H}] = [\text{H}]_0 \{1 + 2[\text{CH}_3]_0 k_4 t\}^{-k_1/2k_4} \exp \{-(k_3[\text{CH}_3\text{N}_2\text{CH}_3] + k_{\text{diff}})t\}$$

in which k_1 is the only unknown parameter.

Fig. 1 shows a plot of the pressure dependence of k_1 at room temperature.



References

1. J.E. Baggott, M. Brouard, M.A. Coles, A. Davis, M.T. Macpherson and M.J. Pilling, submitted to J. Phys. Chem.
2. M.T. Macpherson, M.J. Pilling and M.J.C. Smith, Chem. Phys. Lett., 1983, 94, 430.
3. M.T. Macpherson, M.J. Pilling and M.J.C. Smith, to be published.

Calculation of the $\text{H}+\text{CH}_3\text{---}\rightarrow\text{CH}_4$
Bimolecular Recombination Rate Constant

William L. Hase and Ronald J. Duchovic
Department of Chemistry
Wayne State University
Detroit, Michigan 48202

Using an accurate potential energy surface obtained in part from ab initio calculations¹, the $\text{H}+\text{CH}_3\text{---}\rightarrow\text{CH}_4$ bimolecular rate constant determined from a Monte Carlo classical trajectory study. As shown in Table I this calculated rate constant is in excellent agreement with experimental measurement. An important feature of the potential energy surface is the C-H stretching potential which differs significantly from that of a Morse oscillator. In Figure 1 the C-H stretching potential for the accurate surface is given by a dashed curve and compared with that for the Morse oscillator which is given by the solid curve.

The shape of the C-H stretching potential strongly influences the recombination rate constant. If a Morse function is used for the stretching potential instead of that derived from the ab initio calculations, the calculated recombination rate constant is an order of magnitude larger than the experimental value. Another feature of the potential energy surface which strongly influences the recombination rate constant is the attenuation of the $\text{H}_3\text{C---H}$ bending motions between methane and the methyl radical asymptotic limit. Ab initio calculations with a hierarchy of basis sets and treatment of electron correlation indicate that this attenuation is properly described.

The classical trajectory calculations also provide the $\text{H}+\text{CH}_3\text{---}\rightarrow\text{CH}_4^*$ excitation function and opacity function. Also of interest are the dynamical details of the trajectories which lead to recombination.

1. R. J. Duchovic, W. L. Hase and H. B. Schlegel, J. Phys. Chem. 88, 1339 (1984).
2. J.-T. Cheng and C.-T. Yeh, J. Phys. Chem. 81, 1982 (1977).
3. M. J. Pilling and J. A. Robertson, Chem. Phys. Letters 33, 336 (1975).
4. R. Patrick, M. J. Pilling and G. J. Rogers, Chem. Phys. 53, 279 (1980).
5. M. J. Pilling, J. A. Robertson and G. J. Rogers, Int J. Chem. Kinet. 8, 883 (1976).

TABLE I. $\text{H}+\text{CH}_3 \rightarrow \text{CH}_4$ BIMOLECULAR RATE CONSTANT^a

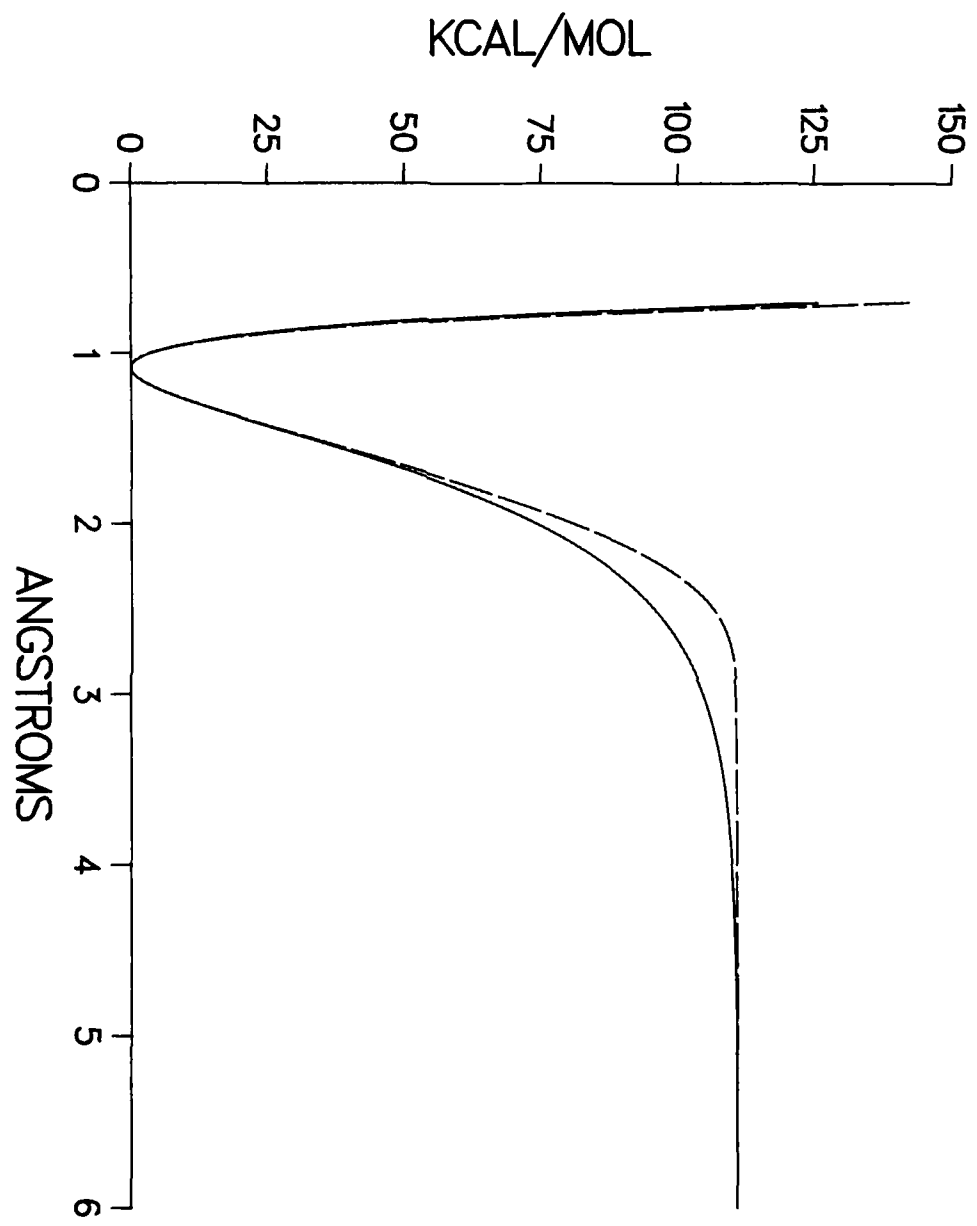
RATE CONSTANT	TEMPERATURE	SOURCE
$(3.32 \pm 1.49) \times 10^{-10}$	308.0	ref 2 (expt) ^b
1.0×10^{-10}	298.0	ref 3 (expt) ^c
$(1.5 \pm 0.7) \times 10^{-10}$	298.0	ref 4 (expt) ^b
2.0×10^{-10}	298.0	ref 5 (expt) ^b
$(1.65 \pm 0.53) \times 10^{-10}$	300.0	this work (stiff Morse) ^d
$(1.97 \pm 0.24) \times 10^{-9}$	300.0	this work (standard Morse)

a. Rate constants in $\text{cm}^3 \text{ molecule}^{-1} \text{ s}^{-1}$; temperature in Kelvin.

b. Direct experimental measurement.

c. Inferred from kinetic model used to analyze experimental data.

d. The term stiff Morse describes the ab initio potential for C-H stretching.



NOTES

PHOTOENHANCED ELECTRON ATTACHMENT
PROCESSES IN THE GAS PHASE

M. J. Rossi, H. P. Helm, and D. C. Lorents
Chemical Physics Laboratory
SRI International
Menlo Park, CA 94025

Abstract

Electron attachment rate coefficients and cross sections have been measured in a drift cell, whose cathode-anode gap has been illuminated in order to produce volume excitation of the attaching gas. The rate enhancement of the following reactions upon photoexcitation and the absolute rates of the following reactions will be reported:

- (1) $\text{HF}^{\dagger} (v = 4 \text{ or } 5) + e^{-} \rightarrow \text{H}^{\bullet} + \text{F}^{-}$
- (2) $\text{HCl}^{\dagger} (v = 4 \text{ or } 5) + e^{-} \rightarrow \text{H}^{\bullet} + \text{Cl}^{-}$

The vibrationally excited HF^{\dagger} and HCl^{\dagger} will be generated in two ways:

- Photoelimination of HCl or HF from $\text{C}_2\text{H}_3\text{Cl}$ and $\text{C}_2\text{F}_3\text{H}$ upon excimer laser irradiation at 193 nm.
- Energy transfer from IR TEA laser heated SiF_4 to HCl and HF.

The rate enhancements upon photoexcitation will be discussed in light of previous results for the temperature dependence of the electron attachment cross sections for HCl and HF.

SLOW UNIMOLECULAR DISSOCIATIONS OF
POLYATOMIC IONS AT NEAR THRESHOLD ENERGIES

C. Lifshitz

Department of Physical Chemistry

The Hebrew University of Jerusalem, Jerusalem 91904, Israel

Unimolecular dissociations of many polyatomic cations have microcanonical rate coefficients $k(E) \approx 1 \text{ s}^{-1}$ or less at near threshold energies. We have constructed a Time-resolved Photoionization Mass Spectrometer (TPIMS)¹ to study these slow dissociations. Pulsed ionization in the VUV produces photoions which are trapped for variable times in a Cylindrical Ion Trap (CIT) before being ejected for mass analysis.

The main effort has concentrated recently on two reaction systems:



and



in bromobenzene and phenol, respectively.

Figure 1 represents data for bromobenzene; the photoionization efficiency (PIE) of the phenyl cation is plotted as a function of photon energy. The points (open circles, at 2 ms; squares, at 5 μs) are experimental and the curves are calculated. The calculation is based on an RRKM-QET model of Rosenstock et al.² The agreement between experiment and theory is remarkably good, and demonstrates that we can detect dissociations having rate coefficients of $\sim 1 \text{ s}^{-1}$. The transition state for this reaction is loose with an activation entropy at 1000°K, of $\Delta S^\ddagger = 8.07 \text{ e.u.}$ and the pre-exponential A_∞ factor is closely similar to that for the analogous neutral reaction.

An upper limit on the lifetime of a metastable ion decomposition is imposed by the competing relaxation of internal excitation by IR radiative cooling.³ We have included a radiative term in our model calculations for

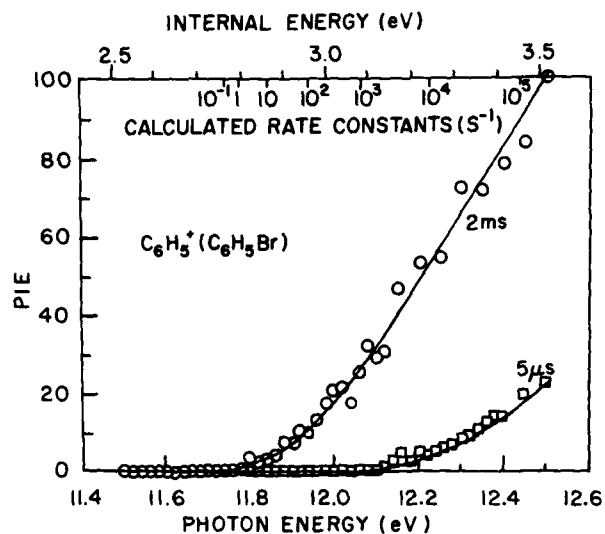


Figure 1

bromobenzene and found no effect on the dissociative channel, provided we limit ourselves to low overall conversions.

The phenol ion reaction possesses a relatively high activation energy for the reverse reaction. This may be ascribed to a surface crossing between the \tilde{X}^2B_1 and \tilde{A}^2A_2 states. The computed $k(E)$ at threshold energies is $^4 \leq 10^{-3} \text{ s}^{-1}$. No dissociation has been observed at these energies by ordinary mass spectrometric techniques. Data on this reaction obtained by TPIMS will be presented.

1. C. Lifshitz, M. Goldenberg, Y. Malinovich and M. Peres, *Org. Mass Spectrom.* **17**, 453 (1982).
2. H.M. Rosenstock, R. Stockbauer and A.C. Parr, *J. Chem. Phys.* **73**, 773 (1980).
3. R.C. Dunbar, *Int. J. Mass Spectrom. & Ion Processes*, **54**, 109 (1983).
4. M.L. Fraser-Monteiro, L. Fraser-Monteiro, Jos de Wit and T. Baer, *J. Phys. Chem.*, in press.

COLLISIONAL ENERGY TRANSFER IN THE VERY LOW-PRESSURE
PYROLYSIS OF SOME tert-BUTYL HALIDE SYSTEMS

Trevor C. Brown and Keith D. King

Department of Chemical Engineering

University of Adelaide, Adelaide, S.A. 5001, Australia

and

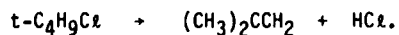
Robert G. Gilbert

Department of Theoretical Chemistry,

University of Sydney, Sydney, N.S.W., 2006, Australia.

An understanding of the probability distribution function for collisional energy exchange between a highly vibrationally excited reactant and a bath gas is essential for the interpretation of rate data for unimolecular and termolecular reactions in the fall-off regime [1]. The development of viable models for this process requires reliable experimental data, particularly data wherein only a small number of controllable parameters (such as temperature, bath gas mass, etc.) are varied. Deuteration of reactant and/or bath gas will clearly provide especially useful data, since deuteration changes only the masses while leaving unchanged the potential function which governs the interaction dynamics.

We report here results obtained using the technique of pressure-dependent very low-pressure pyrolysis [2, 3] to study the effects of deuteration on collisional energy transfer quantities. The reactions studied were HX elimination from tert-butyl halides, e.g. as in the thermal decomposition of tert-butyl chloride:



Although this is only a single channel system, the data are still quite sensitive to the average downward collisional energy transfer ($\langle \Delta E_{\text{down}} \rangle$), because of the "calibration" provided by wall activation data (in the absence of bath gas) and high-pressure data. Both the absolute values of $\langle \Delta E_{\text{down}} \rangle$ and, more importantly, the change in this quantity on perdeuteration, provide both a useful test of current theories and an indication of how such theories can be improved.

The technique of pressure-dependent very low-pressure pyrolysis is well established [2, 3]. Firstly, one obtains the temperature dependence of the reaction rate at pressures so low that activation is solely by gas/wall collisions; this is conventional very low-pressure pyrolysis (VLPP) [4]. By fitting with RRKM theory, while taking account of temperature-dependent non-unit gas/wall collision efficiency, $\beta_w(T)$ [2], one obtains the energy dependences of the microscopic reaction rate, $k(E)$. Although single-channel experiments do not in themselves provide sufficient information to determine $\beta_w(T)$, extensive data on this quantity using multiple channel pressure-dependent VLPP [2] and the variable encounter method (VEM) [5] have resulted in a semi-empirical theory [6] which enables $\beta_w(T)$ to be reliably calculated for any system to the accuracy necessary for the present purpose. A series of experiments is then carried out with reactant highly dilute in bath gas. The pressure-dependent rate coefficients so obtained are fitted by solution of the reaction-diffusion master equation [3], utilizing the $k(E)$, $\rho(E)$ and $\beta_w(T)$, and varying $\langle \Delta E_{\text{down}} \rangle$ to fit the data.

The high-pressure rate coefficient (k_∞) for $\text{C}_4\text{H}_9\text{Cl}$ decomposition is given by $k_\infty(\text{s}^{-1}) = 10^{13.6} \exp(-187 \text{ kJ mol}^{-1}/RT)$. This is in good agreement with the high-pressure parameters reported using other techniques [7]: $A_\infty = 13.9 \text{ s}^{-1}$, $E_\infty = 191 \text{ kJ mol}^{-1}$. The high-pressure parameters obtained for $\text{C}_4\text{D}_9\text{Cl}$ are $A_\infty = 10^{14.2} \text{ s}^{-1}$, $E_\infty = 196 \text{ kJ mol}^{-1}$.

While there is no previously reported study of the C_4D_9Cl decomposition, these results are in accord with the expected isotope effect.

The average downward collisional energy transfer ($\langle \Delta E_{down} \rangle$) was obtained for highly vibrationally excited tert-butyl chloride, both undeuterated and perdeuterated, with Kr, N_2 , CO_2 and C_2H_4 bath gases, at ca. 760 K. Reactant internal energies to which the data are sensitive are in the range 200 - 250 $kJ\ mol^{-1}$. For C_4H_9Cl , the $\langle \Delta E_{down} \rangle$ values (cm^{-1}) are 255 (Kr), 265 (N_2), 440 (CO_2) and 585 (C_2H_4), and for C_4D_9Cl , 245 (N_2), 370 (CO_2) and 540 (C_2H_4). The value for Kr is in agreement with theoretical predictions of a biased random walk model for internal energy change in monatomic/substrate collisions [8]. The effect of deuteration on $\langle \Delta E_{down} \rangle$ is also in accord with that predicted by a modification of the theory.

References

1. B. S. Rabinovitch and D. C. Tardy, Chem. Rev., 77, 369 (1977).
2. See, for example, T. T. Nguyen, K. D. King and R. G. Gilbert, J. Phys. Chem., 87, 494 (1983) and references therein.
3. R. G. Gilbert, B. J. Gaynor and K. D. King, Int. J. Chem. Kinet., 11, 317, (1979).
4. D. M. Golden, G. N. Spokes and S. W. Benson, Angew. Chem., Int. Ed., 12, 534 (1973).
5. See, for example, W. Yuan, B. S. Rabinovitch and R. Tosa, J. Phys. Chem., 86, 2796 (1982) and references therein.
6. P. G. Dick, R. G. Gilbert and K. D. King, Int. J. Chem. Kinet., in press.
7. H. Heydtmann, B. Dill and R. Jonas, Int. J. Chem. Kinet., 7, (1975) and references therein.
8. R. G. Gilbert, J. Chem. Phys., in press.

Quantitative Intermolecular Energy Transfer
Efficiencies from Thermal Studies

by C.D. Eley and H.M. Frey

Chemistry Dept., University of Reading,
Whiteknights, Reading RG6 2AD.

The problem of obtaining a quantitative measure of the average energy transferred during collision between an energised molecule, containing sufficient energy for chemical reaction and an inert bath gas is of both experimental and theoretical interest. There are considerable difficulties in obtaining the required information from conventional thermal studies on unimolecular reactions and it is the purpose of this paper to highlight some of these difficulties and suggest systems capable of yielding satisfactory data. We believe there is still value in this approach despite the development of rather more sophisticated methods for solution of the problem in the last few years, since even those studies have not produced results that are completely consistent or indeed provide a large data base of reliable constants.^(1,2,3)

Ideally, to obtain values of $\langle \Delta E \rangle$, $\langle \Delta E \rangle_d$ or β (collision efficiency) one needs to study a unimolecular reaction from its 1st to its 2nd order region. This is rarely possible for experimental reasons and few molecules of any complexity have been followed far into the 'fall off' region. On the other hand for very simple species the high pressure Arrhenius parameters are often ill-defined.

If one can only obtain information for part of the 'fall off' curve the values calculated for collision efficiencies are very sensitive to the exact values of the Arrhenius parameters used. We illustrate the difficulty of obtaining accurate high pressure Arrhenius parameters as well as the sensitivity of the extracted values of collision

efficiencies by considering some experimental data on the thermal unimolecular decomposition of some lactones.

A more satisfactory situation is presented by the study of reactants which decompose by two separate but competitive pathways provided they have different energies of activation. This intramolecular competition produces a 'gearing effect'. We illustrate this by a series of RRKM calculations. However, even here, accurate Arrhenius parameters are required. Finally we will present some experimental results on a two channel system together with the calculated values for energy transfer.

1. J.R. Barker and R.E. Golden, J. Phys. Chem., 1984, 88, 1012.
2. H. Hippler, J. Troe and H.J. Wendelken, J. Chem. Phys., 1983, 78, 6718.
3. V.V. Krongauz and B.S. Rabinovitch, J. Chem. Phys., 1983, 78, 3872.

LIF STUDIES OF METHOXY AND VINOXY
RADICAL REACTIONS

B. Fritz, K. Lorenz, D. Rhäsa, and R. Zellner

Institut für Physikalische Chemie
Universität Göttingen, FRG

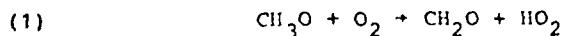
Methoxy (CH_3O) and vinoxy (or formyl-methyl, CH_2CHO) radicals are important reaction intermediates during the gas-phase oxidation of most hydrocarbons. Whereas CH_3O is only formed in simple abstraction reactions (i.e. $\text{OH} + \text{CH}_3\text{OH}$ [1]), CH_2CHO has also been observed in reactions with multiple potential well surfaces (i.e. $\text{O} + \text{C}_2\text{H}_4$ [2], $\text{OH} + \text{ethylene oxide}$ [3] and $\text{OH} + \text{C}_2\text{H}_2$ [4]) as a result of bond rupture or isomerization of energy rich primary species.

The present work focusses on the kinetics and mechanism of the consecutive reactions of CH_3O and CH_2CHO radicals in atmospheric and combustion environments: reactions with O_2 and NO . In the experiments CH_3O and CH_2CHO are generated by excimer laser photolysis of CH_3ONO ($\lambda = 248 \text{ nm}$) and methyl-vinyl-ether ($\lambda = 193 \text{ nm}$), respectively. Their decay is monitored by LIF using a frequency doubled dye laser. Time resolution is obtained by varying the delay between both laser systems.

1. Reactions of CH_3O with O_2 and NO

These reactions have been studied over the pressure region 13 - 250 mbar (He) and at temperatures between 298 and 520 K.

Reaction (1)



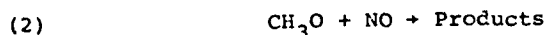
is confirmed to be a slow process. At 298 K we obtain $k_1 = (1.5 \pm 0.4) 10^{-15} \text{ cm}^3/\text{s}$, which considerably reduces

previous uncertainties associated with this rate coefficient. The temperature dependence of k_1 is found to be

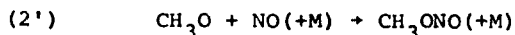
$$k_1(T) = (5.5 \pm 2.0) 10^{-14} \exp(-1000 \text{ K}/T) \text{ cm}^3/\text{s}$$

in reasonable good agreement with the previous determination by Gutman et al. [5]. Our pressure dependent studies reveal little increase of k_1 (+ 20 %) between 13 and 210 mbar. The formation of HO_2 as the only product ($p = 1.0 \pm 0.1$) has been confirmed in independent experiments, in which we have determined the absolute yield of OH arising from chemical titration of HO_2 with NO.

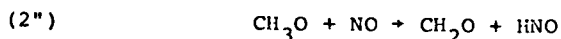
The reaction (2)



is found to be strongly pressure dependent with k_2 increasing from $1.1 \times 10^{-11} \text{ cm}^3/\text{s}$ to $2.5 \times 10^{-11} \text{ cm}^3/\text{s}$ between 13 and 245 mbar of He, in agreement with a dominant recombination process



The overall temperature dependence, however, is more complicated than one might expect on the basis of (2') only. k_2 decreases with temperature; it becomes independent of T though around 500 K. We attribute this effect to the increasing importance of an abstraction channel



for which we deduce $k_{2''} \sim 4 \times 10^{-12} \text{ cm}^3/\text{s}$ around 500 K. This is the order of magnitude previously estimated by Batt et al. [6]. Direct product studies of the formation of HNO are presently carried out.

2. The Reaction of CH_2CHO with O_2

Vinoxy reacts with O_2 more than two orders of magnitude faster than methoxy. The overall rate coefficient is found to show a fall-off behaviour with $k^\infty = (2.6 \pm 0.5) 10^{-13} \text{ cm}^3/\text{s}$, which is best explained by assuming a primary recombination process:



This is also supported by a strong negative temperature dependence:

$$k_3(T) = 2.7 \times 10^{-14} \exp(670 \text{ K}/T) \text{ cm}^3/\text{s}$$

between 298 and 500 K and at 130 mbar of He. These results confirm and extend previous observations by Gutman and Nelson [7].

The product of reaction (3), however, does not appear to be stable under all conditions of our experiments. We observe the formation of OH radicals very early in the reaction and with a time constant comparable to the decay of vinoxy. This suggests intramolecular H-atom shift and subsequent decomposition. A qualitative energy diagram accounting for these observations will be presented.

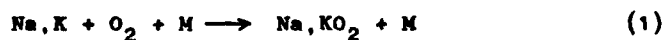
- [1] J. Hägele, K. Lorenz, D. Rhäsa, R. Zellner, Ber. Bunsenges. phys. Chem. 87, 1023 (1983)
- [2] H.E. Hunziker, H. Knepe, H.R. Wendt, J. Photochem. 17, 377 (1981). K. Kleinternann, A.C. Luntz, J. Phys. Chem. 85, 1966 (1981)
- [3] K. Lorenz, R. Zellner, Ber. Bunsenges. phys. Chem.; submitted
- [4] K. Lorenz, D. Rhäsa, R. Zellner, to be published. V. Schmidt, G.Y. Zhu, K.H. Becker, E.H. Fink, 3rd Europ. Symp. physico-chemical behaviour of atmospheric pollutants, Varese 1984
- [5] D. Gutman, N. Sanders, J.E. Butler, J. Phys. Chem. 86, 66 (1982)
- [6] L. Batt, R.T. Milne, R.D. McCulloch, Int. J. Chem. Kin. 9, 567 (1977)
- [7] D. Gutman, H.H. Nelson, J. Phys. Chem. 87, 000 (1983)

Termolecular Reactions of the Alkali Elements Na and K
with O_2 and OH at Elevated Temperatures Determined by
Time-Resolved Spectroscopic Methods

by David Husain, John M.C. Plane and Chen Cong Xiang

The Department of Physical Chemistry,
The University of Cambridge,
Lensfield Road,
CAMBRIDGE CB2 1EP.

There is extensive current interest in the fundamental
termolecular reactions



on account of their importance in flames¹ and in the
chemistry of the mesosphere.² Termolecular reactions of OH



are receiving renewed attention of account of their roles
in the chemistry of the after burning region of flames
seeded with alkali metals.^{1,3} We have recently described
direct measurements on the determination of the absolute
third-order rate constants for both Na and K in reaction (1)
by time-resolved atomic resonance absorption spectroscopic
monitoring of the alkali atoms generated by pulsed
irradiation of the alkali metal iodide at elevated temperat-
ures.^{4,5} In this paper, we give a detailed account of the
first direct measurement of the absolute third-order rate
constant for process (2) where the metal is atomic potassium.
This requires special techniques as both K and OH in this

process are effectively transient species which must be both generated and monitored simultaneously at elevated temperatures.

A complex experimental system has been constructed in which a heat pipe oven, from which atomic potassium is generated, is coupled to a high temperature stainless steel reactor for time-resolved resonance fluorescence measurements on OH following pulsed irradiation. The apparatus is a slow flow system kinetically equivalent to a static system. Ground state $\text{OH}(X^2\Pi)$ was generated by the repetitively pulsed irradiation of water vapour through CaF_2 optics using an N_2 flash lamp directly coupled to the high temperature reactor. This was then monitored in the time-resolved mode at $\lambda = 307$ ($\text{OH}(A^2\Sigma^+ - X^2\Pi)$, (0,0)) following optical excitation with pre-trigger photomultiplier gating, photon counting and signal averaging. Atomic potassium was monitored in the steady mode using resonance fluorescence of the Rydberg transition at $\lambda = 404$ nm ($\text{K}(5^2P_J) - \text{K}(4^2S_{1/2})$) coupled with phase sensitive detection. Thus the time-dependence of $[\text{OH}(X^2\Pi)]$ is studied both as a function of the excess concentrations of $\text{K}(4^2S_{1/2})$ and He, yielding the absolute rate constant

$$k_2(\text{K} + \text{OH} + \text{He}) = 8.8 \pm 1.2 \times 10^{-31} \text{ cm}^6 \text{ molecule}^{-2} \text{ s}^{-1}$$

(T = 530 K, error = 20)

This system exploits an effective "chemical window" through measurements at a temperature at which reaction of the equilibrium concentration of K_2 with OH is negligible and under conditions in which there is no significant fluorescence quenching of $\text{OH}(A^2\Sigma^+)$ by the third-body. Extrapolation of

the present data to the temperatures and conditions of fuel-rich flames using the method of Tree⁶ yields a result in general accord with that derived from modelling calculations on such flames by Jensen et al.³

The kinetic results for the reaction between $K + OH + He$ are compared with preliminary data for the analogous reaction of Na derived from similar measurements at a somewhat higher temperature (650 K). A general summary is presented of recent investigations of both groups of termolecular reactions (1) and (2) together with results for other alkali metals recently reported in the literature.

- (1) A.J. Hynes, M. Steinberg and K. Scheffield, J.Chem.Phys., (1984) 80, 2585.
- (2) L. Thomas, M.C. Isherwood and M.R. Bowman, J.Atmos. Terrestrial Phys., (1983) 45, 587.
- (3) D.E. Jensen, G.A. Jones and A.C.H. Mace, J.Chem.Soc. Faraday Trans. I (1979) 75, 2377.
- (4) D. Husain and J.M.C. Plane, J.Chem.Soc.Faraday Trans. II (1982) 78, 163.
- (5) D. Husain and J.M.C. Plane, J.Chem.Soc. Faraday Trans. II (1982) 78, 1175.
- (6) J. Tree, J.Chem.Phys., (1977) 66, 4745, 4758.

Temperature and pressure dependence of the reaction
of atomic chlorine with acetylene

L. J. Stief and J. Brunning
NASA/Goddard Space Flight Center
Laboratory for Extraterrestrial Physics
Greenbelt, Maryland 20771, U. S. A.

The absolute rate constant for the reaction $\text{Cl} + \text{C}_2\text{H}_2 + \text{M} \rightarrow \text{C}_2\text{H}_2\text{Cl} + \text{M}$ has been investigated using the flash photolysis technique coupled with time resolved detection of atomic chlorine by Cl resonance radiation. Experiments at 298 K and total pressures ranging from 10 to 200 torr argon demonstrate a significant pressure dependence, the rate constant increasing from $2.1 \times 10^{-12} \text{ cm}^3 \text{ molecule}^{-1} \text{ s}^{-1}$ to $1.3 \times 10^{-11} \text{ cm}^3 \text{ molecule}^{-1} \text{ s}^{-1}$ over this pressure range. Experiments over the temperature range 210–360 K reveal that the reaction rate decreases with temperature. This is opposite to the temperature dependence observed in our laboratory for reaction of H, OH and NH_2 with C_2H_2 .

The Pressure Dependence of the Recombination $2\text{NO}_2 \longrightarrow \text{N}_2\text{O}_4$

P. Borrell

Department of Chemistry, University of Keele, Staffordshire, England,

K. Luther and J. Troe

Institut für Physikalische Chemie der Universität Göttingen,
Tammannstraße 6, D-3400 Göttingen, Germany

The rate constant of the reaction $\text{NO}_2 + \text{NO}_2 \longrightarrow \text{N}_2\text{O}_4$ has been measured over wide range of inert gas pressures up to 200 bar. Concentration-time profiles were monitored by absorption spectroscopy in a high pressure cell where $\text{NO}_2/\text{N}_2\text{O}_4$ equilibrium mixtures in N_2 were irradiated by laser pulses at 248 nm. The experimental data cover most of the fall-off range of the recombination reaction and show that the limiting high pressure rate constant k_∞ is only reached at very high pressures. The experimental results are discussed in connection with a detailed theoretical calculation of the fall-off curve.

NOTES

THERMAL REACTIONS OF ETHYLENE INDUCED BY PULSED INFRARED LASER RADIATION

L. GIROUX and M.H. BACK, University of Ottawa,
and
R.A. BACK, National Research Council of Canada

The decomposition of ethylene induced by a pulsed infrared CO₂ TEA laser has been explored at pressures from 500 to 3000 Torr, using the strongly absorbed P(14) line at 949.5 cm⁻¹. Under these conditions the reaction zone is a thin disc at the front window of the reaction vessel, which consisted of two salt windows separated by a brass annulus 5mm thick and 2 cm internal diameter. The gas expands as it is heated during the 0.5 microsecond pulse, so that to a fair approximation the maximum temperature reached is determined by C_p rather than C_v, and the reaction time is controlled by cooling of the reaction zone after the pulse by conduction

The reversible reactions, $2 \text{C}_2\text{H}_4 \rightleftharpoons \text{cyclobutane}$, for which the rate parameters are well known, are operative in the system. Experimentally, it is observed that with successive pulses, cyclobutane increases and then levels out to a steady value. Within a certain range of pulse energies and pressures, an "effective temperature" of reaction can be measured by assuming that the steady concentration of cyclobutane corresponds to an equilibrium. Simple computer modelling of the system by numerical integration shows that this effective temperature is appreciably less than the maximum temperature reached at the end of the pulse.

Other products of the decomposition include 1,3-butadiene, acetylene, hydrogen, 1-butene, propylene, methane, ethane, allene and 2-butene, in approximate order of diminishing importance. It is suggested that these are formed largely by free-radical chains initiated by the reaction,

$2 \text{C}_2\text{H}_4 \rightarrow \text{C}_2\text{H}_3 + \text{C}_2\text{H}_5$, and followed by $\text{C}_2\text{H}_5 \rightleftharpoons \text{H} + \text{C}_2\text{H}_4 \rightarrow \text{H}_2 + \text{C}_2\text{H}_3$ and by further addition reactions of C₂H₃ and C₂H₅ and of the higher radicals thus formed. Some evidence is presented for reactions of the type

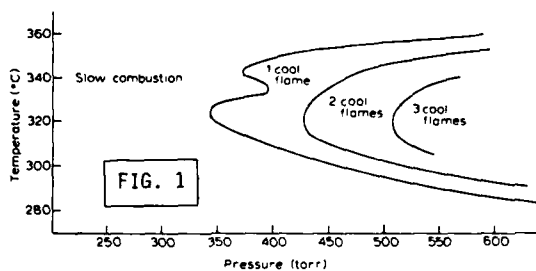
$$\text{RCH}_2\text{CH}_2 + \text{C}_2\text{H}_4 \rightarrow \text{RCH=CH}_2 + \text{C}_2\text{H}_5.$$

COMPARISON OF THE OXIDATION KINETICS OF ACETONE, METHYL ETHYL KETONE AND DIETHYL KETONE

by E. LE ROUX*, G. SCACCHI and F. BARONNET

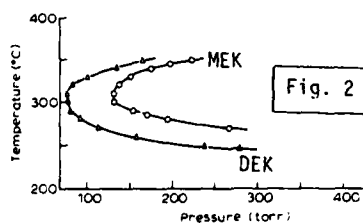
Département de Chimie-Physique des Réactions - L.A. n° 328 CNRS
1, rue Grandville F-54042 NANCY France

The low-temperature combustion of light aliphatic ketones generally resembles that of hydrocarbons ; cool flames are observed and there is the usual pressure-temperature diagram with three regions : slow reaction, cool flames and ignition.



This is the case for instance for the oxidation of acetone ; a rather detailed review of this reaction was published by BARNARD ⁽¹⁾. The cool flame limits of equimolecular mixtures acetone-oxygen

are shown in fig. 1 [from ref. ⁽¹⁾]. The induction period of cool flames is approximately 25 sec. at 330°C.



The behaviour of diethyl ketone (DEK) is rather similar [see fig. 2 from ref. ⁽¹⁾]. The induction periods are also relatively short (around 30 sec. at 310°C).

In the case of methyl ethyl ketone (MEK) pressure-temperature diagrams were mapped out ⁽²⁾ [see also fig. 2]. A striking and unexpected feature of MEK oxidation is the very long induction period which precedes the cool flame. AKBAR and BARNARD found 7 h at 250°C ⁽³⁾ ; HOARE and TING MAN LI mentioned 5 h ⁽⁴⁾ and in our own experimental conditions (350°C, equimolecular mixtures, 100 torr), we observed induction periods longer than half an hour.

It is well known that there is a close relationship between the tendency of a fuel to knock in an engine and its oxidation characteristics

* Present address : Rhône-Poulenc, Centre de Recherches d'Aubervilliers, 93308 AUBERVILLIERS, France.

at low pressure (⁵). It has been shown again here that this correlation holds since MEK has rather interesting antiknock properties (⁶). This observation has also a rather fundamental interest, since it seems rather difficult to explain such a different behaviour for these three light ketones.

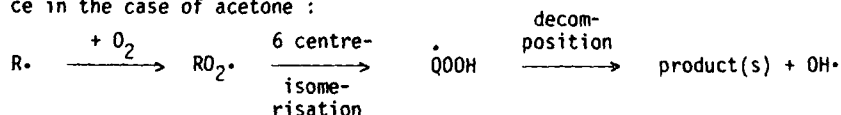
In an attempt to explain the rather specific behaviour of MEK, we have investigated its oxidation around 350°C, especially by identifying and measuring the major primary reaction products at moderate extents of reaction. At the same time, we have performed some complementary comparative investigations on the oxidation reaction of acetone and DEK.

The analysis of the reaction products shows that, in the case of MEK, methyl vinyl ketone (MVC) is largely predominant [in agreement with WALSH's results (⁷)]. The mass balances are reasonably good when we compare the consumption of reactants (MEK and O₂) and the formation of the various products which suggests that we have not missed an important organic reaction product.

To build a reaction scheme accounting for these experimental results, we have also used the experimental results obtained in the investigation of the pyrolysis of MEK (⁸); the kinetic characteristics of this reaction can be explained by taking into account a rather unreactive isomeric form of the radical derived from the MEK molecule by hydrogen abstraction, CH₃CHCOCH₃, which is, according to BENSON (⁹) a "wrong radical" because of its rather low reactivity.

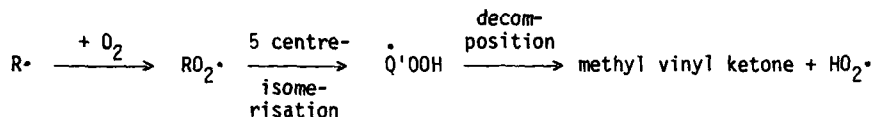
If we write all the possible elementary steps involving this radical, the reaction scheme becomes very complicated; this scheme can be simplified by omitting the elementary steps which do not account for a sufficient consumption of the initial reactants. Since most of the required rate constants are not available in the literature, they have been evaluated by the methods of Thermochemical Kinetics, according to BENSON (⁹) and co-workers. The resulting simplification of the reaction scheme leads to a good understanding of the rate determining elementary steps.

Basically, if we consider the radical (R•) derived from the ketone molecule (RH) by hydrogen abstraction, we obtain the following sequence in the case of acetone:



The hydroxyl radical is very reactive and can propagate the reaction, in agreement with the rather high reactivity of acetone.

In the case of methyl ethyl ketone, the largely predominant reaction path can be summarised as follows :



It is well known that $HO_2\cdot$ cannot be a very reactive chain carrier around 350°C and, therefore, the rather low reactivity of MEK compared with that of acetone can be explained.

If we consider the case of diethyl ketone, the reaction scheme becomes more complex ; but there is again a rather easy reaction channel which transforms $R\cdot$ into $OH\cdot$ and therefore, the same kind of behaviour as that of acetone can be expected.

The antiknock effect of MEK can be interpreted by the same kind of mechanism, the ketone acts as a transfer agent which transforms active chain carriers of the oxidation of hydrocarbon mixtures into rather unreactive $HO_2\cdot$ radicals via a complex reaction scheme.

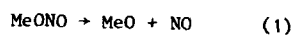
- (¹) J. BARNARD - "Gas phase combustion of organic compounds other than hydrocarbons and aldehydes" in "Comprehensive Chemical Kinetics", C.H. BAMFORD and C.F.H. TIPPER editions, 17, 441 (1977).
- (²) J. BARDWELL and Sir C.N. HINSHELWOOD - Proc. Roy. Soc., A 205, 375 (1951).
- (³) M. AKBAR and J.A. BARNARD - Trans. Faraday Soc., 64, 3035 (1968).
- (⁴) D.E. HOARE and TINGMAN LI - Combust. Flame, 12, 145 (1968).
- (⁵) W.S. AFFLECK and A. FISH - 11th Symp. (Int.) on Combustion, The Combustion Institute, Pittsburgh USA, 1003 (1967).
- (⁶) F. BARONNET, J.C. BROCARD, M. NICLAUSE, A. AHMED, R. VICHNIEVSKY and L. CHARPENET - Communication at the 1st Specialists' Meeting of the Combustion Institute, Université de Bordeaux I, 20th-24th July 1981, Book of preprints p. 425.
- (⁷) A.D. WALSH - 9th Symp. (Int.) on Combustion, The Combustion Institute, Pittsburgh, USA, 104 (1963).
- (⁸) E. LE ROUX, G. SCACCHI and F. BARONNET - Communication at the Gas Kinetics Meeting "Reactive intermediates in gas phase kinetics", Department of Chemistry, University College, Cardiff (Wales), 26th-27th September 1983.
- (⁹) S.W. BENSON - Thermochemical Kinetics, 2nd ed., John Wiley (1976).

UNIMOLECULAR DECOMPOSITION OF METHYL NITRITE

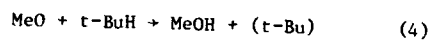
L. Batt and P.H. Stewart

Department of Chemistry, University of Aberdeen, Aberdeen AB9 1FX
Scotland

A study is made of the unimolecular decomposition of methyl nitrite at 200°C and up to 2 atm:



1 Torr of MeONO is decomposed in a bath of isobutane (t-BuH) such that all of the methoxy radicals produced in step (1) are converted to methanol:



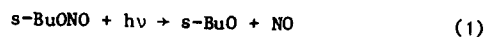
The results are subjected to an RRKM analysis.

UNIMOLECULAR DECOMPOSITION OF THE S-BUTOXY RADICAL

L. BATT AND M. MCKAY

Department of Chemistry, University of Aberdeen, Aberdeen AB9 1FX,
Scotland

S-butoxy radicals have been generated via the near
U-V photolysis of s-butyl nitrite:



The rate constant for the decomposition of the s-butoxy radical is determined as a function of pressure and compared both with RRKM theory and previous results for the decomposition of the t-butoxy radical.

Kinetic studies using a laser photolysis/atomic resonance absorption system. I Rate constants for $I^2P_{3/2}$ and $I^2P_{1/2} + F_2$ at room temperature.

M.R. Berlman and D.P. Whitefield

McDonnell Douglas Research Laboratories, P.O. Box 516, St. Louis, MO. 63166, U.S.A.

Rate constants for the reactions $I^2P_{3/2} + F_2$ and $I^2P_{1/2} + F_2$ will be reported, in time resolved atomic resonance absorption experiments, under pseudo first-order kinetic conditions. Iodine atoms were produced in preset mixtures of alkyl iodide + F_2 . $I^2P_{3/2}$ and $I^2P_{1/2}$ were measured by atomic resonance emission at 183 nm and 206.2 nm. The significance of the results to proposed mechanisms for an IF chemical laser will be discussed.

PYROLYSIS OF N-DECANE / STEAM MIXTURES
IN A HIGH TEMPERATURE MICROPILOT FURNACE

Francis BILLAUD* and Edouard FREUND**

* Département de Chimie-Physique des Réactions, L.A. n° 328 CNRS, INPL-ENSIC, 1, rue Grandville 54042 NANCY Cedex, France

** Département de Physique et Analyse, Institut Français du Pétrole,
1 et 4, avenue de Bois Préau, BP 311, 92506 RUEIL MALMAISON Cedex, France

If the technology of the steam-cracking (pyrolysis in the presence of steam) of light petroleum gases (LPG) is satisfactorily mastered, this is not the case for the steam-cracking of gas-oil, especially the cracking of vacuum gas-oil (VGO). This has prompted fundamental studies to elucidate the a priori very complex mechanisms operating in the case of heavy feeds.

The pyrolysis of n-decane in the presence of steam at temperature around 810°C (1083 K) is a part of a larger project and will be used as a reference for studies of co-reactions n-decane-gas-oil components.

POSSIBLE MECHANISMS FOR HYDROCARBON DECOMPOSITION

The distribution of products issued from the thermal cracking of light alkanes, $C_n H_{2n+2}$, can be interpreted by a RICE-HERZFELD mechanism (1931-1933-1934). In what follows, we shall use the symbolism proposed by GOLDFINGER et al. (1947-1948).

The stoichiometries of decomposition of the alkane μH can be written : $\mu H = \beta H + \alpha$ -olefin.

For higher alkanes, the alkyl radicals do not decompose only by carbon-carbon β scission, they may also isomerise intramolecularly through a transfer which needs a chain of 6 carbon atoms [RICE and KOSSIAKOFF (1943)] or at least a 5-atom chain [GORDON and Mc NESBY (1959)].

A review paper on these problems has been published by DOUE and GUIOCHON (1968).

At 1083 K (810°C), by using the methods and data of BENSON (1976), we have estimated the absolute and relative values of unimolecular isomerisation processes of μH produced by 1.4, 1.5 and 1.6 transition state including hydrogen atoms (elementary steps (5) (6) and (7)) ; if k_{C-C} is the rate constant by C-C decomposition, the rate constants are such as $k_6 > k_5 > k_{CC} > k_7$ in the ratio $115 > 34 > 2 > 1$.

EXPERIMENTAL RESULTS

The apparatus and the analytical procedures have been described previously [see BILLAUD, AJOT and FREUND (1982)].

The main and characteristic products of thermal decomposition obtained for different residence times at 1083 K are H_2 , CH_4 , C_2H_4 , C_3H_6 , 1,3 C_4H_6 , 1- C_4H_8 , 1- C_5H_{10} , Benzene, Toluene, α -olefins ($C_5^+ - C_{10}$), ..., overall gas, naphta and 200⁺. As an example, Figure 1 describes C_2H_4 , C_3H_6 , Benzene and Toluene formation vs residence times.

INTERPRETATION

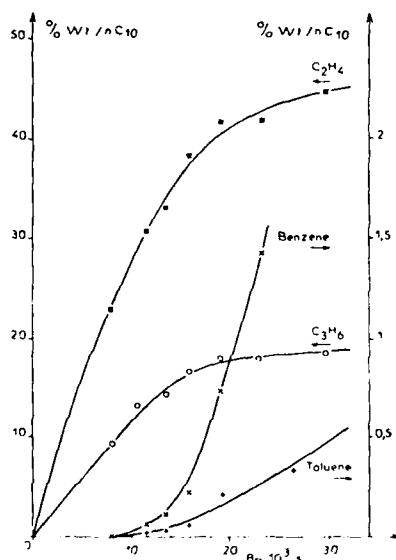
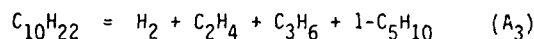
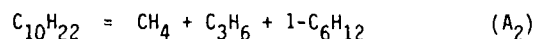
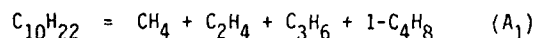


Figure 1 : C_2H_4 , C_3H_6 , Benzene, Toluene formations vs residence times

C_2H_4 and C_3H_6 are primary (non zero initial rate of formation whereas Benzene and Toluene are secondary products (zero initial rate of formation) (cf. figure 1).

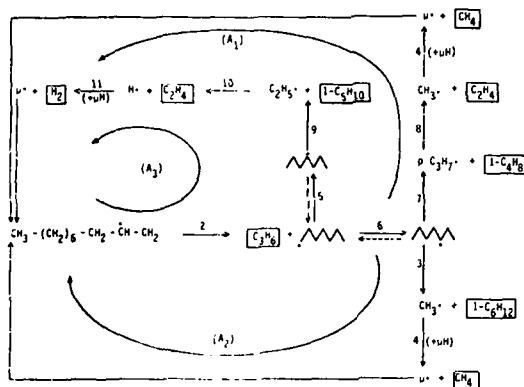
We can show by a classical kinetic scheme that all radicals formed in initiation reactions yield a $C_{10}H_{21}^{\bullet}$ radical.

Let us consider for instance the μ_1 radical (one of the four isomeric forms of μ^{\bullet}) and let us write the three different closed sequences, (A_1) (A_2) and (A_3), which will yield a μ radical (μ_1 or other). With μ_1 , the thermal decomposition of n -decane is described by three primary stoichiometries :



Taking into account the four isomeric forms of the μ^{\bullet} radical the closed sequences lead to a satisfactory description of the thermal decomposition of n -decane by 9 main primary stoichiometries.

The secondary formation of monoaromatics (Benzene and Toluene) can be interpreted either by a DIELS-ALDER mechanism, or direct bimolecular



μ_1 radical transformation

reaction of two radicals formed during primary product pyrolysis or direct cyclisation of an α -olefin.

The abstraction of an hydrogen from α -olefin by a $R\cdot$ radical and the subsequent steps are mainly responsible for the formation of diolefins.

CONCLUSION

Despite the length (ten atoms) of the carbon chain of the hydrocarbon, the description of the main primary products is still rather simple and can be analysed in terms of radical mechanism.

The above distinction between primary and secondary products and the selectivity ratio : light olefins/monoaromatics are very important from a practical point of view ; they clearly point out the possibility of vastly improving the steam cracking process by increasing the selectivity ratio and reducing tar and coke production.

Literature cited

- BILLAUD F. and FREUND E., 1983, Rev. Inst. Fr. Pétrole, 38 (6), 763.
 BENSON S.W., Thermochemical Kinetics, Wiley, New-York, 1976.
 DOUE F. and GUIOCHON G., J. Chimie Phys., 1968, 65, 395.
 FREUND E., 1982, French Patent, Registration number 82/06715.
 GOLDFINGER P., LETORT M. and NICLAUSE M., Volume commémoratif Victor Henri, Contribution à l'étude de la structure moléculaire, p. 283, Desoer, Liège (1947-48).
 GORDON A.S. and M.C. NESBY J.R., J. Chem. Phys., 1959, 31, 853.
 RICE F.O., J. Amer. Chem. Soc., 1931, 53, 1959-1933, 55, 3035.
 RICE F.O. and HERZFELD K.J., J. Amer. Chem. Soc., 1934, 56, 284.
 RICE F.O. and KOSSIAKOFF A., J. Amer. Chem. Soc., 1943, 65, 590.

MODEL STUDIES OF ATOM AND MOLECULE DIFFUSION ON SURFACES^{a)}S.C. PARK AND J.M. BOWMAN

Department of Chemistry, Illinois Institute of Technology, Chicago,
IL 60616, U.S.A.

We report a classical trajectory study of the diffusive dynamics of a rigid rotor N_2 trapped on a rigid but corrugated LiF(001) surface. An analogous study is also made for a fictitious atom with the atomic weight of N_2 . The ensemble-averaged square displacement as well as the velocity autocorrelation functions are computed for a range of kinetic energies, each exhibiting the standard signatures for diffusive behaviour. The "temperature" dependence of the diffusion coefficients determined show Arrhenius behaviour, with an activation energy which can be approximately related to barriers on the three-dimensional potential surface.

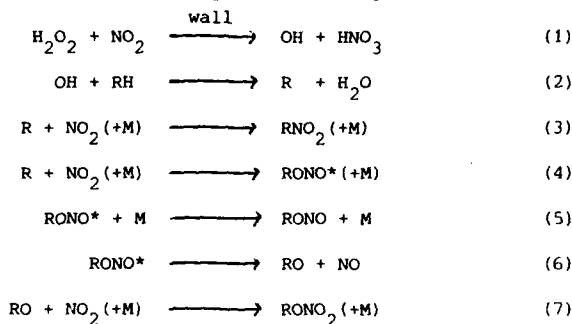
a) Support from the National Science Foundation (CHE-811784) is gratefully acknowledged.

Kinetics and Mechanism of the Formation of Alkyl Nitro-Compounds in Flowing

 $\text{H}_2\text{O}_2 + \text{NO}_2 + \text{N}_2 + \text{O}_2 + \text{Alkane Vapour Systems.}$ by D.L. Baulch, I.M. Campbell and J.M. Chappel.

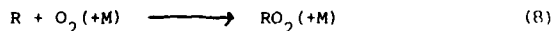
(School of Chemistry, The University, Leeds LS2 9JT).

The effects of oxygen on the product distribution from the surface-initiated reactions in flowing mixtures of H_2O_2 , NO_2 , N_2 and RH, where RH = ethane, propane, n-butane and n-pentane, at 298 K have been studied. In the absence of O_2 , the principal products are the corresponding nitroalkane, alkyl nitrite and alkyl nitrate, formed by the following mechanism.



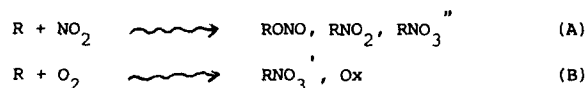
where RONO^* is an internally excited species and reaction (1) occurs on the boron-acid-coated walls of the flow tube.

In the presence of O_2 at >20% the predominant product is the alkyl nitrate and the only other products of significance are the corresponding carbonyl compounds. The general nature of the mechanism in the presence of O_2 seems clear. Under our conditions the OH radical from reaction (1) will react predominantly with RH to generate alkyl radicals, R. Thereafter there is competition between the NO_2 and O_2 for reaction with R, the former leading to nitro alkane, alkyl nitrite and some alkyl nitrate (denoted RNO_3), the latter leading to alkyl peroxy radicals

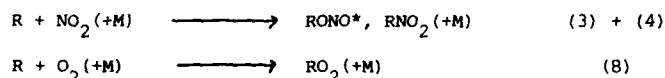


The ultimate products from the RO_2 radicals are the alkyl nitrates

(denoted RNO_3') and carbonyl species (collectively denoted as Ox). Thus as $[\text{O}_2]$ increases the yields of alkyl nitrate and Ox increase at the expense of the nitroalkane, alkyl nitrite and the part of the alkyl nitrate yield resulting from reactions (6) and (7) as a result of the two general competitive routes represented as



The total yields of respective products from these two pathways are determined by the relative rates of the initiating elementary steps:



On this basis we obtain the equation

$$\frac{k_8[\text{O}_2]}{(k_3 + k_4)[\text{NO}_2]} = \frac{[\text{RNO}_3'] + [\text{Ox}]}{[\text{RONO}] + [\text{RNO}_2] + [\text{RNO}_3'']} = \frac{\Sigma P(\text{A})}{\Sigma P(\text{B})}$$

where $\Sigma P(\text{A})$ and $\Sigma P(\text{B})$ represent the total product yields arising via pathways (A) and (B) respectively. Plots of $\Sigma P(\text{A})/\Sigma P(\text{B})$ against $[\text{O}_2]$ at constant $[\text{NO}_2]$ give the rate-constant ratios shown below at total pressures of 40 kPa.

Alkane	$k_8/(k_3 + k_4)$
ethane	0.14 ± 0.01
propane*	0.17 ± 0.01
n-butane*	0.20 ± 0.01
n-pentane*	0.22 ± 0.01

(* 10% in N_2 carrier)

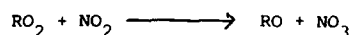
The results can also be used to derive values for the relative reactivities of O_2 and NO_2 at the primary and secondary radical centres of the R species and these are shown in the next table.

The tabulated data show that primary and secondary radical centres have distinctly different relative reactivities to O_2 and NO_2 , O_2 being significantly favoured over NO_2 for reaction at a secondary carbon as compared to a primary

<u>R</u>	$10^2 k_8/(k_3 + k_4)$	
	<u>Primary</u>	<u>Secondary</u>
1-C ₃ H ₇	7.6 ± 0.4	
2-C ₃ H ₇		23 ± 1
1-n-C ₄ H ₉	6.8 ± 0.3	
2-n-C ₄ H ₉		22 ± 1
2+3-n-C ₅ H ₁₁		27 ± 1

carbon. Also, although separate data for the 2- and 3- positions in n-C₅H₁₁ were not derived, the increased average value of $k_8/(k_3 + k_4)$ for the secondary site for n-pentane compared with those for propane and n-butane may suggest that O₂ reaction at the 3-position is even more favoured over NO₂ reaction there than is the case for the 2-position.

In common with other studies^{1,2} we find that the generation of RO₂ radicals in the presence of NO₂ leads predominantly to the formation of alkyl nitrates. It seems extremely probable that the reaction between RO₂ and NO₂ forms ROONO₂ in the initial stages. The most likely homogeneous process for the formation of the alkyl nitrates appears to be the reaction



and hence through the alkoxy radicals as intermediates: in the case of R = CH₃ this was suggested by Cox et al³, but there is little positive evidence for it. The only alternative seems to be the possibility of a heterogeneous process.

1. C.W. Spicer, A. Villa, H.A. Wiebe and J. Heicklen, J. Am. Chem. Soc., 1973, 95, 13.
2. R. Simonaitis and J. Heicklen, J. Phys. Chem., 1974, 78, 2417.
3. R.A. Cox, R.G. Derwent, P.M. Holt, and J.A. Kerr, J. Chem. Soc., Faraday Trans. 1, 1976, 72, 2044.

STUDY OF THE SO_2 INFLUENCE ON SLOW OXIDATION OF HYDROGEN BY A "SEMI-STATIC" METHOD

by J. CHAMBOUX, V. VIOSSAT, F. JORAND, K.A. SAHETCHIAN

Laboratoire de Chimie Générale, Equipe de Recherche Associée au CNRS n°457,
Université P. et M. Curie, 4 Place Jussieu, 75230-PARIS CEDEX-05, FRANCE

In order to study the $\text{H}_2 + \text{SO}_2$ reaction we took an interest in the influence of sulfur dioxide on the hydrogen slow oxidation at 773 K and 400 torr.

As this influence could appear in the first stages of the reaction it is necessary to avoid the thermal disturbances caused by introduction of the reactants in an empty vessel. So we used a "semi-static" procedure (1). The reacting gases flow through the reactor, and at a given moment, two magnetic valves confine the gas inside the reactor. Then the reaction takes place as in a static system and it is monitored by the pressure change.

Different gaseous mixtures were used: $\text{H}_2 + \text{O}_2 / \text{N}_2 + \text{SO}_2$: 80/20, with richness from 1/8 to 2, and SO_2 percent from 0 to 20.

In the absence of SO_2 , curves of the pressure change $\Delta P = f(t)$ are characteristic of hydrogen slow oxidation and can be compared to others obtained in literature.

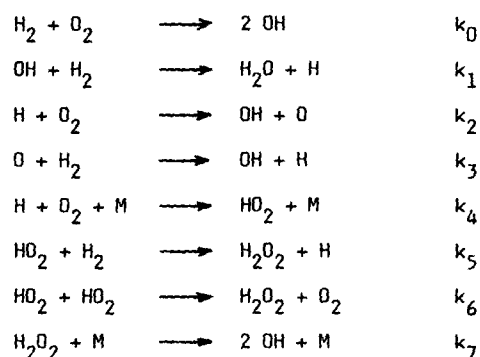
Two SO_2 effects are observed: an accelerating effect in the earliest stages of the reaction, and an inhibitor effect for the latter reaction stages. The acceleration is manifested by a pressure decrease (ΔP) and a rate $d \frac{\Delta P}{dt}$ more important at a given time, while the inhibitor effect is manifested by weaker values of ΔP and $d \frac{\Delta P}{dt}$.

Both effects depend on the mixture richness and the SO_2 concentration. Thus, according to the H_2/O_2 ratio, the maximum rate \dot{V}_m increases or decreases with the addition of SO_2 .

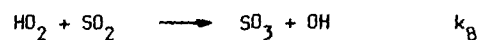
These results lead to propose the reaction $\text{H}_2 + \text{SO}_2 \longrightarrow \text{SO}_3 + \text{H}_2$ in order to explain the accelerating effect.

The kinetic study was performed for SO_2 percents varying from 0 to 5, and at weak conversion ratios ($\Delta P \leq 0,1$ torr), for which an accelerating effect was clearly observed.

In these conditions, the following mechanism can be used for hydrogen slow oxidation:



The addition of the reaction:



leads to a rate acceleration.

From experimental ΔP values (measured on curves) and calculated ΔP values (from the mechanism) the rate constants k_5 and k_6 are estimated:

$$\begin{array}{l}
 k_5 \approx 2 \cdot 10^{-17} \text{ molec.}^{-1} \cdot \text{cm}^3 \cdot \text{s}^{-1} \\
 k_6 \approx 10^{-12} \quad " \quad " \quad "
 \end{array}$$

Further work will be extended to precise these values with the aim to determine the rate constant k_8 .

(1) J. CHAMBOUX, V. VIOSSAT, F. JORAND, K.A. SAHETCHIAN
J. Chim. Phys. (to be published).

ELECTRONIC BRANCHING RATIO BETWEEN $CN(A^2\Pi_1)$ AND $CN(X^2\Sigma^+)$ PRODUCED
FROM THE REACTION $C + N_2O \rightarrow CN + NO$ AT 300K.

M. Costes, C. Naulin and G. Dorthé

Université de Bordeaux I, Laboratoire de Chimie-Physique A,
L.A. 348, 33405 Talence cédex, France

A large variety of chemical and photochemical reactions have been shown to produce CN radicals in low lying electronic states ; $X^2\Sigma^+$ and $A^2\Pi_1$, and even in the $B^2\Sigma^+$ state. The spectroscopic data available concerning the $CN(A-X)$ and $CN(B-X)$ systems makes possible the determination of quantum state distributions in CN from these processes, by analysis of spontaneous emission for A and B states, and by laser induced fluorescence (LIF) for the X state. Recently $CN(A)$ state LIF probing has been proved to be also possible¹ ; radicals are optically pumped from A to B state and the fluorescence is observed on B-X transitions. This new possibility allows now to determine the electronic branching ratio between $CN(A)$ and $CN(X)$ states and is applied to the reaction $C(^3P) + N_2O(X^1\Sigma^+) \rightarrow CN(X^2\Sigma^+, A^2\Pi_1) + NO(X^2\Pi_r)$ produced in bulk conditions at 300 K.

Ground state carbon atoms were generated by mixing bromoform with atomic hydrogen produced by microwave dissociation of hydrogen with helium as carrier gas in a flow system. The CN excitation was

achieved using a Nd-Yag/dye laser system. This system, operated with rhodamine 610 dye, provided the suitable photons to excite (B-A)(0-0) transitions near 600 nm and the (B-X) transitions at $\Delta v = 0$, by frequency mixing of the dye output with the fundamental Yag. Fluorescence was observed on the (B-X) transitions at $\Delta v = 0$ in the case of the (B-A) excitation and at $\Delta v = -1$ in the case of the (B-X) excitation.

Choosing the same fluorescent rotational level in the B state for the two LIF : $v = 0$, $K = 5$, the ratio of populations of the probed levels : $A^2\Pi_{1/2}$, $v' = 0$, $K' = 5$ and $X^2\Sigma^+$, $v'' = 0$, $K'' = 6$, could be deduced as a product of ratios of fluorescence intensities, laser powers, filter transmissions, photomultiplier quantum efficiency, rotational transition probabilities in absorption, and Einstein coefficients in absorption and emission. The only unknown ratio appeared to be the ratio of the following Einstein coefficients $A_{0-1}^{B-X}/A_{0-0}^{B-A}$. It was determined by exciting the level $X^2\Sigma^+$, $v'' = 0$, $K'' = 6$ and analysing the fluorescence with a monochromator. The ratio of populations of the single rotational levels was finally converted in the steady state branching ratio $N_A/(N_A + N_X)$ knowing the relative vibrational and rotational distributions in the A and X states ^{2,3}. It was thus evaluated to be 6.5×10^{-5} in our conditions.

1. C. Conley, J.B. Halpern, J. Wood, C. Vaughn and W.M. Jackson, Chem. Phys. Letters 73 (1980) 224
2. M. Costes, G. Dorthe and M. Destriau, Chem. Phys. Letters 61 (1979) 588
3. M. Costes, G. Dorthe and P. Caubet, J. Chem. Phys. 74 (1981) 6523

NO($B^2\Pi_r$, $A^2\Sigma^+$) CHEMILUMINESCENCE FROM THE REACTION $C + NO_2 \rightarrow$
CO + NO AT 300 K.

G. Dorthé, J. Caille, Ph. Caubet and M. Costes
Université de Bordeaux I, Laboratoire de Chimie-Physique A,
L.A. 348, 33405 Talence cédex, France

Taking a value for the dissociation energy of the NO-O bond :
 $D_0 = 3.12$ eV, the $C + NO_2$ reaction is exoergic by 7.97 eV for
reactants and products in their ground electronic states. Each
electronic state of CO or NO whose energy lies below 7.97 eV has
thus a chance to be produced and among them, four NO radiative
states : $A^2\Sigma^+$, $B^2\Pi_r$, $C^2\Pi_r$ and $D^2\Sigma^+$ whose energies above the ground
state $X^2\Pi_r$ are respectively 5.48, 5.64, 6.49 and 6.60 eV. The
corresponding transitions to the ground state are called respectively
the γ , β , λ and ϵ bands and lie in the ultraviolet (γ : 220-300 nm,
 β : 240-450 nm, λ and ϵ : 190-220 nm).

Atomic carbon was produced by the microwave dissociation of CO
diluted in He in a flow system. The flow speed was 3 m.s^{-1} . NO_2 was
added 25 cm downstream to avoid the reaction of excited atomic carbon.
Pressure conditions were typically 3 Torr for He, 40 mTorr for CO
and 1 mTorr for NO_2 .

In the range 190-500 nm the emission spectrum of the discharge
products 25 cm downstream from the discharge was characterized by two

C_2 "high pressure" bands, at 436.9 and 468.0 nm, attributed to the reaction $C + C_2O \rightarrow C_2 + CO$, C_2O being produced by the consecutive reactions: $C + O + M \rightarrow CO + M$ followed by $C + CO + M \rightarrow C_2O + M$. The addition of NO_2 decreased the C_2 emission and simultaneously arose a strong chemiluminescence of NO β bands and extremely faint γ bands. No λ or ϵ bands could be observed.

The steady state branching ratio between $NO(B^2\Pi_r, v' = 0)$ and $NO(A^2\Sigma^+, v' = 0)$ was found equal to 150 ± 30 . It was deduced a rate production branching ratio for these two vibronic states equal to 10 ± 2 .

From a C_s symmetry correlation diagram the products $NO(B^2\Pi_r) + CO(X^1\Sigma^+)$ are correlated to the ground state reactants $C(^3P) + NO_2(X^2A_1)$ through one $^2A''$ potential energy surface. However this surface crosses the surface connecting $C(^1D) + NO_2(X^2A_1)$ to $NO(A^2\Sigma^+) + CO(X^1\Sigma^+)$ so that a branching must occur between the $NO(B^2\Pi_r)$ and $A^2\Sigma^+$ states. Ground state reactants cannot lead to $NO(C^2\Pi_r)$ or $D^2\Sigma^+$ either directly or by surface crossing. Thus the observation of intense NO β bands and weak γ bands without λ and ϵ bands is consistent with the correlation diagram.

The nascent vibrational temperature on the $NO(B^2\Pi_r)$ state was found to fit a much lower temperature, 2200 K, than the prior statistical one, 7200 K. This indicates a direct character for the pathway leading to $NO(B^2\Pi_r) + CO(X^1\Sigma^+)$.

HIGH TEMPERATURE PYROLYSIS OF 1,3-BUTADIENE

R.J. DENNING and R. FOON

School of Chemistry, University of New South Wales,
Kensington, NSW, 2033, Australia

Recent studies of the pyrolysis of unsaturated hydrocarbons including 1,3-butadiene have been motivated by interest in the mechanism of soot formation(1). The thermal stability of 1,3-butadiene was first investigated over the temperature range 1200-1400K by Skinner and Sokoloski(2) who detected it as a product from the pyrolysis of ethylene. The radical chain mechanism and rate parameters of the individual steps proposed by Benson and Haugen(3) have been applied in original and modified form in computer simulations of the rate of the overall reaction, measured in the present work by time-resolved uv absorption spectroscopy of the reactant.

The kinetics of the pyrolysis of *cis*-1,3-butadiene behind reflected shock waves at temperatures from 1480 to 1560K of 0.2 to 0.6% mixtures in argon were investigated by time-resolved absorption spectroscopy at 240 nm over the first 500 microseconds of the reaction. The shock tube, high pressure xenon lamp, optical and pressure recording instruments were as described previously(4). The ultraviolet spectra have been reported for the two conformations of 1,3-butadiene(5). Isomerisation from *s-trans*- to *s-cis*-1,3-butadiene, the high energy form, occurs rapidly at temperatures behind the incident shock wave. A broad absorption maximum for *cis*-1,3-butadiene around 240 nm was obtained at temperatures around 1400K behind the reflected shock wave. Fig. 1a shows the decay in the *cis*-1,3-butadiene absorption to a non-zero residual absorption which, at higher temperatures (see Figure 1b) rises due to formation of absorbing species from the vinyl acetylene and acetylene initially produced. Numerical integration of the rate equations (Table 1) was computed by Gear's method to match

within 5% the observed cis-1,3-butadiene profile, corrected for the end absorption, at 1560, 1520 and 1490K by adjustment of the rate parameters for reactions 1 and 11, the only reactions to which the computed profiles proved to be sensitive. A value for ΔH_f^0 of the vinyl radical of 279 kJ mol^{-1} has been determined which supports the most recent value of $64 \pm 2 \text{ kcal mol}^{-1}$ obtained by Holmes & Lossing(9).

References

1. Frenklach, M., Taki, S., Durgaprasad, M.B. & Matula, R.A., *Combustion & Flame*, **54**, 81 (1983)
2. Skinner, G.B. & Sokoloski, E.M., *J. Phys. Chem.* **64**, 1028 (1960)
3. Benson, S.W. & Haugen, G.R., *J. Phys. Chem.* **71**, 1735 (1967)
4. Denning, R.J. & Foon, R., *Fourteenth Intl. Symposium on Shock Tubes & Waves*, Sydney eds. B.E. Milton & R.D. Archer
5. Squillacote, M.E., Sheridan, R.S., Chapman, O.L. and Anet, F.A.L., *J. Amer. Chem. Soc.* **101**, 3657 (1979)
6. Westbrook, C.K., Dryer, F.L. & Schug, K.P., *19th Symp. (Intl.) Combustion*, 153 (1982)
7. Payne, W.A. & Stief, L.J., *J. Phys. Chem.* **64**, 1150 (1976)
8. Just, T., Roth, P. & Damm, R., *16th Symp. (Intl.) Combustion*, 961 (1977)
9. Holmes, J.L. & Lossing, F.P., *Intl. J. Mass Spectrometry & Ion Processes*, in press (1984).

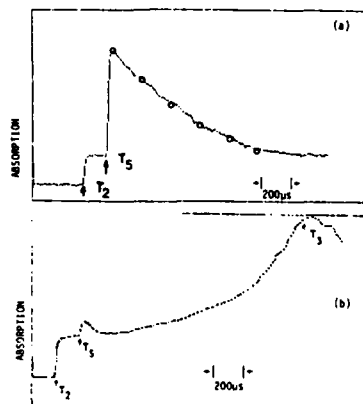


Fig. 1. Absorption-time profile of 1,3-butadiene pyrolysis at 240 nm (a) 0.2% at 1490K, circles are computed points (b) 0.9% at 1700K. T_2 = time at which the incident wave arrives at the window; T_5 and T_3 mark the arrival of the reflected and cooling wave respectively.

TABLE 1. 1,3-BUTADIENE PYROLYSIS MECHANISM AND RATE CONSTANTS^a

Reaction		Forward rate		Ref.	Reverse rate		Ref.
		log A	E _a		log A	E _a	
1. C ₄ H ₆	→ C ₂ H ₃ + C ₂ H ₃	17.34	440	b	12.95	0	b
2. C ₄ H ₆	→ C ₄ H ₄ * + H ₂	12.40	340	c	12.66	208	c
3. C ₄ H ₆	→ 1-C ₄ H ₅ + H	14.30	410	c	12.0	0	c
4. C ₄ H ₆	→ 2-C ₄ H ₅ + H	14.0	400	c	12.0	10.0	c
5. C ₄ H ₆ + H	→ 1-C ₄ H ₅ + H ₂	13.0	19.7	3	12.4	24.7	3
6. C ₄ H ₆ + H	→ 2-C ₄ H ₅ + H ₂	13.0	19.7	3	12.3	80.3	3
7. C ₄ H ₆ + H	→ C ₂ H ₃ + C ₂ H ₄	14.02 ^d	4.2	3	11.7	8.2	3
8. 1-C ₄ H ₅	→ C ₄ H ₄ + H	14.70	191	3	13.0	0	3
9. 2-C ₄ H ₅	→ C ₄ H ₄ + H	14.8	246	3	13.7	0	3
10. 1-C ₄ H ₅	→ C ₂ H ₃ + C ₂ H ₂	13.7	167	3	11.3	0	3
11. C ₂ H ₃	→ C ₂ H ₂ + H	12.26	200	b	12.79	10	7
12. C ₂ H ₃ + H	→ C ₂ H ₂ + H ₂	13.0	0	6	13.1	285	6
13. C ₂ H ₃ + H + M	→ C ₂ H ₄ + M	17.3	0	6	18.80	455	6
14. C ₂ H ₄ + M	→ C ₂ H ₂ + H ₂ + H	17.4	332	8	12.66	153	6 ^a
15. C ₂ H ₄ + M	→ C ₂ H ₃ + H ₂	14.85	60	6 ^a	12.9	30.9	6 ^a

a rate constants are expressed as $k = AT^n \exp(-E_a/RT)$; $n=0$ for all reactions except no. 15 where $n=2$ for both forward and reverse rates and no. 14 where $n=1$ for the reverse rate; units are s, mol, cm³, kJ, K.

b from this work by computer simulation

c estimated from thermochemical data

d this value^b differs from ref. 2 value of 12.8

* vinyl acetylene; 1-C₄H₅ and 2-C₄H₅ are the radicals formed by loss of H from carbon atoms 1 and 2 respectively in C₄H₆.

Multiphoton excitation of CS₂ with a narrow-band, tunable KrF laser

by

C. Fotakis, D. Zevgolis, P. Papagiannacopoulos and T. Efthimiopoulos

Research Center of Crete, Institute of Electronic Structure and Lasers

and

Department of Physics, University of Crete

Iraklion, P.O. Box 470, Crete, GREECE

Molecular multiphoton excitation in the ultraviolet allows the access of highly excited states, which may undergo a variety of competing processes such as ionization, fluorescence, or fragmentation. The latter may lead to the formation of substantial concentrations of excited or ground state free radicals and can provide a basis for interesting kinetic and fragmentation studies. Particularly interesting in this respect is the study of centrosymmetric molecules, mainly due to the differences in the parity selection rules, which operate for single and two-photon excitation.

In the present work we have used the focused output of a frequency narrowed ($\Delta\lambda_{\text{Laser}} = 0.3 \text{ cm}^{-1}$), tunable KrF laser (248 nm) to excite CS₂ molecules and observed the ionization and photofragment fluorescence as a result of multiphoton excitation. The dominant emission features can be assigned to sequences of the CS($A^1\Pi \rightarrow X^1\Sigma_g^+$) transition, as shown in figure 1. Weak emission from the $d^3\Delta$ and $a^3\Pi$ states of CS can also be observed. These results differ markedly from those obtained in previous work by using a broad band KrF laser, which caused laser induced fluorescence from ground state CS, which dominated the emission spectra and obscured the analysis [1]. Thus, it is now possible to determine the vibrational distribution in the CS($A^1\Pi$), which is found to be nearly identical to that obtained by single photon excitation at 123.6 nm [2].

CS_2 is fully transparent at 248 nm. On energetic grounds, at least two photons should be involved in the multiphoton excitation process in order to observe excited CS. This is compatible with the observed quadratic dependence of photofragment fluorescence on laser intensity. A similar dependence has been found for the total ion yield. Possible excitation and fragmentation mechanisms are discussed within the context of known higher Rydberg and autoionizing states of CS_2 .

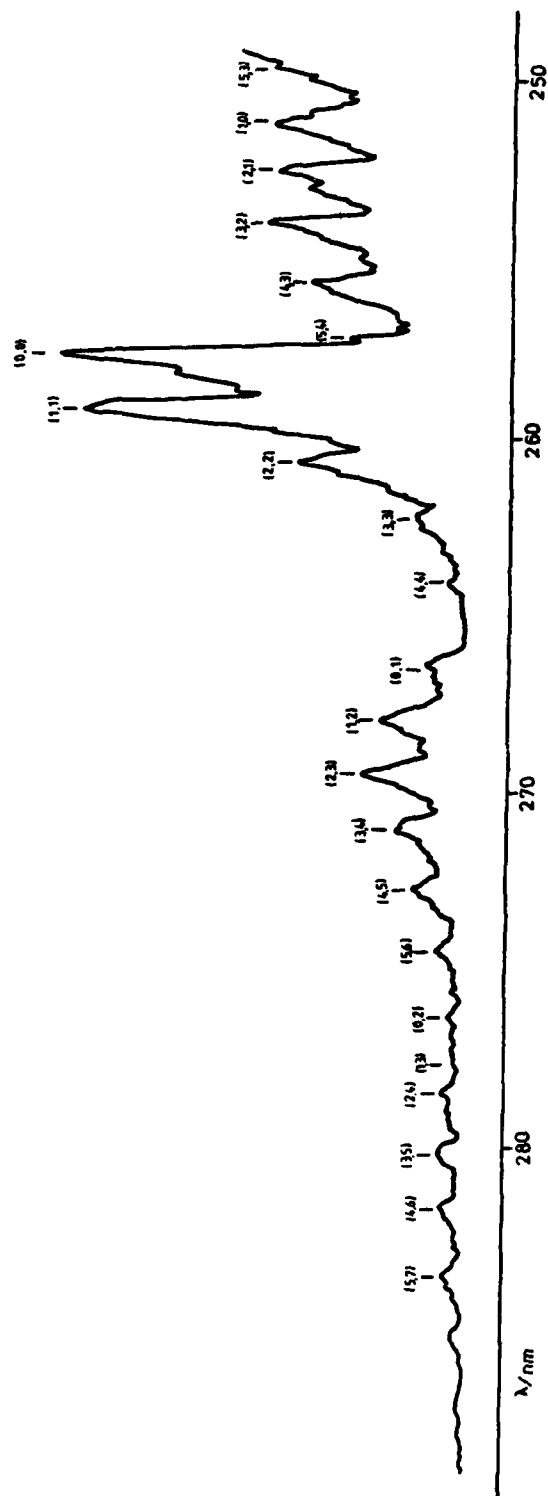
Finally, it is demonstrated that the multiphoton excitation of CS_2 at 248 nm, can provide the basis for kinetic measurements of $\text{CS}(\text{A}^1\Pi)$ in the presence of various reagents, under optically thin conditions and without the difficulties usually associated with photolysis in the vacuum ultraviolet [3]. Rate constants have been measured for the removal of $\text{CS}(\text{A}^1\Pi)$ by reactive and non-reactive species, such as Ar, CO, SF_6 and O_2 .

REFERENCES :

1. M. Martin and R.J. Donovan, J. Photochem., 18 (1982) 245
2. M.N.R. Ashfold, A.M. Quinton and J.P. Simons, J.C.S. Faraday II, 76 (1980) 905
3. M.N.R. Ashfold, A.M. Quinton and J.P. Simons, J.C.S. Faraday II, 76 (1980) 915

Figure 1 : Photofragment fluorescence observed following multiphoton
excitation of CS₂ with a frequency narrowed, tunable KrF laser.

CS(A'' π →X'Z) emission spectrum
p=80 mbar; λ_{exc} =248.5 nm
resolution: 0.04 nm



Mobility of a Platinum Surface During the Heterogeneous
Oxidation of Carbon Monoxide

A.K. Galwey*, J.F. Griffiths and S.M. Hasko

* Department of Chemistry, The Queen's University of Belfast

Department of Physical Chemistry, The University of Leeds

Introduction

In the last 10-15 years there have been many and varied investigations of the oxidation of carbon monoxide at a platinum surface. In most cases attention has been directed to oscillatory events and their interpretation; rarely has the surface itself been studied. The present contribution concerns the stationary-state oxidation of carbon monoxide at the surface of a very fine platinum wire (25 μm dia., 2.5 cm length). Macroscopic restructuring of the wire surface was observed during the course of the work.

Experimental

The catalytic wire was used as a responsive resistance thermometer in such a way as to maintain a virtually constant surface temperature. However, even though a tight coil-spring was used (11 turns, 1 mm dia.) it was not without a temperature gradient at the ends since heat conduction occurred to the more substantial supporting wires. The wire was mounted in a tube (2 cm dia.) at laboratory temperature through which flowed carefully controlled gas compositions ($300 \text{ cm}^3 \text{ min}^{-1}$, generally in the proportions $\text{CO}:\text{O}_2:\text{N}_2 = 1:11:50$).

Different wires were exposed in more than 10 ways to various preliminary or reactive treatments over prescribed intervals. Re-texturing

of the surface is a difficult and slow process, and in some instances treatment involved some hundreds of hours of exposure.

Results

There are two distinct modes of stationary reaction in lean $\text{CO} + \text{O}_2$ mixtures, whose existence depend on surface temperature. The one, at low wire temperatures, is a kinetically controlled reaction; the other is diffusion controlled, and is achieved by a discontinuous transition when the wire temperature is raised. The present results pertain to reaction in the kinetically-controlled regime ($T_w < 500 \text{ K}$). Reaction rates were monitored and kinetic parameters measured. Scanning electron micrographs (magnification 4-30 K) were obtained and changes to the surface documented.

(a) Kinetic measurements. Some of the principal observations may be summarized as follows. Wires, previously unused, showed quite substantial variations in reactivity. This discrepancy was much reduced by preliminary heating to beyond 1200 K in an $\text{N}_2 + \text{O}_2$ flow. The initial reactivity was also marginally diminished by this fore-treatment. Repeated experiments under kinetically-controlled conditions brought about a gradual increase in surface reactivity, although the overall activation energy for reaction remained approximately constant ($185 \pm 15 \text{ kJ mol}^{-1}$). So far no major kinetic distinctions have been revealed between relatively "young" surfaces and those at which very extensive re-texturing has occurred.

(b) Scanning electron microscopy. At the microscopic level the 25 μm wire is not perfectly uniform. The drawn wires show longitudinal striations, often $\sim 1 \mu\text{m}$ in height and width. There may be surface irregularities but there are no sharp-edged features. Annealing causes smoothing of the surface, but leaves grain boundaries. Exposure to non-reactive gases at any temperature up to the annealing point produces no discernable change.

Oxidation of carbon monoxide at the surface always brings about a restructuring comprising the development of crystallographic planes of dense occupancy, probably (111), possibly (100). The strong parallel orientation of the texture is indicative of crystallographic control of the mobility of the surface. The surface is not affected similarly everywhere: global differences may be attributed partly to the temperature gradient; local variations may be attributed to different crystals that make up the surface. The extent of the re-textured surface does not necessarily increase with duration of reaction, but within zone so affected the effect becomes more pronounced. X-ray scattering has revealed that the oxygen content to a depth of several microns is a few percent.

PHOTODISSOCIATION DYNAMICS OF CYANOGEN HALIDES**S. Hay, F. Shokoohi, I. Nadler, H. Reisler, and C. Wittig****Chemistry Department, University of Southern California****Los Angeles, CA 90089-0484**

Photodissociation dynamics of cyanogen halides, following absorption in the spectral region of their longest wavelength absorption known as the \tilde{A} continuum, have been investigated both at 300 K and in a free jet expansion. Vibrational and rotational distributions in $CN(X^2\Sigma^+)$ were measured under collision-free conditions at selected photolysis wavelengths, and Doppler-shift measurements of completely resolved CN states were carried out. Our work demonstrates the effects of the initial quantum state of the parent cyanogen halide molecule on the vibrational and rotational energy distributions in the fragments. This is done by exciting the molecules in the long wavelength region of the \tilde{A} continuum, where absorptions originating from bending vibrations of BrCN and ICN may be favored, and by comparing the resulting CN energy distributions with those obtained at the same wavelength when dissociating expansion cooled molecules. At certain wavelengths, striking differences are found between the spectra obtained at 300 K and with expansion-cooled samples.

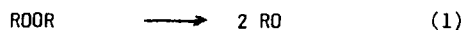
Doppler-shift measurements of **completely resolved** rovibronic levels in CN yield information on the electronic state(s) of iodine associated with particular rotational levels of CN, the symmetry of the electronic transition(s), and state specific effects associated with the potential surfaces involved in the dissociation.

A COMPARATIVE STUDY OF THE IMPORTANCE OF DIFFERENT WALL TREATMENTS ON THE DECOMPOSITION OF A DIALKYL PEROXIDE

by Adolphe HEISS, Renée RIGNY and Krikor A. SAHETCHIAN

Laboratoire de Chimie Générale, Equipe de Recherche Associée au CNRS n°457,
Université P. et M. Curie, 4 Place Jussieu, 75230-PARIS CEDEX-05, FRANCE

The mechanism of the thermal decomposition reaction of a dialkyl peroxide (~ 10 p.p.m.) in oxygen, between 130 and 220°C is the following:



The source of HO_2 radicals is represented by reaction (2).

We have made a comparative study in order to select wall conditions such as neither the peroxide ROOR, nor the radicals formed, RO as well as HO_2 , might be decomposed heterogeneously. Experiments were carried out in a flow system. The evolution of the reaction has been followed by analysing the H_2O_2 formation as produced by the homogeneous decomposition and the occurrence of other peroxides, of ROOH or R-CH(OH)-OOH type, as a consequence of heterogeneous reactions. The organic peroxides and H_2O_2 were detected by thin layer chromatography.

Five treatments on quartz vessels have been used : 1) cleaning with the sulfo-chromic mixture and several rinsings with distilled water; 2) boric acid coating; 3) boric acid coating heated at 380°C; 4) treatment (3) followed by the slow reaction H_2/O_2 ; 5) coating with a teflon solution.

With treatment (4), only H_2O_2 is formed while with the others, peroxides of ROOH type are occurring. The amount of ROOR decomposed does not practically change with treatments (1) to (4).

With treatment (1), the concentration of the ROOH peroxides formed is very large whereas $[\text{H}_2\text{O}_2]$ is very low. With (2) and (3) $[\text{ROOH}]$ decreases whereas $[\text{H}_2\text{O}_2]$ increases. The teflon coating (5) promotes homogeneous and heterogeneous decomposition of ROOR, even at low temperatures (90-100°C).

In conclusion, treatment (4) is by far the best.

A crossed beam study of the collision induced dissociation of CS_2^+

D. M. Hirst, K.R. Jennings, J. A. Laramee and A. K. Shukla

Department of Chemistry, University of Warwick, Coventry, CV4 7AL.

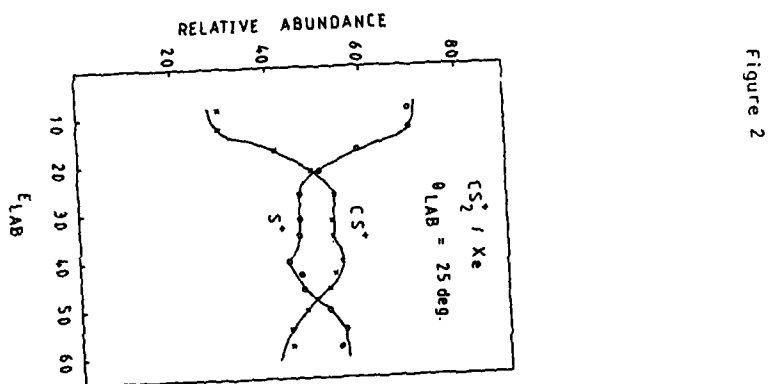
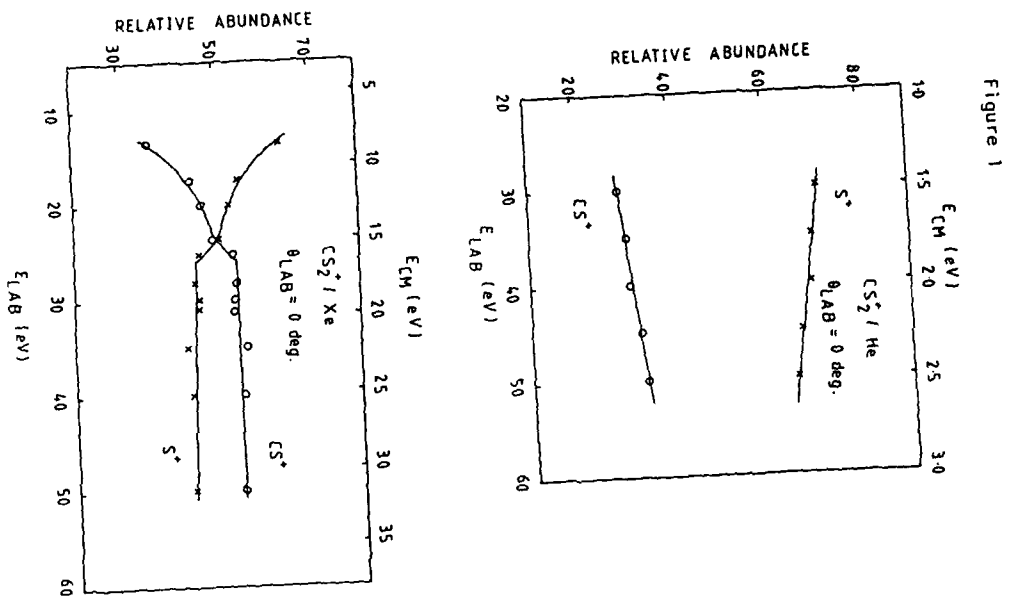
CS_2^+ ions are produced by electron impact mass selected by a quadrupole mass spectrometer and focused by an electrostatic octopole lens to yield a beam with an angular spread of less than 2° (FWHM). The ion beam is intersected at right angles by a beam of target molecules (usually a rare gas) from a differentially pumped effusive capillary array. The detector, which can be rotated about the crossing point, consists of a quadrupole mass spectrometer and a channeltron electron multiplier operated in pulse counting mode.

In a series of experiments at zero scattering angle, the relative abundances of fragment ions CS^+ and S^+ were measured as functions of ion kinetic energy for target gases He, Ar, Kr, Xe. For low centre of mass energies S^+ is the dominant product but as the initial relative energy is increased the $[\text{CS}^+]/[\text{S}^+]$ ratio increases and at the higher energies CS^+ is the major product. Some of these results are shown in figure 1. The formation of S^+ is the least endothermic dissociation channel and these data are interpreted in terms of the vibrational excitation of CS_2^+ increasing with the centre of mass collision energy. This is in contrast with the results at high energies where helium is found to be the most effective rare gas target for promoting collision induced dissociation. Polyatomic targets are found to be less effective than monatomic targets for a given centre of mass energy.

The variation of the ratio of the relative abundances of S^+ and CS^+ with scattering angle, for a given ion kinetic energy, has been measured. For the heavier targets (Ar, Kr, Xe), the $[\text{CS}^+]/[\text{S}^+]$ ratio decreases as the angle increases.

It is assumed that the amount of energy transferred to internal modes increases with increasing scattering angle. The increase in the relative abundance of S^+ with respect to that of CS^+ is interpreted in terms of a second dissociation channel leading to $S^+ + CS$ which is more endothermic than the lowest CS^+ channel. This is supported by measurements of the relative abundances as functions of ion energy taken at an angle of 25° (figure 2) in which S^+ becomes the dominant product at large energies.

In the case of the xenon target, the relative abundances of S^+ and CS^+ have been measured as functions of angle for a range of centre of mass collision energies from 26 to 37 eV. For a given value of the energy E_{CM} , the value of θ_{CM} for which the ratio $[CS^+]/[S^+]$ equalled unity was determined and the product $E_{CM}^{\theta_{CM}}$ was found to be approximately constant over the range of energies considered.



The Reaction of OH Radicals with Butadiyne

by

M. Bartels, P. Heinemann, and K. Hoyermann

Institute of Physical Chemistry

University of Göttingen

Tammannstr. 6, D-3400 Göttingen

W-Germany

The reaction of OH radicals with butadiyne (C_4H_2) has been studied at low temperatures (300 K, <300 K) and low pressures (1 torr, < 2 torr), using an isothermal flow reactor and a Laval nozzle reactor. The OH/OD radicals were produced via the reactions $H/D + NO_2$ and $F + H_2O/D_2O$. Samples were withdrawn continuously by a molecular beam sampling system; the identification of stable and labile species were performed by high resolution mass spectrometry, combined with a chemical modulation technique and synchronous ion counting.

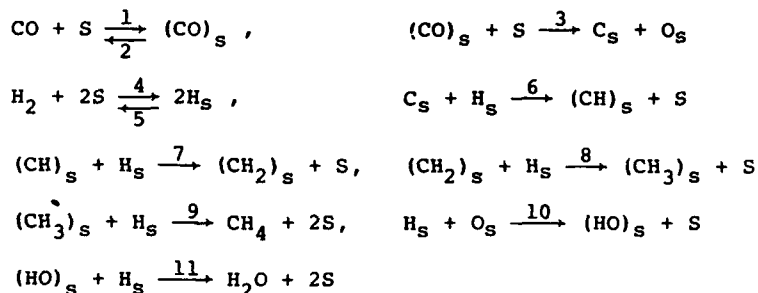
The reaction of $OH + C_4H_2$ is fast; the rate of this reaction has been determined with reference to the reaction $OH + CH_3OH$. The primary products can be explained best by a mechanism of OH addition to the triple bond, forming an adduct $C_4H_2 \cdot OH$, undergoing dissociation/isomerization. The adduct was observed at higher pressures; the contribution of the stabilization route to the total reaction can only be estimated, for the reason of the absence of an absolute calibration of the C_4H_2 OH concentration.

Study of a Mechanism for the Fischer-Tropsch Synthesis

Yean-Jang Lee, Jenn-Tai Hwang, and Kuei-Jung Chao
 Department of Chemistry, National Tsing Hua University
 Hsinchu, Taiwan 300, Republic of China

The process of polymerization and hydrogenation of CO to give hydrocarbons and oxygenated products, the Fischer-Tropsch synthesis, has recently attracted considerable research interest because of (1) the politically unstable petroleum supplies, and (2) the potential of the process in producing chemical feedstocks or motor fuels without the production of environmentally harmful compounds. Although the synthesis has been studied for more than 50 years, no understanding of its mechanism exists that is sufficient to predict products under various conditions or to unify the observations in a detailed way. The present work proposed a scheme for tackling this problem, or problems of a similar nature.

A simplified 11-step mechanism leading from CO and H₂ to CH₄ was utilized for illustrative purpose:



The rate constant of each elementary step was either measured experimentally or estimated theoretically. For initial theoretical estimation, (crude) semi-empirical theories like the modified extended Hückel theory¹ (MEHT) could be employed. The activation barrier of a reaction step was calculated and the pre-exponential frequency factor was identified with the average collision number between adsorbed species. Note that initially we only needed a rough order-of-magnitude estimation. The mechanism was then subjected to computer simulation and sensitivity study.² Kinetic importance of each elementary step was determined, reaction pathways of chemical species were elucidated,

and functional dependence of chemical species upon rate constants was unravelled. These important kinetic details were conveyed to experimentalists such that new experiments could be designed or a "better" mechanism could be set up. Kinetically important rate constants were then measured or calculated more carefully, and the refined mechanism was returned for further computer simulation and sensitivity study. This whole procedure was iterated until finally a satisfactory mechanism was built.

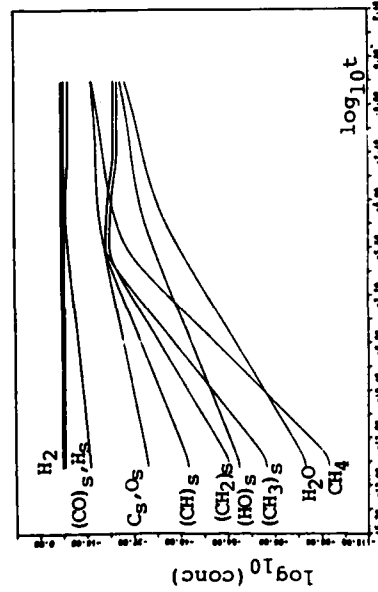
In this work, we used MEHT¹ to estimate the activation barrier of a reaction step with unknown rate constant. The newly developed

reaction step no.	6	7	8	9	10	11
activation barrier (kcal/mole)	13	13	9	33	58	36

Pt(111) surface was modeled by a 4-atom cluster.

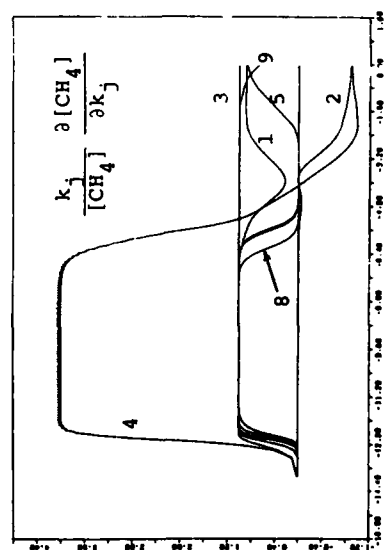
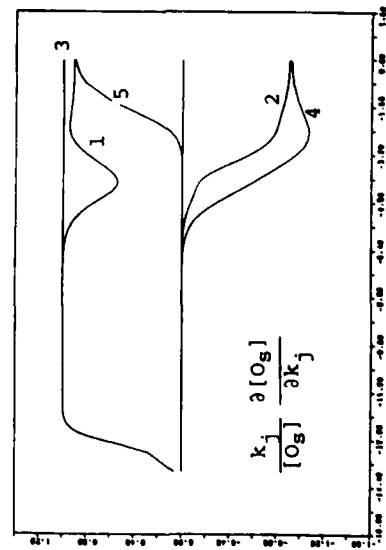
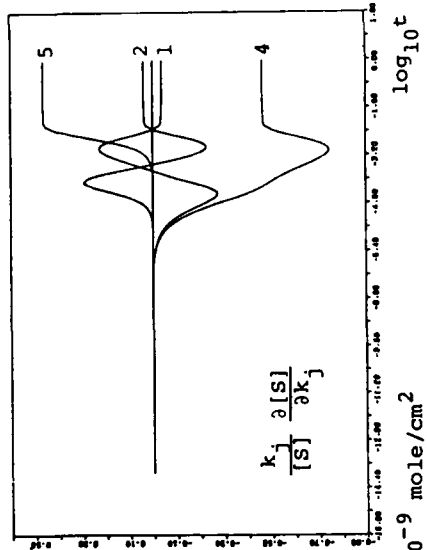
Polynomial Approximation Method² (PAM) was then applied to the 11-step mechanism to extract dynamical information. It was found, for example, that the most influential step for both H₂O and CH₄ was the dissociative adsorption of H₂, and that to increase the yield of CH₄ the ratio [H₂]:[CO] should be decreased.

1. A. B. Anderson, J. Chem. Phys., 62, 1187 (1975).
2. J.-T. Hwang, Int. J. Chem. Kinet., 15, 959 (1983).



$[\text{CO}]_0 = 4.26 \times 10^{-9}$ mole/c.c., $[\text{S}]_0 = 1.74 \times 10^{-9}$ mole/cm²

$[\text{H}_2]_0 = 1.70 \times 10^{-8}$ mole/c.c., temperature = 573°K



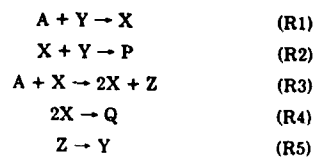
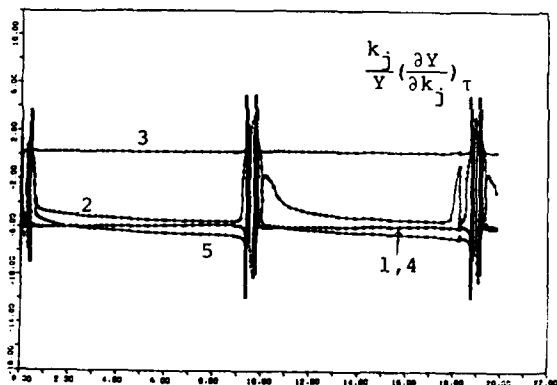
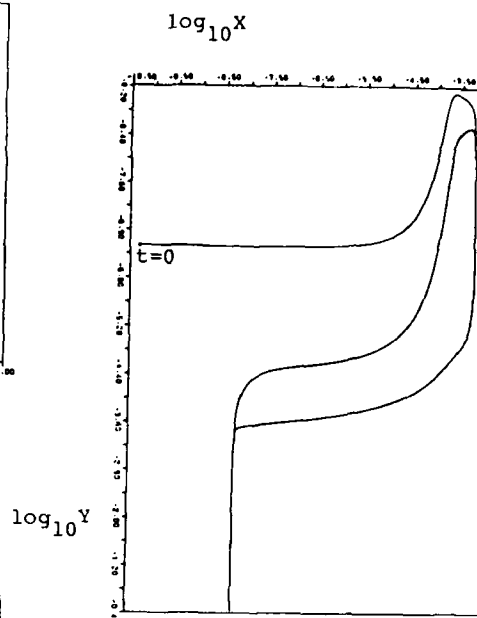
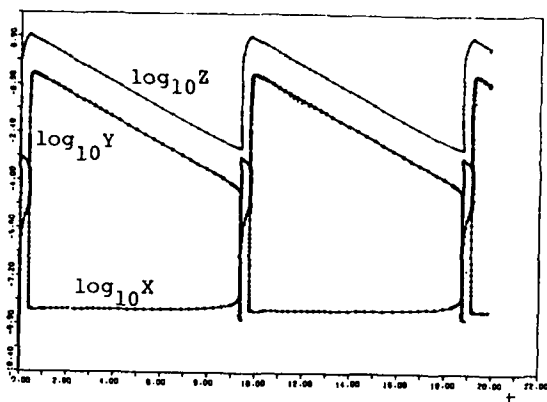
Computational Sensitivity Study of Oscillating Chemical Reaction
Systems — The Overall Temporal Sensitivity Behavior of the
Oregonator

Jenn-Tai Hwang

Department of Chemistry
National Tsing Hua University
Hsinchu, Taiwan 300
Republic of China

Recently some interest has been shown in studying oscillating chemical reaction systems with sensitivity analysis.^{1,2} A careful application of sensitivity analysis can yield information concerning kinetic importance of the elementary steps in determining characteristic features of the oscillation. In this work we applied the newly developed Polynomial Approximation Method³ (PAM) to the Oregonator and obtained the entire temporal behavior of the sensitivity coefficients (time span: ca. 3 oscillations in species concentrations). In view of the complexity of the system behavior, every two steps employed by the ODE solver, GEAR, in integrating the coupled rate equations of the Oregonator (relative error tolerance = 5×10^{-3}) was counted for simplicity as a subinterval. On the average, the PAM took ca. 2 sec CP execution time for each sensitivity profile. This should be compared with the computation time of 10 CP sec required by GEAR in solving the Oregonator.

Dynamical informations were readily extracted from the sensitivity profiles. For example, it was observed that initially the autocatalytic nature of R3 produced X and Z, and destructed Y explosively. This action was not retarded because [Y] started at a low value. As R4 and R5 gained their influence (due to the accumulation of X and Z), R3 started to help the production of Y via the sequence R3→R5. Y was therefore regenerated. This regeneration was kept slow because of R2. X maintained a (large) steady-state quantity through R3 and R4 ($[X] = \text{function of } k_3/k_4$) and steadily produced Z through R3. As Y slowly increased, R2 slowly became influential. This decreased X. The importance of R2 then dropped accordingly and R5 generated Y relatively unretarded, etc.



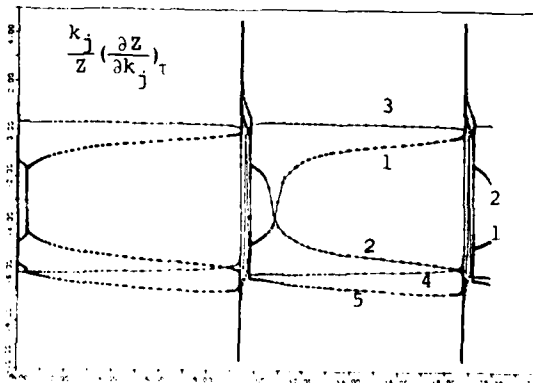
$$\begin{array}{ll}
 k_1 = 1.34 & k_4 = 4.00 \times 10^3 \\
 k_2 = 1.60 \times 10^3 & k_5 = 1.00 \\
 k_3 = 8.00 \times 10^3 &
 \end{array}$$

$$\begin{array}{ll}
 \text{Initial Conditions} & \\
 [A]_0 = 6.00 & [Y]_0 = 3.00 \times 10^{-3} \\
 [X]_0 = 5.025 \times 10^{-11} & [Z]_0 = 2.41 \times 10^{-4}
 \end{array}$$

Time and concentrations in arbitrary units.

In the lower two diagrams, normalized modified sensitivity coefficient s is assigned a value

$$\begin{cases}
 -3, & \text{if } |s| \cdot 10^{-3} \\
 \log_{10} s, & \text{if } s \cdot 10^{-3} \\
 -6 + \log_{10} |s|, & \text{if } s < -10^{-3}
 \end{cases}$$



After (not before) system had reached limit cycle, it was observed that modified sensitivity coefficients²

$$\left(\frac{\partial c}{\partial k_j}\right)_\tau = \left(\frac{\partial c}{\partial k_j}\right) + \frac{t}{\tau} \left(\frac{\partial \tau}{\partial k_j}\right) \left(\frac{\partial c}{\partial t}\right),$$

where τ = period of the oscillation (≈ 9.36), must be used. This was necessary for a periodic system because only modified sensitivity coefficient could exhibit the correct effects, by eliminating secular terms, that each elementary step had upon the system behavior. For example, using "raw" sensitivity coefficients, an erroneous constructive effect of R2 upon Y would be inferred during most of the time span. Modified sensitivity coefficients at the time points where the corresponding species concentration attained extrema gave information concerning the shape of the limit cycle. This was understandable because

$$c(t) = \sum_n \left(a_n \cos \frac{2n\pi t}{\tau} + b_n \sin \frac{2n\pi t}{\tau} \right)$$

implied

$$\left(\frac{\partial c}{\partial k}\right)_\tau = \sum_n \left[\left(\frac{\partial a_n}{\partial k}\right) \cos \frac{2n\pi t}{\tau} + \left(\frac{\partial b_n}{\partial k}\right) \sin \frac{2n\pi t}{\tau} \right].$$

Sensitivity data indicated that R5 and then R3 were the most influential. Effects of elementary steps on the induction period could also be read directly from the (raw) sensitivity profiles. For the induction period, R3 appeared to be the most important.

We have developed a generalized PAM⁴ for sensitivity study of non-uniform reaction systems. The equations of the generalized PAM for kinetics-diffusion problems were (similar in form to those of PAM³)

$$A \underline{z} = \underline{g},$$

where \underline{z} = vector of sensitivity coefficients at $L_a \times L_b$ collocation points (x_a, t_b) (L_a, L_b : degree of interpolation polynomials), and where A and \underline{g} , both independent of \underline{z} , contained the input information (i.e., initial and boundary conditions, diffusion constants of chemical species, kinetic mechanism of the reaction system, etc.). Sensitivity study of the trigger wave phenomenon (by coupling the Oregonator to diffusion) will be reported in a future publication.

1. D. Edelson and V. M. Thomas, J. Phys. Chem., **85**, 1555 (1981).
2. R. Larter, J. Phys. Chem., **87**, 3114 (1983).
3. J.-T. Hwang, Int. J. Chem. Kinet., **15**, 959 (1983).
4. J.-T. Hwang, "Sensitivity Analysis of Non-uniform Chemical Reaction Systems. Method of Polynomial Approximation", to be submitted.

KINETIC MODELING OF HIGH TEMPERATURE, HIGH PRESSURE
HYDROCARBON OXIDATION IN A WELL-STIRRED REACTOR

J.C. BOETTNER, M. CATHONNET, P. DAGAUT, F. GAILLARD,
H. JAMES, J.P. ROUAN

C.N.R.S., Centre de Recherches sur la Chimie de la Combustion
et des Hautes Températures, 45045 Orléans-Cedex, France.

The increasing use of numerical simulation methods to model combustion phenomena requires the development of accurate kinetic schemes, valid over a wide range of experimental parameters. Recent attempts have been carried out to improve detailed mechanisms of low molecular weight hydrocarbon oxidation (1, 2, 3, 4, 5). However, very few studies have been achieved on high pressure gas phase reaction kinetics. In this respect, our Laboratory has conducted since a few years a research on high temperature and high pressure oxidation of light hydrocarbons; among them, propane is under study, together with the main intermediate of alkane combustion: ethylene.

Previous data have been obtained on both fuel oxidations (6, 7, 8), proceeding in a tubular quartz reactor, under laminar flow conditions, for temperatures up to 1200 K, pressures up to 10 atmospheres and equivalence ratios between 0,25 and 4. Provided that the kinetic measurements were limited to a zone of moderate temperature gradient, this reactor could be approximated as a plug flow reactor. Therefore, a detailed kinetic scheme could be set up for these reactions only for low conversions. In fact, it is very difficult to realize ideal plug flow, except when radial diffusion is important. Moreover, the radial heat transfer arising from reaction exothermicity, when conversion becomes important (carbon monoxide consumption), is a limiting factor.

As a consequence, the investigation of high conversion oxidation of propane and ethylene was performed by means of a continuous flow stirred tank reactor (9). The reactor, designed and built in C.R.C.C.H.T., is a quartz sphere. It is 4 cm in diameter and includes four injection holes (0,5 mm in diameter) directed as to ensure an optimal mixing of the reactants in the whole volume of the sphere (fig. 1).

The reactor is located inside a pressure resistant jacket and can be operated up to 10 atmospheres. Reaction temperature is measured by means

of a thermocouple chromel-alumel and molecular species are sampled through a quartz probe. In order to test its homogeneity, thermocouple and sampling may be shifted along a diameter of the sphere, and it can be shown that, under working conditions, the reactor is well-mixed between 0,02 s and a few seconds.

Furthermore, adequate preheating of input flow and diluting the reactants allow to obtain a negligible temperature gradient in the reactor. Thus, in our experimental conditions, this reactor is very close to a perfect mixer and is very suitable for kinetic studies.

Experiments are performed between 1033 and 1150 K and for pressures up to 10 atmospheres. Equivalence ratios are varied between 0,5 and 4 for ethylene and between 0,3 and 1 for propane.

Concentrations of main molecular species: propane, ethylene, carbon monoxide, carbon dioxide, methane and hydrogen are measured by gas phase chromatography. Small amounts of acetylene, acetaldehyde, ethanol and propene are also detected.

Therefore, concentration profiles are established as a function of the residence times for a wide variety of experimental conditions. As shown in figures 2 and 3, the well-stirred reactor allows investigation of the reaction over a very large extent of conversion. Therefore, it can supply more complete kinetic data than the tubular reactor technique which, in similar experimental conditions (7, 8), could not be previously applied to fuel consumption exceeding 60% of its initial concentration.

A numerical model incorporating detailed chemical kinetics is used for the interpretation of the experiments; thus, comparison between experimental and computed profiles allows to improve the detailed mechanism of ethylene and propane oxidation and to validate it until high completion of the reaction.

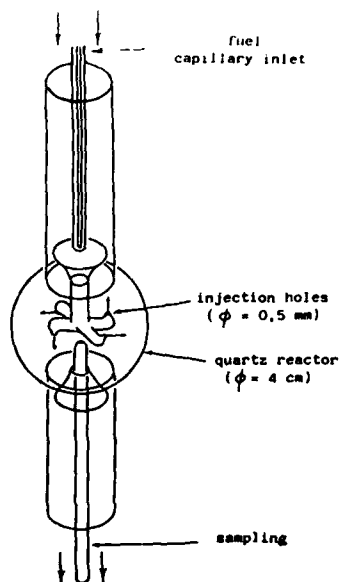


Fig. 1
The well-stirred reactor

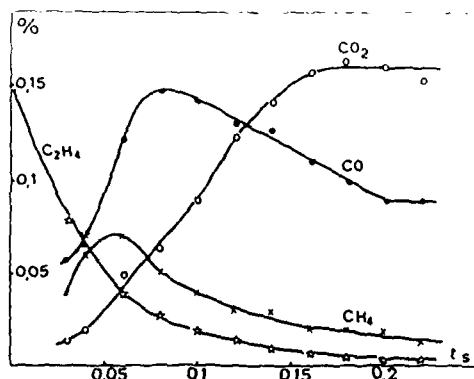


Fig. 2

Concentration profiles
of main molecular species
in C_2H_4 oxidation

$T = 1033 \text{ K}$
 $P = 1 \text{ atm}$
Equivalence ratio = 0,4

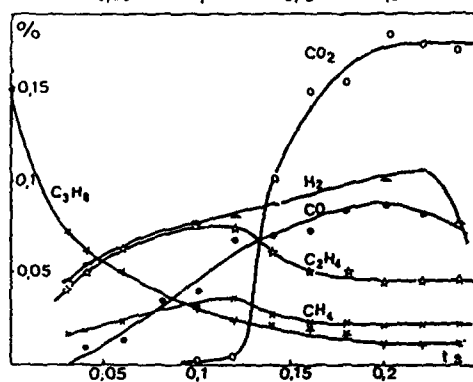


Fig. 3

Concentration profiles
of main molecular species
in C_3H_8 oxidation

$T = 1150 \text{ K}$
 $P = 1 \text{ atm}$
Equivalence ratio = 1

REFERENCES

- (1) C. K. WESTBROOK, F.L. DRYER, K.P. SHUG: 19th Symp. (International) on Combustion, 1983 p. 153.
- (2) C.K. WESTBROOK, W.J. PITZ: Private communication
- (3) A. MILLER, R.E. MITCHELL, M.D. SMOOKE, R.J. KEE: 19th Symp. (International) on Combustion, 1983, p. 181.
- (4) S.M. HWANG, W.C. GARDINER, J. WARNATZ: 9th Intern. Coll. Dyn. Gas, Explosions and Reactive Systems, Poitiers, juil. 1983.
- (5) J. WARNATZ: Comb. Sci. and Technology, 1983, vol. 34, p. 177.
- (6) M. CATHONNET, J.C. BOETTNER, H. JAMES: 18th Symp. (International) on Combustion, 1981, p. 903.
- (7) M. CATHONNET, F. GAILLARD, J.C. BOETTNER, H. JAMES: "Propulsion and Energetics Panel" 62^d Symposium, AGARD, Turquie, oct. 1983.
- (8) M. CATHONNET, F. GAILLARD, J.C. BOETTNER, P. CAMBRAY, D. KARNED, J.C. BELLET: 20th Symp. (International) on Combustion, to be published.
- (9) R. DAVID, D. MATRAS: Can. J. Chem. Eng. Science, 53, 1975, p. 297.

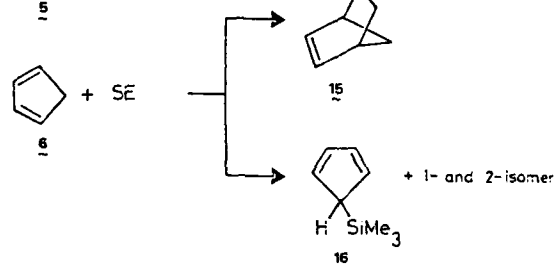
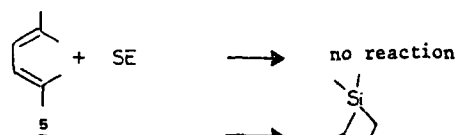
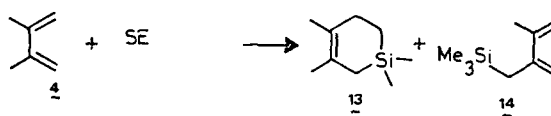
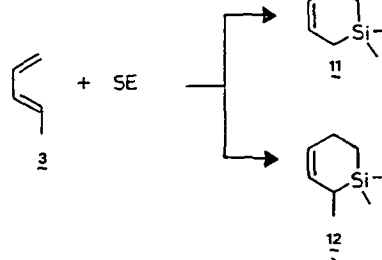
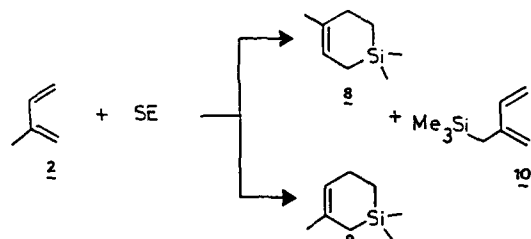
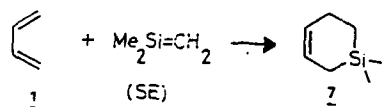
Kinetics of the Addition Reactions of
 $\text{Me}_2\text{Si}=\text{CH}_2$ with Conjugated Dienes

P. John, B.G. Gowenlock and P. Groome,
Department of Chemistry, Heriot-Watt University,
Riccarton, Currie, Edinburgh EH14 4AS, UK.

Abstract

The kinetics of the addition of 1,1-dimethyl-1-silaethylene, $\text{Me}_2\text{Si}=\text{CH}_2$, with butadiene (1), isoprene (2), 1,3-pentadiene (3), 2,3-dimethyl-1,3-butadiene (4), 2,5-dimethyl-2,4-hexadiene (5) and cyclopentadiene (6) has been studied in the gas phase. The named reactions (1) - (6) were investigated in the temperature range 670 - 740K using a conventional static system and the pyrolysis of 1,1-dimethylsilacyclobutane, DMSCB, as the precursor to $\text{Me}_2\text{Si}=\text{CH}_2$.

For the reaction with butadiene, the expected [2 + 4] cycloaddition product, 1,1-dimethylsilacyclohex-3-ene, was formed in addition to C_2H_4 and 1,1,3,3-tetramethyl-1,3-disilacyclobutane. The latter products arise from the pyrolysis of DMSCB in the absence of the conjugated diene. In contrast, the reaction of $\text{Me}_2\text{Si}=\text{CH}_2$ with the dienes (2) - (6) yielded the corresponding isomeric [2 + 4] cycloaddition products plus the trimethylsilyl derivatives listed below:



In the case of (5) no products other than C_2H_4 or 1,1,3,3-tetramethyl-1,3-disilacyclobutane were detected under the conditions of the experiment. The rates of formation of the products obeyed the expression:

$$\frac{R_a^0}{R_d^0} = \frac{k_a}{k_d} [\text{diene}]_0$$

where R_a^0 and R_d^0 are the initial rates of formation of product and 1,1,3,3-tetramethyl-1,3-disilacyclobutane respectively, k_a , k_d are the rate constants for the addition of $Me_2Si=CH_2$ to the conjugated diene and self-dimerisation respectively. $[\text{diene}]_0$ is the initial diene concentration. Arrhenius parameters for the individual reactions will be reported. The relative rate constants at 723K with respect to cyclodimerisation of $Me_2Si=CH_2$ are given below.

Diene	Product	k_a/k_d ($l^2 mol^{-1} s^{-1}$)	Relative Rate
butadiene	(7)	8.91 ± 0.3	1
isoprene	(8)+(9)	10.2 ± 0.4	1.14
	(10)	1.6 ± 0.2	0.18
1,3-pentadiene	(11)	5.0 ± 0.2	0.60
	(12)	0.19 ± 0.01	0.02
2,3-dimethyl-1,3-butadiene	(13)	2.1 ± 0.3	0.23
	(14)	1.3 ± 0.2	0.15
cyclopentadiene	(15)	3.7 ± 0.6	0.41
	(16)	1.2 ± 0.3	0.13

VIBRATIONAL RELAXATION OF XeX(B) (X = Br, I, Cl) BY Ar

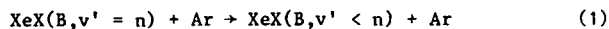
Agúst Kvaran and Inga Dóra Sigurðardóttir

Raunvísindastofnun Háskólans, Science Institute, University of Iceland,
Dunhaga 3, 107 Reykjavik, Iceland, and

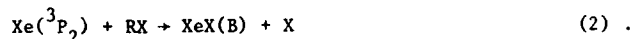
J.P. Simons

Chemistry Department, The University, Nottingham NG7 2RD, United Kingdom

XeX; X = Br, I, Cl chemiluminescence spectra excited in the reaction of Xe(³P₂) with RX (RBr = Br₂, CH₂Br₂, HBr, I₂ and Cl₂) were recorded in a flowing afterglow apparatus using Ar buffer gas at pressures in the range 0.5 - 5 torr. Vibrational distributions in the B(1/2) states were derived from the spectra, using an inversion technique [1]. We describe a method of estimating the rate of vibrational relaxation of XeX(B) by Ar as a function of v'.



from the population distributions determined after the formation reactions



The analysis assumes a knowledge of the Einstein coefficients A_v, for



Relative coefficients A_v/A_{v'=0}, calculated via uniform WKB wavefunctions using corrected ab initio potential curves and transition moment functions [2,3] were set on an absolute basis by reference to A_{v'=0}-values. Average rate constants obtained for reactions (1) increase monotonically with v'.

Rate constants for XeBr rise from 0.1 x 10⁻¹⁰ cm³ molecule⁻¹ s⁻¹ at v' < 10 to 10 x 10⁻¹⁰ cm³ molecule⁻¹ s⁻¹ at v' = 150. XeBr spectra

excited in the reaction of $\text{Xe}(^3\text{P}_2)$ with CBr_4 recorded by D.W. Setser et al. [2] were also analysed for comparison, to yield analogous results for $25 < v' < 110$. The unrelaxed vibrational population distributions in the Xe^*/Br_2 and Xe^*/I_2 systems differ significantly from those determined previously [2]. The vibrational relaxation data for XeCl(B) are compared with results obtained elsewhere [4].

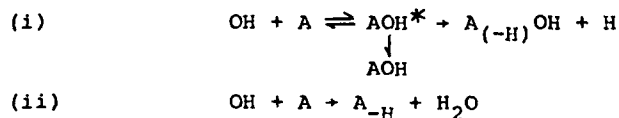
- [1] Keith Johnson, Agust Kvaran and John P. Simons, *Molec. Phys.*, 1983, 50, 981.
- [2] K. Tamagake, D.W. Setser and J.H. Kolts, *J. Chem. Phys.*, 1981, 74, 4286.
- [3] P.J. Hay and T.H. Dunning, jr., *J. Chem. Phys.*, 1978, 69, 2209.
- [4] T.D. Dreiling and D.W. Setser, *J. Chem. Phys.*, 1981, 75, 4360.

KINETICS OF THE REACTIONS OF OH RADICALS
WITH BENZENE, NAPHTHALENE, AND PHENANTHRENE
BETWEEN 400 AND 1000 K

K. Lorenz and R. Zellner

Institut für Physikalische Chemie
Universität Göttingen, FRG

Aromatic hydrocarbons (A) react with OH radicals by two different routes: (i) addition - followed by stabilization or exchange - and (ii) abstraction, viz:

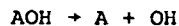


The relative yield of these channels depends strongly on temperature. Whereas benzene and its substitutes have been studied extensively [1], essentially no information is yet available about the corresponding behaviour of polycyclic aromatics (PCAs). The kinetic of these compounds, however, is of substantial relevance to their oxidation in atmospheric and combustion environments. Moreover, it is of fundamental kinetic interest to deduce, whether the kinetic behaviour of PCAs is analogous to the one of its simplest representative (benzene) or, alternatively, how it is modified.

Our studies were performed in an all-quartz reaction system, capable of temperatures up to 1100 K. OH radicals are generated by excimer laser photolysis (at 193 nm) of either HNO_3 or H_2O (at $T \geq 600$ K). Their decay is monitored by A-X resonance fluorescence excited normally by a conventional microwave discharge lamp. Considerable improvement in signal-to-noise ratio was however obtained by the use, in some experiments, of our frequency doubled cw-ring-dye laser system.

As an extension of our previous studies on (1) OH + benzene [1], which was limited to below 520 K, we have first determined k_1 up to 950 K. The results are essentially identical to those reported by Tully et al. [2], i.e. confirming the dominance of the abstraction channel (ii) at temperatures above 500 K.

For the reaction (2), OH + naphthalene, the same qualitative behaviour of $k(T)$ as for OH + benzene is found. However, the addition reaction (dominant at $T < 410$ K) is more than an order of magnitude faster and has a negative activation energy, $k_2(T < 410 \text{ K}) = 2.2 \times 10^{12} \exp(440 \text{ K}/T) \text{ cm}^3/\text{mol}\cdot\text{s}$. Moreover, the transition to dominant abstraction (ii) occurs at higher temperatures, $T \sim 450$ K, as opposed to $T \sim 375$ K for OH + benzene. In terms of the thermal dissociation of the adducts, i.e.



this suggests a larger stability for naphthalene - OH ($E_{\text{N-OH}} = 95 \pm 6 \text{ kJ/mol}$, $E_{\text{B-OH}} = 79 \pm 6 \text{ kJ/mol}$).

A further increase in adduct stability, however, is not observed for (3) OH + phenanthrene. Its kinetic behaviour is almost identical to that of OH + naphthalene. Therefore, it appears that with naphthalene a limiting case is established and that the kinetics of still larger PCAs can be reasonably well predicted from these measurements.

[1] K. Lorenz, R. Zellner, Ber. Bunsenges. phys. Chem. 87, 629 (1983) and references therein.

[2] F.P. Tully, A.R. Ravishankara, R.L. Thompson, J.M. Nicovich, R.C. Shah, N.M. Kreutter, P.H. Wine, J. Phys. Chem. 85, 2262 (1981)

OSCILLATORY CONTINUUM EMISSION FROM I₂ AND Br₂

M. MacDonald, K.P. Lawley, J.P.T. Wilkinson and R.J. Donovan

Department of Chemistry, University of Edinburgh,

West Mains Road, Edinburgh EH9 3JJ

M.C. Gower

SERC Rutherford Appleton Laboratory,

Chilton, Didcot OX11 0QX

The ion-pair states of the halogens ($E \approx 50,000 \text{ cm}^{-1}$) exhibit a number of interesting chemical and physical properties. Chemically they are very aggressive, reacting readily with hydrocarbons^(1,2) and attacking even perfluorinated hydrocarbons⁽³⁾. It has also been shown that they can react with noble gas atoms to yield electronically excited noble gas halide molecules⁽⁴⁾.

The ion-pair states of the halogens are also interesting spectroscopically as their main fluorescence systems are generally structured (oscillatory) continua⁽⁵⁻¹⁰⁾.

We will present new data on oscillatory continuum emission from I₂, excited by means of a line-narrowed ArF laser (Figure 1). These spectroscopic data are then used to derive the interatomic potential for the lower electronic state. The procedure for carrying out this inversion will be discussed.

The radiative life-time for the D(0_u^+) state of I₂ has also been measured using synchrotron radiation in a pulsed (single bunch) mode, together with single photon counting techniques.

We will also present new data on oscillatory continuum emission from Br_2 excited at 157 nm using an F_2 laser. These spectra are more complex as overlapping features from the three possible isotopic pairs obscure some of the oscillatory structure. The observed spectra will be compared with computer simulated spectra derived by the same methods as those used for $\text{I}_2^{(9)}$.

References

1. L.C. Glasgow and J.E. Willard, J.Phys.Chem., 77, 1585 (1973).
2. R.J. Donovan, B.V. O'Grady, L. Lain and C. Fotakis, J.Chem.Phys., 78, 3727 (1983).
3. Zhang Yun-Wu, W. Fuss and K.L. Kompa, J.Photochem., 23, 311 (1983).
4. J.P.T. Wilkinson, M. MacDonald and R.J. Donovan, Chem.Phys.Letters, 101, 284 (1983).
5. R.S. Mulliken, J.Chem.Phys., 55, 309 (1971).
6. J. Tellinghuisen, Chem.Phys. Letters, 29, 359 (1974).
7. M. MacDonald, J.P.T. Wilkinson, C. Fotakis, M. Martin and R.J. Donovan, Chem.Phys. Letters, 99, 250 (1983).
8. M. MacDonald, R.J. Donovan and M.C. Gower, Chem.Phys. Letters, 97, 72 (1983).
9. K.P. Lawley, M. MacDonald, R.J. Donovan and A. Kvaran, Chem.Phys. Letters, 92, 322 (1982).
10. M. Martin, C. Fotakis, R.J. Donovan and M.J. Shaw, Nuovo Cimento, B63, 300 (1981).

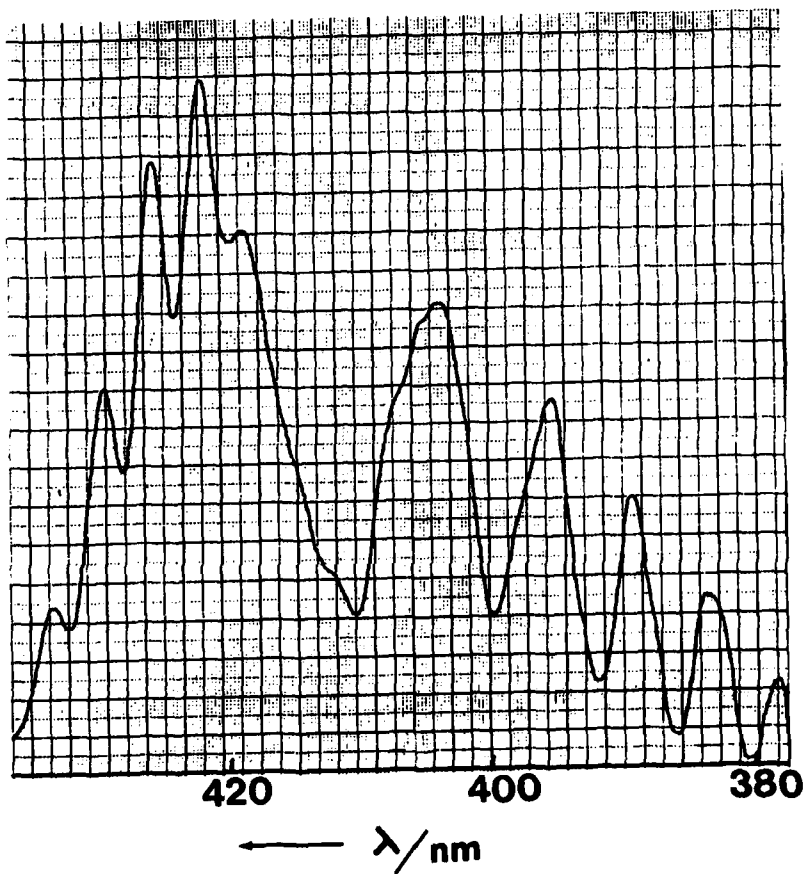


Figure 1 Fluorescence from I_2 excited at 193.3 nm
using a line-narrowed ArF laser

Kinetics of the Reaction $O + ClO \rightarrow Cl + O_2$ James J. Margitan

Jet Propulsion Laboratory
California Institute of Technology
Pasadena, California 91109

The reaction $O + ClO \rightarrow Cl + O_2$ (k_1) plays a uniquely important role in stratospheric chemistry since it is the rate determining step in the chlorine-catalyzed destruction of ozone, completing the cycle initiated by $Cl + O_3 \rightarrow ClO + O_2$. The calculated potential depletion of the stratospheric ozone column, caused by anthropogenic sources of chlorine, is thus very sensitive to the value and uncertainties of k_1 .

In this work the kinetics of the reaction $O + ClO \rightarrow Cl + O_2$ (k_1) were studied in a combined discharge flow/laser photolysis/resonance fluorescence system (Figure 1). A discharge flow system was used to generate ClO via the reaction of Cl_2O with excess Cl . A laser (266 nm) was used to photolyze a small (~ 1%) fraction of the ClO , and generate O atoms, whose decay via reaction 1 was followed by resonance fluorescence. The concentration of ClO was measured directly via absorption at 277 nm in a 6 pass White cell in a room temperature, 20 cm long cell 0.2 sec downstream of the photolysis/fluorescence region. The concentration of ClO was corrected for loss due to the $ClO + ClO$ reaction between the fluorescence and absorption regions. These corrections were less than 20% at the highest $[ClO]$.

A typical semilogarithmic O -atom decay plot is shown in Figure 2, the slope of which is k^I , the pseudo first order rate constant. The linearity of

the decay over greater than an order of magnitude indicates the absence of complicating, secondary reactions. The value of k_1 is determined from a plot of k_1^I vs. $[ClO]$, as shown in Figure 3. As can be seen in that figure, the data show no significant temperature dependence over the 241-298 K range of this study. The composite slope is $k_1 = (4.17 \pm 0.07) \times 10^{-11} \text{ cm}^3 \text{ s}^{-1}$ (uncertainty 1σ , precision only). The limit on E/R determined from this study is $\approx 200 \text{ K}$. An analysis of possible systematic errors leads to the expression $k_1 = (4.2 \pm 0.8) \times 10^{-11} \text{ cm}^3 \text{ s}^{-1}$.

The results of this study are in good agreement with the existing literature data, which had all been obtained in discharge flow studies. The present results and the data of Clyne and co-workers¹ ($k_1(298) = 5.3 \times 10^{-11} \text{ cm}^3 \text{ s}^{-1}$, E/R = 224 K), Zahniser and Kaufman² ($k_1(298) = 4.2 \times 10^{-11} \text{ cm}^3 \text{ s}^{-1}$, E/R = 11 K) and Leu³ ($k_1(298) = 3.6 \times 10^{-11} \text{ cm}^3 \text{ s}^{-1}$, E/R = 96 K) can be averaged to obtain a composite $k_1(298) = 4.3 \times 10^{-11} \text{ cm}^3 \text{ s}^{-1}$, or $k_1(T) = 6 \times 10^{-11} \exp(-100/T)$. An Arrhenius plot of the data is shown in Figure 4.

The research described in this paper was carried out by the Jet Propulsion Laboratory, California Institute of Technology, under contract with the National Aeronautics and Space Administration.

1. P. P. Bemand, M. A. A. Clyne and R. T. Watson, J. Chem. Soc. Faraday I, **69**, 1356-74 (1973); M. A. A. Clyne and W. S. Nip, J. Chem. Soc. Faraday I, **72**, 2211-17 (1976).
2. M. S. Zahniser and F. Kaufman, J. Chem. Phys. **66**, 3673-3681 (1977).
3. M. T. Leu, J. Phys. Chem. **88**, 1394-98 (1984).

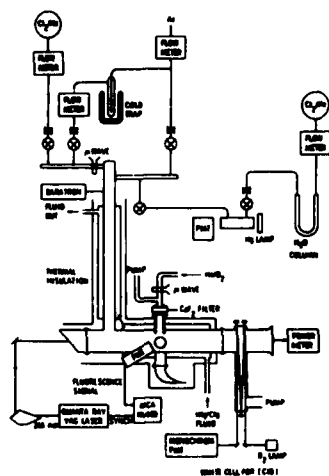


Figure 1

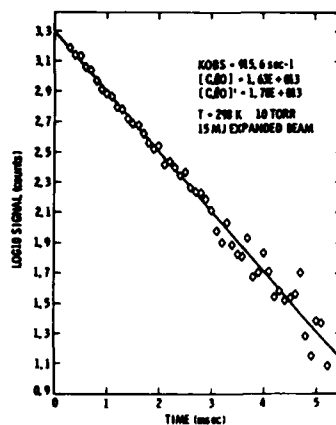


Figure 2

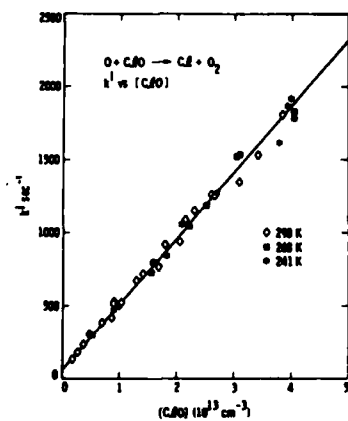


Figure 3

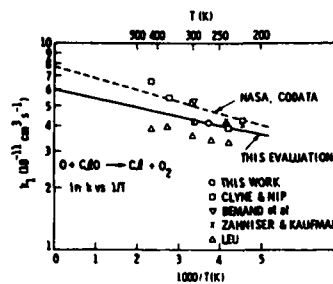


Figure 4

NON QUASI-STATIONARY STATE PYROLYSIS OF ETHANE

Serge CORBEL, Paul-Marie MARQUAIRE and Guy-Marie CÔME

Département de Chimie Physique des Réactions, L.A. CNRS 328
Université de Nancy I et Institut National Polytechnique de Lorraine
1, rue Grandville, 54000 NANCY, France

The study of a pyrolysis reaction in non Quasi-Stationary State (QSS) conditions provides very direct information about reaction mechanisms and radical reactivities. Induction periods have been observed in the pyrolysis of neopentane in a Continuous Flow Stirred Tank Reactor (CFSTR) around 440°C [1] and in a tubular reactor at 550°C [2]. These non QSS experiments have provided kinetic parameters for the initiation, propagation and termination steps occurring in neopentane pyrolysis.

Here, we report on the observation of an induction period in the pyrolysis of ethane in a CFSTR at 530°C. From these experiments, independent values of the rate constants of the initiation step, and of the determining propagation and termination steps of ethane pyrolysis have been deduced.

EXPERIMENTAL RESULTS

The principle of the apparatus used in this study has been described previously [1]. The reactor is a Pyrex CFSTR, operated at constant temperature and pressure, and steady-state gas flow.

A singular perturbation theory of chain radical reaction mechanisms [3] allows one to predict a priori, from an assumed reaction mechanism and corresponding kinetic parameters, experimental conditions for which non QSS kinetics can be observed. In the case of ethane pyrolysis, it was concluded that an induction period of the order of 1 s should occur around 530°C. Accordingly, experiments were carried out at 530°C, under constant ethane pressures between 10 and 80 Torr and for space times from 0.7 to 7 s*. Under these conditions, the degree of conversion of ethane was very low (between 10^{-3} and 10^{-2} %).

We observed the formation of ethylene and hydrogen in equal amounts, and methane.

* Our first results at 40 Torr have already been published [4].

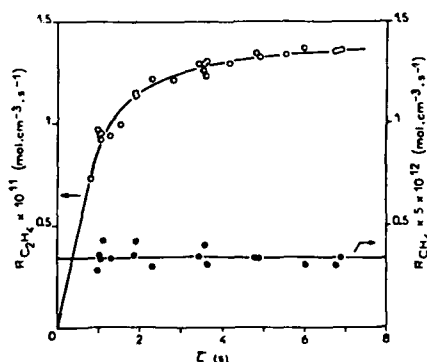
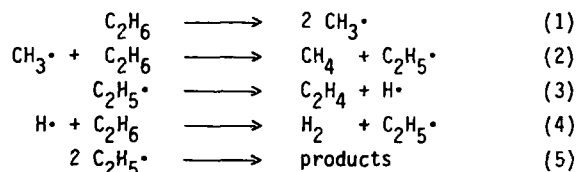


Fig. 1. Rates of formation of ethylene and methane as a function of space time τ . $T = 530^\circ\text{C}$; $P_{\text{C}_2\text{H}_6} = 40$ Torr. $\circ R_{\text{C}_2\text{H}_4}$, $\bullet R_{\text{CH}_4}$ (experimental), — theoretical line.

At constant temperature and ethane pressure, the rate of formation of ethylene increases with space time, whereas the rate of formation of methane remains constant [Figure 1].

INTERPRETATION

The pyrolysis of ethane at small extents of reaction has been generally interpreted by the following straight chain radical mechanism :



Since methane only appears in the elementary process (2) and since ethylene mainly appears in process (3) (i.e. chains are long), the rates of formation of these two products are given by :

$$\begin{aligned}
 R_{\text{CH}_4} &= k_2 [\text{C}_2\text{H}_6] [\text{CH}_3\cdot] \\
 R_{\text{C}_2\text{H}_4} &= k_3 [\text{C}_2\text{H}_5\cdot]
 \end{aligned}$$

At constant temperature, k_2 and k_3 are constant and, since ethane concentration is also constant, the concentrations of methyl and ethyl radicals are proportional to R_{CH_4} and $R_{\text{C}_2\text{H}_4}$ respectively. From the results shown in fig. 1, it can be concluded that the concentration of methyl radicals is constant and that the concentration of ethyl radical increases with space time. These facts are evidences of the existence of an observable induction period for the ethyl radicals, and thus, for the overall reaction.

From our measurements, we have got independent values of the rate constants of elementary processes (1), (3) and (5) at 530°C and different pressures.

$P_{C_2H_6}$ (Torr)	10	20	40	80
$k_1 (s^{-1}) \times 10^8$	2.7	3.8	4.0	4.3
$k_3 (s^{-1}) \times 10^{-2}$	0.9	1.2	2.0	2.8
$k_5 (mol^{-1}.cm^3.s^{-1}) \times 10^{-12}$	5.8			

k_1 and k_3 show a pressure dependence, already observed.

Our values of these kinetic parameters are in agreement with others of the literature, and particularly with those of Pacey and Wimalasena [5], obtained by means of a plug flow reactor at 630°C and 0.05 to 0.5 space times.

In conclusion, Non Quasi-Stationary State Pyrolysis appears to be a powerful method for both elucidating reaction mechanisms and for determining independent rate constants of chain radical reactions.

REFERENCES

- [1] P.M. Marquaire, Thèse de 3ème cycle, Nancy (1976) ;
P.M. Marquaire and G.M. Côme, Fifth International Symposium on Gas Kinetics, Paper 2, The Chemical Society, London (1977) ;
P.M. Marquaire and G.M. Côme, React. Kin. Cat. Lett., 9, 165 and 171 (1978).
- [2] P.D. Pacey and J.H. Wimalasena, Chem. Phys. Lett., 53, 593 (1978) ;
J. Phys. Chem., 84, 2221 (1980).
- [3] G.M. Côme, J. Phys. Chem., 81, 2560 (1977).
- [4] S. Corbel, P.M. Marquaire and G.M. Côme, Chem. Phys. Lett., 80, 34 (1981).
- [5] P.D. Pacey and J.H. Wimalasena, Chem. Phys. Lett., 76, 433 (1980) ;
Can. J. Chem., 61, 1086 (1983).

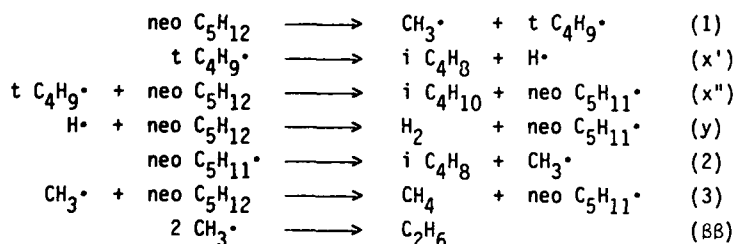
DETAILED MECHANISM OF NEOPENTANE PYROLYSIS AROUND 700°C

by P. AZAY, P.M. MARQUAIRE and G.M. CÔME

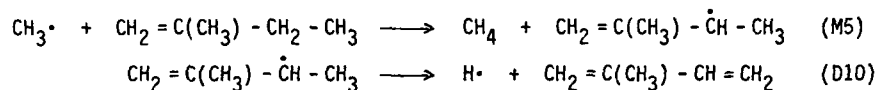
Département de Chimie Physique des Réactions, L.A. C.N.R.S. 328,
 Université de Nancy I et Institut National Polytechnique de Lorraine,
 1, rue Grandville, 54000 NANCY, France

The pyrolysis of neopentane has been studied by means of a continuous flow stirred tank reactor, at temperatures between 635 and 735°C, at space times between 0.05 and 0.35 s, at partial pressures of hydrocarbon between 4.1 and 16.4 Torr, the total pressure being 350 Torr, using oxygen free nitrogen as carrier gas. In these conditions, the conversion of neopentane is comprised between 0.3 and 30 %.

There are 4 main primary reaction products : isobutene, methane, hydrogen and ethane. Isobutane is believed to be a primary product though it cannot be quantitatively measured. There are 7 minor secondary products : 2-methyl 1-butene, propene, ethylene, allene, isoprene, propyne, 2-methyl 2-butene. The system is described by 3 stoichiometries at zero conversion, and by 10 stoichiometries at any extent of the reaction. The relative importances of these stoichiometries greatly vary with the temperature. Initial stoichiometries, reaction orders and activation energies are in favour of the following classical initial mechanism :



The building up of the mechanism at any extent of the reaction has been done by the following procedure. An exhaustive secondary reaction mechanism has been written by means of a specific computer program (¹). The reactants considered in this mechanism were neopentane and the 4 major primary products. Only β type free radicals were involved in metatheses, H^\bullet and CH_3^\bullet in addition processes, and CH_3^\bullet and $\text{i C}_4\text{H}_7^\bullet$ (resonance stabilized) in termination processes. This mechanism accounts for all the reaction products except isobutane and isoprene. Therefore, processes (M5), (D10) and (x'') have been added :



Process (x") has already been written previously. This reaction mechanism includes 44 elementary processes, involving 14 molecular species and 10 free radicals. A sensitivity analysis ⁽²⁾ of this reaction mechanism has shown that only 5 processes among the 44 ones are determining : (1), (y), (3), (ββ) [cf. supra], and (4β) :



The Arrhenius parameters of these elementary processes have been determined by optimization :

$$\begin{aligned} \log k_1 &= 17.3 - 82\,000/\text{RT} \\ \log k_y &= 16.1 - 12\,500/\text{RT} \\ \log k_3 &= 13.6 - 16\,500/\text{RT} \\ \log k_{4\beta} &= 12.8 - 11\,000/\text{RT} \\ \log k_{\beta\beta} &= 12.3 + 3\,900/\text{RT} \quad (P_{\text{neo C}_5\text{H}_{12}} = 16.4 \text{ Torr}) \end{aligned}$$

Units : mol, cm³, s, cal

Figures 1, 2, 3, 4 show the fit of the corresponding theoretical lines to the experimental points, for the 4 major products, at $P_{\text{neo C}_5\text{H}_{12}} = 16.4 \text{ Torr}$, and at various temperatures and space times.

The Arrhenius parameters of the above elementary processes are in good agreement with the literature, as it is shown in table 1 for $\log A_1$ (s⁻¹) and E_1 (kcal.mol⁻¹), at different temperatures between 703 and 1240 K.

Table 1

$\log A_1$	17.6	18.2	16.8	16.1	17.7	16.9	17.3	16.5	16.1
E_1	84.0	85.8	82.0	78.9	85.2	80.5	80.8	80.4	78.2
Ref.	3	4	5	6	7	8	9	10	11

REFERENCES

1. L. HAUX-VOGIN, P.Y. CUNIN, M. GRIFFITHS and G.M. CÔME - to be published.
2. G.M. CÔME - Comprehensive Chemical Kinetics, Vol. 24, Chap. 3, Elsevier (1983).
3. P.M. MARQUAIRE and G.M. CÔME - React. Kin. Catal. Lett., 9, 165, 171 (1978).

4. M.P. HALSTEAD, R.S. KONAR, D.A. LEATHARD, R.M. MARSHALL and J.H. PURNELL - Proc. Roy. Soc. London, Ser. A, 310, 525 (1969).
5. F. BARONNET, G.M. CÔME and M. NICLAUSE - J. Chim. Phys., 71, 1214 (1974).
6. R.M. MARSHALL, J.H. PURNELL and P.D. STOREY - J.C.S. Faraday Trans. I, 72, 85 (1976).
7. P.D. PACEY - Can. J. Chem., 51, 2415 (1973).
8. J.E. TAYLOR, D.A. HUTCHINGS and K.J. FRECH - J. Am. Chem. Soc., 91, 2215 (1969).
9. A.C. BALDWIN, K.E. LEWIS and D.M. GOLDEN - Int. J. Chem. Kin., 11, 529 (1979).
10. J.N. BRADLEY and K.O. WEST - J.C.S. Faraday Trans. I, 72, 8 (1976).
11. W. TSANG - J. Chem. Phys., 44, 4283 (1966).

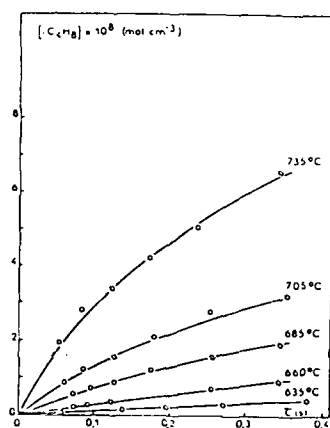


Figure 1

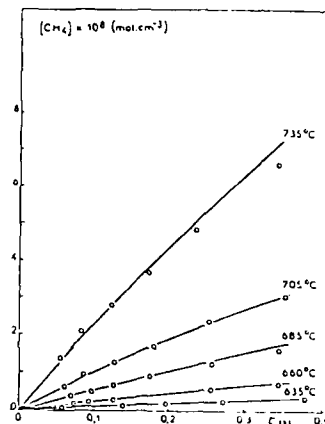


Figure 2

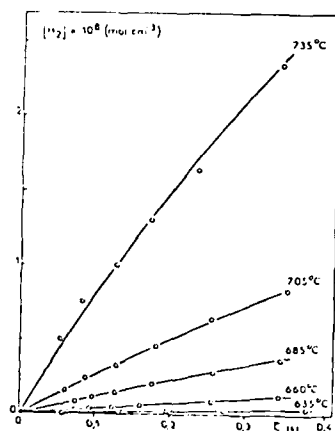


Figure 3

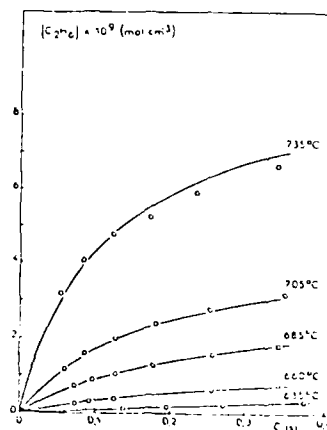


Figure 4

THE THERMAL REACTION OF BUTENE-2-CIS IN A STAINLESS STEEL
REACTOR OR SURFACE EFFECTS AS A MEANS TO ACCELERATE AND
ORIENTATE COMPLEX OLEFIN REACTIONS.

C. COLLONGUES, C. RICHARD and R. MARTIN

University of Nancy I, France.

The thermal reaction of butene-2 cis has been successively studied in a Pyrex and in a stainless steel reactor at about 500°C.

In the Pyrex reactor, the reaction was shown to be reproducible and homogeneous. Its kinetic features were interpreted in terms of molecular and free-radical processes ⁽¹⁾ ⁽²⁾.

By contrast in the stainless steel reactor, the reaction is less reproducible and much dependent on the type of wall-conditioning which has been effected and on how long the reactor has been steadily evacuated before a run (one hour, one day, one week). With a definite order of procedure, very reproducible results may be obtained for a first class of products, such as CH₄ (see figure), C₃H₆, trans-2-C₄H₈ ..., whereas more erratic results are obtained for a second class of products such as 1-C₄H₈ (see figure), butadiene-1,3, n-butane,...

As compared to the Pyrex reactor, the initial rates of product formation in the stainless steel reactor are selectively increased and the magnitude of this effect is much dependent on wall-conditioning (see figures and tables).

The latter results can only be interpreted in terms of heterogeneous catalytic reactions which add to homogeneous molecular processes and to a "hetero-homogeneous" free-radical reaction which is partly initiated at the walls - probably as a consequence of the catalytic reactions - and partly initiated in the gas phase.

Table I

Ratios, $(v_p^0)_{ss} / (v_p^0)_{py}$, of initial rates of product P
in the stainless steel and in the Pyrex reactors at 521°C

Stainless steel reactor	olefin cond.	olefin cond.	air cond.
$P_o(\text{cis } 2\text{-C}_4\text{H}_8)$ torr	10	101	
CH_4	3	3	33
C_3H_6	3	4	24
$1\text{-C}_4\text{H}_8$	63 — 73	20 — 25	~ 120
$\text{trans } 2\text{-C}_4\text{H}_8$	1,3	1,2	~ 2,5
$1,3\text{-C}_4\text{H}_6$	3 — 4	3	7
$n\text{-C}_4\text{H}_{10}$		~ 60	~ 7

Table II

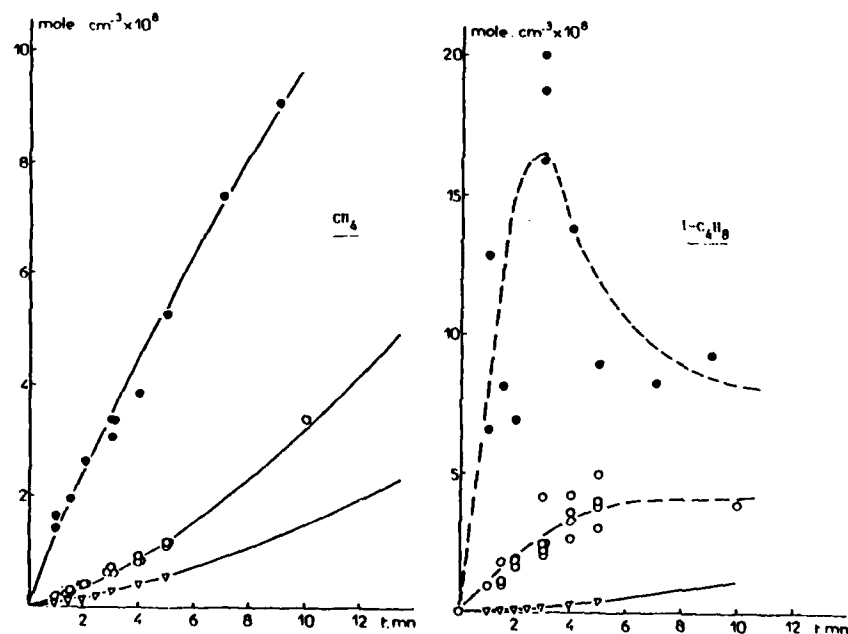
Relative importances of primary stoichiometries
at low extent of reaction in various reactors

$T = 521^\circ\text{C}$; $P_o(\text{cis } 2\text{-C}_4\text{H}_8) = 101$ torr

Kind of reactor	Pyrex	stainless steel	
		olefin cond.	air cond.
(1) $\text{cis } 2\text{-C}_4\text{H}_8 = \text{trans } 2\text{-C}_4\text{H}_8$	96,0	78,3	43,25
(2) $\text{cis } 2\text{-C}_4\text{H}_8 = \text{H}_2 + 1,3\text{-C}_4\text{H}_6$	2,2	5,3	19,42
(3) $\text{cis } 2\text{-C}_4\text{H}_8 = \frac{1}{2} (\text{CH}_4 + \text{C}_3\text{H}_6 + 1,3\text{-C}_4\text{H}_6)$	1,2	3,7	7,35
(4) $\text{cis } 2\text{-C}_4\text{H}_8 = 1\text{-C}_4\text{H}_8$	0,6	12,2	29,92
(8) $\text{cis } 2\text{-C}_4\text{H}_8 = \frac{1}{2} (1,3\text{-C}_4\text{H}_6 + n\text{-C}_4\text{H}_{10})$	-	0,5	0,06
total	100	100	100

References

- (¹) C. RICHARD and R. MARTIN, J. Chim. Phys. 73, 745 (1976).
D.R. POWERS and H. CORCORAN, "Industrial and Laboratory Pyrolyses",
Am. Chem. Soc. Symp. Series, 32, Washington D.C., 1976, p. 117.
- (²) C. RICHARD, A. BOIVEAUT and R. MARTIN, Int. J. Chem. Kinet. 12, 921
(1980).
C. COLLONGUES, C. RICHARD and R. MARTIN, Int. J. Chem. Kinet., 15, 5
(1983).
C. RICHARD, A. BOUCHY, G. ROUSSY and R. MARTIN, C.R. Acad. Sci. Fr.,
296, série II, 47 (1983).



Product formation in the thermal reaction of pure butene-2 cis. T = 521°C ; P₀(cis-2-C₄H₈) = 101 torr.

- stainless-steel reactor conditioned by air
- stainless-steel reactor conditioned by 2-butene
- ▽ Pyrex reactor

I,R LASER PHOTO OXIDATION OF n BUTANE AND CARBON MONOXIDE

by J. MASANET, C. LALO, F. LEMPEREUR, J. TARDIEU de MALEISSYE

Laboratoire de Chimie Générale, Equipe de Recherche Associée au CNRS n°070457
Université P. et M. Curie, 4 Place Jussieu, 75230-PARIS CEDEX-05, FRANCE

Bimolecular reactions were activated by using a tunable CW CO₂ laser between 9 and 11 μm. The thermal bath obtained from the rovibrational excitation of one of the gaseous mixture components is able to drive an homogeneous phase reaction. The available energy in the reacting medium depends on the difference between the energy captured through the absorbing species and the energy relaxed by the collisions and then removed by heat and mass transports.

The two reactions of oxidation described are developed in similar thermal bath and pressure conditions.

I. n-BUTANE-OXYGEN REACTION

a) The conditions of irradiation.

The n C₄H₁₀ has a weak absorption band in the range of emission of the CO₂ laser between the R 10 and R 28 lines from the 00°1-10°0 CO₂ transition. By using the R 28 at 10.195 μm we dispose of a 100 W laser power and have determined for the first time an absorption coefficient:

$$\epsilon(n\text{ C}_4\text{H}_{10}) = 3.10 \pm 0.15 \cdot 10^{-4} \text{ cm}^{-1} \cdot \text{torr}^{-1}$$

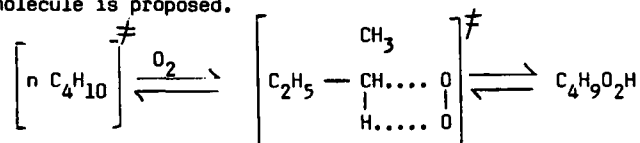
Despite of the weak absorption coefficient, the thermal bath generated in mixtures of 150 and 100 torr respectively of n butane and oxygen, can entail a slow oxidation in focused conditions.

b) Results.

By measuring the temperature out of the irradiation zone, close to the walls, it is possible to observe the development of the slow reaction (fig. 1).

The dramatic increase which follows the slow and uniform slope of the temperature points out the evolution of a branching and degenerate chain reaction. The analysis of the condensed products by thin layer chromatography at different steps of the reaction, shows that the formation of butyl hydroperoxide precedes the apparition of dibutyl peroxide as the hydrogen peroxide; the later is produced in great quantity just after the thermal

acceleration. The first electronic excited state of n butane is repulsive so it does not seem plausible that such a thermal bath leads to its decomposition ($n\text{C}_4\text{H}_{10} - \text{H} = 385 \text{ KJ.mole}^{-1}$). Therefore a primary process of formation of butyl hydroperoxide via the O_2 biradical insertion within the n butane molecule is proposed.



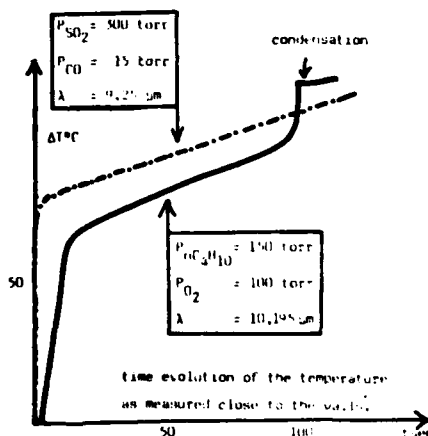
II. SULFUR DIOXIDE-CARBON MONOXIDE REACTION

a) The conditions of irradiation.

The vibrational photo excitation of SO_2 was performed at $9.25 \mu\text{m}$, corresponding to the R 22 line from the 00^01-02^00 CO_2 transition, with a power of 100 W. The weak absorption coefficient in our experimental conditions was measured at this wavelength:

$$\epsilon(\text{SO}_2) = 2.20 \pm 0.10.10^{-4} \text{ cm}^{-1}.\text{torr}^{-1}$$

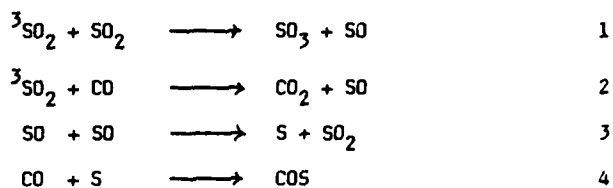
Mixtures of SO_2 at partial pressures ranging from 250 to 350 torr and of transparent CO from 15 to 100 torrs were irradiated. The absorption coefficients of SO_2 and $n\text{C}_4\text{H}_{10}$ do not differ significantly and we observe (fig.1) that the thermal conditions are similar for the two systems outside of the laser beam.



b) Results.

The analysis of gaseous products performed by mass spectrometry and gas chromatography shows the formation of CO_2 with traces of SO_3 and COS . The yield of formation of CO_2 becomes noteworthy beyond 15 torr of CO and is directed towards a limiting formation rate of $10^{-3} \text{ torr.s}^{-1}$ at upper pressures. The kinetics of the CO_2 formation is influenced for irradiation times beyond 120 s, by the coating on the walls of S, COS and SO_3 which catalyses the oxidation of CO. The formation of CO_2 is typical of a metastable SO_2

triplet state reacting with CO. In a same way, SO_3 is issued from the interaction between this triplet state and the SO_2 ground state, while COS proceeds from a radical mechanism:



Actually, studies are in progress with the aim to settle the energy level of this SO_2 metastable state of SO_2 . Theoretical calculations locate the ${}^3\text{A}_2$ and ${}^3\text{B}_2$ states near of 2 eV. Both states may interact with the vibrational levels of SO_2 populated by the laser excitation. Some preliminary calculations point out an average temperature of 1800 K inside the reaction zone.

LASER STUDIES ON THE REACTION OF Mg WITH OXIDANTS.

Bernard BOURGUIGNON, June MCCOMBIE, Joëlle ROSTAS and
Guy TAIEB⁺

Laboratoire de Photophysique Moléculaire CNRS
Bâtiment 213, Université de Paris-Sud,
91405 - ORSAY - CEDEX. France.

The reactions of excited Mg atoms with the oxidants N_2O and NO_2 have been studied extensively under bulk conditions ⁽¹⁾. Interpretation of reactive collision dynamics requires detailed understanding of the triplet state spectroscopy and this is now in progress.

Laser excitation spectra of MgO , formed under bulk conditions in the reaction between $Mg(^3P, ^1P)$ and N_2O , have been recorded between 3630 Å and 3860 Å. In the uv numerous new bands have been seen in emission ⁽²⁾. Among those, bands at 3672.1, 3674.6 and 3677.4 Å have been assigned for the first time to the (0,0), (1,1) and (2,2) bands of the intermultiplet transition $D^1\Delta - a^3\Pi_1$, (see fig. 1). Identification of these bands gives evidence that the $a^3\Pi$ states are populated under bulk conditions, confirming the conclusion of Field ⁽³⁾.

Preliminary analysis of the strong bands at 3720 Å, previously assigned by Schamps ⁽⁴⁾ to the $d^3\Delta - a^3\Pi$ transition, questions his assignment of the individual band heads since, similarly to the spectra obtained by Field et al ⁽⁵⁾ on the $CaO D^1d^1, ^3\Delta - a^3\Pi$ system, the rotation-vibration analysis and deperturbation of the (0,0) and (1,1) bands is not simple. The value of the spin orbit constant $A(^3\Delta) \approx -20 \text{ cm}^{-1}$ which our crude analysis has yielded is in agreement with his original calculation, but not with his experimentally derived value of $\approx -30 \text{ cm}^{-1}$.

Further investigation of the triplet transition is planned using the OODR technique. Two excimer pumped dye lasers are employed, one to scan the $d^3\Delta - a^3\Pi$ transition whilst the second pumps the known $B^1\Sigma^+ - a^3\Pi$ transition. Wavelength scanning and data accumulation are controlled by a

⁺ and UER Claude Bernard, Université de Rennes I, 35000-RENNES.

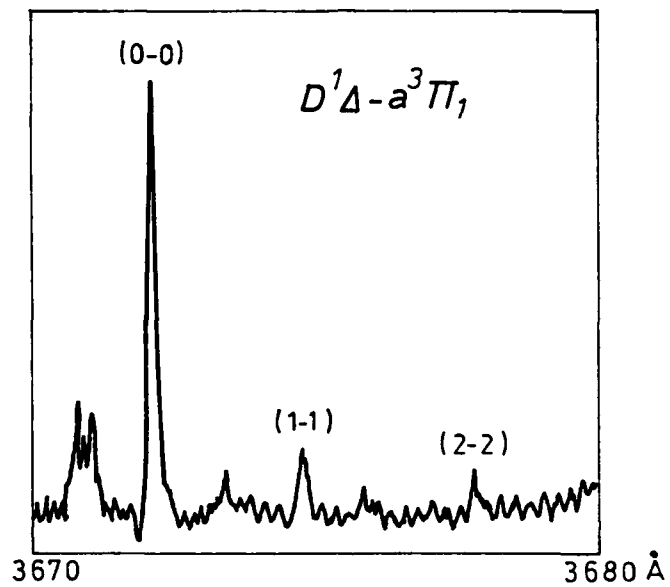


Figure.1. Part of the excitation spectrum of MgO formed in the reaction between Mg ($^3P, ^1P$) and N_2O .

microprocessor. Initial results of this are presented here. On the other hand a computer simulation of the spectra obtained by Dagdigian ⁽⁶⁾ has given an estimate of the vibrational and spin-orbit populations of the nascent MgO $a^3\Pi$ state in the $Mg + N_2O$ reaction.

A study of the reaction with NO_2 has been carried out. The rotational and vibrational temperatures in the $B^1\Sigma^+$ state have been estimated by simulating the chemiluminescence spectra. As theoretical investigations ⁽⁷⁾ strongly suggest that for the $Mg + N_2O$ reaction the N_2 molecule must take a large amount of the exothermicity of the reaction, we intend to probe the energy distribution of the NO fragment by laser induced fluorescence.

References

1. B. Bourguignon, J. Rostas and G. Taïeb, J. Chem. Phys., 77, 2979 (1982)
2. J. Schamps, Thèse d'Etat, Université de Lille I, (1973)
3. P. Chuey Fong Ip, Ph.D. Thesis, M.I.T. (1983)
4. J. Schamps and G. Gandara, J. Mol. Spectr. 62, 80 (1976)
5. R.F. Marks, R.A. Gottscho and R.W. Field, Physica Scripta 25, 312 (1982)
6. P.J. Dagdigian, J. Chem. Phys. 76, 5375 (1982)
7. D.R. Yarkony, J. Chem. Phys. 78, 6763 (1983).

LASER POWERED HOMOGENEOUS PYROLYSIS OF NITROAROMATICS:
THE MECHANISM OF HOMOGENEOUS, GAS-PHASE DECOMPOSITION OF NITROTOLUENES

Donald F. McMillen, C. W. Larson, Alicia Gonzalez, and David M. Golden
SRI International
Menlo Park, CA 94025

Abstract

Laser Powered Homogeneous Pyrolysis (LPHP) has been used to characterize the initial step(s) in the homogeneous thermal decomposition of ortho-nitro-toluene. Using SF_6 as the unreactive absorber, this technique provides conditions in which ortho-substituted nitro-toluenes have no opportunity to undergo wall-catalyzed reactions. LPHP has provided the first successful test of the speculation that the "abnormal" rate parameters and products commonly reported for gas phase decomposition of the ortho isomers result from wall reactions and not from some homogeneous elimination reaction operating via a complex transition state. Preliminary measurements of o-nitrotoluene decomposition rates indicate an activation energy ~ 66 kcal/mole, in line with the ca. 70 kcal/mole "normally" expected for Ph-NO_2 bond scission. Similarly, the principal decomposition product of ortho-nitrotoluene (>80%) under these conditions was toluene, as expected if phenyl- NO_2 bond scission was the initial decomposition step, and the methyl-phenyl radical was effectively scavenged. The implications that these "normal" rate parameters and products have for the origin of the commonly observed "abnormal" decomposition will be discussed.

Pressure Effects on Some Bimolecular
Reactions of the OH Radical*

M. J. Molina, L. T. Molina, and R. Stachnik

Molecular Physics and Chemistry Section
Jet Propulsion Laboratory
California Institute of Technology
Pasadena, California 91109

Abstract

The kinetics of several reactions of the OH radical of importance in the atmosphere have been investigated using a laser photolysis-long path resonance absorption apparatus. We have studied the reactions with species such as HNO_3 and CO which are likely to involve the formation of a bound intermediate with a sufficiently long lifetime to suffer collisions before decomposing to products or back to reactants. We are studying the pressure and temperature dependency of the rate constants in order to obtain information about the reaction mechanism. Our preliminary room temperature results indicate some pressure effect for the $\text{OH} + \text{HNO}_3$ reaction between 10 and 50 torr helium, but no significant effect between 50 torr and 760 torr He, N_2 , or O_2 .

* The Study was supported by NASA Contract No. NAS7-918.

Spectrokinetic studies of HO_2 and OH involved in the chain reactions (2) $\text{H} + \text{O}_2 \rightarrow \text{HO}_2$; (3) $\text{H} + \text{HO}_2 \rightarrow 2\text{OH}$; and (4) $\text{OH} + \text{H}_2 \rightarrow \text{H} + \text{H}_2\text{O}$ under experimental conditions where (7) $\text{OH} + \text{HO}_2 \rightarrow \text{H}_2\text{O} + \text{O}_2$ is the predominant termination reaction for OH .

by

Jette Munk, O.J. Nielsen, A. Sillesen and P. Pagsberg
Chemistry Department
Risø National Laboratory
DK-4000 Roskilde, Denmark.

Abstract:

The yield of H-atoms produced by pulse radiolysis of 10% H_2 in Ar at 1 atm. and 298 K was determined by monitoring the transient absorption at 215 nm due to formation of HO_2 radicals via reaction (2) in the presence of 0.2–10 mbar O_2 . Reaction (3) provides a highly efficient source of OH radicals in this system. The formation and decay of OH was studied by monitoring the transient absorption at 3090 Å. The decay of OH was approximately exponential, $[\text{OH}] = [\text{OH}]_0 \exp(-k^*t)$ and with a ten-fold variation of k^* in the range of $p(\text{O}_2) = 0.2\text{--}10$ mbar. A strong correlation with the yield of long-lived HO_2 radicals indicates that $k^* \approx k_7[\text{HO}_2]$, i.e. that the OH decay is primarily controlled by reaction (7). A computer model including eight elementary reactions accounts for all of the experimental observations when $k_2 = 4.5 \times 10^8 \text{ M}^{-1}\text{s}^{-1}$, $k_3 = 6.5 \times 10^{10} \text{ M}^{-1}\text{s}^{-1}$, $k_4 = 4 \times 10^6 \text{ M}^{-1}\text{s}^{-1}$, and $k_7 = 6.0 \times 10^{10} \text{ M}^{-1}\text{s}^{-1}$.

THE PHOTOPHYSICS AND PHOTOCHEMISTRY OF NCNO

I. Nadler, M. Noble, J. Pfab,* H. Reisler, and C. Wittig

Chemistry Department, University of Southern California,

Los Angeles, CA 90089-0484

The spectroscopy and photodissociation dynamics of NCNO were studied throughout the 450-900 nm wavelength region both at 300 K and in a free jet expansion. The $\tilde{A}^1A'' \leftarrow \tilde{X}^1A'$ absorption system of NCNO was monitored in a free jet expansion by using either 1- or 2-photon dissociation followed by LIF detection of the CN photofragment. The frequencies of the fundamental vibrations in the excited \tilde{A}^1A'' state were accurately assigned, and 1-photon photodissociation was observed with photolysis wavelengths < 585 nm, corresponding to $D_0 = 17,085 \pm 10 \text{ cm}^{-1}$. We show that dissociation following $\tilde{A}^1A'' \leftarrow \tilde{X}^1A'$ excitation transpires via vibrational predissociation, and that the $\text{CN}(\tilde{X}^2\Sigma^+)$ fragments are extremely cold near reaction threshold. Only $v''=0$ is observed, $> 90\%$ of the CN is in $N''=0$, and it is translationally cold as well. By tuning the photolysis laser to wavelengths < 585 nm, expansion cooled NCNO is photodissociated via 1-photon excitation, and we obtain detailed V,R,T energy distributions of the CN fragment at all photolysis wavelengths. These distributions are compared to statistical calculations such as those embodying the phase space theory of molecular

reactions (PST). We find that when the excess energy is smaller than what is necessary to access product vibrations, the agreement between experiment and theory is excellent. However, when product vibrations are accessible, PST cannot be used, and we offer another statistical theory to explain our results.

At room temperature, 1-photon photodissociation is observed even with photolysis wavelengths > 592 nm. We show that it occurs predominantly from "hot bands," whereas molecules near the ground state dissociate only following the stepwise absorption of 2-photons. With photolysis wavelengths ≤ 592 nm only 1-photon dissociation is observed.

TEMPERATURE DEPENDENCE OF $\text{NH} (a^1\Delta)$ REACTIONS

J.W. Cox, H.H. Nelson and J.R. McDonald
Chemistry Division, Naval Research Laboratory, Washington, DC 20375, USA

Kinetic information concerning rates for $\text{NH} (a^1\Delta)$ electronic quenching or reaction with simple molecules such as H_2 and various hydrocarbons has developed steadily in recent years (1). Little information is available which would directly determine the nature of the mechanism involved in these gas-phase reactions. Such information is of more than passing interest as it would make it possible to make detailed comparisons of $\text{NH} (a^1\Delta)$ with its more extensively studied isoelectronic analogs $\text{CH}_2(^1A_1)$ (2) and $\text{O}(^1D)$ (3).

Several studies of NH kinetics in solution indicate the existence of competition among CH-insertion, C-C addition, and electronic deactivation processes for hydrocarbon reactions (4). Whether such competition exists for $\text{NH} (a^1\Delta)$ vapor phase reactions in analogy to those of gas phase $\text{CH}_2(^1A_1)$ and $\text{O}(^1D)$ reactions is unclear. In an attempt to better characterize the gas phase reactions we have undertaken a study of the temperature dependence of $\text{NH} (a^1\Delta)$ reactions with hydrogen and several hydrocarbons.

We have examined the temperature dependence of $\text{NH} (a^1\Delta)$ reactions over the 25-250°C range with hydrogen and saturated and unsaturated hydrocarbons. Kinetic studies were carried out in a flow cell enclosed in an oven. A Nd:YAG laser, frequency-quadrupled to 266 nm, photolysed HN_3 to form $\text{NH} (a^1\Delta)$ with >95% conversion efficiency (5). A counter-propagating excimer-pumped, frequency-doubled dye laser beam served to measure $\text{NH} (a^1\Delta)$ concentration by monitoring the fluorescence from $\text{NH} (a^1\Delta \rightarrow c^1\Pi) \text{ O-O } Q(2)$ excitation at 325.78 nm as a function of time delay between the photolysis and interrogation pulses. Linear least squares fits of pseudo first-order fluorescence decay curves provide rate constants. By measuring first order rate constants as a function of temperature

and fitting to an Arrhenius form, we obtain the A factors and activation energies given in Table 1. Typical Arrhenius plots are shown in Figure 1.

TABLE 1: NH ($a^1\Delta$) A Factors and Activation Energies E

Reactant	A ($\text{cm}^3\text{sec}^{-1}$, $\pm 2\sigma$)	E (KJ/Mole, $\pm 2\sigma$)
H ₂	$(8.0 \pm 0.5) \times 10^{11}$	0.40 ± 0.02
CH ₄	*	*
C ₃ H ₈	$(1.5 \pm 0.1) \times 10^{-10}$	0.21 ± 0.03
C ₂ H ₄	$(8.5 \pm 0.3) \times 10^{-11}$	0
cis-2-Butene	$(2.4 \pm 0.1) \times 10^{-10}$	0
Methyl Acetylene	$(1.4 \pm 0.1) \times 10^{-10}$	0

*Data show some curvature at low T. Experiments at lower temperatures are in progress.

The NH ($a^1\Delta$) reactions with unsaturated hydrocarbons show no statistically significant variation in rate over the 25-250°C range, with the rates $k \approx 10^{-10} \text{ cm}^3 \text{ sec}^{-1}$ being essentially gas kinetic. Methane, propane and H₂ reactions show definite temperature dependent rates, with activation energies of about 0.3 KJ/mole. The rate constants for the latter reactants at 25°C are similar to those of CH₂(1A_1) (2), but considerably slower than for O(1D) (3). On the basis of the preliminary data reported here, we believe the existence of nonlinear Arrhenius behavior tentatively observed for the H₂ and CH₄ reactions with NH ($a^1\Delta$) provides evidence for competition between two mechanistic channels. We are extending measurements to lower temperatures to better characterize the nonlinear behavior demonstrated in Fig. 1. In addition, temperature dependent kinetic studies of NH ($X^3\Sigma^-$) reactions are in progress.

REFERENCES

1. a. J. R. McDonald, R. G. Miller, and A. P. Baronavski, Chem. Phys. 30, 133 (1978);
 b. L. G. Piper, R. H. Krech, and R. L. Taylor, J. Chem Phys. 73, 791 (1980).
 c. O. Kajimoto and T. Fueno, Chem. Phys. Lett. 80, 484 (1981); and references therein.
2. W. L. Hase and J. W. Simons, J. Chem. Phys. 54, 1277 (1971).
3. a. P. Michaud and R. J. Cventanovic, J. Phys. Chem. 76, 1375 (1972).
 b. C. L. Lin and W. B. Demore, J. Phys. Chem. 46, 2500 (1976).
4. a. S. Tsunashima, J. Hamada, M. Hotta, S. Sato, Bull. Chem. Soc. Jpn. 53, 2443 (1980).
 b. J. Hamada, S. Tsunashima, and S. Sato, Bull. Chem. Soc. Jpn., 55, 1739 (1982).
5. J. R. McDonald, R. G. Miller, and A. P. Baronavski, Chem. Phys. Lett. 51, 57 (1977).

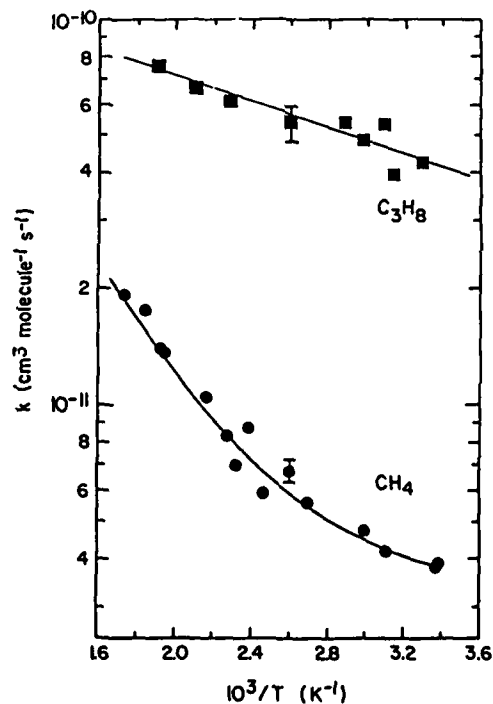


FIG. 1. Arrhenius plot for the reaction of $\text{NH} (a^1\Delta)$ with propane and methane. The error bars are $\pm 2\sigma$. The fit to the CH_4 data is the sum of two second order rates.

Classical trajectory calculations of the Br₂-graphite surface
scattering

Gunnar Nyman and Leif Holmlid
Department of Physical Chemistry
University of Göteborg and
Chalmers University of Technology
S-412 96 Göteborg

Classical trajectory calculations have been carried out to model the experiments made by Holmlid et al. on Br₂ colliding with a graphite surface [1]. The experiments show very low intensity in the specular direction. The main aim of the calculations have therefore been to investigate the conditions for inelastic scattering.

We have solved the equations of motion for these systems using a variable-order variable-step Gear method intended for stiff systems. The incoming Br₂ particle is taken as spherical with no internal degrees of freedom. This particle interacts with one particle in a flat surface through a Lennard-Jones 12-6 potential, giving a one-dimensional problem.

The graphite surface has been modelled in two ways. In the first model the surface particle is tied to a fixed point below with a force constant corresponding to the force between two graphite layers. In the second model there are two

identical particles, corresponding to two layers moving relative to the fixed point.

The Br_2 mass is so large that multiple collisions with the surface is necessary to scatter the Br_2 particle. A trajectory with one carbon atom in the surface is shown in Fig. 1. Note that the scattering is elastic despite the Br_2 bounce and the total of eight hits against the C atom. To get inelastic scattering the vibrational period of the graphite lattice must be comparable to the time of strong interaction. Otherwise, the Br_2 will feel an approximately "symmetric" time variation of the force around the turning point, which will give elastic scattering.

Br_2 is further large enough to collide with more than one carbon atom. To model this the mass of the surface particle has been varied, taking care that the vibrational amplitude is not changed. Increased mass of the surface particle, larger potential well depth and a higher speed of incidence tends to increase the inelasticity.

In Fig. 2 the elastic scattering for the surface particle with $M=12$ is compared to the inelastic pattern for $M=72$ with no other differences in the two runs. The $M=72$ figure is very similar to the experimental results and to the simple one-phonon transfer model used previously [1,2] to interpret our experiments. Note especially the very small elastic fraction.

References

1. L. Holmlid, A. Sigurdsson and G. Nyman, Surface Sci. 119(1982)107.
2. L. Holmlid and G. Nyman, to be published.

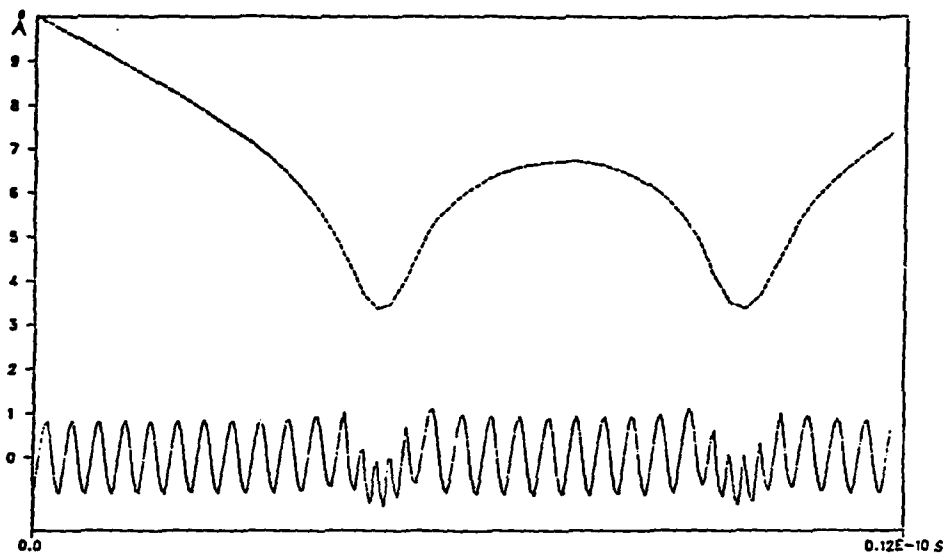


Fig. 1.

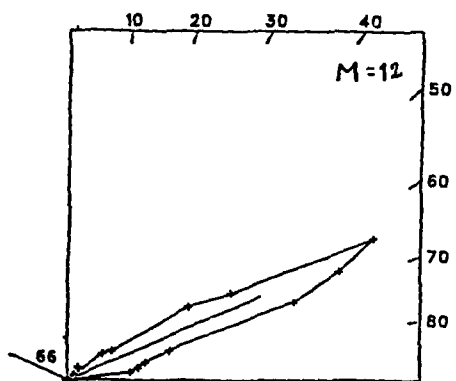


Fig. 2, M=12.

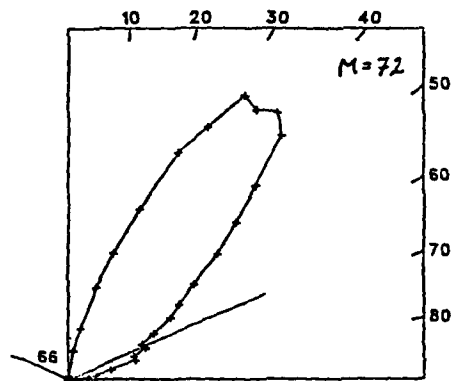


Fig. 2, M=72.

THE REACTION OF METHYL RADICALS WITH NEOPENTANE
IN FLOW PHOTOLYSIS AT 607 - 823 K

Hiroshi Furue, Kim C. Manthorne, Philip D. Pacey

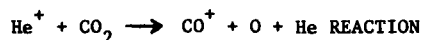
Department of Chemistry
Dalhousie University
Halifax, Nova Scotia, Canada
B3H 4J3

Reaction 1 has previously been studied by pyrolysis of neopentane above 700 K

$$[1] \quad \text{CH}_3 + \text{C}(\text{CH}_3)_4 \rightarrow \text{CH}_4 + (\text{CH}_3)_3\text{CCH}_2$$

and by photolysis of acetone, azomethane and dimethyl mercury in neopentane below 600 K. These studies revealed a significant difference in activation energies, (67 - 90 kJ mol⁻¹ above 800 K, 42 - 50 kJ mol⁻¹ below 600 K) suggesting that the Arrhenius plot for the reaction is curved. In the present study, data have been obtained from 607 to 823 K, where data had been scarce, by generating methyl radicals by photolysis of acetone in a flow reactor. An intermediate activation energy, 62(±2) kJ mol⁻¹, has been found. (Quoted uncertainties are standard deviations.) In combination with data from the literature for the temperature range 245 - 953 K, the Arrhenius plot is found to be strongly curved, with a heat capacity of activation, dE_A/dT , of 71(±4) JK⁻¹ mol⁻¹. This value will be discussed.

A STUDY OF THE PRODUCT STATES OF THE



D.C. Parent, M. Chevrier, G. Mauclaire, M.T. Bowers^o and R. Marx

LREI, Bât. 350, Université de Paris-Sud, 91405 Orsay Cedex, FRANCE

Dept. of Chemistry, University of California, Santa Barbara, Ca. 93106 USA

Thermal energy charge transfer reactions have been studied for several years by measuring the product ion kinetic energy by an ion cyclotron resonance (ICR) technique developed at Orsay.¹ In this paper the study of the dissociative charge transfer reaction



is presented. Five pairs of $\text{CO}^+, 0$ electronic states are energetically accessible. The exoergicity of the reaction

$$\Delta E = 5.12 \text{ eV} = \text{KE}(\text{He}, \text{CO}^+, 0) + \text{IE}(\text{CO}^+, 0) \quad (2)$$

can be partitioned into excess kinetic energy of the products or internal (electronic, vibrational and rotational) energy of CO^+ and O. (He cannot be electronically excited with the available energy.)

The experimental kinetic energy curve is shown in Figure 1, where f is the fraction of ion trapped and is given by

$$\begin{aligned} f &= (V_o/E_k)^{1/2} && \text{when } V_o \leq E_k \\ f &= 1 && \text{when } V_o \geq E_k \end{aligned} \quad (3)$$

where V_o is the trapping well depth and E_k is the kinetic energy of the ion, CO^+ in this case. The kinetic energy of CO^+ is obtained directly from the "breaks" in the curve.

The total kinetic energy cannot be determined from the kinetic energy of CO^+ alone. In order to proceed it is necessary to assume that the charge transfer proceeds via a resonant long-range electron jump. This

has been found to be valid for all other dissociative charge transfer reactions.¹⁻³ Then the He has no excess energy and that of O is calculated by momentum conservation from the measured CO⁺ kinetic energy. The results are given in Table 1. For both kinetic energies observed three sets of products are possible.

A study of the spontaneous emission from this reaction found CO⁺ in the A state with high v.⁴ This could correspond to the product at 0.48 eV kinetic energy or it could represent only a small fraction of the products which was not observed in the kinetic energy study, which has an observation sensitivity limit of about 10% of the total products.

Laser-induced fluorescence studies of the X state of CO⁺ are underway in order to obtain more information on this reaction.

References:

- ¹ G. Mauclaire, R. Deraï, S. Fenistein and R. Marx, J. Chem. Phys., 70, 4017, (1979).
- ² R. Deraï, G. Mauclaire and R. Marx, Chem. Phys. Lett., 86, 275, (1982).
- ³ G. Mauclaire, R. Deraï, S. Fenistein and R. Marx, J. Chem. Phys., 70, 4023, (1979).
- ⁴ M. Gérard-Aïn and T.R. Govers, unpublished results.

Figure 1. Kinetic Energy Curve of CO^+

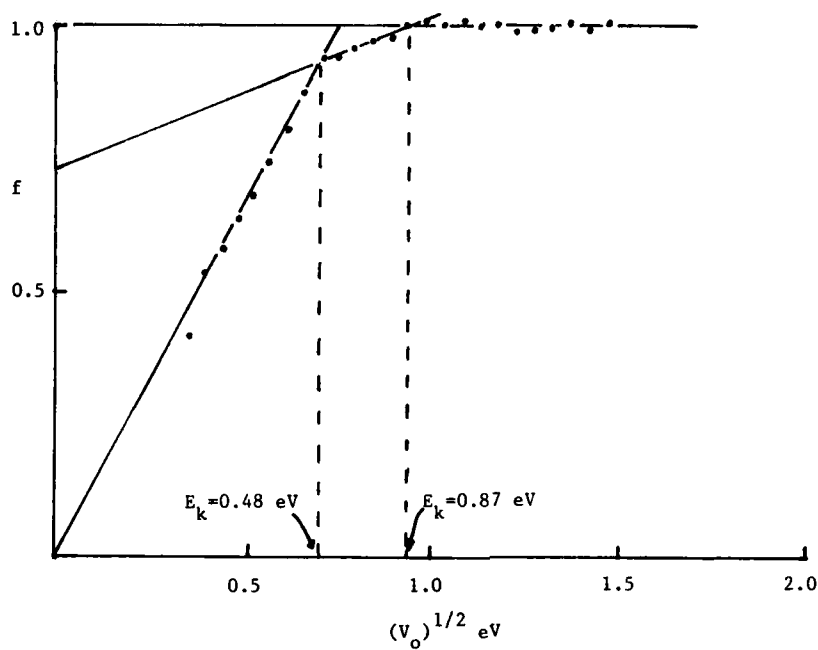


Table 1. $\text{He}^+ + \text{CO}_2 \rightarrow \text{CO}^+ + \text{O} + \text{He}$

Total KE (eV)	Total IE (eV)	Possible Product States [°]	%
1.36 ± 0.04	3.76	$\left\{ \begin{array}{l} \text{CO}^+(\text{X}, 14-15) + \text{O}(^3\text{P}) \\ \text{CO}^+(\text{X}, 6) + \text{O}(^1\text{D}) \\ \text{CO}^+(\text{A}, 6) + \text{O}(^3\text{P}) \end{array} \right\}$	70-75
2.43 ± 0.12	2.69	$\left\{ \begin{array}{l} \text{CO}^+(\text{X}, 9-10) + \text{O}(^3\text{P}) \\ \text{CO}^+(\text{X}, 1-2) + \text{O}(^1\text{D}) \\ \text{CO}^+(\text{A}, 0-1) + \text{O}(^3\text{P}) \end{array} \right\}$	25-30

[°] CO^+ notation is electronic state, vibrational level.

ABSOLUTE RATE CONSTANTS FOR THE REACTION OF $O(^3P)$ ATOMS WITH
 ETHENE, PROPENE, PROPENE-d6, 1,BUTENE, CIS-2-BUTENE,
 TRANS-2-BUTENE AND ISOBUTENE OVER THE TEMPERATURE RANGE 260-860 K*

---Robert A. Perry, Sandia National Laboratories,
 Livermore, California 94550

ABSTRACT

A laser photolysis chemiluminescence technique has been used to measure O atom reaction rate coefficients for ethene, propene, deuterated propene and the isomers of butene over the temperature range 260-860 K. A fluorine laser (157 nm, 10 mJ/pulse) was used to produce the O atoms via O_2 photolysis in an argon-oxygen-nitric oxide-olefin mixture. The following empirical expressions are the best fits to the data:

$$\begin{aligned} k_{\text{ethene}} &= 1.6 \times 10^{-14} T^{1.0} e^{-1040/RT} , \\ k_{\text{propene}} &= 3.4 \times 10^{-19} T^{2.56} e^{1130/RT} , \\ k_{\text{propene-d6}} &= 3.4 \times 10^{-19} T^{2.53} e^{1210/RT} , \\ k_{1,\text{butene}} &= 1.2 \times 10^{-18} T^{2.34} e^{1050/RT} , \\ k_{\text{cis-2-butene}} &= 7.1 \times 10^{-18} T^{2.07} e^{1750/RT} , \\ k_{\text{trans-2-butene}} &= 4.1 \times 10^{-18} T^{2.17} e^{1800/RT} , \\ k_{\text{isobutene}} &= 7.1 \times 10^{-18} T^{2.11} e^{1800/RT} \text{ cm}^3 \text{ molecule}^{-1} \text{ sec}^{-1} . \end{aligned}$$

*Work supported by the U.S. Department of Energy, Office of Basic Energy Sciences.

Figure 1 shows a summary of the data for ethene, propene, and propene-d6 while Fig. 2 shows the the plots of the data for the isomers of butene. While efforts were made to fit this data using a simple transition state theory model, as discussed by this author (1) and Singleton and Cvetanovic (2), the pronounced curvature in the plots for the isomers of butene requires a three parameter fit with unreasonably low vibration frequencies for C_2O vibration mode and a negative activation energy in addition to the temperature dependent A factor.

These results will be compared to the predictions of Singleton and Cvetanovic and the implications that these results imply for combustion modeling will be discussed.

References

1. R. A. Perry, J. Chem. Phys. 80, 153 (1984).
2. D. L. Singleton and R. J. Cvetanovic, J. Am. Chem. Soc. 98, 6812 (1976).

Fig. 1. Arrhenius plots of rate constants for reactions of $O + \text{ethene}$, \circ , propene, Δ ; and propene- d_6 , $+$. Solid lines are best fit to data.

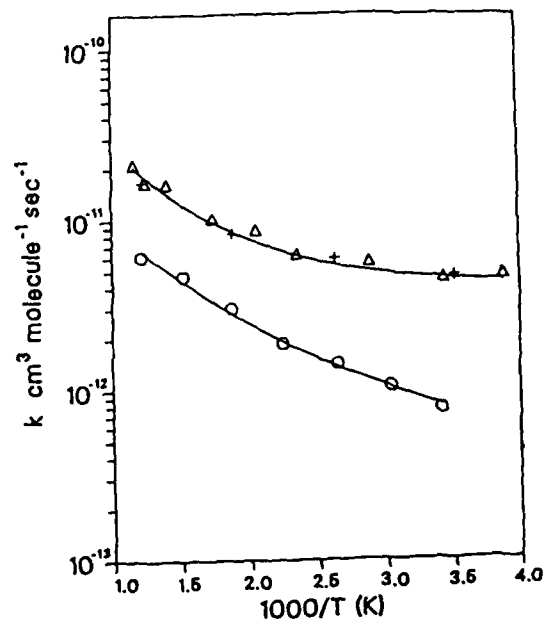
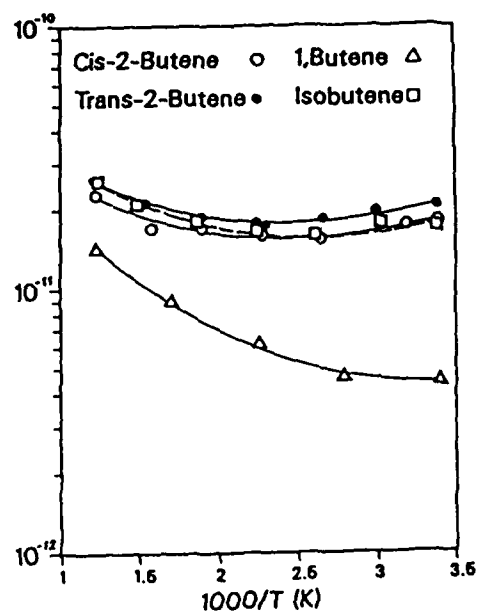


Fig. 2. Arrhenius plots of rate constants for reactions of $O + 1, \text{butene}$, Δ ; trans-2-butene, \bullet ; cis-2-butene, \circ ; and isobutene, \square .



A COMPREHENSIVE STUDY OF THE "WALL EFFECTS" MECHANISM
DUE TO GAS/SURFACE REACTIONS BY USE OF HIGH SURFACE AREA PARTICLES

J.C. PETIT, H. JAMES

C.N.R.S. - Centre de Recherches sur la Chimie de la Combustion
et des Hautes Températures, 45045 ORLEANS CEDEX, FRANCE

Although the heterogeneous effects occurring during combustion and pyrolysis have long been observed, it is only recently that attention has been focused toward the "wall effects" mainly for fundamental understanding. The chemical role played by the reactor walls has been postulated but only considered in a few occasions (1); however, in the majority of pyrolysis studies, it is the physical role which has been studied.

In the present work, we have used the system cyanogen/silica in conditions allowing an enhancement of the "wall effects" (previously observed in the slow combustion of this compound in a silica reactor (2)) hence allowing us to study in a systematic manner both the chemical evolution of the solid surface and of the gas phase.

A significant increase of the interface ($\times 10^5$) has been obtained by evenly distributing along the length of the reactor a silica sample of high surface area (AEROSIL DEGUSSA $300 \text{ m}^2.\text{g}^{-1}$).

Due to the complexity of the reactions occurring, the work has been divided in three studies :

1. Chemisorption of cyanogen on silica at 693 K accompanied by $\geq \text{SiNCO}$, $\geq \text{SiCN}$, $\geq \text{SiNC}$ formation (3) (4).
2. Pyrolysis of surface species formed in 1 by a Thermal Programmed Desorption (5).
3. Isothermal pyrolysis of cyanogen at 1273 K. Only this third step will be considered hereafter.

When successive equal doses of cyanogen are admitted for a 24 hour pyrolysis period, the removal (before each new introduction) and the subsequent analysis of the resulting gas phase lead to the results reported. These show clearly (Fig. 1) that two regions are present.

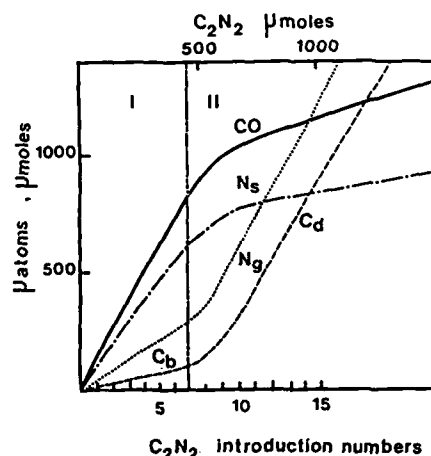
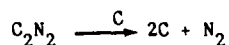


Fig. 1. Evolution of the quantity of gas formed (CO and nitrogen N_2), versus the cyanogen converted; N_s , C_b , C_d represent respectively the nitrogen and the carbon remaining bound on the carbon deposited on the surface.

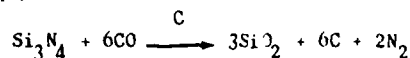
where the different theoretical ratios of CO/N_2 , CO/C_2N_2 are experimentally verified.

This heterogeneous oxidation of cyanogen is stopped when almost a monolayer of silicon nitride has replaced the silica surface. At this time, oxygen is no more available, and a silicon carbide is assumedly formed, leading ultimately to a carbon deposit.

Region II corresponds mainly to the elemental heterogeneous decomposition reaction of cyanogen on the carbon deposit :

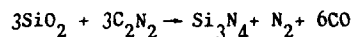


A minor source of carbon deposition has been observed when carbon deposits are already present. Under these conditions carbon monoxide reacted (probably in the adsorbed state on carbon) with Si_3N_4 to produce silica, carbon and nitrogen :



Region I corresponds to the oxydative pyrolysis of cyanogen

where the surface species : $\geq SiNCO$, $\geq SiNC$ and $\geq SiNC$ are successively formed and destroyed (with CO and N_2 release). The major part of carbon is liberated as CO (and a quasi total carbon liberation is possible by increasing the pyrolysis period up to 100 hours) whereas only a small part of the nitrogen is liberated in the gas phase (1/3) the main part remaining bound onto the surface as a silicon nitride Si_3N_4 . The corresponding reaction being :



In consequence, to prevent a partial reoxidation of the surface when carbon deposits are present, CO must be removed as soon as formed.

The evolution of silica surface during the course of the interaction cyanogen/silica can be summarized :

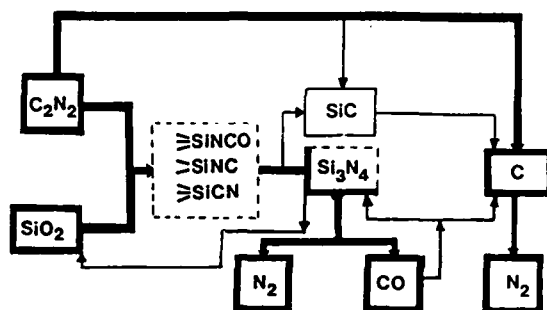


Fig. 2. Schema of cyanogen reactions with silica

This work is an example of the chemical evolution undergone by a silica surface in the course of a pyrolysis reaction where the major products have been identified and measured.

REFERENCES

1. L.R. MARTIN, A.G. WREN and M. WUN, Int. J. Chem. Kinet. 11 (1979) 543.
2. J. JEANJEAN, H. JAMES, 2ème Symposium sur la Combustion, Orléans 1975, I p. 109.
3. B.A. MORROW and I.A. CODY, J. Chem. Soc. Farad. Trans. I, 71 (1975) 1021.
4. J.C. PETIT, H. JAMES, Thermochimica Acta 35 (1980) 111.
5. J.C. PETIT, H. JAMES, Thermochimica Acta 69 (1983) 323.

MODEL CALCULATIONS ON THE METHANE PYROLYSIS

M. H. Back, University of Ottawa

R. A. Back, National Research Council, Canada

J. M. Roscoe and M. J. Thompson, Acadia University

The literature on the thermal decomposition of methane is extensive and has recently been reviewed.¹ In spite of this, there are several unexplained features of the decomposition even at comparatively small conversions. One of these is the marked autocatalysis, particularly evident in the C_2H_6 yield, which sets in shortly after the appearance of C_2H_2 and allene. Computer modelling of the methane pyrolysis has not been reported and it seemed that such an approach might elucidate the origin of the autocatalysis.

The set of differential equations defined by the mechanism was integrated numerically using an extended form of the integration package described by Stabler and Chesick.² Kinetic parameters were obtained from recent critical compilations. The pressure dependence of the rate constants for radical decomposition was estimated from experimental data where possible or by careful downward adjustment from their high pressure limits when fitting to experimental yields.

Rate constants were adjusted to fit the very extensive data of Chen *et. al.*³ fitting one product at a time. The rate constants to be adjusted were chosen on the basis of a first order sensitivity analysis to indicate those rate constants which would achieve the desired result with the smallest change from their initial values. The fitting was done in three stages, based on extent of reaction, since the sensitivity coefficients were strongly time dependent and suggested three fairly distinct phases of reaction at the conversions for which calculations were feasible. When a rate constant had been adjusted to give optimum fit in the time regime where it had its maximum effect, its value was not altered in the other time domains. Reactions were discarded only if they produced less than 1% change in any product yield when dropped from the mechanism.

The final fitting was done with a 62-step mechanism including the following classes of reactions:

- (a) Hydrogen abstraction from CH_4 , C_2H_6 , C_2H_4 and C_3H_6 by H and by all radicals smaller than C_4 .
- (b) Addition to C_2H_2 , C_2H_4 and C_3H_6 by H and by all radicals smaller than C_3 .
- (c) Dissociation of all radicals larger than CH_3 .
- (d) Recombination and cross-combination of all radicals smaller than C_3 .
- (e) Isomerization of C_3 radicals.
- (f) Dissociation of CH_4 , C_2H_6 and C_3H_6 .

The products C_2H_6 , C_2H_4 , C_2H_2 , C_3H_6 , allene and H_2 were used for fitting and the calculations were stopped at conversions slightly less than those at which carbon formation is first observed.

It was possible to obtain agreement with experiment to within the stated uncertainty of the experimental data for all the main reaction products to well into the autocatalytic stage of the reaction. The radicals to which autocatalysis was most sensitive were CH_3 and $1\text{-C}_3\text{H}_7$ although there was some sensitivity to all radicals and, in fact, to nearly half the reactions retained in the final mechanism. As expected, the concentration of CH_3 is predicted to be much larger than that of any other radical. The concentrations of C_2H_5 and C_2H_3 reach values about three orders of magnitude less than CH_3 . The concentrations of C_3H_5 and CH_3CHCH rise to about one tenth that of the C_2 radicals and the concentrations of $1\text{-C}_3\text{H}_7$ and $2\text{-C}_3\text{H}_7$ rise to comparable concentrations which are some ten times smaller than those of the unsaturated C_3 radicals.

The concentrations of the products are very sensitive to the decompositions of the radical intermediates, presumably because hydrogen abstraction from the parent molecule is more difficult than in the pyrolysis of the higher alkanes. This is also reflected in the preponderance of unsaturated products. However, the comparatively high temperature required for pyrolysis of CH_4 , combined with the large CH_4 concentration, makes hydrogen abstraction from CH_4 more important than hydrogen abstraction from reaction products for radicals other than CH_3 .

Radical addition to unsaturated products is the only route to high molecular

weight species and is therefore important. However, addition reactions of CH_3 predominate both because of the comparatively large concentration of this species and because of the trend to decreasing rate constants with increasing complexity of the radical. Among other reactions, isomerization is unimportant and the only significant termination step is recombination of CH_3 .

While it is not possible to assign responsibility for autocatalysis to any single reaction, some reactions seem to be particularly important. Autocatalysis is particularly sensitive to $\text{C}_3\text{H}_6 \xrightarrow{1} \text{CH}_3 + \text{C}_2\text{H}_3$ but is insensitive to the analogous decompositions in which a H atom is eliminated. The only other product decomposition resulting from C-C bond cleavage is $\text{C}_2\text{H}_6 \xrightarrow{2} 2 \text{CH}_3$. The sensitivity to this reaction is fairly large throughout the reaction. Autocatalysis is not particularly sensitive to it although drastic changes in k_2 or $k_{2(R)}$ cause large changes in autocatalysis. The addition reaction to which autocatalysis is most sensitive is $\text{CH}_3 + \text{C}_2\text{H}_4 \xrightarrow{3} 1\text{-C}_3\text{H}_7$. The H atom addition $\text{H} + \text{C}_2\text{H}_4 \xrightarrow{4} \text{C}_2\text{H}_5$ is also important although to a lesser extent. The radical decompositions to which autocatalysis shows the greatest sensitivity are $1\text{-C}_3\text{H}_7 \xrightarrow{5a} \text{C}_3\text{H}_6 + \text{H}$ and $1\text{-C}_3\text{H}_7 \xrightarrow{5b} \text{CH}_3 + \text{C}_2\text{H}_4$. Reaction 5a increases the extent of autocatalysis while 5b has the opposite effect. Reactions leading to C_3H_6 tend to accentuate autocatalysis by promoting the build up of radicals via reaction 1. Reactions leading to C_2H_5 , except via C_2H_6 , also accentuate autocatalysis via abstraction reactions such as $\text{C}_2\text{H}_5 + \text{CH}_4 \rightleftharpoons \text{C}_2\text{H}_6 + \text{CH}_3$. Bimolecular reactions of unsaturated products such as $2 \text{C}_2\text{H}_4 \rightleftharpoons \text{C}_2\text{H}_5 + \text{C}_2\text{H}_3$ had no significant effect on the autocatalysis.

REFERENCES:

1. M. H. Back and R. A. Back in "Pyrolysis: Theory and Industrial Practice", Academic Press, New York, 1983.
2. R. N. Stabler and J. P. Chesick, Int. J. Chem. Kinet., 10, 461 (1978).
3. C.-J. Chen, M. H. Back and R. A. Back, Can. J. Chem., 53, 3580 (1975);
C.-J. Chen, M. H. Back and R. A. Back, Can. J. Chem., 54, 3175 (1976).

Laser Induced Fluorescence Studies of the Quenching Kinetics of N_2 $B^3\Pi_g$, $v = 1-11$ and $B'^3\Sigma_u^-$, $v = 4-6$ I. Bar, A. Rotem and S. Rosenwaks

Department of Physics
Ben-Gurion University of the Negev
Beer-Sheva, Israel

Extended Abstract

Selective excitation of $N_2(B^3\Pi_g, v = 1-11)$ was obtained by applying a pulsed electrical discharge followed by a pulsed laser beam to mixtures of N_2 , Ar and Ne at pressures in the Torr range. The wavelength- and time-resolved fluorescence of the excited levels was measured and analysed as a function of gas composition. In all cases, multiple exponential decay was observed. The fast, initial decay is attributed to collisional equilibration of B, v with an adjacent, strongly coupled vibronic level (or levels) and the subsequent, slower decays, to weaker coupling of B, v and its adjacent mate to other levels.

By comparing the measured amplitude ratios between the first and the second decay curves of $N_2(B, v)$ to statistical mechanics calculations, the main route for the initial decay has been identified. It has been concluded that in most cases the triplet states (mainly W but also B' and A) are strongly coupled to the B, v levels. The quenching kinetics of $N_2(B', v = 4-6)$, collisionally populated following the laser production of $N_2(B, v+4)$, was studied as well.

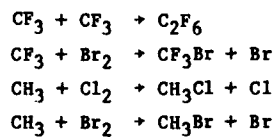
The rate constants for the strong collisional coupling between B,v and adjacent levels by N_2 and Ar are found to be very large, of the order of $10^{-10} - 10^{-11} \text{ cm}^3 \text{ s}^{-1}$. This implies that interpretations of the quenching kinetics of electronically excited N_2 in an environment which is not collision-free should take into account the energy flow between adjacent N_2 levels. An example of such an environment is the upper atmosphere. The characteristics of the auroral optical emission can be explained taking into account the rate constants for the collisional coupling in the N_2 triplet manifold found in the present work.

ABSOLUTE RATES OF FREE RADICAL REACTIONS
AND THEIR TEMPERATURE DEPENDENCE

Nur Selamoglu, Michel Rossi, and David M. Golden
SRI International, Menlo Park, CA 94025

Abstract

Absolute rates of free radical reactions and their temperature dependence have been studied by the VLF Φ technique. Among these are methyl and trifluoromethyl radicals and their reactions with bromine and chlorine, e.g.,



The Reactivity of Hydrogen and Deuterium
Atoms Trapped at a Glass Surface

G. McLeod and D.B. Sheen
 University of Strathclyde

Hydrogen and deuterium atoms, generated by molecular dissociation at an incandescent filament, are trapped on the surface of a 1dm³ Pyrex glass bulb, and their reactions studied using mass spectrometric and ultra high vacuum techniques. The changes in pressure of hydrogen that occur under dynamic flow conditions during and after dissociation are used to determine the rates of adsorption and recombination of the atoms. A kinetic analysis can be carried out by relating the rates to the amount of hydrogen present on the surface.

For recombination at 273K, both Eley-Rideal and Langmuir-Hinshelwood processes are identified. It is observed that only a minor portion (3 - 7%) of the adsorbed hydrogen participates in either of the recombination reactions. As the amount of this weakly bound hydrogen increases proportionately with the total hydrogen present on the surface, it is suggested that the more strongly bound atoms act as the trapping sites for those weakly bound atoms involved in recombination. The steady state coverage of these weakly bound atoms appears to be maintained by fast adsorption and recombination reactions.

A model, based on these observations, is developed to explain the kinetic data. In this model, $(2R_A(t) - R_{LH}(t)) / (2R_{ER}(t) + R_{LH}(t)) = (R_f(t) + R(t)) / (R_f(t) - R(t)) = K_1(1/n(t)) + K_2$ where $R_f(t)$ and $R(t)$ are the experimentally determined rates of dissociation of hydrogen at the filament

and uptake by the glass wall at time t , $R_{ER}(t)$ and $R_{LH}(t)$ the rates of recombination by Eley - Rideal(ER) and Langmuir-Hinshelwood(LH) mechanisms, $R_A(t)$ the rate of adsorption, $n(t)$ the amount of hydrogen present on the surface and K_1 and K_2 constants. A similar model is used to interpret the results at 77K.

The absence of HD as a product in deuterium experiments implies that surface hydroxyl groups present on the glass surface in no way participate in the recombination reactions.

When hydrogen atoms are trapped at 77K and the glass allowed to warm up under dynamic flow conditions, a number of peaks occur in the desorption 'spectrum' corresponding to maxima in the rates of desorption. These peaks are identified with different sorbed states of the hydrogen atoms. Several such states occur in the range 77 - 600K. If the warm up process occurs in the presence of molecular oxygen, the water profile obtained coincides almost precisely with that for the recombining hydrogen. Thus oxygen does not appear to react with hydrogen atoms on the surface unless they are undergoing recombination and are hence mobile. The reaction with oxygen that occurs leads to a surface modification which affects the recombination reactions and which is permanent up to temperatures in excess of 600K.

Primary Process in the Photolysis of Acetaldehyde.G.N. Bagnall and H.W. Sidebottom

Chemistry Department, University College, Dublin, Ireland.

ABSTRACT

The photochemistry of acetaldehyde has been extensively studied both with regard to the nature of the primary dissociative processes and the subsequent secondary radical reactions. However, uncertainty still remains concerning the nature and extent of the primary photodissociative reactions. Recent work indicates that the major dissociation pathway occurs from the vibrationally rich first excited triplet state. Since the decay of triplets is controlled to a significant extent by the rate constant for triplet decomposition, triplet lifetime data should provide information on the mechanism and rate constants for triplet state decomposition. The triplet lifetime of acetaldehyde has been determined in the gas phase as a function of temperature and concentration utilising time-resolved laser-excited phosphorescence. The results help to clarify the role of the triplet state in the photodissociative processes.

REACTIONS OF POLYAROMATIC MOLECULES IN GAS AND
LIQUID PHASES

S.E. Stein

National Bureau of Standards, United States Department
of Commerce, Washington DC 20234, U.S.A.

This research has determined elementary rate constants and mechanisms for reactions of multi-ring aromatic molecules and radicals in gas and condensed phases. Very low pressure pyrolysis was used for gas studies; high temperature liquid pyrolysis (250 - 500°C) was used for condensed phase studies. Elementary kinetics studies involved resonance stabilised radicals such as diphenylmethyl and mechanistic studies focussed on anthracene and phenanthrene dimerisation.

Elementary reactions of the SO radical

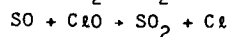
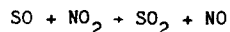
by

J. Brunning and L. J. Stief

Laboratory for Extraterrestrial Physics

NASA/Goddard Space Flight Center, Greenbelt, Maryland 20771, U. S. A.

The kinetics and temperature dependence of the ground state $\text{SO } X^3\Sigma^-$ radical have been studied using the discharge flow - mass spectrometric technique near 1 Torr total pressure. Ground state SO radicals were generated by a microwave discharge in dilute SO_2/He mixtures. S and O atom impurities were removed using a discharge bypass technique. Mass spectrometric detection of the SO radical has been used to study the kinetics for the following reactions in the temperature range 210-400 K:



TEMPERATURE DEPENDENCE OF O-ATOM REACTIONS WITH OLEFINS

R. Browarzik and F. Stuhl

Ruhr-Universität, Physikalische Chemie I,

D-4630 Bochum, West Germany

Extended Abstract

Beginning with the pioneering work of Cvetanovic¹⁾, reactions of oxygen atoms with olefins have been studied for decades. Recently, this field of reactions has gained renewed interest since molecular beam²⁾ and modulated spectroscopy³⁾ studies have given detailed insight into the formation of primary products^{2,3)} and into threshold energies for the various reaction pathways²⁾. Moreover, pressure dependent kinetic parameters have been suggested from recent photolysis work³⁾.

Therefore, we have reinvestigated several O atom reactions with simple olefins using H₂ laser ($\lambda \approx 160$ nm, $\tau \approx 1$ ns) photolysis of NO to produce the atoms. The O atoms were sensitively monitored by the O + NO-chemiluminescence. Decays of O atom concentrations ranging from initial values of about 10^{10} to about 10^8 atoms cm⁻³ were measured in the temperature range 197 to 373 K. So far, temperature dependent rate constants were determined for the reactions O + ethene, propene and 1-butene. The rate data for ethene ($E_a = (6.3 \pm 1.0)$ kJ mol⁻¹ and $A = (8.4 \pm 2.7) \cdot 10^{-12}$ cm³s⁻¹) agree well with most of the recent literature⁴⁾. The Arrhenius plots for the rate constants for propene and 1-butene are found to be slightly curved. Fig. 1, for example, shows the data for propene in an Arrhenius presentation. This figure clearly demonstrates that the activation energy in this temperature range is significantly different from zero and therefore is at variance with a

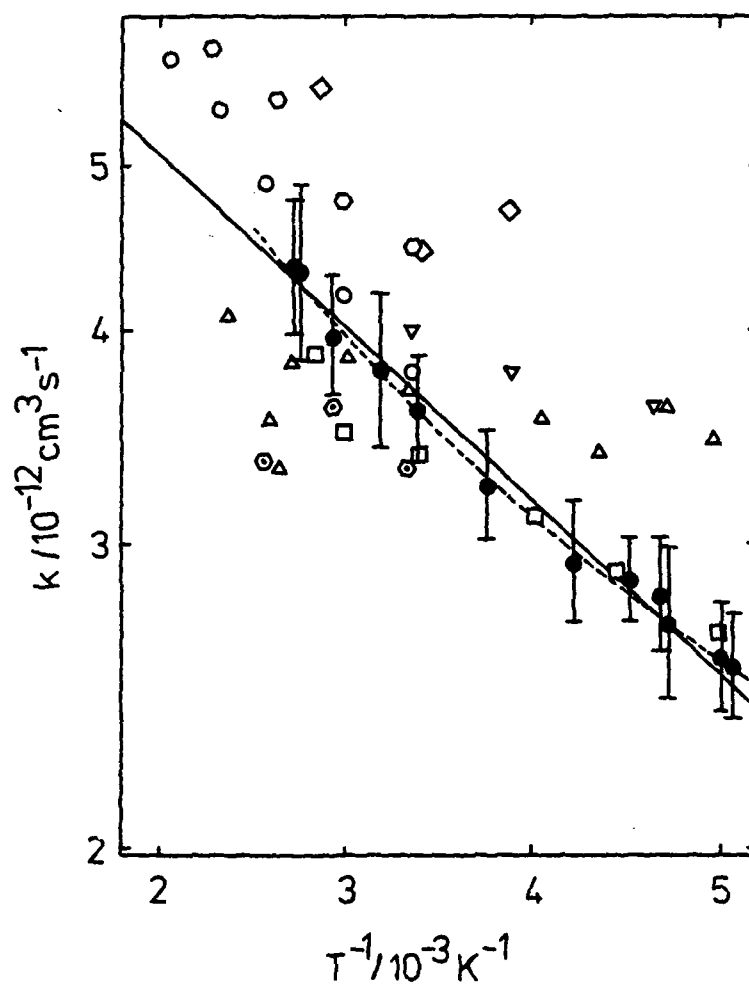


Fig. 1 : Arrhenius plot for the rate constants of the reaction $\text{O} + \text{C}_3\text{H}_6$ (full circles). The indicated error limits represent three times the standard deviation. Included are the data reported in Ref. 5, Δ ; 6, \square ; 7, \circ ; 8, \diamond ; 9, ∇ ; 10, \odot ; 11, \ominus .

previous recommendation⁵⁾.

No pressure dependence of the rate constants was observed for pressures ranging from 2.2 to 34 mbar.

A comparison with literature data for all three reactants⁴⁻¹¹⁾ shows that the data previously obtained by Singleton and Cvetanovic⁷⁾ is in good agreement with the data obtained in the present work. Their data hence appears to be an appropriate addition at higher temperatures for our low temperature data. We found that simple transition state theory can explain the curvature in the Arrhenius plot^{7,8)}, but does not provide unique values for E_a , A and ω . The present data will be discussed with respect to the threshold energies recently reported²⁾.

Financial support of the Deutsche Forschungsgemeinschaft is gratefully acknowledged.

References

- 1) R.J. Cvetanovic, Adv. Photochem., 1, 115 (1963).
- 2) K. Kleinermanns and A.C. Luntz, J. Phys. Chem., 85, 1966 (1981).
- 3) H.E. Hunziker, H. Knepe and H.R. Wendt, J. Photochem., 17, 377 (1981).
- 4) A.A. Westenberg and N. de Haas, 12th Symp. (Int.) on Combustion, p. 289 (The Combustion Institute, Pittsburgh (1969)).
- 5) J.T. Herron and R.E. Huie, J. Phys. Chem. Ref. Data, 2, 467 (1973).
- 6) K. Kohse-Höinghaus, Dissertation, Ruhr Universität Bochum, 1978.
- 7) D.L. Singleton and R.J. Cvetanovic, J. Am. Chem. Soc., 98, 6812 (1976).
- 8) R.A. Perry, J. Chem. Phys., 80, 153 (1984).
- 9) M.J. Kurylo, Chem. Phys. Lett., 14, 117 (1972).
- 10) R. Atkinson and J.N. Pitts, Chem. Phys. Lett., 27, 467 (1974).
- 11) R. Atkinson and J.N. Pitts, J. Chem. Phys., 67, 38 (1977).

Radiative Lifetime and Quenching of Metastable $\text{NH}(\text{b}^1\Sigma^+)$ U. Blumenstein, F. Rohrer and F. Stuhl

Ruhr-Universität, Physikalische Chemie I, D-4630 Bochum, West Germany

Long Abstract

Since its forbidden transition to the ground state has been observed^{1,2)} several experiments have been performed to determine the radiative lifetime and the quenching of the metastable $\text{NH}(\text{b}^1\Sigma^+)$ -state.³⁻⁶⁾ While, in general, the results from various quenching studies^{4,5,7-9)} (which all have been performed at room temperature) do not greatly deviate, the literature values for the radiative lifetime are spread over almost two orders of magnitude ranging from 0.23⁵⁾ to 17⁴⁾ ms. We have therefore initiated a program to reinvestigate the radiative lifetime of $\text{NH}(\text{b}^1\Sigma^+)$. Moreover, for a better understanding of the mechanism, we have begun a study of the temperature dependence of its quenching.

Two different photolysis systems were used to study the decays of $\text{NH}(\text{b}^1\Sigma^+)$. The first system uses the vuv flash photolysis of NH_3 to generate the metastable radicals. Emission from the forbidden $\text{NH}(\text{b}^1\Sigma^+ \rightarrow \text{X}^3\Sigma^-)$ -transition at 471 nm was monitored by an interference filter and a photomultiplier.

The second method uses the newly observed generation of $\text{NH}(\text{b}^1\Sigma^+)$ in the ArF laser photolysis (193 nm) of HN_3 . This process was found to be so efficient that sufficient amounts of $\text{NH}(\text{b}^1\Sigma^+)$ could be generated by photolysing the HN_3 molecules being desorbed from the walls of the photolysis cell. Their decays were monitored by a 0.25 m-monochromator and a photomultiplier.

In the present experiments, the (extrapolated) zero pressure lifetime was taken to represent the radiative lifetime of $\text{NH}(\text{b})$. In the flash photolysis experiments, constant mixing ratios of NH_3 and Ar were

irradiated. In the laser experiments, the partial pressure of HN_3 was found to be so low that quenching by HN_3 was negligible. Hence, simply Ar, He or N_2 was flowed through the cell after the walls had been covered with HN_3 . The presence of an inert gas was necessary in order to minimize diffusion of $\text{NH}(b)$ to the walls at the long lifetimes measured. However, even at pressures around 40 Torr Ar, diffusion could not be eliminated completely. Therefore, a correction for diffusion was introduced by taking the diffusional loss rate to be inversely proportional to the total pressure.

Measured decay rates, τ^{-1} , are plotted vs. the total pressure in Fig. 1. Clearly, at low pressures, diffusion determined the measured value of τ^{-1} . The dashed lines in this figure represent the decay rates corrected for diffusion. It should be noted that the decay rates in the flash photolysis experiments are larger because NH_3 participates in the quenching process besides Ar. The common intercept in Fig. 1 represents the zero pressure decay rate. It determines the radiative lifetime to be $(53 \pm 17; -13)$ ms for these and three additional runs using He and N_2 as buffer gas. This value is much longer than all previous values, but is in good agreement with a recent preliminary theoretical value.¹⁰⁾

From the slopes of plots such as those in Fig. 1 we determined the values for the quenching by HN_3 , He, Ar and N_2 at room temperature to be $k_{\text{He}} = 0.77 \times 10^{-16}$, $k_{\text{Ar}} = 1.0 \times 10^{-16}$, $k_{\text{N}_2} = 5.0 \times 10^{-16} \text{ cm}^3\text{s}^{-1}$, respectively. Additionally, for the flash photolysis system, we have varied the temperature of the cell between 209 and 493 K. Temperature dependent rate constants for the quenching by NH_3 , H_2 , D_2 , Ar, N_2 and He will be reported and discussed.

Financial support by the Deutsche Forschungsgemeinschaft (SFB 42) and Fonds der Chemischen Industrie is gratefully acknowledged.

References

1. A. Gilles, J. Masanet, and C. Vermeil, *Chem. Phys. Lett.* **25** (1974) 346.
2. J. Masanet, A. Gilles, and C. Vermeil, *J. Photochem.* **3** (1975) 417.
3. C. Zetzsch and F. Stuhl, *Chem. Phys. Lett.* **33** (1975) 375.
4. B. Gelernt, S.V. Filseth, and T. Carrington, *Chem. Phys. Lett.* **36** (1975) 238 and *J. Chem. Phys.* **65** (1976) 4940.
5. J. Masanet, C. Lalo, G. Durand, and C. Vermeil, *Chem. Phys.* **33** (1978) 123 and *J. Photochem.* **9** (1978) 171.
6. C. Nguyen Xuan, G.D. Stefano, M. Lenzi, and A. Margani, *J. Chem. Phys.* **74** (1981) 6219.
7. C. Zetzsch and F. Stuhl, *Ber. Bunsenges. Phys. Chem.* **80** (1976) 1354.
8. C. Zetzsch and F. Stuhl, *J. Chem. Phys.* **66** (1977) 3107.
9. C. Zetzsch, *Ber. Bunsenges. Phys. Chem.* **82** (1978) 1098.
10. C. Marian and R.Klotz, to be published

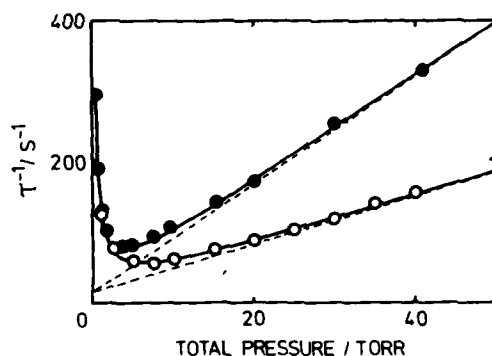


Fig. 1

Decay rates of $NH(b^1_2^+)$ as a function of total pressure. The data of the flash photolysis experiment is shown by full circles; here, the mixing ratio $[NH_3]/[Ar] = 0.00014$. The data of the ArF laser experiment are shown by open circles; only traces of NH_3 are used in Ar. The full curves represent computer fits to the data including diffusion. The straight broken lines represent decay rates corrected for diffusion.

THE STUDY OF ION-MOLECULE REACTIONS IN THE GAS PHASE
USING A TRIPLE QUADRUPOLE MASS SPECTROMETER

BY Alan Mitchell, J. K. Conner and J. M. Tedder

Department of Chemistry, The University, St. Andrews,
Fife KY16 9ST, Scotland

A triple quadrupole mass spectrometer has been used to study the reactions of simple even electron ions (*e.g.* CH_3^+ , CH_2F^+ , *etc.*) with acetylene and substituted acetylenes.

The triple quadrupole mass spectrometer consists of a conventional electron impact ion source attached in series to the first quadrupole (mass filter); the second r.f. only quadrupole (collision chamber); the third quadrupole (mass filter) and to an electron multiplier. Ions formed by electron impact in the ion source are mass-analysed by the first quadrupole. The selected ions pass on into the second quadrupole which holds ions in stable trajectories and into which the collision gas is admitted at relatively high pressure. Differential pumping between the ion source and the collision region prevents mixing of the neutral gases. Ions formed in the collision zone are mass-analysed by the third quadrupole and detected by the electron multiplier.

The base peaks for the reactions of methyl cations and the three fluoromethyl cations with acetylene, propyne and 3,3,3-trifluoropropyne are listed in Table 1.

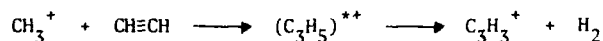
The secondary ion formed in largest yield is C_3H_3^+ from acetylene and the methyl cation. It seems probable that C_3H_3^+ is the cyclopropenium cation. Evidence supporting this conclusion comes from the observation

TABLE I. The Base Peaks in the Reactions of CH_3^+ and Fluoromethyl Cations with Acetylene, Propyne and 3,3,3-Trifluoropropyne

$\text{R}^+ + \text{CH}\equiv\text{CH}$			$\text{R}^+ + \text{CH}_3\text{C}\equiv\text{CH}$			$\text{R}^+ + \text{CF}_3\text{C}\equiv\text{CH}$		
1°	base		1°	base		1°	base	
CH_3^+	C_3H_3^+	(1,600)	CH_3^+	C_2H_3^+	(17)	CH_3^+	C_3HF_2^+	(5)
CH_2F^+	C_3H_3^+	(50)	CH_2F^+	C_3H_5^+	(18)	CH_2F^+	C_3HF_2^+	(74)
CHF_2^+	$\text{C}_3\text{H}_4\text{F}^+$	(9)	CHF_2^+	C_3H_5^+	(20)	CHF_2^+	C_3HF_2^+	(22)
CF_3^+	CHF_2^+	(6)	CF_3^+	$\text{C}_3\text{H}_4\text{F}^+$	(21)	CF_3^+	C_3HF_2^+	(78)

Figures in brackets represent $[\text{Secondary Ions}]/[\text{Total Primary Ions}] \times 10^3$

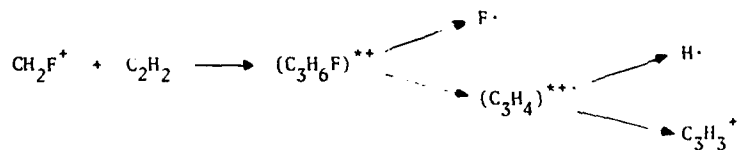
that when CH_3^+ ions are replaced by CD_3^+ , $\text{C}_3\text{H}_2\text{D}^+$ (m/e 40) and C_3HD_2^+ (m/e 41) are formed in equal yield; thus the thermally excited addition complex $(\text{C}_3\text{H}_5)^{++}$ must be symmetrical, and C_3H_3^+ is not therefore the propargyl cation ($\text{CH}_2=\text{C}=\text{CH}^+$) but



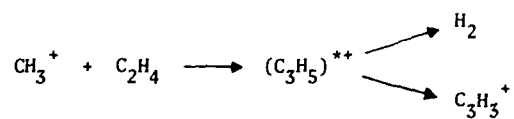
cyclopropenium.

The reactions with propyne yield C_3H_5^+ (C_3H_5^+ and $\text{C}_3\text{H}_2\text{F}^+$) as the most abundant secondary ions with the fluorinated methyl radicals in contrast to the reactions with 3,3,3-trifluoropropyne which all yield C_3H_3^+ (C_3HF_2^+) as the predominant secondary ion.

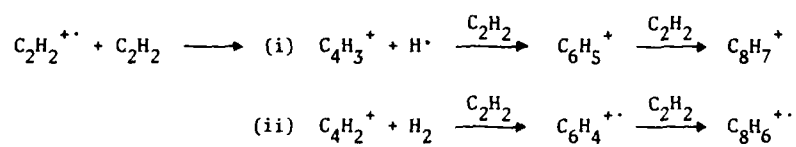
The very high cross-section for $\text{CH}_3^+ + \text{C}_2\text{H}_2$ compared with that for $\text{CH}_2\text{F}^+ + \text{C}_2\text{H}_2$ may be due to an initial loss of a fluorine atom from the latter adduct cluster.



In contrast no such predissociation is likely with methyl cations.



The reaction of acetylene radical cations with acetylene was also studied and two parallel pathways were observed:



Some evidence was also seen of $\text{H} \cdot$ and/or H_2 ions from the higher order ions, contrary to an earlier i.c.r. study by Brill and Eyler.

Determination of the Absolute Rate Constant for the Reaction of OH with
CO by cw-UV-Laser-Absorption at Atmospheric Conditions

A. Wahner and C. Zetzsch

Ruhr-Universität Bochum, Physikalische Chemie I, Postfach 102148,
4630 Bochum, West Germany

and

Fraunhofer Institut, ITA Hannover, Stadtfeldweg 35, 3000 Hannover,
West Germany

The reaction of OH with CO is of major importance for combustion processes and tropospheric chemistry. Since 1974 several studies observed the dependence of the rate constant on the partial pressure of inert gas. This work reports absolute measurements of the rate constant for the reaction in air and in N₂ by means of a sensitive cw-UV-Laserabsorption-technique. The OH radicals were detected in absorption of the electronic transition $\text{OH} (A^2\Sigma^+ \leftrightarrow X^2\Pi)$ using a long light path and they are generated by photolysing H₂O with 193 nm radiation (ArF-Excimer laser) or H₂O₂ with 248 nm radiation (KrF-Excimer laser).

Figure 1 shows the schematic experimental set-up. A frequency doubled cw-Ar-Ion laser pumped ring-dye laser (Rhodamin 6G) generates the UV-radiation (308 nm) in order to detect the OH-radicals. The wavelength of the dye laser radiation (616 nm) is actively stabilized by an interferometer system. The frequency doubling is accomplished externally by using an angle tunable LiIO₄ crystal. 1 mW output intensity can be achieved at 308 nm. The bandwidth of the frequency-doubled laser radiation is about 1000 times smaller than the Doppler and pressure broadened absorbing rotational line Q₁(2) of the electronic transition $(A^2\Sigma^+ \leftrightarrow X^2\Pi)$ of the OH radical. In order to tune the dye laser in this transition, the fluorescence signal of continuously generated OH-radicals by a microwave discharge is used. The main portion of the laserlight is directed into the longpath absorption cell. The longpath absorption cell consists of a 1.5 m long glass tubing (dia. 15 cm) with mirror holders made of stainless steel.

The non-confocal mirror arrangement allows to adjust an absorption path of 151.2 m at a mirror distance of 0.98 m (focal length of the concave mirror is 0.5 m). The mirrors (Suprasil substrate) are dichroitically coated. They have a high reflectivity at 308 nm (98.7%) and a high

transmission at 193 nm and 248 nm (70%). To generate a homogeneous distribution of OH radicals, the reaction cell is illuminated axially by the 10 times enlarged excimer laser beam. The detection of the absorption is accomplished by a differential measurement of the laser light intensities before and after passing the reaction cell (rise time: 40 μ s). The time resolved differential absorption signal is accumulated 50 times in a computer.

Concentrations of OH ranging from $5 \cdot 10^9$ to $1.5 \cdot 10^7$ cm^{-3} in the presence of 1 atm of synthetic air or N_2 could be detected. To avoid accumulation of reaction products, measurements were performed under slow flow conditions. Because of the large excess of CO in comparison with OH, decay curves obeying pseudo first order time behaviour were observed. Exponential decays of OH were followed over 2 to 3 orders of magnitude in air or in N_2 , respectively. Radical-radical reactions are unimportant in the observed time range of less than 20 ms because of the low OH concentrations.

The reaction of OH with CO was investigated in N_2 with H_2O_2 and H_2O as source of OH in the pressure range of 8.6 - 1480 mbar and in air with

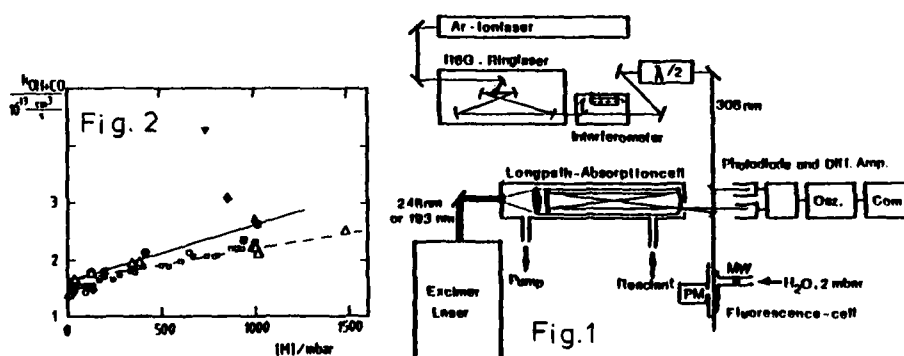


Fig. 1 : Schematic experimental set-up.

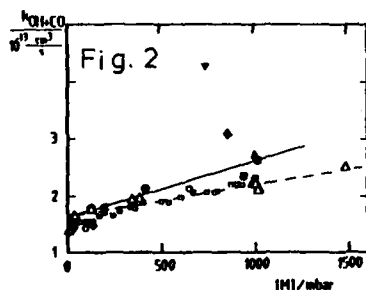


Fig. 2 : Linear plot of the rate constants of the reaction $\text{OH} + \text{CO}$ against the total pressure. Measurements in N_2 : Hofzumahaus et al.¹ \circ ; Paraskevopoulos et al.² \square ; this work \triangle . Relative measurements in N_2/O_2 : Cox et al.³ \blacktriangle ; Chan et al.⁴ \blacklozenge ; Butler et al.⁵ \blacktriangledown ; Niki et al.⁶ \blacksquare ; absolute measurements in air: this work \bullet . The broken line fits to the set of data in N_2 , the full line to the data in air.

H₂O₂ as source of OH in the pressure range of 21 - 1012 mbar. Linear dependences of the reciprocal lifetimes of OH radicals on the concentration of CO were found. The slopes yield the rate constants for the reaction of OH + CO depending on the total pressure. Figure 2 shows a linear plot of the measured bimolecular rate constant against the total pressure. (Symbol: Δ measurements in N₂; symbol: \bullet measurements in air) The broken line is a least squares fit to the complete set of data in N₂ at 300 K:

$$k(\text{N}_2) = (1.65 \pm 0.2) \cdot 10^{-13} \cdot (1 + 3.36 \cdot 10^{-4} [\text{N}_2]/\text{mbar}) \text{ cm}^3 \text{ s}^{-1}$$

The full line is a least squares fit to the complete set of data in air at 300 K:

$$k(\text{air}) = (1.63 \pm 0.2) \cdot 10^{-13} \cdot (1 + 6.02 \cdot 10^{-4} [\text{air}]/\text{mbar}) \text{ cm}^3 \text{ s}^{-1}$$

The scatter of the data allows a linear fit only. The stated error limits are estimated from individual data points.

The data of Hofzumahaus et al.¹ and Paraskevopoulos et al.² are shown in figure 2 for comparison (symbol \circ and \square). These data were obtained by using the flash photolysis/resonance fluorescence method. Good agreement was found within the error limits. Relative measurements of this reaction in smog chambers show large discrepancies among them (see figure 2, symbols: \blacktriangle , \blacklozenge , \blacktriangledown , \blacksquare). The value of the rate constant at 1480 mbar N₂ ($k = 2.51 \cdot 10^{-13} \text{ cm}^3 \text{ s}^{-1}$) found in this work shows that the high pressure limit is not reached under these conditions. The measurements performed in air show a stronger pressure dependence.

- 1 A. Hofzumahaus and F. Stuhl, to be published in Ber. Bunsenges. Phys. Chem.
- 2 G. Paraskevopoulos and R.S. Irwin, J. Chem. Phys. 80, 259 (1984)
- 3 R.A. Cox, R.G. Derwent and P.M. Holt, Faraday Trans. I 72, 2031 (1976)
- 4 W.H. Chan, W.M. Uselman, J.G. Calvert and J.H. Shaw, Chem. Phys. Let. 45(2), 240 (1977)
- 5 R. Butler, I.J. Solomon and A. Snelson, Chem. Phys. Let. 54(1), 19 (1978)
- 6 H. Niki, P.D. Maker, C.M. Savage and L.P. Breitenbach, to be published in J. Phys. Chem.

OH internal state distributions from the reactions of $O(^3P)$ with cyclic and aromatic hydrocarbons.

N.J. Dutton, I.W. Fletcher and J.C. Whitehead

Department of Chemistry, University of Manchester, Manchester M13 9PL, U.K.

The dynamics of the hydrogen abstraction reactions of $O(^3P)$ atoms with cyclohexane, cyclohexene, 1,4-cyclohexadiene and benzene have been investigated by measuring the OH product rotational and vibrational state distributions by laser-induced fluorescence under crossed-molecular beam conditions. The molecular beams were seeded to provide the translational energy necessary to overcome the barriers to reaction. The oxygen atoms were produced by a microwave discharge of an O_2/He mixture.

The rotational state distributions (Figure 1) are very similar for all the reactions and show that only a very low fraction ($\langle F_R \rangle \sim 1-7\%$) of the available energy goes into OH rotation. This indicates that abstraction is a direct process taking place only when the O atom is collinear with the C-H bond under attack. The invariance of these distributions to the total available energy ($37-155 \text{ kJ mol}^{-1}$) shows that the potential energy in the entrance channel of the reaction surface must rise rapidly for all but very collinear encounters.

The OH vibrational state distributions (Figure 2) show a modest increase in vibrational energy ($\langle F_V \rangle = 0.16-0.22$) in going along the series $O + C_6H_{12}$, C_6H_{10} , C_6H_8 . (For the last two reactions, information theory has been used to predict the population in vibrational levels $v \geq 2$ which cannot be probed by L.I.F.). A model in which the hydrocarbon radical is regarded as structureless would predict a large increase in OH vibrational energy as the reaction exoergicity increases. For these reactions, the timescale for the direct H atom abstraction is short compared with the time taken for the hydrocarbon radical product to rearrange and thus the radical stabilisation energy which is then not available

for OH vibrational excitation becomes internal excitation of the radical.

For $O + \text{benzene}$, the beam energy is insufficient to allow population of OH in $v = 1$. Estimates of the OH product yield, suggest that above the threshold for OH production, OH is produced with a branching ratio close to unity. OH production would then be dominant in $O + C_6H_6$ at high temperatures ($T > 2500 \text{ K}$).

(kJ/mol)

	ΔH_r	E_{trans}	$\langle F_R \rangle$	$\langle F_V \rangle$
$O + c-C_6H_{12}$	-29	28	0.03	0.16
$O + c-C_6H_{10}$	-73	23	0.03	0.17
$O + c-C_6H_8$	-135	20	0.01	0.22
$O + C_6H_6$	+32	69	0.07	-

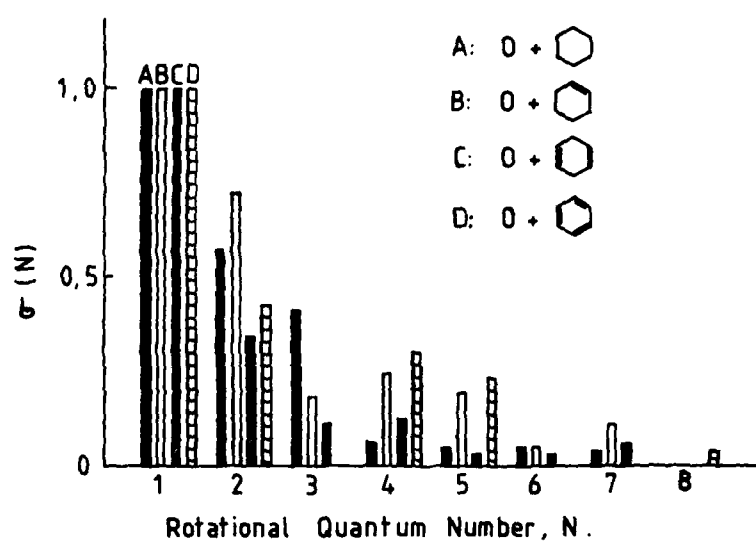


Figure 1

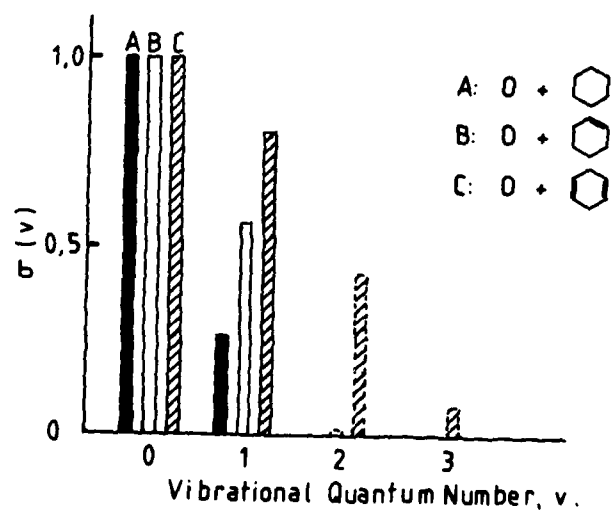


Figure 2

Visible Chemiluminescence from the Multiple Collision Reactions of F atoms with Organic Iodides

H.S. Braynis, D. Raybone and J.C. Whitehead

Department of Chemistry, University of Manchester, Manchester, M13 9PL, U.K.

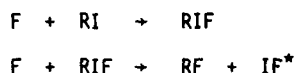
The visible chemiluminescence produced in the reactions of F atoms (formed by microwave dissociation of a 5% F₂/He mixture) with various organic iodides (CH₃I, CH₂I₂, CHI₃, CI₄, allyl iodide, iodobenzene and ortho- and meta-iodotoluene) in a flowing system at ~ 0.5-1.0 mbar has been measured in the spectral region 400-890 nm. Strong flames are observed with the substituted methanes and allyl iodide and weaker emissions in the case of iodobenzene and the iodotoluenes. Examples of the observed spectra are shown in the figure and the identified emitters are listed below.

Reactant	Emitting Species
CH ₃ I	IF [*] (B), CH [*] (A), HCF [*] (\tilde{A}), HF ^z
CH ₂ I ₂	IF [*] (B), CH [*] (A), HCF [*] (\tilde{A}), HF ^z
CHI ₃	IF [*] (B), HCF [*] (\tilde{A}) _w , HF ^z
CI ₄	IF [*] (B)
allyl iodide	IF [*] (B) _w , C ₂ [*] (d), CH [*] (A), HF ^z
iodobenzene	IF [*] (B) _{vw} , CH [*] (A) _w , HF ^z
o-iodotoluene	IF [*] (B) _{vw} , CH [*] (A), HCF [*] (\tilde{A}), HF ^z
m-iodotoluene	IF [*] (B) _{vw} , CH [*] (A), HCF [*] (\tilde{A}), HF ^z

All the spectra are complex, except for F + CI₄ which shows a high yield of only IF^{*}.

IF^{*}(B) For the reactions with substituted methanes, this is produced in vibrational levels up to v' = 8 with a non-Boltzmann population that shows some inversion. For the other systems emission could only be detected up to v' = 2.

In all cases the IF^* was rotationally relaxed. The primary reaction ($F + RI \rightarrow R + IF$) has insufficient energy to produce IF^* and a two step mechanism is proposed



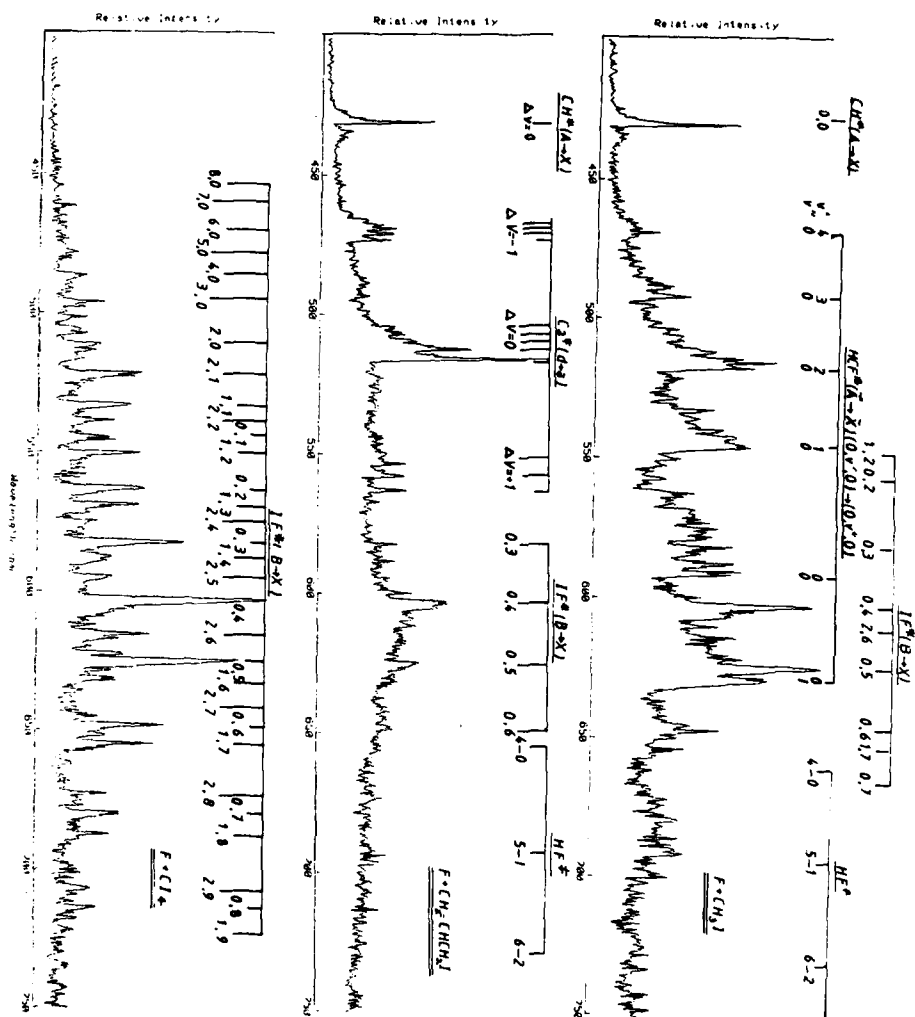
The intermediate RIF is known to be stable when $R = CH_3$.

$HCF^*(\tilde{A})$ This is observed in all cases except $F +$ iodobenzene and allyl iodide with vibrational excitation up to $v_2' = 4$. This suggests that it is produced by reaction with a CH_n fragment, possibly the recombination



HF^* Vibrationally-excited $HF(X^1\Sigma^+)$ is detected in levels up to $v = 8$. The primary reactions ($F + RI \rightarrow HF$) are known to produce HF only up to $v = 3$. The HF observed in these systems must then be produced by the reaction of an F atom with some radical product from a previous reaction. In all cases, the HF is rotationally relaxed.

$C_2^*(d)$ and $CH^*(A)$ $C_2^*(d)$ is only produced in the $F +$ allyl iodide system, presumably by breaking the C_3 chain. It has a non-Boltzmann vibrational distribution extending up to $v' = 4$. The rotational temperature of the C_2^* is ~ 1500 K. A similar rotational temperature (~ 1000 - 1500 K) is found for the $CH^*(A)$ which is observed in all systems except CHI_3 and CI_4 . The method of production of $CH^*(A)$ is not clear, although it is a commonly-observed feature in F_2 /hydrocarbon flames.



A COMPREHENSIVE MECHANISM FOR THE OXIDATION OF CARBON MONOXIDE

by

R.A. Yetter and F.L. Dryer
Department of Mechanical and Aerospace Engineering
and
H. Rabitz
Department of Chemistry
Princeton University, Princeton, New Jersey

ABSTRACT

A comprehensive reaction mechanism for the oxidation of carbon monoxide is proposed. Model predictions are compared with experimental data over wide ranges of physical conditions. The data, obtained from shock tube experiments and various types of reactor experiments, encompassed a combined temperature range of 800-3000K, fuel-air equivalence ratios between 0.025 and 6.0 and pressures between 0.3 and 3 atmospheres. Validation of the reaction mechanism is obtained with accurate reproduction of the experimental results by the model predictions and from sensitivity analysis calculations which provide a quantitative measure of the sensitivity of the model predictions to the imposed input parameters.

Evaluation of Smog Chamber Experiments with Dilution:
Rate Constants for the Reactions of OH with Alkanes up to C₁₂

W. Behnke, F. Nolting and C. Zetzsch

Fraunhofer Institut für Toxikologie und Aerosolforschung
Stadtfelddamm 35
D-3000 Hannover 61, W.-Germany

Smog chamber studies or similar chemical or photochemical static experiments in closed reaction vessels in principle suffer from the limitation in vessel volume. Each sampling dilutes the contents of the vessel, especially in smog chamber experiments where the concentrations of NO_x and O₃ need to be monitored continuously by highly gas consuming methods. Previously, the dilution had to be either calculated from the gas consumption, or an unreactive component had to be added to the reaction mixture as a concentration standard in order to detect leaks or variations of the analytic sensitivity. The present study introduces a method, where several compounds (and reactive components as well) serve as mutual standards.

In the approximation of pseudo first order kinetics (mostly applied to competitive reactions) of a species, C, in the presence of OH radicals one obtains the equation:

$$\ln \frac{[C]}{[C]_0} = -k_1 [OH]t - d, (1)$$

where d denotes the relative dilution by the sampling, which may include variations of the analytic sensitivity as well.

The dilution, d , can either be eliminated by monitoring several species, C_i , simultaneously leading to the equation

$$\frac{\sum_{i=1}^N \ln \frac{[C_i]}{[C_i]_0} - \sum_{j=1}^M \ln \frac{[C_j]}{[C_j]_0}}{\sum_{i=1}^N k_i - \sum_{j=1}^M k_j} = [OH]t, (2)$$

where the concentration of OH can be determined, or the dilution can be determined from eq. (1) and (2):

$$d = - \frac{1}{N+M} \sum_{i=1}^{N+M} \left(\ln \frac{[C_i]}{[C_i]_0} + k_i [OH]t \right) \quad (3)$$

Using the equations (2) and (3) time profiles of the concentration of OH and the dilution can be obtained. In an iterative manner, several compounds i and j with differing reactivity are used to optimize the fit to rate constants, k . First results on the rate constants for the reactions of OH radicals with n -alkanes (relative to n -butane¹⁾, $k = 2.58 \times 10^{-12} \text{ cm}^3 \text{ molecule}^{-1} \text{ s}^{-1}$) up to dodecane will be presented.

1) Recent results on n -alkanes by Atkinson et al.

A new theory for vibrational and rotational energy transfer
in the collisions of symmetric top molecules with atoms

D.C. Clary,
University Chemical Laboratory,
Lensfield Road,
Cambridge, CB2 1EW.

A new three-dimensional quantum theory has been developed for calculating vibrational and rotational relaxation cross sections and rate constants for the collisions of atoms with prolate symmetric or near-symmetric top molecules. The technique uses a scattering wavefunction expansion in vibrational states coupled with azimuthal rotational functions which describe the spinning of the top about its symmetry axis. The infinite order sudden approximation is used for the total rotational angular momentum of the molecule.

The technique has been applied to the computation of vibrational relaxation rate constants for the collisions of C_2H_4 with He atoms. The results have been compared with those obtained using the less accurate VCC-IO5 method¹ in which the sudden approximation is applied to both the total and azimuthal rotational motion. The rate constants of the two methods differ on average by a factor of two. This is due to the effect of the azimuthal rotational levels in reducing the effective energy gap for a vibrational transition, and hence making the vibrational energy transfer more efficient. The new method also gives improved agreement with experimental vibrational relaxation rate constants.

1. D.C. Clary, J. Am. Chem. Soc., 1984, 106, 970.

Photodissociation Dynamics of Small Cluster Ions

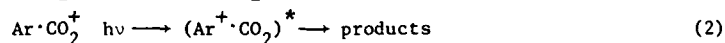
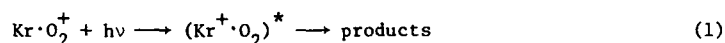
Michael T. Bowers
 Department of Chemistry
 University of California, Santa Barbara, CA 93106

We have recently developed techniques for photodissociating mass selected beams of cluster ions by single visible photons from an Argon Ion Laser system [1]. These methods allow determination of absolute photodissociation cross sections, branching ratios, information on excited state symmetry and lifetime, angular dependence of the photofragments in the center of mass frame, high resolution kinetic energy analysis of the products and, in favorable cases, product vibrational state distributions, information on rotational excitation, cluster ion structure, and cluster ion binding energy. To date information has been obtained on the clusters $(\text{NO})_2^+$, $(\text{NO})_3^+$, $(\text{N}_2)_2^+$, $(\text{N}_2\text{O})_2^+$, $(\text{CO}_2)_2^+$, $(\text{CO}_2)_3^+$, $(\text{SO}_2)_2^+$, $(\text{CS}_2)_2^+$, Mn_2^+ , $\text{CS}_2\cdot\text{S}_2^+$, KrO_2^+ , ArCO_2^+ and KrCO_2^+ .

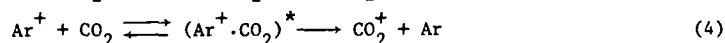
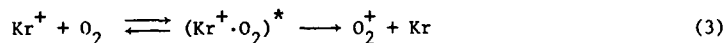
The symmetric clusters are relatively strongly bound (0.5 to 1.1 eV) and generally dissociate via photoexcitation to a repulsive state that yields ground state A^+/A products. Exceptions to this rule are $(\text{SO}_2)_2^+$ which accesses a bound excited state that dissociates via vibrational predissociation after interconversion to the ground state and

Mn_2^+ that forms a variety of electronically excited products in addition to the ground state. The $(\text{CO}_2)_2^+$ dimer dissociates via two pathways; one that directly accesses a repulsive state and one that accesses an excited state that is long-lived, which dissociates via vibrational predissociation after interconversion to the ground state.

In the mixed clusters, the processes are quite specific and often several product channels are observed. In this talk we'll concentrate on the two reactions



In both reactions the rare gas atom is initially clustered to the molecular ion. Absorption of a photon results in "charge transfer" to the rare gas ion/neutral molecule surfaces. From these surfaces dissociation can take place. Reactions (1) and (2) allow sampling of the intermediate complexes for the bimolecular charge transfer reactions (3) and (4):



At thermal energies reaction (3) proceeds at about 8% efficiency [2] and (4) at about 50% efficiency [3]. The photodissociation processes (1) and (2) are accomplished at about the same total energy as reactions (3) and (4). The advantage in (1) and (2) is that the energy is precisely known and that the "half" reaction is initiated from $\text{Kr}^+ \cdot \text{O}_2$ or $\text{Ar}^+ \cdot \text{CO}_2$ in a specific geometric configuration. A

detailed discussion will be given that will elucidate the details of the dynamics of both reactions (1)/(2) and (3)/(4) including discussion of the detailed energy disposal in all four reactions.

- [1] M.F. Jarrold, A.J. Illies and M.T. Bowers, J. Chem. Phys. 79, 6086 (1983); *ibid* (in press).
- [2] T.T.C. Jones, K. Birkinshaw, J.D.C. Jones and N.D. Twiddy, J. Phys. B 15, 2439 (1982).
- [3] J.B. Laudenslager, W.T. Huntress and M.T. Bowers, J. Chem. Phys. 61, 4600 (1974).

Mode Specificity in the Reaction $C_2H_4^+(v_2, v_4) + C_2H_4 \rightarrow C_3H_5^+ + CH_3$.

Kenichiro Tanaka, Tatsuhisa Kato, and Inosuke Koyano
Institute for Molecular Science, Myodaiji, Okazaki,
444 Japan

The threshold electron-secondary ion coincidence (TESICO) technique, which we have developed recently,¹⁾ has been applied to the selection of reactant vibrational states in the reaction $C_2H_4^+ + C_2H_4 \rightarrow C_3H_5^+ + CH_3$. (1) Threshold electron spectrum of $C_2H_4^+$ shows peaks corresponding to v_2 and v_4 progressions of the ground state $C_2H_4^+$ ions. Thus, the system involving $C_2H_4^+$ provides an unique opportunity to investigate mode specificity in chemical reactions.

Relative reaction cross sections have been determined for the four vibrational states $(v_2, v_4) = (0, 0), (0, 2), (1, 0)$, and $(1, 2)$. The experimental results, given in Fig.1, showed that, at intermediate collision energies around 0.2 eV, the former two states have cross sections of essentially the same magnitude which is definitely larger than that for the last two states, the last two states again having the same cross sections. These results indicate that while v_2 vibration has prohibiting effect on reaction (1), v_4 vibration has nothing to do with the reaction. At lower and higher collision energies, however, the cross sections behaved quite differently as the vibrational states were varied, as shown in Fig. 1.

Reaction (1) is known to proceed via an intermediate complex at low collision energies.²⁾ Thus, the above results are considered as reflecting the mode specificity in the uni-

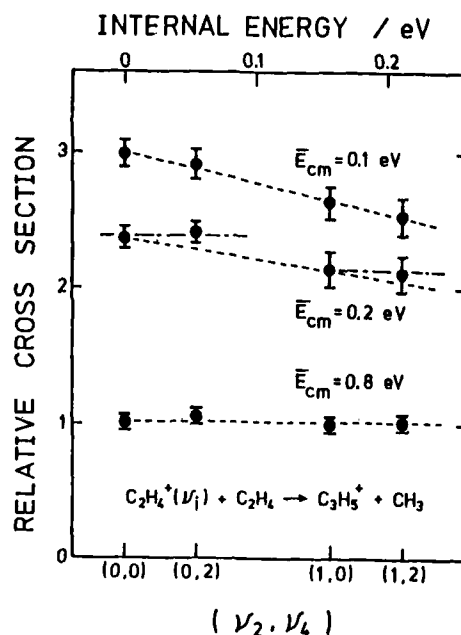


Fig. 1. Vibrational state dependence of the reaction cross section.

molecular decomposition of the intermediate complex. At the moment, we interpret the results as indicating that the ν_2 vibration of the original ion effectively enhances the decomposition of the complex back to the reactants, thus reducing the probability of the forward decomposition, whereas the ν_4 vibration does not effectively couple with either of these decomposition coordinates.

- 1) I. Koyano and K. Tanaka, J. Chem. Phys. 72, 4858 (1980).
- 2) Z. Herman, A. Lee, and R. Wolfgang, J. Chem. Phys. 51, 452 (1969).

COMPARISON OF THE ENERGY PARTITIONING IN CHARGE
TRANSFER REACTIONS OF Ar^+ AND N_2^+

R. Marx, G. Mauclaire, R. Derai, D.C. Parent, A. O'Keefe[°] and M.T. Bowers[°]

LREI, Bât. 350, Université de Paris-Sud, 91405 Orsay Cedex, FRANCE

[°]Dept. of Chemistry, University of California, Santa Barbara, Ca. 93106 USA

The kinetic/internal energy partitioning in the products of thermal energy charge transfer reactions can be determined by an ion cyclotron resonance (ICR) measurement of the product ion kinetic energy.¹ For a reaction of the type



the exoergicity ΔE and energy partitioning are given by

$$\Delta E = \text{RE}(\text{A}^+) - \text{IP}(\text{M}) = \text{KE}(\text{A}, \text{M}^+) + \text{IE}(\text{A}, \text{M}^+) \quad (2)$$

where RE is the recombination energy of the ion, IP is the ionization potential of the neutral, KE is the excess kinetic energy of the products and IE is the internal energy. If a rare gas ion is used, the internal energy of A is zero and the energy partitioning is completely specified. Many studies of the type have been done.¹⁻⁵

We were interested to see what changes would be observed if the rare gas ion was replaced by a molecular ion of similar recombination energy. To this end the reactions of Ar^+ and N_2^+ with a series of small neutrals were studied. The range of total kinetic energy measured and the percentage of the reaction exothermicity this represents are given in Table 1.

The addition of one vibration and two rotations (from N_2^+) to the ion-neutral system seems to have almost no effect on the energy partitioning when the neutral has more than two atoms. (The only exception is CO_2 , where some of the products formed by N_2^+ have more kinetic energy than if

formed by Ar^+ . This is the opposite of what one might expect, as the system with more internal modes should have more internal energy.) Two possible explanations can be proposed. One is that the energy of the N_2 vibration is sufficiently large that it is not excited, and that only the lower frequency modes of the ion are excited by the charge transfer from either Ar^+ or N_2^+ . The other explanation is that the Ar^+ -neutral system already has three to six vibrational modes, so that the addition of one more with N_2^+ has little effect. In this case, a system with a diatomic neutral might show an effect as the number of vibrations is increased from one with Ar^+ to two with N_2^+ . With O_2 it is observed that a greater percentage of energy is found in the internal modes when N_2^+ is the reactant. But it is not known if this represents excitation of the N_2 or of the O_2^+ vibration. Data on other reactions of N_2^+ with diatomics is needed to see if any trends emerge.

References:

- ¹ G. Mauclaire, R. Deraï, S. Fenistein and R. Marx, J. Chem. Phys., 70, 4017, (1979).
- ² R. Deraï, G. Mauclaire and R. Marx, Chem. Phys. Lett., 86, 275, (1982).
- ³ G. Mauclaire, R. Deraï, S. Fenistein and R. Marx, J. Chem. Phys., 70, 4023, (1979).
- ⁴ R. Marx, G. Mauclaire, T.R. Govers, M. Gérard-Aïn, S. Fenistein and R. Deraï, J. Chim. Phys., 7, 1077, (1979).
- ⁵ R. Marx in Ionic Processes in the Gas Phase, M.A. Almoester Ferreira, ed., D. Reidel Publishing Co., Dordrecht, Holland, (1984).
- ⁶ D.C. Parent, PhD Thesis, Dept. of Chemistry, University of California, Santa Barbara, 1983.
- ⁷ M. Heninger, R. Deraï and G. Mauclaire, unpublished results.

Table 1. Energy Partitioning in Charge Transfer Reactions

Neutral	Total KE (eV)		ZKE of E=RE-IP		
	Ar ^{+,5}	N ₂ ^{+,6}	Ar ^{+,5}	N ₂ ^{+,6}	uncer- tainty
O ₂	1.8	0.86-2.14 ⁷	49	24-61	±3
N ₂ O	0.61-1.41	0.49-1.39	21-49	18-52	±4
CO ₂	0.65-1.05	0.58-1.52	33-53	32-84	±5
H ₂ O	0.30-1.00	0.33-1.12	10-32	11-38	±3
NH ₃	0.41-1.08	0.34-0.93	7-19	6-17	±2

PRODUCT STATE DISTRIBUTIONS OF THERMAL ENERGY ION-MOLECULE REACTIONS*

Stephen R. Leone[†]

Joint Institute for Laboratory Astrophysics
University of Colorado and National Bureau of Standards
and Department of Chemistry, University of Colorado
Boulder, Colorado 80309 USA

Abstract

A flowing afterglow apparatus is used to study the dynamics of ion-molecule reactions by detection with infrared chemiluminescence and laser-induced fluorescence. A number of simple proton transfer reactions have been studied, e.g. $F^- + HX \rightarrow HF(v) + X^-$ ($X = Cl, Br, I$), in order to determine the vibrational state distributions in the HF product.¹ The results show distinct differences from the analogous neutral reactions, $F + HX \rightarrow HF(v) + X$; these differences can be attributed to the long-range ion-dipole and ion-induced dipole forces present in the ion reactions. Further work is in progress on the deuterated analogues. Other reactions of polyatomic molecules have been studied to test whether the products are formed in a "direct" fashion or through a long-lived collision intermediate. For example, the reaction, $H + SF_6^- \rightarrow HF(v) + SF_5^-$, is found to have a high degree of vibrational excitation, indicative of an early "attractive" energy release followed by a strong "repulsive" release.²

A new apparatus combines a flowing afterglow ion source with a free jet expansion to produce high fluxes of ions for single collision molecular beam

*Co-workers on this project are Veronica M. Bierbaum and G. Barney Ellison, together with past and present students, Timothy S. Zwier, James C. Weisshaar, Charles E. Hamilton, Michael A. Duncan, Andrew O. Langford, Dean R. Guyer, Lutz Hüwel, Lin Guang-Hai, and Jürgen Maier.

[†]Staff Member, Quantum Physics Division, National Bureau of Standards.

type studies of thermalized ions. The kinetic energies are 0.1-0.2 eV. In this device, charge transfer reactions of $\text{Ar}^+ + \text{N}_2 \rightarrow \text{Ar} + \text{N}_2^+(v=0,1,J)^3$ and $\text{N}^+ + \text{CO} \rightarrow \text{N} + \text{CO}^+(v=0,1,2,J)^4$ have been studied with laser-induced fluorescence probing of both vibrational and rotational distributions. The results show that the regions of the potential surfaces where the electron is transferred are different for the two different reactions. For example, in $\text{N}^+ + \text{CO}$, the vibrational distribution is nearly approximated by the Franck-Condon distribution for the isolated CO, which favors the $v''=0$ state of CO^+ . The rotational excitation in this state is low (400 K). In contrast, the $\text{Ar}^+ + \text{N}_2$ reaction produces N_2^+ predominantly in $v''=1$, with a ratio of $v''=1/v''=0$ of nearly 10. In the $v''=1$ state, the rotational excitation is substantial (700 K, which corresponds to 15% of the energy).

New results are also being obtained on the vibrational distribution of $\text{N}^+ + \text{CO}$ in the flowing afterglow apparatus. To carry out these experiments, several improvements to the original⁵ ion source production were necessary. In this case, because there are collisions with the helium buffer gas, there is no ambiguity concerning analysis of the velocities of individual vibrational product states (the density-to-flux conversion is unambiguous). A definitive vibrational distribution for this reaction is possible by this method. These results will be discussed in light of the relevant charge transfer mechanisms.

References

1. J. C. Weisshaar, T. S. Zwier and S. R. Leone, J. Chem. Phys. 75, 4873 (1981).
2. C. E. Hamilton, V. M. Bierbaum and S. R. Leone, J. Chem. Phys. (in press).
3. L. Hüwel, D. R. Guyer, G. H. Lin and S. R. Leone, J. Chem. Phys. (submitted).
4. D. R. Guyer, L. Hüwel and S. R. Leone, J. Chem. Phys. 79, 1259 (1983).
5. C. E. Hamilton, M. A. Duncan, T. S. Zwier, J. C. Weisshaar, G. B. Ellison, V. M. Bierbaum and S. R. Leone, Chem. Phys. Lett. 94, 4 (1983).

SPECTROSCOPY AND QUENCHING BEHAVIOUR OF SOME
EXCITED STATES OF IODINE MONOBROMIDE

J.P.T. Wilkinson, M.A. MacDonald and R.J. Donovan

Department of Chemistry, University of Edinburgh,

West Mains Road, Edinburgh EH9 3JJ

The emission spectra produced when iodine monobromide is excited by photons of wavelengths near 200 nm have been studied. In addition to studies using 193 nm laser excitation of IBr we have also studied the spectra produced using a conventional spectrofluorimeter with wavelength selection of both the excitation and emission beams. In the absence of any quenching gas we detect oscillatory continuum emission in the 200 - 600 nm wavelength range which can be ascribed to fluorescence from the initially populated level(s) to at least two lower states. These systems are analogous to those previously detected in the 193 nm excitation of molecular iodine and can be ascribed to bound-free transitions. Examination of the excitation wavelength dependence of the IBr fluorescence shows that the initially populated state of IBr is not the E Rydberg state which may be populated by absorption around 193 nm, but must be due to an ion-pair state underlying this transition (labelled the D state).

The addition of quenching gases to iodine monobromide can cause a number of processes to occur. When the quenching gas is either argon or helium then the fluorescence spectrum observed shows diminished emission from the IBr(D) state and the concomitant growth of a new system which can be ascribed to the IBr (D' \rightarrow A') system. The IBr(D) fluorescence

yield as a function of added inert gas pressure follows Stern-Volmer kinetics and the quenching rate constants are

$$k_{\text{argon}} = (1.77 \pm 0.04) \times 10^{-3} \text{ m}^2 \text{ N}^{-1}$$

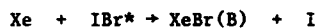
$$k_{\text{helium}} = 1.11 \times 10^{-3} \text{ m}^2 \text{ N}^{-1}$$

Using a value of the radiative lifetime of IBr(D) of 13.5 ns, found in studies using the Synchrotron Radiation Source at Daresbury, leads to values of

$$k_{\text{argon}} = (5.47 \pm 0.12) \times 10^{-10} \text{ cm}^3 \text{ molecule}^{-1} \text{ s}^{-1}$$

$$k_{\text{helium}} = 3.2 \times 10^{-10} \text{ cm}^3 \text{ molecule}^{-1} \text{ s}^{-1}$$

When the inert gas used was xenon of an additional channel, the formation of xenon bromide, was detected by the appearance of the characteristic XeBr (B \rightarrow X) band at 280 nm. The XeBr(B) was formed by the direct interaction between the excited IBr molecule and a xenon atom



This reaction will be compared with the analogous reaction involving electronically excited Xe atoms and ground state IBr.

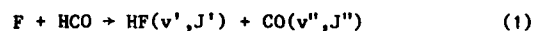
The actual interaction between the excited iodine monobromide and the inert gas atom will be discussed in terms of the potential curves corresponding to the covalent interaction between IBr* and Xe and that corresponding to the ionic intermediates Xe^+ and IBr^- which are produced by an electron jump from the xenon atom to the halogen molecule.

ENERGY PARTITIONING IN THE REACTION OF F ATOMS WITH FORMYL RADICALS

D.J. Donaldson and J.J. Sloan

National Research Council of Canada, 100 Sussex Drive, Ottawa, Canada K1A 0R6

The energy disposal in the reaction:

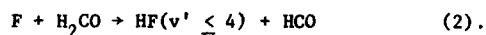


has been determined by direct measurement of the vibrational and rotational excitation in both the HF and CO reaction products. The measurements were carried out using a variant of the low-pressure infrared chemiluminescence technique, developed in this laboratory to permit the measurement of energy partitioning in atom/radical reactions.

The experimental apparatus consists of a cylindrical vacuum chamber, 25 cm. diameter by 25 cm. high, evacuated through a cryobaffle and slide valve by a diffusion pump which provides a speed of about 6000 litres/sec. at the bottom (outlet) of the chamber. The total pressure during an experiment is in the 10^{-2} to 10^{-4} Torr range. An atomic and a molecular reagent are admitted at the top of the chamber, where they rapidly mix and react as they expand through an observation zone located at the chamber centre. The observation zone is defined by a multipass infrared light collection cell consisting of two gold-coated spherical mirrors. These collect infrared emission from the vibrationally excited reaction products and focus it into a Fourier Transform Spectrometer which is optically matched to the multipass cell.

Two successive chemical reactions occur as the reagents expand into the reaction chamber. Radicals are generated in the first reaction; they react with an atomic reagent in the second. The latter is the reaction of

interest in these studies. In the present work, the radicals are produced via the abstraction of a hydrogen atom from formaldehyde:



This reaction occurs very rapidly upon the injection of formaldehyde into a region in which the F atom density is about 10^{-3} Torr. As they expand further towards the lower pressure region at the outlet of the reaction chamber, the HCO radicals encounter a second source of F atoms, where reaction (1) occurs. The high exothermicity of reaction (1), $116 \pm 5 \text{ kcal mole}^{-1}$, permits the population of HF up to $v'=13$, and of CO up to $v''=21$. The much lower exothermicity of the primary reaction (2) can populate HF only up to the $v'=4$ level, hence the observed $\text{HF}(v' > 4)$ is known to originate in reaction (1).

The populations of the observed vibrational levels of HF and CO, are calculated using known Einstein A-factors. A complete picture of the dynamics of the reaction is provided by the resulting map of the probability with which the internal energy levels of the products are created by the reaction. The maximum level which is observed to be populated in the CO product is $v''=5$; that of the HF is $v'=10$. For the purposes of this analysis, all of the observed CO levels, and those HF levels originating in reaction (1), $\text{HF}(5 \leq v' \leq 10)$, were used.

For both products, the vibrational populations were observed to decrease monotonically with increasing vibrational level. Since this behaviour is characteristic of reactions in which a long-lived intermediate is formed, and since the latter mechanism is expected to distribute the reaction exoergicity statistically among all available product states, appropriate statistical distributions were calculated, for comparison with

the measured populations. It was found that the measured populations conform to those predicted by a restricted phase space calculation in which statistical behaviour (free flow of energy among all modes of the intermediate species) is permitted only until the first part of the product separation phase of the reaction; the HF and CO must not be energetically coupled in the last part of the exit channel.

This result is consistent with ab initio reaction coordinate calculations which indicate that the nascent HF bond remains slightly extended until the system is well into the exit channel, whereas the CO bond is much closer to its asymptotic (isolated) length during product separation. As a consequence, slightly more than the statistical amount of energy is partitioned into vibration of the HF, whereas the CO is vibrationally colder than a purely statistical model would predict.

MOLECULAR BEAM STUDIES OF THE INTERACTIONS OF P STATE ATOMS

V. Aquilanti,

Dipartimento di Chimica dell'Università di Perugia,

06100 Perugia, Italy

The interactions of atomic halogen and oxygen atoms with other atoms and molecules are being studied in our group by molecular beam techniques, using magnetic selection of sub-levels. The analysis of experimental data, and their use for chemical kinetics, rely on the development of a theoretical framework for the description of atoms carrying internal angular momentum.

The theory is being extended to the analysis of related experiments in our laboratory, on chemiionization reactions by metastable rare gases.

The Reaction and Relaxation of Vibrationally Excited OH and OD with other Radical Species.

M.J. Howard, I.W.M. Smith and M.D. Williams,
Department of Physical Chemistry,
University Chemical Laboratories,
Lensfield Road,
Cambridge CB2 1EP

Collisions between free radicals are likely to proceed via transitory collision complexes, because the formation of a chemical bond will lead to a deep well on at least one of the potential surfaces correlating with the separated radicals. The rates at which radicals collide to form complexes may then be reflected in the rate constants of three types of radical-radical process : (i) recombination of radicals in the limit of high pressure; (ii) vibrational relaxation in collisions between radicals, and (iii) exothermic atom-transfer reactions between radicals.

In order to explore these connections further we have initiated measurements on the kinetics of OH and OD in levels $v=0$ and $v=1$ with other radicals, both NO_2 and NO, which can be handled easily, and unstable atomic radicals, H, D, O and N. The experiments are based on the creation of small OH, OD concentrations by pulsed photolysis of H_2O or HNO_3 (or the corresponding deuterated molecules), and the sensitive and state-selective detection of OH or OD by laser-induced fluorescence (LIF) using a flashlamp-pumped dye laser. Kinetic information is obtained by scanning the delay between the flash photolytic and laser pulses.

For OH,OD + NO, NO_2 , gas mixtures can be prepared and handled conventionally, a slow flow of gas being maintained merely to prevent depletion of reagents and accumulation of products. The results for OH($v=0$) + NO, NO_2 (+ M) are in satisfactory agreement with previously determined data for

this recombination. For $\text{OH}(v=1) + \text{NO}, \text{NO}_2$, rate constants are found of $k = (3.8 \pm 1.1) \times 10^{-11} \text{ cm}^3 \text{ molecule}^{-1} \text{ s}^{-1}$ and $(6.4 \pm 1.2) \times 10^{-11} \text{ cm}^3 \text{ molecule}^{-1} \text{ s}^{-1}$, respectively. Although not a radical-radical reaction, we shall also report rate data for the $\text{OH} + \text{CO}$ system. Here, at low total pressure, $\text{OH}(v=1)$ is removed 5.4 times faster than $\text{OH}(v=0)$. This appears to confirm proposals that the reaction: $\text{OH} + \text{CO} \rightarrow \text{CO}_2 + \text{H}$ proceeds first by addition to an HOCO radical which can either decompose back to $\text{OH} + \text{CO}$ or, with lower probability, to $\text{CO}_2 + \text{H}$.

We shall also report new kinetic data on the kinetics of $\text{OD}(v=0,1)$ with NO, NO_2 and CO and discuss what additional light these results shed on the mechanisms for reaction and relaxation in these systems. Finally, experiments will be described in which the same basic flashphotolysis-LIF technique is used in conjunction with a discharge-flow apparatus to study the kinetics of $\text{OH}, \text{OD}(v=0,1)$ with $\text{N}, \text{O}, \text{H}$ and D atoms and some preliminary results will be given.

NOTES

INDEX

Abramson, E. D1	Billaud, F. K6
Ács, G. C1, C39	Billington, A. C8
Agrawal, P.M. C46	Binkley, J.S. B2
Al-Niami, K.H. C37	Black, G. C7
Alvariño, J.M. C31	Blumenstein, U. K50
Anderson, J.G. H2	Blyth, R.G.C. C42
Anner, O. C25	Boettner, J.C. K21
Apel, E.C. D2	Booth, D. C34
Aquilanti, V. L7, C2	Borrell, P. J8, C8
Ashfold, M.N.R. G2, G3	Borrell, P.M. C8
Atkinson, R. C3	Bourguignon, B. K31
Axelsson, E. C4	Bowers, M.T. L1, L3, C9, C10, K39
Azay, P. K28	Bowman, J.M. C11, C12, K7
	Braynis, H.S. K54
	Brouard, M. I6, C40
Back, M.H. C5, K1, K42	Browarzik, R. K49
Back, R.A. K1, K2	Brown, T.C. D4, J3
Bagnall, G.N. K46	Brunning, J. J7, K48
Baldwin, R.R. C56	Burrows, J.P. C13, C14
Bar, I. K43	Buxton, J. D3
Barker, J.R. D4	
Barnes, I. C6	Caille, J. K11
Baronnet, F. K2	Callear, A.B. E1
Barry, M.D. G5	Calpini, B. C55
Bartels, M. K18	Campbell, I.M. K8
Bastian, V. C6	Cao, J.R. C5
Batt, L. K3, K4	Caralp, F. E4
Baughcum, S.L. I3	Carter, W.P.L. C3
Baulch, D.L. K8	Cathonnet, M. K21
Bayes, K.D. C41	Caubet, Ph. K11
Bayley, J.M. G2, G3	Cavalli, S. C2
Becker, K.H. C6	Chamboux, J. K9
Behnke, W. K56	Chandler, D.W. C36
Bércecs, T. C33	Chao, K-J. K19
Berlman, M.R. K5	

Chappel, J.M. K8
Chevrier, M. K39
Child, M.S. A1
Chou, M.S. F1
Clary, D.C. A5, K57
Cohen, N. C15
Collongues, C. K29
Côme, G-M. C16, C17, K27, K28
Conner, J.K. K51
Connor, J.N.L. C18
Corbel, S. K27
Costes, M. K10, K11
Cox, J.W. K36
Cox, R.A. C19
Cunin, P.Y. C17
Curtis, M.C. C45

Dagaut, P. K21
Dai, H-L. D1
David, J-M. C16
Davidson, I.M.T. E2
Dean, A.M. F1
Denning, R.J. K12
Derai, R. L3, C9
Dixon, R.N. G2, G3
Dognon, A.M. E4
Dombi, A. C20
Donaldson, D.J. L6
Donovan, R.J. L5, K25
Dorthe, G. K10, K11
Dove, J.E. C27
Drewery, G.R. C56
Dryer, F.L. K55
Duchovic, R.J. I7
Dutton, N.J. K53
Dzelzkalns, L.S. C21

Efthimiopoulos, T. K13
Eley, C.D. J4
Ertl, G. H1

Farantos, S.C. C22
Feldmann, D. I2
Field, R.W. D1
Fink, E.H. C6
Fletcher, I.W. K53
Foon, R. K12
Forst, W. C23
Fotakis, C. K13
Fowles, M. C19
Freund, E. K6
Frey, H.M. J4
Fritz, B. J5
Furue, H. K38

Gaillard, F. K21
Galwey, A.K. K14
Garcia, E. C31
Garland, N.L. D2
Gilbert, R.G. J3
Giroux, L. K1
Golden, D.M. B1, K32, K44
Goldsmith, J.E.M. B3
Gonzalez, A. K32
Gorry, P.A. G5
Gould, P.L. C37
Gowenlock, B.G. K22
Gower, M.C. K25
Gozel, P. C55
Gray, P. F2
Griffith, D.W.T. C14
Griffiths, J.F. F2, K14

Griffiths, M. C17
Groome, P. K22
Grossi, G. C2
Gutman, D. I5, C24

Haas, Y. I2, C25
Hack, W. C30
Hackett, P.A. C43
Hancock, G. I1, C26
Harman, A. C34
Harrison, R.G. C29
Hase, W.L. I7
Hasko, S.M. K14
Haux-Vogin, L. C17
Hay, S. K15
Heaven, M.C. C24
Heinemann, P. K18
Heiss, A. K16
Helm, H.P. J1
Hernandez, M.L. C31
Hippler, H. C27
Hirst, D.M. K17
Hodgson, A. G3
Hoffmeyer, H. E3
Holbrook, K.A. C37
Holmlid, L. C4, K37
Honma, K. C28
Howard, M.J. L8
Hoyer mann, K. K18
Huhn, P. C1, C20, C39
Hughes, K.J. E2
Husain, D. J6
Hwang, J-T. F4, K19, K20

Ijadi-Maghsoodi, S. E2
Innes, K.K. D1

Jackson, P.A. C45
Jackson, W.M. I4
James, H. K21, K41
Jennings, K.R. K17
John, P. C29, K22
Johnson, K.M. C42
Jorand, F. K9
Joseph, T. C47
Jourdain, J.L. C32
Jusinski, L.E. C7

Kajimoto, O. C28
Kato, T. L2
Kaufman, F. H3, C21
King, K.D. D4, J3
Kinsey, J.L. D1
Klemm, R.B. F3
Koszykowski, M.L. B2
Koyano, I. L2
Kresin, V.Z. A3
Kurzke, H. C30
Kvaran, A. K23

Laganà, A. C2, C31
Lalo, C. K30
Laramée, J.A. K17
Larson, C.W. K32
Laukemper, J. I2
Laverdet, G. C32
Lawley, K.P. K25
Le Bras, G. C32
Lee, E.K.C. D2

Lee, Y-J. K19
Lempereur, F. K30
Leone, S.R. L4
Le Roux, E. K2
Lesclaux, R. E4
Lester, W.A. A3
Li, X. I4
Lifshitz, C. J2
Lightfoot, P.D. C40
Liu, S. C9
Lorents, D.C. J1
Lorenz, K. J5, K24
Lungstrom, E. C19
Luther, K. J8

Macdonald, M.A. L5, K25
Macpherson, M.T. I6
MacRobert, A.J. C26
Manthorne, K.C. K38
Margitan, J.J. K26
Marković, N. A2
Marquaire, P-M. K27, K28
Márta, F. C33
Martin, H.D. C57
Martin, R. K29
Marx, R. L3, K39
Masanet, J. K30
Mauclaire, G. L3, K39
McAndrew, H. C34
McCombie, J. K31
McDonald, J.R. K36
McGuire, R.G. C29
McKay, M. K4
McKendrick, K.G. C26
McLeod, G. K45
McMillen, D.F. K32
McQuigg, R.D. H5

Melius, C.F. B2
Metcalf, E. C34
Miller, J.A. C35, C36
Miller, W.H. A4
Mitchell, A. K51
Mohan, V. C46
Molina, L.T. K33
Molina, M.J. K33
Monot, R. C54
Moortgat, G.K. H5, C13, C14
Moulton, D. C19
Muller, C. C16
Munk, J. K34

Nacsa, A. C48
Nadler, I. K15, K35
Naulin, C. K10
Nelson, H.H. K36
Nielson, O.J. K34
Noble, N. K35
Nolting, F. K56
Nyman, G. K37

O'Keefe, A. L3, C10
Oldenborg, R.C. I3
Oldershaw, G.A. C37
Oref, I. C38

Pacey, P.D. K38
Pagsberg, P. K34
Papagiannacopoulos, P. K13
Parent, D.C. L3, C10, K39
Park, S.C. K7
Patrick, R. C7
Perry, R.A. K40

Péter, A. C1, C39
Petit, J.C. K41
Pfab, J. K35
Philippoz, J.M. C54
Pilling, M.J. I6, C40, C41
Pitts, J.N. Jr. C3
Plane, J.M.C. J6
Potzinger, P. E3
Poulet, G. C32
Powis, I. C42
Preuss, M. I2
Prince, J.D. G2

Rabitz, H. F3, K55
Ratajczak, E. C24
Ravishankara, A.R. H4
Raybone, D. K54
Rayner, D.M. C43
Reimann, B. E3
Reisler, H. K15, K35
Rhäsa, D. J5
Rigny, R. K16
Richard, C. K29
Richards, D.S. C8
Robaugh, D. C52
Rohrer, F. K50
Romanowski, H. C12
Roscoe, J.M. K42
Rosenwaks, S. K43
Rossi, M.J. J1, K44
Rostas, J. K31
Rotem, A. K43
Rouan, J.P. K21
Ruhman, S. I2, C25
Rynefors, K. A2

Sahetchian, K.A. K9, K16
Santamaría, J. C44
Sarre, P.J. C45
Sathyamurthy, N. C46, C47
Sayah, N. I4
Scacchi, G. C16, K2
Scampton, R.J. E2
Schatz, G.C. A6
Schroeder, J. A7
Scott, S.K. F2
Selamoglu, N. K44
Seres, L. C48
Shapiro, M. G4
Sheen, D.B. K45
Shokoohi, F. K15
Shukla, A.K. K17
Sidebottom, H.W. K46
Sigurðadóttir, I.D. K23
Sillesen, A. K34
Simons, J.P. G3, C58, K23
Simpson, C.J.S.M. D3
Slagle, I.R. C24
Slanger, T.G. C7
Sloan, J.J. L6
Smith, C.A. H4
Smith, G.B. E1
Smith, I.W.M. L8
Smith, M.J.C. C41
Snider, N. C49
Sohm, R. D3
Southall, W.J.E. C18
Stace, A.J. C50
Stachnik, R. K33
Stein, S.E. K47
Stern, D. F1
Stewart, P.H. K3
Stief, L.J. J7, K48
Stocker, D. C19

Stuhl, F. K49, K50
Suck Salk, S.H. C51
Sundberg, R. D1
Suzuki, K. C58
Szilágyi, I. C33

Taieb, G. K31
Tanaka, K. L2
Tardieu de Maleissye, J. K30
Tedder, J.M. K51
Thompson, M.J. K42
Troe, J. A7, J8, C27
Tsang, W. C52
Tulloch, J.M. I6
Tully, F.P. B3
Tung Lee, K. C11
Tyndall, G.S. C13, C14
Tzidoni, E. C38

Urbanek, T. C57
Ureña, A.G. C53

Vaccaro, P.H. D1
Van den Bergh, H. C54, C55
Van Koppen, P.A.M. C9
Viossat, V. K9

Wagner, A.F. C24
Wagner, H. Gg. C30
Wagner-Redeker, W. C10
Wahner, A. K52
Walker, R.B. C11
Walker, R.W. C56
Walsh, R. C57

Washington, C. C58
Wayne, R.P. C19
Welge, K.H. I2
Whitefield, D.P. K5
Whitehead, J.C. K53, K54
Wilkinson, J.P.T. L5, K25
Williams, J.H. C26
Williams, M.D. L8
Williamson, A.P. I6
Wilson, C.L. C29
Wine, P.H. H4
Winer, A.M. C3
Wittig, C. G1, K15, K35
Woolley, W.D. C34

Xiang, C.C. J6

Yetter, R.A. F3, K55
Yu, C-R. F4

Zalotai, L. C33
Zellner, R. J5, K24
Zellweger, J.M. C54
Zetzsch, C. K52, K56
Zevgolis, D. K13